



INVESTIGATION OF THE OPERATION OF THE SUPERREGENERATIVE RECEIVER

by

Arthur Gardner Fox

and

Gordon Kendrick Burns

Submitted in Partial Fulfillment of the Requirements

for the degree of

MASTER OF SCIENCE


from the


Massachusetts Institute of Technology

1935

Signatures of Authors.....

.....
Department of Electrical Engineering, May 16, 1935

Signature of Professor in Charge of Research.....

Signature of Chairman of Departmental
Committee on Graduate Students.....

√

TABLE OF CONTENTS

Chapter		Page
I.	Foreword	1
II.	Review of Work of Previous Investigators	7
	A. Edwin H. Armstrong	7
	B. Pierre David	10
	C. Hens Kohn	15
	D. Von G. Hassler	20
III.	Theory	26
	A. Fundamental Circuit Equations	26
	B. Beats and Multiple Resonance Phenomena	35
IV.	Experimental Apparatus	53
V.	Experimental Investigation	62
	A. The Vacuum Tube as a Source of Negative Resistance	63
	B. The Superregenerative Process	86
	C. Operating Curves	103
	D. Multiple Resonance Phenomena	134
VI.	Conclusion	148

Appendix		Page
A.	Translations and Abstracts	155
	I. Armstrong	155
	II. David, Dufour, Mesny	163
	III. David	170
	IV. Kohn	186
	V. Hassler	238
B.	Standard Signal Generator	295
C.	Preliminary Outline of Automobile Antenna Investigation	304

CHAPTER I

FOREWORD

CHAPTER I

FOREWORD

Significance of a Study of Superregeneration

The superregenerative receiver at present occupies a peculiar position in radio. While Armstrong's announcement of a circuit in which the resistance of the tuned circuit alternated periodically about zero was made in 1922, it is only in the last five years that superregeneration has reached a place of practical importance.

This development has come about, not because of marked improvements in the circuit, but because of the new interest in ultra-high frequencies, where, at least until very recently, the use of conventional receivers has been impracticable. First amateur radio and then police and other types of communication have been established in the region below ten meters. The superregenerative circuit has been a favorite in these classes of service on account of the simplicity and portability of equipment which it makes possible without sacrifice of necessary sensitivity.

In spite of its growing practical importance, however, progress toward a true understanding of the process of superregeneration has been slow. Radio engineers in this country seem to have avoided the subject almost entirely, and even in Europe, where it has interested such men as Heinrich Barkhausen, the number of scientific and comprehensive papers which have been published on superregeneration may be counted on the fingers of one hand.

It is not surprising, however, that this condition has prevailed. The superregenerative receiver is essentially a non-linear circuit of one of the worst possible types for theoretical analysis, namely, an oscillatory circuit in which the resistance is a function both of time and of the amplitude of oscillating current in the circuit. This function, furthermore, is generally quite complicated, and depends upon the arrangement and values of the circuit elements. As a result, it has not only been rare for experimenters to duplicate each other's results; it has been unusual for them to succeed in repeating even their own observations. Indeed, to persons familiar only with the more conventional and straightforward types of radio circuits, the superregenerative receiver has often seemed to operate utterly "without rhyme or reason".

History of the Present Investigation

The present thesis study developed from an attempt to account for certain peculiarities of behavior of a superregenerative receiver, which was desired for use as a field-strength measuring set. In order to indicate more clearly the route by which this investigation of superregeneration was approached, a brief account of the evolution of the thesis problem from its original to its final form will be given here.

The original problem pertained to antennas and radiation measurements, rather than to receivers. In the spring of 1934 we set as our objective the determination of the best forms of ultra-

high-frequency antennas to use on an automobile in two-way police radio service. In Appendix C, at the rear of this volume, is included a more complete statement of this problem, as well as a fairly detailed outline of the series of measurements which it was proposed to make. Here it will suffice to state that the entire experimental program hinged upon the development of apparatus and technique for the measurement of ultra-high-frequency field strengths.

This preliminary problem seemed at the outset to be nearly solved. There was at our disposal an RCA superregenerative receiver, of a type built commercially for ultra-high-frequency police radio communication. A brief test of this receiver indicated that it was apparently in satisfactory operating condition.

The next requirement was a means of calibrating the receiver. For this purpose it was decided to construct a standard signal generator, having a range of 30 to 60 megacycles. Such a generator was designed, being based upon a circuit suggested to us by Mr. G. W. Pickard of the General Radio Company, and was built during the summer of 1934. It is described in Appendix B, in somewhat more detail than would be appropriate here.

When this signal generator was connected to the superregenerative receiver mentioned above, a number of unexpected phenomena were observed. One of the most puzzling of these was the presence of multiple resonance points. It was thought at first that the receiver was reacting upon the generator in such a way as to substitute a complicated reactance network, having a number of resonant

frequencies, for the simple tuned circuit of the generator. Subsequent experiments showed, however, that this was not the case, and that the cause of the multiple resonance points was entirely within the receiver.

Efforts were made to isolate and remove the cause of this phenomenon, using a cathode-ray oscillograph as an aid to investigation. It was soon realized, however, that the receiver being used was poorly adapted to experimental work, on account of the difficulty of adjusting voltages and circuit parameters, and because of its relatively complicated circuit. To overcome these difficulties, another ultra-high-frequency superregenerative receiver was constructed for use as a field-strength measuring set, employing a circuit suggested by Mr. G. W. Pickard. This receiver and a summary of the observations made with it are described in Chapters IV and V, on "Experimental Apparatus" and "Experimental Investigation", respectively.

Up to this point, the matter of securing a suitable receiver had been considered simply as a preliminary step toward the originally scheduled program of antenna measurements. It now became apparent, however, that the problem of superregenerative reception could not be adequately solved in time to permit this plan to be carried out, but were themselves sufficiently important to warrant devoting the remainder of our time to them alone. Accordingly, in October, we changed the objective of our thesis from a study of antennas to an investigation of superregeneration.

As our first and most important task, it was now necessary to determine the operating characteristics of superregenerative

receivers in general, and the causes of their peculiarities. As a second objective, to be attacked only when progress had been made toward the first, we hoped to formulate practical rules for the design and adjustment of superregenerative receivers, particularly for use in field-strength measurement.

The program of procedure which was adopted consisted of (1) assembling previously published contributions to the theory of superregeneration into a convenient form, in English; (2) critically examining these papers in order to appraise their conclusions on theoretical grounds alone; (3) conducting a series of experiments with a low-frequency model of a superregenerative circuit; and (4) combining the findings of these theoretical and experimental investigations into a discussion and summary of the theory of the superregenerative receiver, as it stands at the present time. The following chapters take up these steps in the order given, except that the abstracts and translations of previous papers are removed from the body of the thesis, and appear in Appendix A.

Division of Responsibility Between Authors

To a very great degree, the planning and execution of this thesis investigation have been performed jointly by the two authors, so that it would be impossible to draw a sharp line of division between their respective contributions. In general, however, Mr. Fox has been particularly concerned with the formal mathematical work on

the superregenerative circuit, and Mr. Burns has dealt especially with the experimental program.

In the writing up of the thesis, the division of responsibility has been as follows. Mr. Fox has written part of Chapter II, Chapter III, a portion of Appendix A, and Appendix B. Mr. Burns has written Chapter I, part of Chapter II, Chapter IV, Chapter V, Chapter VI, part of Appendix A, and Appendix C.

Acknowledgements

We wish to record our appreciation of the advice and assistance given us by Messrs. Shaw and Pickard, of the General Radio Company. Through them an ultra-high-frequency transmitter was made available to us for our originally planned series of antenna measurements. Mr. Pickard, in particular, helped us greatly in the design of the ultra-high-frequency signal generator and superregenerative receiver referred to in the foregoing pages. Thanks are also due to Dr. W. L. Barrow, our thesis advisor, for the particular interest which he has taken in our problem, and for the assistance which he has given us in the mathematical analysis of the superregenerative receiver as a circuit with periodically-varying resistance.

CHAPTER II

REVIEW OF WORK OF PREVIOUS INVESTIGATORS

CHAPTER II

REVIEW OF WORK OF PREVIOUS INVESTIGATORS

A. EDWIN H. ARMSTRONG

Superregeneration was first described by Edwin H. Armstrong in an article appearing in the August 1922 number of the Proceedings of the Institute of Radio Engineers.¹ In this article Armstrong outlined the theory of superregeneration in a general way and presented several circuits by means of which it was possible to obtain superregenerative amplification.

No mathematical analysis was made of the circuit, and the theory presented was principally qualitative in nature. Nevertheless, Armstrong had a fairly clear physical picture of the superregenerative process, and his explanations, as far as they go, are essentially correct. He was the first to make use of the concept of negative resistance in analyzing the problem, and most of those who have interested themselves in the subject since that time have continued to make use of this concept. In short, it consists in assuming that the effect of feed-back in a simple regenerative oscillator in the presence of oscillations in the tuned circuit, may be considered to be the same as the insertion into the tuned circuit of a hypothetical negative resistance. If this negative resistance is large enough, it may neutralize the

1 - See Appendix A, Part I.

effect of the inherent positive resistance of the circuit, and render the net resistance negative, in which case energy may be fed into the circuit and any oscillations present will be increased in magnitude. The superregenerative process is then explained by saying that the periodically varying quenching voltage causes the negative resistance due to feed-back, and hence the net resistance of the tuned circuit, to vary periodically in such a way that part of the time any oscillations existing in the circuit will be damped out, and part of the time they will be increased.

In this article, Armstrong proposed using the superregenerative circuit as a simple amplifier for the purpose of amplifying modulated radio frequency signals before detection had been performed. As such, he intended that the function of detection should be performed in a separate stage, and most of the superregenerative circuits which he shows are simple amplifiers. He suggested, however, that when operating at high radio frequencies, it might be advisable to combine the functions of amplification and detection in one stage, and he presented a circuit in which this is accomplished. He also pointed out that it might be necessary to insert positive resistance into the tuned circuit of the superregenerative stage in order to insure that oscillations existing in that circuit would be sufficiently attenuated during the period when the net resistance of the tuned circuit was positive.

Armstrong had apparently performed enough experimental tests on his circuits to check his conclusions fairly well. On the whole, however, his analysis of superregeneration is fairly elementary, and many problems and phenomena which are of great importance were not mentioned.

He did not give any hint as to the presence of beats or multiple resonance peaks in the operation of the amplifier, and it remained for later experimenters to bring these interesting quirks to light and explain them.

A.G.F.

B. PIERRE DAVID

To David must go the credit for being probably the first writer to attempt a mathematical analysis of the superregenerative receiver by considering it as an oscillatory circuit with periodically varying resistance.

In the article which David, Dufour and Mesny (see Appendix A, Part II) published in L'Onde Electrique, in 1925, this analysis is, to be sure, carried out in a way which is slightly confusing to the reader. Starting with a differential equation for a circuit containing R, L and C, and making use of certain simplifying assumptions, the authors arrive at the following expression for current as a function of R, L, C, the impressed voltage, and time.

$$i = \frac{E}{|R|} \left[\sin \omega t - e^{-\frac{Rt}{2L}} \sin \omega t \right]$$

$$\text{where } \omega = \frac{1}{\sqrt{LC}} .$$

It is not difficult to gain the impression from the paper that this expression is presented as the general equation for the superregenerative receiver, from which, if the proper function of time is substituted for R, the course of oscillations during the quenching-frequency cycle may be determined.

Actually the equation has no such significance, for its very derivation depends upon the assumption of a constant resistance in the oscillatory circuit. Indeed, succeeding paragraphs of the paper indicate that the authors themselves did not consider the above equation to be the general equation for the superregenerative receiver. They use it only as a qualitative aid to an examination of the behavior of

the circuit during various parts of the quenching cycle. For example, the equation shows that, when R is positive, a forced oscillation of finite magnitude is set up by the impressed voltage; while, when R is negative, free oscillations build up exponentially.

David and his colleagues, then, were in a position to draw quantitative conclusions based on theoretical grounds, concerning the speed with which oscillations should build up during the negative-resistance period, and therefore concerning the amplification which should be attainable in a superregenerative receiver. Had they done so, they would undoubtedly have discovered a fact later pointed out by Hassler, namely, that for given values of resistance and reactance in the tuned circuit, the amplification depends upon the ratio of radio frequency to quenching frequency, but not upon either of these alone. Instead, however, the authors were content with an experimental study of the effect of radio and quenching frequencies upon amplification. They rendered a service by refuting Armstrong's surmise that the amplification varied as the square of the ratio of these two frequencies, but overstepped themselves by concluding that provided there was a large number of radio-frequency cycles in one quenching cycle, the value of this number had no effect at all upon the sensitivity of the receiver.

In his 1928 article in L'Onde Electrique, David makes a further contribution to the mathematical analysis of superregeneration by presenting the differential equation which must be solved in order to determine the course of oscillations during the quenching cycle.

His statement of the equation is as follows:

$$L \frac{d^2 i}{dt^2} + R(i, t) \frac{di}{dt} + \frac{1}{C} i = E \omega \cos \omega t$$

The significant point is that he considers R to be a function of current as well as of time. By so doing he paves the way for a rational consideration of the effect of saturation upon the behavior of the circuit. He rightly points out, however, that the formal solution of this differential equation would be extremely difficult. Indeed, strictly speaking, his differential equation itself is not correctly written. It should be as follows:

$$L \frac{di}{dt} + R(i, t) i + \frac{1}{C} \int i dt = E \sin \omega t$$

If this is differentiated with respect to time, then there is obtained the following equation:

$$L \frac{d^2 i}{dt^2} + R(i, t) \frac{di}{dt} + \left[\frac{1}{C} + \frac{d R(i, t)}{dt} \right] i = E \omega \cos \omega t.$$

which contains a term not shown in David's equation.

David not only touches upon the matter of saturation from a theoretical point of view, but also considers its practical effects. He points out that while under some conditions of adjustment a super-regenerative receiver may be made to operate in the linear manner described by Armstrong, whereby the amplitude of oscillations attained during the quenching cycle is always proportional to the initial oscillation giving rise to them, it is also possible to adjust the receiver to such a state of saturation that considerable fluctuations in signal strength have almost no effect on the output of the receiver. David

correctly notes that the former condition is desirable for radiotelephony, while the latter has advantages in telegraphic reception.

David appears also to have been the first writer to mention the subject of multiple resonance phenomena. The fundamental reason for these phenomena -- the reenforcement of the signal voltage by the residual oscillation at the moment of passage from positive to negative resistance, when the frequencies of the transmitter and receiver differ by any integral multiple of the quenching frequency -- is mentioned briefly in the 1925 article, and is considered more fully in the 1928 paper. In the latter, David erroneously implies, however, that any detuning of the receiver from one of these resonance points necessarily produces a heterodyne whistle. Actually, as will be shown in Chapter III, there are additional conditions which must be met in order for multiple beats to occur, even assuming that an appreciable residual oscillation is present and that the frequencies of the receiver and the signal bear the proper relation to each other.

In regard to selectivity, David observed the superregenerative receiver to be inferior to the ordinary regenerative receiver, and offers a rather novel explanation for the difference. He points out that the superregenerative circuit is sensitive to the impressed signal for only a very short period during each quenching cycle; that is, during the time when the resistance is approximately zero, becoming negative. As far as selectivity is concerned, he claims, this brief period is the time constant of the circuit; hence the low time constant and the observed poor selectivity.

This explanation appears to be of rather dubious rigor. It is true that in a circuit of fixed resistance, the initial rate of growth of oscillations when a signal is applied is more or less independent of the tuning of the circuit with respect to the signal, so that in this sense the circuit might be said to be broadly tuned. In the superregenerative receiver, however, the effective resistance of the tuned circuit is not constant during the brief period which David takes to be the time constant, but is continuously changing. Consequently David's explanation is scarcely valid.

In summary, it is interesting to note the trend of David's thinking during the period from 1923 to 1928. In 1923 he wrote a brief "how-to-build-it" article concerning a superregenerative receiver and included a few "rules of thumb" for the adjustment of the receiver. In the 1925 article a more scientific attitude begins to appear, although the paper is not very well organized. The 1928 paper is a first-class piece of work, considering the subject of superregeneration quite comprehensively, from both theoretical and practical standpoints. While it lacks the quantitative exactness of Hassler's article (see Part D of this chapter), it was, at the time of its publication, by far the best treatment of superregeneration in print.

G.K.B.

C. HANS KOHN

Kohn's paper on superregeneration (see Appendix A, Part IV) is rather disappointing in a number of ways. He does make two or three real contributions, including an improved method of taking saturation into account in analyzing the operation of the receiver, and an interesting graphical method of tracing the course of oscillations during the quenching cycle. For the most part, however, the paper stands as evidence of a faulty understanding of the very fundamentals of the action of the superregenerative receiver, on the part of the author.

The paper is composed of two sections: an experimental part, and a theoretical, or mathematical, part. To the experimental work at least two objections must be raised. In the first place, it is not very well planned. Insufficient data is taken to warrant the general conclusions which the experiments are designed to support. In the second place, Kohn often misinterprets the outcome of his experiments and lays down as general truths statements which are either irrelevant or absolutely incorrect.

The mathematical part of the paper starts in a promising way, but so many approximations and assumptions are introduced that it is impossible to place much faith in the results. There is some ground for a feeling that the approximations were chosen with an eye to obtaining the desired expressions at the end of the derivations.

Viewed simply as a piece of technical writing, the article is quite unsatisfactory. The logic and coherence of the presentation are poor. The nomenclature and choice of symbols is unfortunate, the same style of letter often being used for two or more different types of quantities.

* * * * *

In the beginning of the article under "The regenerative oscillator", Kohn presents the equation $\tan \alpha_0 = \frac{1}{2C\delta}$ which he attributes to Moller, and this he proceeds to use for his own purpose. Now this expression for $\tan \alpha_0$ is not strictly correct as he has used it. This is shown by the following considerations. Since $\delta = \frac{R}{2L}$, $\frac{1}{2C\delta} = \frac{L}{RC}$, which is the resistive impedance of the tuned circuit. In Kohn's work, the high frequency tuned circuit was in the plate circuit, and so (using Kohn's notation) $\tan \alpha_0 = \frac{L}{RC} = \frac{U_{st}}{S_a}$ and not $\frac{U_{st}}{S_a}$ as indicated in his diagram (Fig. 1). U_{st} is proportional to U_a, μ, L_1 , and L_2 , and so it would be approximately correct to say that $U_{st} = k U_a$. This means that Kohn's expression should actually read $\tan \alpha_0 = \frac{k}{2C\delta}$.

It might also be of interest to see where the expression, $\tan \alpha = \frac{1}{2C(\delta+a)}$, came from. It appears that Kohn simply figured that for some position on the oscillation characteristic (Fig. 1) where equilibrium had not yet been reached, the ratio of U_{st} to S_a was such as to supply to the tuned circuit sufficient energy to compensate for the natural damping and in addition to cause a certain rate of growth of oscillations. In other words, speaking in terms of the negative resistance concept, the value of $\frac{U_{st}}{S_a}$ defines the negative resistance supplied by the tube such that $(S_a/U_{st}) \frac{L}{C} = R_{neg}$. However, his equation should read $\frac{U_{st}}{S_a} = \frac{k}{2C(\delta+a)}$ for the same reasons as were given in the previous paragraph. His expression for $a = \delta \left(\frac{\tan \alpha_0 - \tan \alpha}{\tan \alpha} \right)$ stands correct.

The above manner in which Kohn obtains the value of negative resistance in the tuned circuit from the oscillation characteristic constitutes one of the few redeeming features of his paper. As a matter

of fact, it should be pointed out here that Kohn went at the problem of superregeneration in quite a different way from other investigators. He has not explicitly used the concept of variable resistance in the tuned circuit, and all of his thinking has been in terms of the oscillation characteristics which it is possible to measure experimentally. For this reason his treatment of saturation in the oscillator has been markedly different from that of most other investigators, and it gives much more reasonable results. For example, Hassler assumed that during the period of net negative resistance in the tuned circuit, oscillations would build up exponentially unless and until they reached a certain definite saturation value, whereupon there would be no further growth and the limiting value would be maintained (see discussion of Hassler's article in Part D of this chapter). Other investigators have not dealt with the question of saturation at all. The results of Kohn's treatment, however, give a much more reasonable picture of what happens, and they show that oscillations do not suddenly strike a limiting value, but that their rate of growth decreases in such a way that the limiting value is approached more or less asymptotically. This is what one would expect, and it arises from the fact that the oscillation characteristics bend over and cross the line of back-coupling (refer to diagrams in Kohn's article, in Appendix A, Part IV), hence producing a point of equilibrium where the energy produced by the tube is just sufficient to compensate for the energy consumed in the tuned circuit.

Although Kohn^{never} tells exactly what the significance of his a is, it is apparent that this quantity represents the coefficient which

appears in the exponent of the damping factor obtained as part of the solution of the differential equation representing the behavior of the tuned circuit with constant parameters. This seems to be borne out by his statement that $a = \frac{1}{S_a} \cdot \frac{dS_a}{dt}$, which means that he has considered that $S_a = e^{at}$. This fact should be kept in mind when reading his paper, for the assumption will only hold true when the effective resistance in the circuit is constant. All of his statements in the part under "The regenerative oscillator" apply only to a simple oscillator when there is no signal being fed in from the outside.

Throughout the paper, Kohn frequently speaks of a "minimum quenching voltage". It is his opinion that the best operation of the superregenerative amplifier will be had when it is first adjusted so that continuous oscillations are obtained, and then a quenching voltage applied which is just sufficient to prevent high frequency oscillations in the absence of a signal. The minimum quenching voltage was considered to be that value which would do this. But there are many ways in which a superregenerative amplifier may be adjusted so as to prevent oscillations in the absence of a signal, and there is no particular significance or importance in the minimum quenching voltage as defined by Kohn. If the amplifier were operating in a linear condition, the application of quenching voltage could not have suppressed oscillations. The reason the quenching voltage did suppress the oscillations must have been that by swinging the grid potential to higher positive values, a condition of saturation existed during part of the negative-resistance period so that the average resistance taken over

one complete quenching cycle was made more positive.

Kohn's conclusions do not mean very much on the whole because they were based upon mistaken and inaccurate premises, the most important one being that the ideal adjustment of the receiver should be that outlined above. At the end of the section on experimental investigations he explains the fact that he obtained higher values of amplification for greater damping in the tuned circuit, by means of the equation,

$$\frac{1}{\mathcal{D}_a} \cdot \frac{d\mathcal{D}_a}{dt} = \delta \left(\frac{\tan \alpha_0 - \tan \alpha}{\tan \alpha} \right) .$$

This explanation is not valid because changing δ changes $\tan \alpha_0$ also.

Kohn's theoretical treatment is interesting for the graphical construction method which he employs to find the course of oscillations during the quenching cycle. In much of the analytical work, however, the number of approximations made throw some doubt on the value of the results he obtains. Nowhere does he make any reference to the phenomenon of beats or multiple resonance peaks.

A.G.F.

D. VON G. HASSLER

Undoubtedly the most comprehensive and scientific treatment of superregeneration yet published is the article by Hassler (see Appendix A, Part V) in Hochfrequenztechnik und Electroakustik, September, 1934. This paper is outstanding in that it places on a quantitative theoretical basis a number of phenomena which previously had been described only in a general, qualitative manner.

The article is to be commended for the logical order in which it is presented. The first subject treated is the simplest and most highly idealized case of superregeneration: that of a square-wave variation of effective resistance, with no saturation effects coming into consideration, and with the residual oscillation small enough to be negligible at the instant of passage from positive to negative resistance. With this simplified case, Hassler explains the fundamental principle of the superregenerative receiver.

Following this exposition, the bulk of the paper is devoted to a quantitative consideration of the effects of departures from the three simplifying assumptions given above. In the first place, Hassler recognizes that the resistance of the tuned circuit does not shift abruptly from a positive to a negative value, and vice versa, but varies continuously and gradually between these two values. Consequently he presents an equation showing the effect upon sensitivity of gradual passage into the negative-resistance condition, or gradual

"dedamping". While he omits the derivation of the equation, it is evidently derived upon the assumption that the resistance of the tuned circuit, instead of jumping directly from the positive to the negative value, drops abruptly to zero, remains there for a short interval τ_0 , and then drops to the negative value. This is a somewhat better approximation to gradual dedamping than the square-wave variation postulated in the preceding paragraph. The equation thus derived indicates that a given signal voltage will give rise to a larger initial oscillation with gradual dedamping than with sudden dedamping. However, as is explained on page 35 in Chapter III, this comparison is not a fair one, for the amplitudes of oscillation which are being compared are not taken at corresponding instants in the quenching cycle. Consequently Hassler's conclusion that greater sensitivity is obtained when the dedamping takes place gradually is not valid.

Saturation is taken into account by Hassler in a rather highly idealized manner. He considers that when the receiver is operating in a saturated condition the oscillations build up exponentially during the negative-resistance period until they strike a definite limiting level, and continue at constant amplitude until the beginning of the positive-resistance period, after which point they decay exponentially. Now, as will be shown in Chapter V, saturation actually manifests itself in a number of different ways, some of which bear little resemblance to this "flat-topped" form. Still, even if Hassler's assumption is only a rough approximation to the truth, it is justified by the useful results which he obtains from it. He finds, for example, that when the oscillating voltage across the tuned circuit is supplied to a square-law

detector, the derivative of the output of the detector with respect to the logarithm of the signal voltage is a constant, independent of the signal voltage, as long as the receiver is in a saturated condition. Furthermore, and much more remarkable, he offers experimental curves to support this conclusion.

The matter of selectivity is considered by Hassler, for both saturated and unsaturated conditions of the receiver. He finds from a quantitative theoretical analysis that in the latter condition the selectivity of the superregenerative receiver is always superior to that of a conventional tuned-radio-frequency receiver employing an identical tuned circuit. In the saturated condition, however, the resonance curve becomes broader and flattened out on top.

To describe the condition in which the residual oscillation is not small enough at the moment of dedamping to be considered negligible, Hassler uses the term "coherence", indicating that successive quenching cycles exert an effect upon one another. "Incoherence" refers to the condition in which the residual oscillation is so small as to be negligible. Hassler places a rather sharp line of demarcation between these two conditions, by making the noise level in the receiver the criterion. If the residual oscillation is smaller than the noise level, he believes it can have no effect, while if it is larger, it can affect the starting of the next train of oscillations.

This conclusion seems quite incorrect. In the first place, leaving noise voltage out of consideration for the moment, there is no critical value below which the residual oscillation cannot affect the succeeding train of oscillations, and above which it can. There can

be no residual oscillation so small that it does not exert some slight effect toward multiple resonance peaks, for instance. Only when the residual oscillation is fairly large, however, does this effect become sufficiently pronounced to produce perceptible peaks in the output signal of the receiver, as the oscillatory circuit is detuned. Thus the difference between coherence and incoherence is really one of degree only.

If now a noise voltage, considerably greater than the residual oscillation, is brought into the picture, there is no reason why any tendency toward multiple peaks that is exerted by the residual oscillation should be at all reduced. As long as the receiver does not become saturated, the superposition of the noise voltage upon the residual voltage cannot destroy the effect of the latter. From a practical point of view, of course, reception does become unsatisfactory when the noise voltage is greater than the signal voltage, for then the noise output of the receiver is so great as to drown out the desired signal.

One of the interesting results of coherence described by Hassler is the fact that, when the receiver is adjusted so that the residual oscillation is nearly as large as the initial oscillation that gives rise to it, it takes several quenching cycles after the signal voltage is first applied for the trains of oscillations to build up to a steady amplitude. Likewise, when the signal voltage is removed, it takes a large number of quenching cycles for the trains of oscillations to die out.

Another consequence of coherence is the occurrence of multiple resonance phenomena. Hassler is concerned particularly with multiple

peaks, rather than multiple beats, and in this respect is almost directly opposite to David (see Part B of this chapter). He correctly explains the high value of amplification at the peaks on the basis of the re-enforcement of the signal voltage by the residual oscillation, when the receiver frequency differs from the signal frequency by an integral multiple of the quenching frequency.

His explanation of the relatively low amplification in the "valleys" between the peaks, however, seems erroneous. He implies that when the receiver is not tuned to one of these peaks a heterodyne process occurs, whereby the phase relation between the signal voltage and the residual oscillation at the instant of dedamping varies in successive quenching cycles; but that, on account of the long building-up and dying-out times referred to above, the level of oscillations responds to these phase variations too sluggishly to build up to any very high amplitude in that part of the heterodyne cycle where the signal voltage and the residual oscillation are in phase.

This explanation appears definitely incorrect. The multiple peaks which Hassler observed were obtained with the receiver adjusted for positive average resistance; that is, so that in any given quenching cycle the residual oscillation was smaller than the initial oscillation which had given rise to it. As will be shown in Chapter III, it is impossible under such a condition for a rotation of phase to occur between the residual oscillation and the signal voltage at successive instants of dedamping. Consequently the fundamental process by which Hassler explains the low amplification observed when the receiver is not tuned to one of the multiple resonance points simply does not occur.

Hassler also observed multiple heterodyne whistles with his receiver. This, of course, is the phenomenon of multiple beats, as distinguished from that of multiple peaks. He errs, however, in stating the conditions under which such beats may occur. He implies that they may always be observed when a signal is present and the receiver is adjusted so as to generate oscillations continuously. Furthermore, he says that beats may even be observed with the receiver adjusted to have a slightly positive average resistance.

Actually, as will be shown in Chapter III, beats do not always occur even when the receiver is generating continuous oscillations, and, except in the case of transient disturbances, can never occur when the average resistance is positive.

Lest a wrong impression be drawn from the criticisms in the foregoing pages, it should be stated here that on the whole the derivations and explanations in Hassler's paper are remarkably sound. He appears to have a firmer grasp of the mechanism of superregeneration than any other writer has shown to date. He has supplied quantitative, theoretical explanations for many phenomena which previously had been observed only in a general way and often had not been accounted for at all. In this accomplishment lies Hassler's contribution to the literature on the superregenerative receiver.

G.K.B.

CHAPTER III

THEORY

CHAPTER III

THEORY

A. FUNDAMENTAL CIRCUIT EQUATIONS

No one has succeeded in performing a completely rigorous mathematical analysis of the superregenerative process as yet, and it appears improbable that anyone ever will. The difficulty arises simply from the fact that the differential equations representing the degrees of freedom of the circuit are too complicated to permit of a formal solution. But since they represent an actual physical system, solutions must exist, and this suggests that graphical analysis making use of the differential analyzer might produce some interesting results.

In attempting a formal analysis it is usual to consider that the superregenerative circuit consists essentially of an oscillatory circuit containing constant inductance and capacitance and a variable resistance, and in which a voltage is induced by an outside signal. Experiment seems to show that such an assumption is entirely justified, and the problem is to determine how the resistance varies. The ideal superregenerative circuit is shown below.

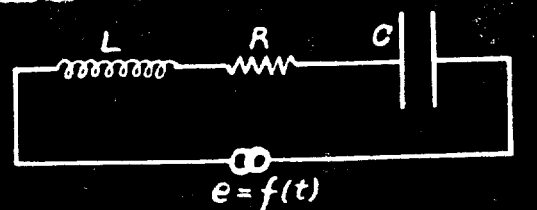


Fig III-1

The fundamental equation for this circuit is,

$$L \frac{di}{dt} + R i + \frac{1}{C} \int i dt = f(t) \quad (1)$$

where i is the instantaneous current in the circuit and $f(t)$ is the signal voltage.

If for the moment it be considered that R is constant, this equation may be written,

$$L \frac{d^2i}{dt^2} + R \frac{di}{dt} + \frac{1}{C} i = f'(t) \quad (2)$$

The solution of this equation is perfectly straight-forward and was performed by David in his 1925 article. David, however, made the mistake of supposing that, once the above equation was solved, the R could be made variable. This is not permissible.

A somewhat more general case is obtained when it is assumed that R is a linear function of time such that $R = a + bt$, where a and b are arbitrary constants. This assumption is obviously not applicable to the superregenerative receiver, but a knowledge of the solution for this condition would be helpful in understanding in a general way the effect of the variation of resistance.

If the resistance is assumed to be a periodic function of time such that $R = a + b \sin(qt + \phi)$ where q is the quenching frequency, a somewhat practical case is represented. In either of the last two cases, R should be considered to be a function of time before equation #1 is differentiated. The resulting equation would then be,

$$L i'' + R i' + \left(\frac{1}{C} + R'\right) i = f'(t) \quad (3)$$

where the primes indicate differentiations with respect to time.

We have not succeeded in obtaining closed solutions to the above equation for the cases of R equal to a linear or to a periodic function of time. A series form of solution may be obtained by assuming a solution for i in the form of a power series for the linear resistance case, or a Fourier series for the periodic resistance case, and computing the coefficients by substituting the assumed values into the differential equation. This method is, however, very laborious and even when the coefficients of the series have been computed it is not easy to see in a general way what the results are.

The solution to equation (2) will represent the current in the tuned circuit accurately as long as the resistance remains constant. It is possible therefore to apply this solution to a given set of initial conditions holding R constant in the meanwhile, and to determine the final conditions which would exist at the end of a brief period time, Δt . Then using these final conditions as the initial conditions for a new solution with the resistance held constant at a new value during a second interval, it is possible to determine a second set of final conditions. Continuing this step by step process, we have found it possible to synthesize an approximate solution for a case where the resistance is allowed to vary by discreet steps, and passing to the limit where the steps become infinite in number and infinitesimal in size, we have obtained an expression for i as follows.

$$i = e^{-\int \frac{R}{2L} dt} \left[A e^{j\int \omega_0 dt} + B e^{-j\int \omega_0 dt} \right] \quad (4)$$

In the above expression A and B are constants of integration and

ω_0 is the resonant frequency of the tuned circuit. This solution is definitely only an approximation and in addition only applies to the case where there is an impressed signal voltage. That the form of the exponential which is outside of the brackets is probably correct is indicated by another method of solution which will be shown presently. The above solution to the homogeneous equation may be used to determine the complete solution for the case of an impressed voltage by the method of the variation of constants. Application of this method leads to a solution in the form of a definite integral which it is impossible to integrate and which is so complex that very little can be learned by examining it.

Proceeding to the most general case of superregeneration, it is known that since amplification is limited by saturation, the effective negative resistance of the circuit must be not only a function of time, but also a function of current. Inserting $R = G(i, t)$ in equation (1) and differentiating with respect to time leads to a differential equation which is not even linear, and which is impossible of formal solution.

The differential analyzer could very easily handle the problem of analysis for any of the cases where resistance is a function of time alone. It would also be possible to perform an analysis with its aid on the last mentioned case where R is a function of current and time. A family of curves representing the variation of resistance with respect to current and time would have to be found experimentally for a particular superregenerative oscillator, and this family could

then be used on one of the input tables of the analyzer to determine R at any instant. Results obtained in this case, however, would not be as accurate as the others since the process of supplying the information to the analyzer from the data curves would involve jumping from one curve to another. In all cases the graphs obtained from these differential equations by the analyzer would include the individual high frequency oscillations as well as the growth and decay of their envelopes.

Energy Considerations:

Because we are primarily interested in determining the magnitude of the high frequency oscillations in the tuned circuit of the superregenerative amplifier at any time, and not in the individual high frequency cycles themselves, it would appear that any method which aims directly at determining the envelope of the oscillations, would avoid needless complications. To this end it will be found advantageous to consider the superregenerative process from the standpoint of the energy which the tuned circuit contains at any time.

Let it be assumed that the current in the tuned circuit is a periodic function of time. In general at any instant some energy will be stored in the electrostatic field of the condenser and the remainder will be stored in the magnetic field of the inductance. Energy will also be in the process of leaving or entering the circuit through the resistance, depending upon whether it is positive or negative. At those points of the high frequency cycle where the current is a maximum, the charge on the condenser will be zero, and all the

energy will be stored in the inductance. Therefore, $W = \frac{1}{2} L i_m^2$ is a measure of the energy in the circuit at any time. i_m is the maximum value of current during the high frequency cycle such that $i_{inst.} = i_m \cdot \varphi(t)$, where $\varphi(t)$ is a periodic function of time, usually sine or cosine.

We now write down the fundamental energy equation.

$$\frac{dW}{dt} = \frac{d}{dt} \left(\frac{1}{2} L i_m^2 \right) = -R i_i^2 + V_i i_i \quad (5)$$

Where, V_i = instantaneous voltage induced in the circuit by the signal

i_i = instantaneous current

V_m = peak value of signal voltage

Then, $L i_m \frac{d i_m}{dt} = -R i_m^2 \varphi^2(t) + V_m \theta(t) i_m \varphi(t)$

$$L \frac{d i_m}{dt} + R i_m \varphi^2(t) - V_m \theta(t) \varphi(t) = 0$$

This last is a linear equation of the first order, and the solution is accordingly,

$$i_m = e^{-\int \frac{R}{L} \varphi^2(t) dt} \left[C + \frac{\int V_m \theta(t) \varphi(t) e^{\int \frac{R}{L} \varphi^2(t) dt} dt}{L} \right] \quad (6)$$

providing that R is assumed to be a function of time alone.

If this solution is now examined for the case where no input signal is impressed, it is seen that

$$i_m = C e^{-\int \frac{R}{L} \varphi^2(t) dt}$$

If $\varphi(t) = \sin \omega_0 t$ as is usually the case, then $\int \frac{R}{L} \varphi^2(t) dt = \int \frac{R}{2L} dt - \int \frac{R}{L} \cos 2\omega_0 t$. When ω_0 is large as compared with the quenching frequency, the second term on the right is unimportant, and hence,

$$i_m = C e^{-\int \frac{R}{2L} dt}, \quad \text{which is the same damping coefficient as}$$

that obtained in equation (4).

In general it may be too difficult to solve the integral in the brackets of equation (6), but presumably a graphical solution could be performed if desired. It should be pointed out here that this equation is also subject to limitations arising from the manner in which it was obtained. For example, it was assumed that R was a function of time alone. It was also assumed that i_i equals i_m times an arbitrary time function, which means that the phase of the current is not affected by the signal voltage, and that is certainly not true. As a matter of fact the only conditions under which the phase of the oscillating current would remain unchanged would be those in which the signal frequency and the natural resonant frequency of the circuit are identical, and the signal voltage is exactly in phase with the oscillating current. Of course, for the purpose of a qualitative analysis it would be entirely possible to make these assumptions, but nevertheless, the use of the equation in general considerations is severely limited to the necessity of making such assumptions.

The foregoing discussion should suffice to show that a rigorous mathematical approach to the problem of superregeneration is beset with formidable, not to say insurmountable, obstacles. It is true, however, that since these differential equations mentioned above, all represent real physical systems of closely similar natures, the solutions to the equations will be similar. Physical systems, unlike mathematical expressions, very seldom exhibit singularities in behavior. That is, when the parameters of a physical system are varied uniformly, the performance or behavior of the system also varies more or less uniformly. It is, therefore, permissible to study the solution of a

solvable equation such as (2) in which the resistance is constant, in order to gain a rough idea of the general character of the solution for the more complicated cases where the resistance is a variable. David and Hassler have discussed different phases of the problem of superregeneration with the aid of the solution to equation (2). While this solution is not strictly applicable to the more complicated practical cases, it nevertheless shows that during a certain part of the quenching cycle there is a growth of oscillations, and during the remainder a damping out of oscillations, etc., in accordance with observable facts.

Hassler attempted to determine what effect the speed of change of resistance would have on the building up of oscillations, and made use of a study of the behavior of a circuit containing constant resistance which was changed suddenly. He believed that the critical period in the superregenerative process was that time when the net resistance of the circuit was just passing through zero, and he concluded that the more slowly the resistance passed through zero the larger would be the oscillations in the subsequent negative resistance period. He considered two cases, in one of which the resistance was changed suddenly from a positive value, a , to a negative value, $-a$, and in the other of which the resistance varied between the same limits, but during the transition, halted for a time, t_0 , at zero resistance. These two cases are illustrated in Figure III-1', "A" being the first mentioned case, and "B" being the second. He calculated the magnitudes of the currents which would exist in the circuit for a given impressed

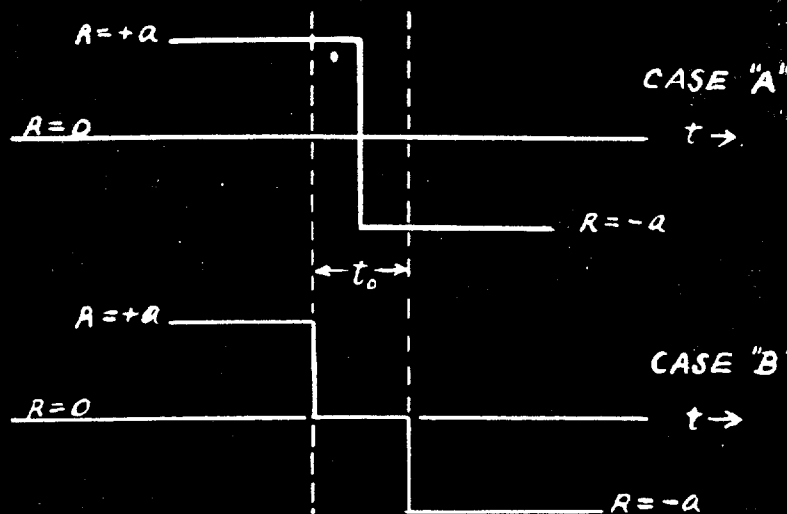


FIGURE III-1'

voltage, in terms of his ρ 's, where ρ (called Q in this country) $= \frac{X}{R}$. For the first case, he calculated that the effective ρ was equal to $(\rho_d - \rho_a)$, where the subscripts d and a refer to the positive and negative-resistance periods, respectively, and that this was a measure of the free oscillations that would exist in the circuit immediately after the change. For the second case the effective ρ was found equal to $(\rho_d - \rho_a) + \frac{\pi t_0}{T}$ and was a measure of the oscillations in the circuit at the end of t_0 just when the resistance reached the value $-a$. Since the effective ρ for the second case contained the extra term $\frac{\pi t_0}{T}$, he concluded that the second case would give larger free oscillations during the negative resistance period. This conclusion is incorrect, for the reason that he was not comparing the two cases properly. His two methods of changing the

resistance are supposed to represent in a general way two different speeds of variation during a period t_0 . His effective ρ for case B has been correctly determined, but in case A the effective ρ was considered for the instant when the resistance became equal to $-a$, and for this reason the two answers are not comparable. In order to make the first case represent a change taking place in the same length of time as the change of case B, the effective ρ should be calculated for a time $t_0/2$ later than the time when the resistance becomes equal to $-a$, in other words at the end of t_0 instead of at $t_0/2$ as previously calculated. When this is done, it is found that the effective ρ for the two cases are exactly equal provided $|R_d| = |R_a| (= a)$, and are approximately so even when this condition is not fulfilled.

B. BEATS AND MULTIPLE RESONANCE PHENOMENA

While attempts to perform a complete analysis of the superregenerative circuit have proven unsuccessful on the whole, the particular problem of beats lends itself fairly well to theoretical treatment. For many adjustments of a superregenerative receiver audible beats may be heard in the presence of an unmodulated signal, and sometimes, as will be pointed out in a succeeding chapter, even when there is no signal being fed into the receiver. For the present we will confine our attention to the more general case of beats in the presence of an unmodulated signal.

To begin with, it is necessary to make certain simplifying assumptions in order to handle the problems which arise in connection

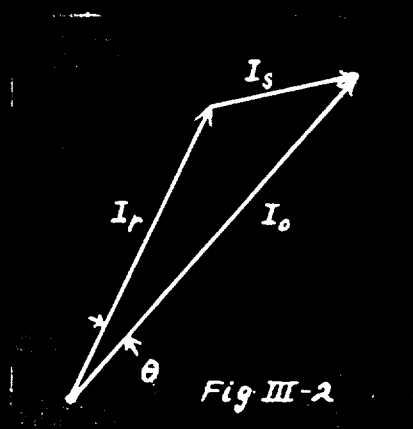
with beat phenomena. It has been fairly well established that for a given adjustment of a superregenerative amplifier, the oscillations which exist in the tuned circuit at the beginning of the negative resistance period determine the course of the ensuing oscillations. During the other parts of the quenching cycle the forced oscillations caused by the signal voltage are so small compared to the free oscillations in the circuit that they may be neglected. A given amount of oscillating current in the tuned circuit at the beginning of the negative resistance period always produces the same size and shape of wave train, and causes the same amount of residual oscillations to be left over at the beginning of the next negative resistance period. However, it is apparent that if only the magnitude of the initial oscillations is to be effective in determining the ensuing wave train so that the phase of the oscillations may be neglected, the critical period during which the net resistance of the circuit passes through zero into the negative region, must be of sufficient duration to contain several high frequency cycles. For if the resistance should pass from positive to negative with great rapidity, the instantaneous current in the circuit at the moment of transition would have to be known in order to calculate the resulting free oscillations. Since we have no way of knowing what is the exact phase relation of the high frequency oscillations to the quenching cycle, it is necessary to make the assumption in the following work that the interval during which the resistance is small is longer than two or three high-frequency periods. While this condition often exists in a superregenerative circuit, we have obtained some oscillograms which show such an extremely rapid growth of oscilla-

tions that we are led to conclude that such an assumption would not hold in the conditions for which these oscillograms were taken.

Hassler explained the formation of beats in the presence of an unmodulated signal as follows. He said that the superregenerative receiver must be in a state where it is generating continuous highly modulated oscillations. If the frequency of these oscillations differs from that of the signal, the current produced by the signal will beat with the natural oscillations of the tuned circuit in such a way that from one quenching cycle to the next, the effective initial current will vary, and this will cause the ensuing wave trains to grow to different heights. Although the beating between the free oscillations and the signal may be at an inaudible frequency, it is still possible to hear an audible output from the receiver if the beat frequency bears the proper relationship to the quenching frequency.

We feel that Hassler's explanation is definitely inadequate because he overlooked one important thing. It is true that the receiver must be generating continuous highly modulated oscillations under such conditions that the residual oscillations at the end of a positive resistance period are of a magnitude comparable to that of the signal current. But Hassler forgets that when the signal current is added to the residual oscillations of one quenching period to form the initial current of the next, this resulting initial current will not necessarily be in phase with the oscillations of the previous period (extending the latter forward in time). And so while the set may be generating continuous oscillations, these oscillations may nevertheless suffer a certain phase shift at the beginning of each

negative resistance period. This immediately raises the question as to whether it might not be possible to have this phase shift just compensate for the net change in phase which occurs between the signal and the free oscillations during the course of a quenching cycle, in such a way that an equilibrium condition is established whereby the wave trains of succeeding quenching periods will be the same. The condition described is illustrated by the following vector diagram in which only the relative phase of the vectors is of importance.



In the above, I_s represents the component of the oscillations which is forced by the signal, I_o represents the initial current in the circuit which determines the size of the wave train, and I_r is the residual current left over at the end of the positive resistance period. The angle θ , between I_r and I_o is the change in phase (considered less than 180°) between the free oscillations and the signal which occurs during one complete quenching period. If the diagram is a closed triangle as shown, so that the addition of the signal current to the residual current of one period is just sufficient to produce a new initial current which has the same magnitude and phase relation to

I_s as the initial current of the previous period, then I_0 will be the same for succeeding periods and equilibrium will be established. If such an equilibrium condition is possible, then it would appear that beats can not occur between the signal and the free oscillations for certain adjustments of the receiver, even when sizable residual currents are being produced.

We have found it possible to determine in a theoretical way whether equilibrium positions of the vectors exist for any particular adjustment of the receiver, but it has not always been possible to demonstrate clearly just when such equilibrium positions are stable and when they are unstable. In the case where the receiver is operating linearly, however, a complete analysis has been possible and this will now be presented.

Linear Operation of Receiver:

During linear operation, the maximum height of any wave train will be directly proportional to I_0 , and this in turn means that the magnitude of I_r will also be directly proportional to I_0 . Hence, the ratio of the magnitudes of the residual current to the initial current is constant and will be represented by k .

The signal frequency is ω .

The frequency of free oscillations is ω_0 .

The period of one complete quenching cycle is T .

I represents a vector quantity.

$$I\theta = e^{j\theta}$$

$$\alpha = \omega T. \quad \beta = \omega_0 T. \quad \theta = |2\pi n - (\beta - \alpha)| < \pi.$$

First digit in the subscript indicates the number of the wave train (starting from one).

The second digit in the subscript indicates o -- initial
 r -- residual.

Starting now with nothing but the signal current in the circuit,

$$I_{1o} = I_s; \quad I_{1r} = k I_s \underline{1\beta}$$

$$\begin{cases} I_{2o} = I_{1r} + I_s \underline{1\alpha} = I_s (k \underline{1\beta} + \underline{1\alpha}) \\ I_{2r} = k I_{2o} \underline{1\beta} = I_s (k^2 \underline{2\beta} + k \underline{1\alpha + \beta}) \end{cases}$$

..... etc.

$$I_{nr} = I_s \left[k^n \underline{n\beta} + k^{(n-1)} \underline{(n-1)\beta + \alpha} + k^{(n-2)} \underline{(n-2)\beta + 2\alpha} + \dots + k^2 \underline{2\beta + (n-2)\alpha} + k \underline{\beta + (n-1)\alpha} \right]$$

$$I_{nr} = I_s \left[k \underline{1(\beta - \alpha) + n\alpha} + k^2 \underline{2(\beta - \alpha) + n\alpha} + k^3 \underline{3(\beta - \alpha) + n\alpha} + \dots + k^n \underline{n\beta} \right]$$

$$I_{nr} = I_s \underline{n\alpha} \left[k \underline{1\beta - \alpha} + k^2 \underline{2(\beta - \alpha)} + k^3 \underline{3(\beta - \alpha)} + \dots + k^n \underline{n(\beta - \alpha)} \right]$$

$$= I_s \underline{n\alpha} k \underline{1\beta - \alpha} \left[1 + ke^{j\theta} + (ke^{j\theta})^2 + (ke^{j\theta})^3 + \dots + (ke^{j\theta})^n \right] \quad (7)$$

where $\theta = \beta - \alpha$.

Now let n approach infinity. The portion in brackets then equals $\frac{1}{1 - ke^{j\theta}}$ as long as k is less than 1. Since, as before stated, only the magnitude of I_{nr} is of interest, the factors $\underline{n\alpha}$ and $\underline{1\beta - \alpha}$ have no meaning and may be dropped. Therefore,

$$|I_{\infty r}| = \frac{k I_s}{\sqrt{k^2 - 2k \cos \theta + 1}} \quad (8)$$

This work shows that if the receiver is started off with only the induced signal current in the tuned circuit, the wave trains will build up in the course of time to a limiting value. The magnitude of the residual oscillations for this limiting value is given by the expression (8), and the vector relationship is accurately represented by the diagram of Figure III-2. That this equilibrium condition is a stable one may be seen from examining expression (7). This shows that within a finite length of time after starting, the magnitude of I_r is oscillating about its final value. In other words the vector diagram does not move smoothly into the equilibrium position, but hops about it in a series of damped undulations. It requires no further proof to show that such a position must be stable.

It is also possible to see by going back to equation (7) that if k should be greater than one, the series will be divergent, and no equilibrium is possible. Of course this particular expression merely shows that no equilibrium can be reached when the receiver is started out with only I_s in the circuit. The very fact that it is possible to draw a closed vector diagram with I_r larger than I_o is sufficient proof that such an equilibrium position is possible. But it may be shown that it is unstable, and that with an infinitesimal displacement of any of the vectors from their equilibrium positions, the condition would break down. Thus, when operating in this condition,

$$k I_o \angle \theta + I_s = I_o \quad \therefore I_s = I_o (1 - k \angle \theta)$$

Suppose that at one instant only there is a change, Δ , in I_o .

Starting the sequence, we have,

$$\begin{aligned} I_{10} &= I_0 + \vec{\Delta} , & I_{1r} &= kL\theta (I_0 + \vec{\Delta}), \\ I_{20} &= I_0 + \vec{\Delta} kL\theta , & I_{2r} &= kL\theta (I_0 + \vec{\Delta} kL\theta), \\ \dots\dots\dots , & & I_{nr} &= I_0 kL\theta + \vec{\Delta} (kL\theta)^n, \end{aligned}$$

and since for equilibrium $I_r = I_0 kL\theta$, it is apparent that the error caused by $\vec{\Delta}$ becomes vanishingly small with the passing of time for $k < 1$, and extremely large for $k > 1$.

The general conclusions that may be made from this analysis are that, as long as the assumptions upon which the analysis was based are permissible, no beats can be maintained while the receiver is operating linearly with k less than one. In the case where k is greater than one, the receiver will build up until it is operating in a saturated condition, and hence this case cannot be considered under the assumption of linear operation.

It might be mentioned here that David claimed that if there were residual oscillations of the same order of magnitude as the signal, and the same frequency as the signal, so that the two always added, then the receiver would build up to saturation. This is not necessarily true at all. If θ is zero so that the residual oscillations and the signal current directly add, the residual oscillations may actually be larger than the signal current and still the receiver will not become saturated as long as $k < 1$.

It will be found upon examination that equation (8) not only serves to tell the magnitude of I_r for equilibrium, but that it

also explains the phenomenon of multiple resonance peaks. Changing θ will cause the magnitude of I_r to vary between the limits of $\frac{k I_s}{k-1}$ and $\frac{k I_s}{k+1}$. Consequently, as a receiver is detuned, the I_r , and hence the I_o , will pass through a series of maxima and minima, and this means that ^{the} amplitude of the wave trains will also pass through a series of maxima and minima. Of course, as the receiver is detuned by a considerable amount, the forced oscillations caused by the signal will decrease, and this will cause the vector diagrams to shrink in size so that the observable peaks become smaller and smaller. Hassler shows some very good pictures of this phenomenon in his article on superregeneration.

100% Saturation of Receiver:

When the receiver is operating at complete saturation so that an increase in I_o has no effect on I_r , analysis of vector equilibriums is very simply made with the vector diagrams alone. It is assumed that under this condition $|I_r|$ is equal to a constant. Therefore, if we let the vector representing I_s be the reference to which the phases of the other vectors are referred, we may construct a diagram as in Figure III-3. In this diagram I_s is always considered to point horizontally to the right. The tip of the vector, I_r , must lie on the circle drawn with the radius equal to $|I_r| = \text{constant}$, and naturally it may have any orientation with respect to I_s . The addition of I_s to I_r at any point gives the I_o which would result. The angle between I_r and I_o which is produced by this addition is called ρ .

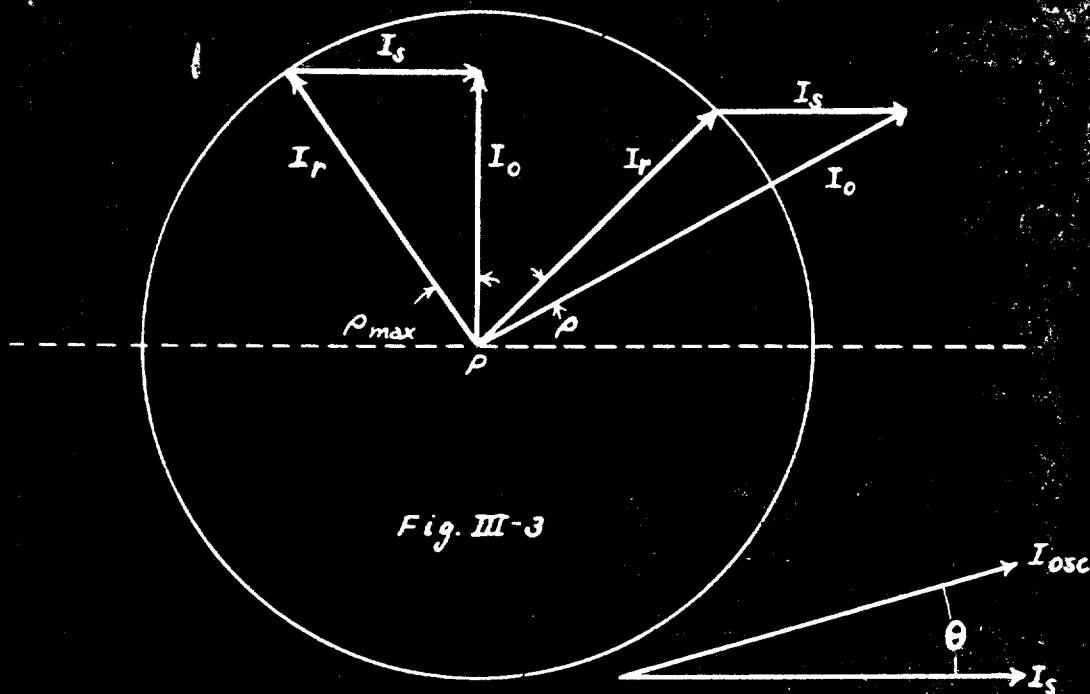


Fig. III-3

The greatest value of ρ will be obtained when I_r is in such a position that after I_s is added, the I_o will be perpendicular to I_s . This is illustrated by the vector triangle on the left. For any other positions of I_r in the upper half of the circle, ρ will be smaller, and it will vanish when I_r is at either 0° or 90° . Therefore, if the change in phase θ between the signal and the free oscillations during one quenching cycle is smaller than the maximum ρ , there will be some position of the vectors as shown by the right-hand triangle, for which a condition of equilibrium will exist. In this position ρ must equal θ , and I_r must lie between 0° and the angle necessary for maximum ρ . When the vectors are in this position, I_r will swing θ degrees to the left of I_o during the quenching cycle. At the end of that time, the addition of I_s will form a new I_o which is exactly the same as the previous one. In other words there

is an equilibrium between two forces, one being the tendency of the phase shift angle, θ , to swing the triangle around the circle to the left, and the other being the restoring influence of ρ which tends to swing the triangle around to the right when it is in the upper half of the circle. That the equilibrium position shown is stable may be seen by the following considerations. If I_r should for some reason swing a little to the left of its equilibrium position, the restoring angle ρ would be increased, and since θ is always a constant, the effect would be to swing the triangle back to its original position. If I_r moves to the right, the restoring angle will be decreased, and the triangle will move back to the left. As the vectors near their equilibrium positions the difference between ρ and θ becomes smaller, and restoration takes place more slowly, so that they approach equilibrium asymptotically. There is a second position of I lying to the left of the position for maximum ρ , where ρ may equal θ and equilibrium result. This equilibrium position is unstable, however, as may be easily seen by observing the effects of a small displacement in the same manner as was done above.

If θ is larger than the largest value of ρ which it is possible to obtain, there can be no equilibrium, and the vector triangle will swing around the circle in a counter-clockwise direction. When the triangle is on the lower side of the circle, it is evident that the addition of I_s to I_r aids rather than opposes the shift caused by θ , and hence on this side of the circle the vectors will be swinging most rapidly. They will be swinging most slowly at the ρ_{max} position.

The swinging of the vectors around the circle can cause audible beats in spite of the fact that the receiver is saturated. This is because the magnitude of I_0 will vary depending on whether I_s adds to or subtracts from I_r , and although the oscillations during the negative resistance period always reach the same value, they will rise to this limit sooner when I_0 is larger. Therefore, the swinging of the vectors will cause the shape of the envelope of oscillations to vary, and audible beats may be heard. It would be expected in view of what was brought out in the previous paragraph, that when beats are obtained for a saturated condition of the receiver, an oscillograph picture of the oscillations would show that the areas of the envelopes of successive wave trains do not increase and decrease in a uniform way, but that they tend to remain at large values longer than at small ones, and that the increase from small to large areas takes place more rapidly than the decrease from large to small.

General Case of Vector Equilibrium:

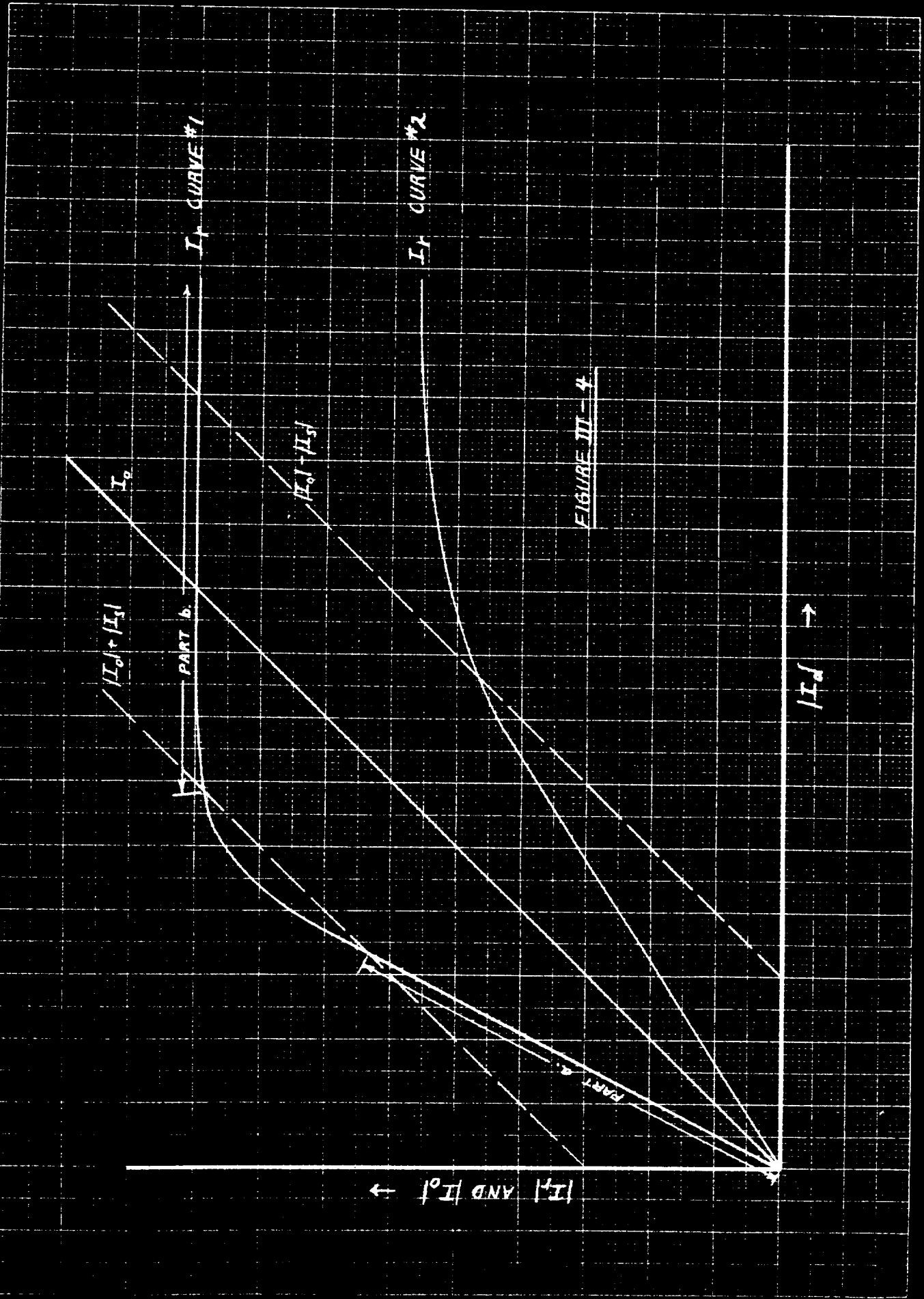
When we come to the general case where the receiver is neither strictly linear nor 100% saturated, the situation becomes decidedly more complicated. We can, at least theoretically, discover whether a vector equilibrium is possible or not, but we have not yet found a fool-proof way of determining whether an equilibrium position is stable or unstable.

Before we can discuss the general case, it is necessary to have some sort of response characteristic for the receiver. A curve

of I_r against I_o for any particular adjustment of the receiver is required. In Figure III-4 two curves of I_r against I_o representing two different adjustments of a superregenerative receiver have been arbitrarily assumed for the purposes of discussion. A line at forty-five degrees has been drawn in so that it is possible to measure the magnitude of I_o in the same direction as I_r . From this it will be seen that the ratio (k) of $|I_r|$ to $|I_o|$ for the linear portion of curve #1 is greater than one, while the k for the corresponding part of curve #2 is less than one. Curve #1 has purposely been drawn so that it will contain a region of strict linearity, another region of 100% saturation, and a third region intermediate to these two.

In Figure III-5 a diagram has been constructed which makes it possible to determine when and where there will be equilibrium positions of the vectors I_s , I_r , and I_o . Except for the greater complication, this diagram is similar to Figure III-3. One important difference is that it has been found more convenient to hold the vector I_s fixed and allow P , the intersection of I_r and I_o , to do the moving. Otherwise the three vectors will be found to have essentially the same space relation.

What has been done is simply this. The curves of Figure III-4 have been replotted in Figure III-5 making use of a bipolar coordinate system. That is, in replotting curve #1, the magnitude of I_o for any particular point on the curve was used as a radius, and an arc was swung using the end of I_s labeled B as a center. The value



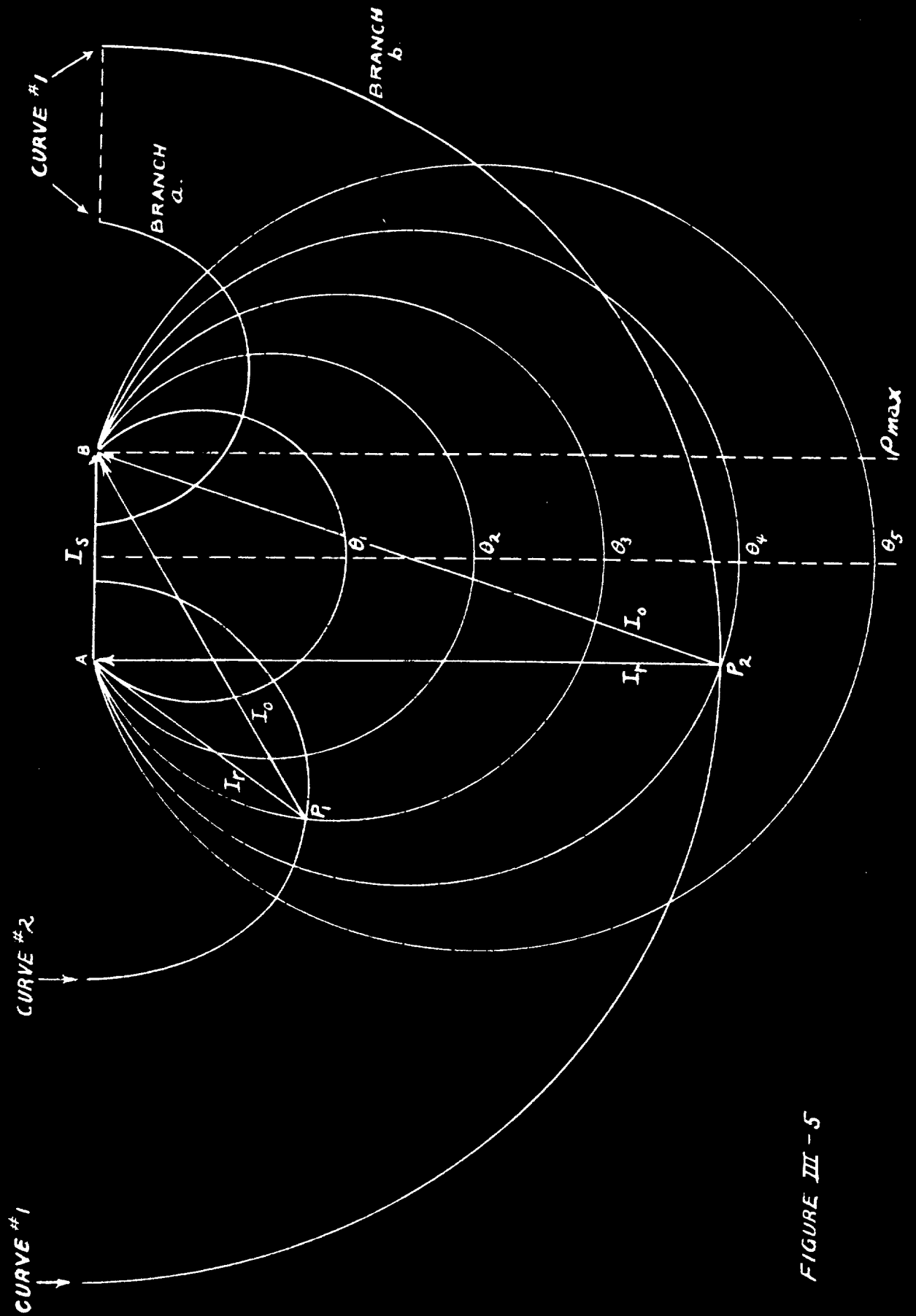


FIGURE III - 5

of I_r for the same point determined the radius of a second arc which had A (the other end of I_s) as a center. Where these two arcs intersected, a point on the replotted curve #1 was established. Hence for any point, P, on one of the replotted curves, the distances PA and PB are the I_r and I_o values respectively of a corresponding point on the corresponding curve of Figure III-4. Wherever the curves in Figure III-4 pass outside of the region contained between the two dashed lines at 45° , the corresponding replotted curve strikes the I_s axis and becomes imaginary. This accounts for the fact that curve #1 consists of two separate branches, a and b, in Figure III-5.

Secondly a series of circles labeled $\theta_1, \theta_2, \theta_3, \theta_4$, and θ_5 were constructed on I_s as a chord. For all points on any one of these circles the chord AB subtends the same angle. The angle subtended decreases for the different circles running outward in the order θ_1 to θ_5 .

Now the process of searching for a possible equilibrium position is as follows. Suppose the receiver is so adjusted that the curve #1 of Figure III-4 represents the relation of residual to initial oscillations. The strength of the signal is known and the vector I_s is drawn. Using the ends of this vector as the poles of the new coordinate system, curve #1 is replotted in the manner described above. The phase change θ (see definition on page 38) is also known, and a circle is constructed on I_s as a chord such that for all points on the circumference of the circle the angle subtended by I_s is

equal to θ . If this circle intersects the curve #1 at any point, that point determines an equilibrium position of the vector triangle. Thus if θ were equal to θ_4 , it will be seen that the point labeled P_2 is an intersection of I_o and I_r for an equilibrium triangle. For this triangle I_r bears the proper relationship to I_o , and the restoring angle ρ is equal to the phase shift angle θ . It will also be seen that there are two other intersections of curve #1 and circle θ_4 . The point P_2 is a position of stable equilibrium as was proven in the section dealing with 100% saturation (the curve is nearly 100% saturated in this region). The other possible point on the same branch of curve #1 is known to be a position of unstable equilibrium (also from section on 100% saturation). The third point, which is on branch a of curve #1, is also an unstable equilibrium since for this region we have linear operation with $k > 1$. This conclusion may be reached somewhat approximately in another way. Suppose that equilibrium had been temporarily established at this point. Then suppose this point became displaced so that it moved toward the right along curve #1. Since this means that it has moved outward across some of the constant angle curves, the restoring angle will have decreased, thus allowing the triangle to swing around still farther in a counter-clockwise direction.

If the value of the phase shift angle should correspond to θ_3 instead of θ_4 , there are no positions of stable equilibrium possible, and beats must occur. The intersections of curve #2 with various θ curves all represent positions of stable equilibrium for

those particular values of θ . This is because this section of curve #2 represents linear operation with $k < 1$. This may also be seen from an examination of the effect of a small displacement from equilibrium.

To the best of our knowledge it is possible to say that any points on branch *a* of a curve of the type #1 are positions of unstable equilibrium. Also, any points of equilibrium which lie to the right of the dashed line labeled ρ_{max} are unstable. All other equilibrium points appear to be stable. This graphical analysis constitutes a method by which it is possible to determine whether beats are permissible under any given set of conditions, and as such it is of considerable theoretical interest, although probably of no practical importance whatever.

It is nevertheless true, that for the general case as well as for the 100% saturated condition, such beats as occur should be characterized by the slow decrease and rapid increase that was mentioned under the section on 100% saturation. In the general case, the phenomenon of multiple resonance peaks will be noticed, since changing the angle θ has the effect of changing the equilibrium triangle and hence the I_0 . The previous analysis suggests, however, that at least for a highly saturated condition of the receiver the phenomenon of multiple resonance peaks should be complicated by a beat phenomenon. Referring to Figure III-5 curve #1, it is seen that as the θ is increased, the point of equilibrium, P_2 , will move toward the position of maximum ρ , and during this time I_0 is decreasing (the receiver is being detuned). But after the position of ρ_{max} has been passed beats will occur

until θ comes to a new value which will once again permit a stable equilibrium.

The effect of noise voltage or a modulated signal upon these equilibrium triangles would be to displace them from their equilibrium positions, and in the case of a modulated signal there is some question as to whether it is possible to speak of equilibrium any more. There will, however, be certain positions which the vectors will try to take even under adverse circumstances. In all cases except the completely saturated condition, the vectors tend to oscillate about their equilibrium positions. It is possible therefore that if some noise voltage should displace the vector triangle an appreciable amount, immediately thereafter a series of decaying beats might be noticed. This may be a partial explanation for a fact which was noticed during our experimental work. It was observed that at times the envelopes of the high frequency wave trains seemed to be in a state of fluctuation which resembled the disturbance caused by noise voltage except for the fact that mixed in with the random effects there seemed to be a certain periodicity in the variation.

In summary it may be stated that the foregoing analysis has shown -

1. That regardless of the adjustment of the receiver, for certain values of I_s and θ it is possible to have an equilibrium relation between I_o , I_r , and I_s such that beats are rendered impossible except during the time in which the equilibrium condition is being established.

2. That for those values of I_0 and θ which render an equilibrium relationship impossible, beats must result.
3. That when beats result, they will in general be of such a nature that the growth in size of the envelopes of oscillations from one quenching cycle to the next will take place more rapidly than the decrease in size. In other words, a sort of "sawtooth" variation will take place.
4. That when an equilibrium between the initial, residual, and signal voltages is permitted, the fact that I_0 depends upon θ means that as the tuning of a receiver is changed continuously over a wide range of values, there will be a number of tunings giving the same value of θ and the same output from the receiver, and hence there will be "multiple resonance peaks".
5. That in a highly saturated condition of operation of a super-regenerative receiver there will be regions between the resonance peaks where beats will take place.
6. That for linear operation of the receiver where the ratio of residual oscillations to initial oscillations is less than one it is impossible to have beats. That it is impossible to maintain linear operation when the ratio is greater than one.

CHAPTER IV

EXPERIMENTAL APPARATUS

CHAPTER IV

EXPERIMENTAL APPARATUS

Ultra-high-frequency receiver:

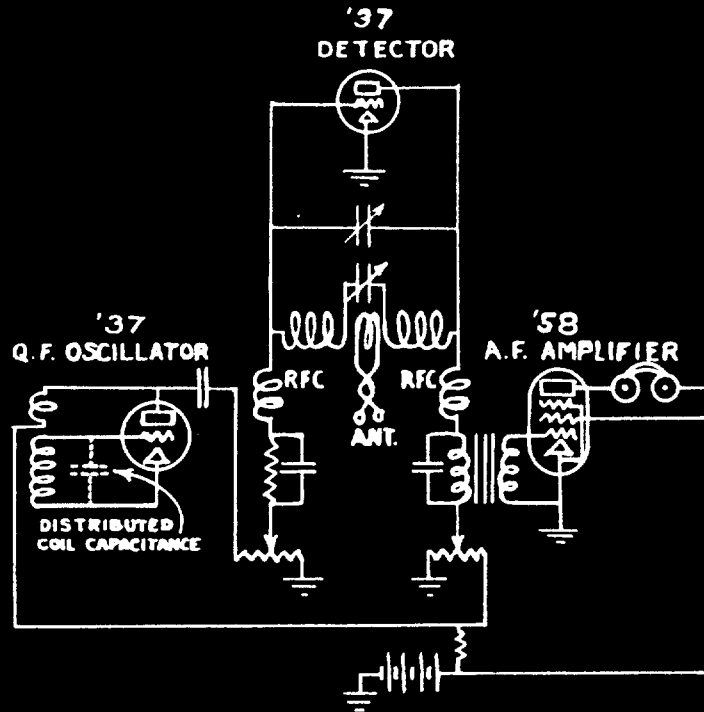
The experimental portion of this investigation was performed with the aid of two different superregenerative receivers. The first of these, designed for operation at about 30 megacycles and based upon a circuit suggested by Mr. G. W. Pickard, was originally constructed as an experimental field-strength measuring set.

Fig. IV-1 (a) shows the circuit employed in this receiver, as initially constructed. It was fundamentally a modified Colpitts circuit, in which the inter-electrode capacitance of the detector tube combined with the two condensers shown in the oscillatory circuit to perform the same function as do the two tuning condensers in the ordinary Colpitts oscillator. Grid leak detection was used. Fig. IV-2

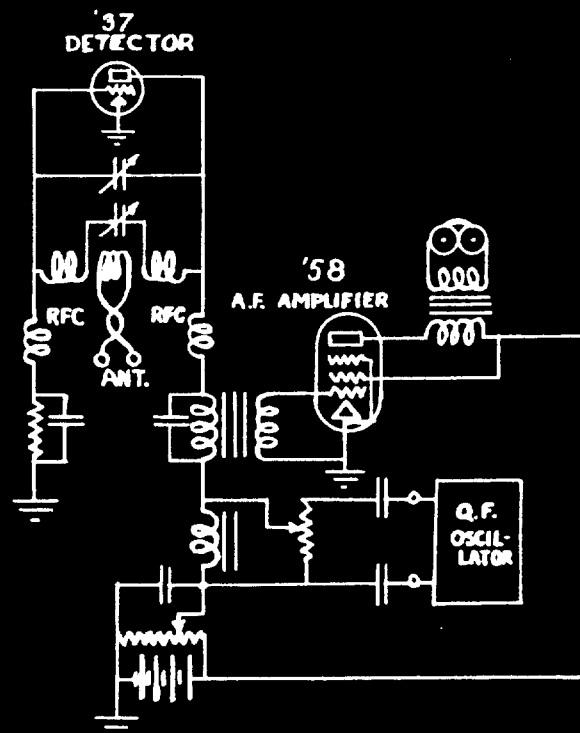


Fig. IV-2. Rear view of 30-megacycle receiver.

30-MEGACYCLE RECEIVER



(a.) QUENCHING VOLTAGE APPLIED TO GRID.



(b.) QUENCHING VOLTAGE APPLIED TO PLATE.

FIG. IV-1

is a rear view of the receiver. It may be observed from the illustrations that three controls were provided with which to adjust the receiver. These were the variable tuning condenser, a potentiometer controlling the d.c. plate voltage, and a potentiometer controlling the quenching voltage applied to the grid of the detector. The quenching frequency was about 10,000 cycles per sec.

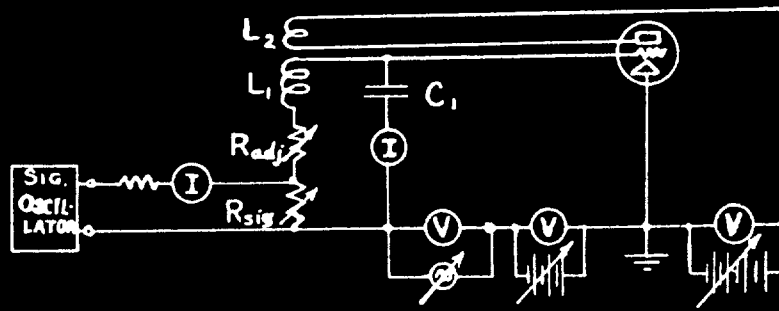
Fig. IV-1 (b) shows a subsequent modification of the circuit, in which the quenching voltage was transferred to the plate side of the tube, and was supplied by an external oscillator. The latter change was made in order to permit varying the quenching frequency and to secure a greater range of quenching voltages.

As was pointed out in the foreword, the receiver just described was soon found to be unsuitable for a quantitative investigation of superregeneration. Measurements of current, voltage and circuit parameters could not have been carried out with any approach to accuracy, both because of the usual difficulties of making accurate radio-frequency measurements and because the stray capacitances and inductances introduced by the measuring instruments would have utterly changed conditions in the receiver.

Low-Frequency Receiver:

A second receiver was therefore designed for laboratory use, the objective this time being quantitative measurement of the important currents, voltages and circuit constants, rather than practical reception of radio signals. The first step in the design was the

(a.) BASIC CIRCUIT



(b.) ACTUAL CIRCUIT

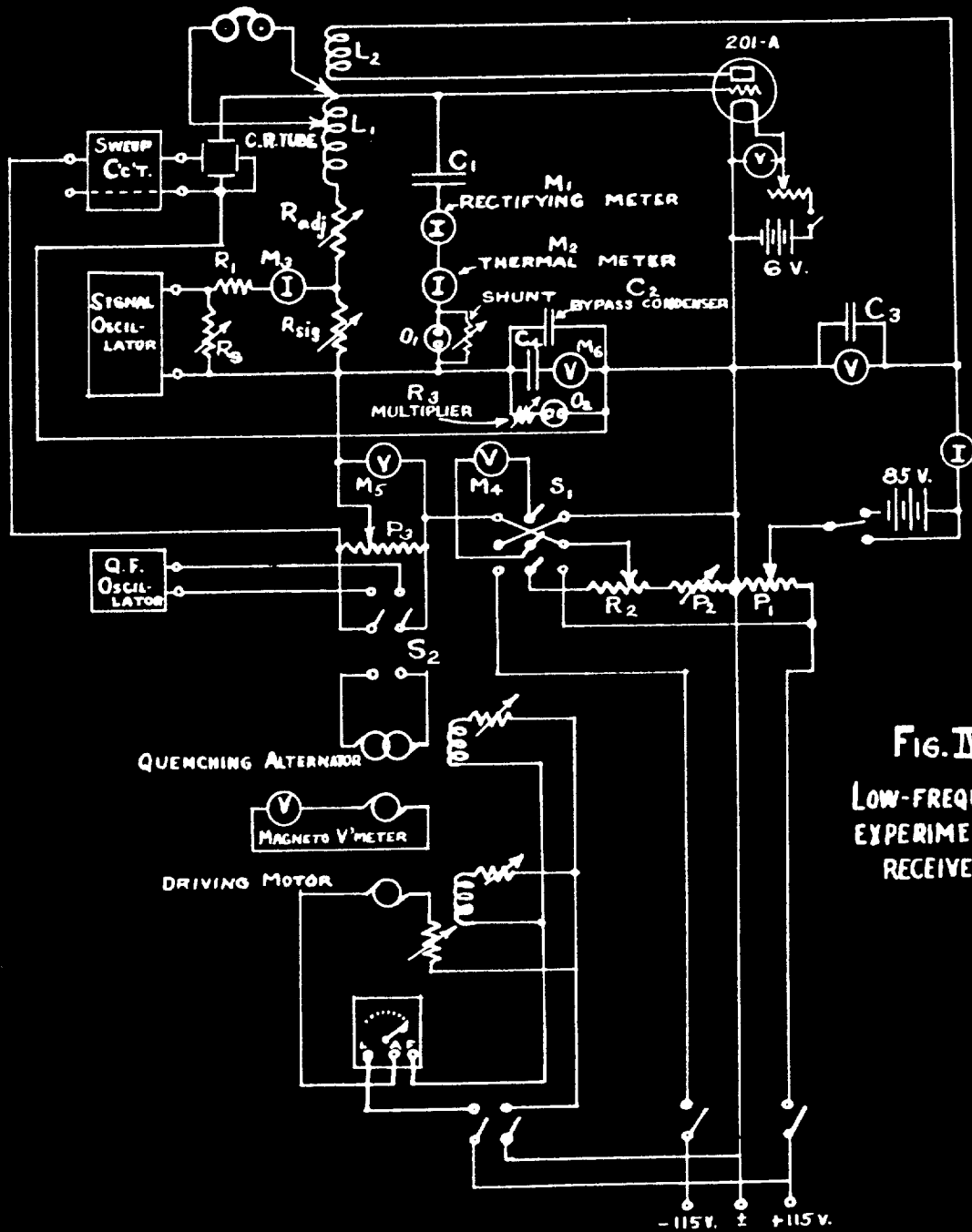


FIG. IV-3.
LOW-FREQUENCY
EXPERIMENTAL
RECEIVER.

choice of much lower frequencies, both for the signal and for the quenching voltage, than were used in the 30-mc. receiver described above. The choice of frequencies was governed somewhat by practical considerations, since it was desired to make the signal frequency about 1000 cycles per second in order to permit the use of a vibration oscillograph, and 5 to 10 cycles per second was the lowest frequency which was practicable for the quenching voltage. Consequently the frequencies employed here were not, strictly speaking, "scaled down" from those used in the previous receiver (which, it will be recalled, were 30,000,000 c.p.s. and 10,000 c.p.s., respectively). They did, however, bear approximately the same ratio to each other as would be used in a practical superregenerative receiver designed for broadcast reception.

The basic circuit of the low-frequency receiver was as shown in Fig. IV-3 (a). This is readily recognizable as a conventional regenerative receiver, with the addition of a source of a.c. quenching voltage in series with the grid bias supply. In order to simplify the measurement of the input signal voltage, the antenna and antenna coil of the ordinary receiver were omitted and the signal oscillator was coupled directly to the tuned circuit, as shown in the diagram. A circuit employing no grid-leak, such as would be used for anode detection, was adopted in order to eliminate one of the variables (the value of the grid-leak) affecting the operation of the receiver.

The details of the circuit of the low-frequency receiver as it was actually constructed may be seen in the diagram, Fig. IV-3 (b).

The tuned circuit was connected as shown in the fundamental circuit diagram, except that an additional milliammeter and an oscillograph element (O_1) for photographic recording of the oscillatory current were inserted. Of the two milliammeters, one (M_2) was a slow-response thermal-type and the other (M_1) a rectifier-type instrument. The reason for including both types will appear in the next chapter. Air core coils were used for L_1 and L_2 , in order to remove any possibility of harmonics being introduced through saturation of an iron core. L_1 had an inductance of 140 mh. and a resistance of about 10 ohms, measured at 1000 c.p.s. The fixed condenser C_1 , combined with the winding capacitance of the coil L_1 , resonated with the inductance of L_1 at a frequency of approximately 1040 c.p.s. The variable resistance R_{adj} was of the decade type and had a range of 0-1111 ohms in 0.1 ohm steps.

It was desired to have a range of measurable input signal voltages extending from about 10 microvolts to 10 or 20 millivolts, inasmuch as readable signals from moderately distant stations usually fall in this range. Accordingly a thermal milliammeter (M_3) having a full-scale deflection of 2.0 ma. and a minimum readable deflection of about 0.1 ma. was used in conjunction with the decade-type resistance R_{sig} , having a range of 0-11 ohms in 0.1 steps, as shown in Fig. IV-3 (b). In order to vary the current through R_{sig} from 0.1 to 2.0 ma., a variable short-circuiting resistance R_s was shunted across the output of the signal oscillator. A resistance of approximately 3000 ohms, shown as R_1 , was placed in series with milliammeter M_3

to limit the current through R_{sig} to about 2.0 ma. when R_s was at its maximum of 11,110 ohms. Later a different signal oscillator having a lower maximum output voltage was used, and R_1 was omitted, the 750 ohms resistance of milliammeter M_3 then being sufficient to limit the current to less than 2.0 ma. Even with R_1 omitted, R_{sig} at its maximum value of 11 ohms, and R_s set at 0, the parallel resistance of R_{sig} and M_3 could differ from the resistance of R_{sig} alone by only about 1.5%, or 0.16 ohms — an amount too small to affect appreciably the operation of the receiver.

The d.c. plate voltage and grid bias were obtained from slide-wire potentiometers, supplied by the laboratory's 230 volt d.c. line. An auxiliary 85 volt battery was arranged so that it could be switched in series with the plate potentiometer P_1 when a plate voltage of more than 115 volts was desired. A rheostat R_2 having a low resistance in comparison with that of the grid potentiometer P_2 was placed in series with the latter, as shown in Fig. IV-3 (b), in order to permit fine adjustment of the grid bias voltage. A reversing switch S_1 made it possible to obtain either positive or negative grid bias, and reversed the connections to the bias voltmeter M_4 in order to keep its deflection positive at all times.

Two alternative sources of quenching voltage were available. One of these was a laboratory vacuum-tube oscillator of the "tea-wagon" type, having a minimum frequency of about 10 c.p.s. and a maximum voltage at this frequency of somewhat less than 10 volts, when connected to slide-wire potentiometer P_3 . The other source was a motor-alternator set (No. 67, from Dynamo Laboratory), operated on 115 volts

d.c. instead of its rated 230 volts, and connected with an adjustable resistance, in the form of stoves, in series with the armature. A magneto voltmeter attached to the shaft of the motor-alternator set indicated the quenching frequency. A range of frequency of approximately 6 to 50 c.p.s. could be obtained. The maximum voltage output, of course, varied directly with the speed of the machine. At 10 c.p.s. approximately 30 volts could be supplied to the potentiometer. Fig. IV-4 shows a general view of the motor-alternator set and its associated equipment. In order to facilitate shifting from the alternator to the vacuum-tube oscillator for quenching voltage, the selecting switch S_2 was included in the circuit.

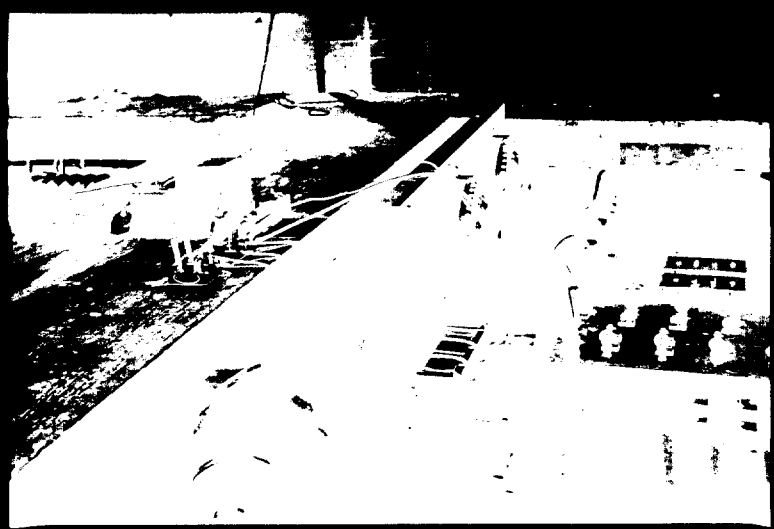


Fig. IV-4. General view of alternator supplying quenching voltage.

In order to reduce noise voltage in the oscillatory circuit to a minimum, bypass condensers C_2 and C_3 , each of about 20 microfarads capacitance, were connected across the plate supply and the entire

grid-bias supply, including the quenching-voltage potentiometer, as shown in Fig. IV-3 (b). Since a condenser of this size has a reactance of only about 250 ohms at 25 cycles, the quenching frequency which was most often used, and since the resistance of the grid-bias potentiometer P_2 was of the order of 700 ohms, a considerable portion of the quenching voltage indicated by the a.c. voltmeter M_5 was lost in P_2 and did not appear between grid and filament at all. Consequently a high-resistance voltmeter M_3 , in series with an 8 microfarad blocking condenser C_4 , was connected in parallel with the 20 microfarad bypass condenser C_2 as shown in Fig. IV-3 (b). The voltage across this instrument was, within a fraction of a per cent, identical with the true quenching voltage supplied to the grid of the tube. An oscillograph element O_2 , in series with the multiplier R_3 , was also connected across this bypass condenser, in order to permit recording the quenching voltage on the same sensitized paper as the oscillating current.

Two types of oscillographs were used in the experimental work. For continuous visual observation, and for photographing envelopes of oscillations when they repeated themselves from one quenching cycle to the next, a General Radio cathode-ray oscillograph was employed. Since such an oscillograph could not simultaneously record two or more currents or voltages, it was necessary to superpose the quenching voltage upon the oscillatory voltage appearing across the coil L_1 in order to show them both in the same picture. The circuit connection by which this was accomplished is shown in Fig. IV-3 (b).

In order to make the pattern remain stationary, the full voltage appearing across the 20-microfarad grid bypass condenser was applied to the input of the sweep circuit as a control voltage. Photographs of the cathode-ray images were taken on film with a Voigtlander Avus camera.

In order to photograph oscillations whose envelopes changed in shape or amplitude from one quenching cycle to the next, a Westinghouse vibration oscillograph was used. One element, as has already been remarked, was connected in series with the tuned circuit, in order to record the oscillatory current. A second element recorded the quenching voltage. An arc lamp was used as a light source, and the records were made on bromide paper.

A general view of the entire apparatus, with the exception of the quenching-voltage supply, is shown in Fig. IV-5. The large

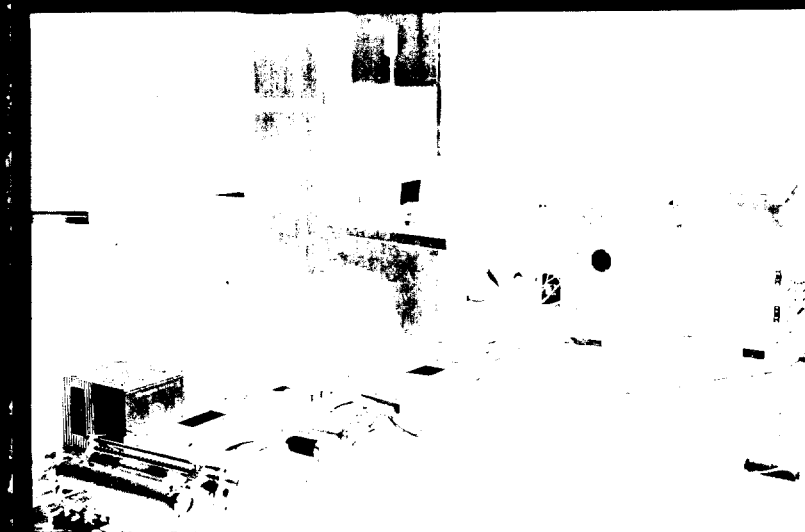


Fig. IV-5. General view of experimental receiver.

metal box in the center of the picture contains the coils L_1 and L_2 and the tuning condenser C_1 . The decade box bearing the number CRC70 is the variable resistance R_{adj} in the tuned circuit. Next to this resistance is a smaller metal box which contains the vacuum tube.

On the table at the end of the bench are the signal oscillator (which may be identified by its tuning dial, half white and half gray), the cathode-ray oscillograph and its sweep circuit. At the rear of the bench may be seen the wooden cases of the two 20-microfarad bypass condensers, and at the near end of the bench are the four slide-wires used in adjusting plate voltage, grid bias and quenching voltage. At the extreme left, in the foreground, is the selecting switch S_2 which connects the quenching-voltage potentiometer to either the vacuum-tube oscillator (not shown) or the motor-alternator set (see Fig. IV-4). Also at the extreme left is located the 85-volt auxiliary plate battery. The table at the extreme right supports the vibration oscillograph, one end of which may be seen in the picture.

The foregoing descriptions cover the essential features of the apparatus. In the next chapter the experiments which were made with this apparatus will be described, their results presented, and the significance of these results discussed.

CHAPTER V

EXPERIMENTAL INVESTIGATION

CHAPTER V
EXPERIMENTAL INVESTIGATION

Introduction:

With the apparatus described in the preceding pages a number of experimental observations and measurements were taken. The present chapter will describe and explain the experimental procedure followed; will present the results of the measurements and observations; and will attempt to pick out the significant experimental conclusions and show their relation to each other, to the theoretical deductions of Chapter III, and to the conclusion of previous writers as summarized in Chapter II.

The investigation may be divided into four parts, having to do with the following topics:

1. The vacuum tube as a source of negative resistance.
2. The superregenerative process; in particular, a study of the course of oscillations during the quenching cycle, from the standpoint of the negative-resistance characteristics of the vacuum tube.
3. Operating curves of the superregenerative receiver.
4. Multiple resonance phenomena.

These subjects will be treated in the above order.

Inasmuch as the experimental program was not originally mapped out in its entirety, but, rather, began with certain funda-

mental measurements and then developed along lines suggested by the outcome of these initial experiments, it will be advantageous to present all three of the above classifications of information -- experimental procedure, results and conclusions -- relating to each phase of the investigation before proceeding to the next phase. Accordingly, the present chapter will follow this procedure.

A. THE VACUUM TUBE AS A SOURCE OF NEGATIVE RESISTANCE

Importance of a Study of Negative Resistance:

The artifice of considering the vacuum tube of a super-regenerative receiver to be a source of negative resistance in the oscillatory circuit is as old as the receiver itself, for, as was pointed out in Chapter II, Armstrong presented this concept in his original paper in 1922. More recent writers, almost without exception, have continued to treat the superregenerative circuit as a circuit whose effective resistance alternates periodically about zero. Now, this effective resistance is simply the sum of the inherent positive resistance of the tuned circuit and the negative resistance supplied by the tube. Consequently a knowledge of how the negative resistance contributed by the vacuum tube varies as a function of time would seem to be of primary importance.

Nevertheless, very little attention has been given this matter by any of the writers to date. Some have been content to consider only the most highly idealized case, that of a square-

wave variation of negative resistance with respect to time. In other words, they have assumed the negative resistance to alternate between two steady values, so that the net effective resistance of the tuned circuit shifted abruptly from a definite positive to a definite negative value and back again. Other authors, seeking a closer approximation, have reasoned that, since the quenching voltage was generally sinusoidal, the variation of negative resistance would in turn be nearly sinusoidal.

One obvious shortcoming of both of these assumptions lies in the fact that they present the resistance of the oscillatory circuit as a function of time alone, and not of current as well; that is, they overlook the fact that in any physical vacuum tube circuit oscillations cannot build up indefinitely, but must tend to level off at a value which has been called the "saturation level". Hessler, it will be recalled, modified his assumption of a square-wave variation of resistance by considering oscillations to build up exponentially until they reached the saturation level, to continue at constant amplitude until the beginning of the positive-resistance period, and then to decay exponentially. In other words, he visualized saturation as a "flat roof" limiting the amplitude of oscillations, but did not investigate the reasons for this "roof". David did point out that the resistance was a function of both time and current, but did not examine the nature of this function either theoretically or experimentally.

In short, previous writers on the subject of the super-

regenerative receiver have established the concept of an oscillatory circuit containing a periodically varying resistance, but have failed to take the next step, that of finding just how this resistance does vary with time. Accordingly, this problem was made the starting point of the present experimental investigation.

Definition of Negative Resistance:

At the outset it is necessary to define what is meant by the term "negative resistance", when it is applied to the type of circuit in consideration here -- for example, that shown in Fig. IV - 3 (a). The justification for the use of the term lies in the fact that an oscillating current in the tuned circuit gives rise to an alternating grid voltage, a pulsating plate current, and finally an induced alternating voltage in the oscillatory circuit which aids, and is in phase with, the oscillating current. The negative resistance, then, might be defined as the ratio of this induced alternating voltage to the alternating current responsible for it. In the normal range of operation of a vacuum tube, the sum of this negative resistance and the inherent positive resistance of the tuned circuit would then be the net resistance which determines the rate of growth or decay of oscillations.

In a superregenerative receiver, the above definition must be modified in order to take into account the loss resulting from the flow of grid current when the grid potential swings positive. As far as its effect upon the growth or decay of oscil-

lations is concerned, this loss is equivalent to that of a resistance R_g shunted across the tuned circuit, or a resistance $R_g' = \frac{L}{R_g C}$ in series with the tuned circuit. The effective negative resistance contributed by the tube is then the ratio of induced voltage to oscillating current, minus R_g' , the equivalent series resistance representing grid loss.

The foregoing analysis reveals an important property of the superregenerative circuit under consideration. Provided the plate and filament voltages and the self and mutual reactances of the grid and plate coils at the oscillatory frequency all remain unchanged, the negative resistance contributed by the tube is a function of only two variables; the amplitude of the oscillating current in the tuned circuit, and the value of the "instantaneous grid bias". By "instantaneous grid bias" is meant the sum of the d.c. grid bias voltage and the instantaneous value of the quenching voltage, or, in other words, all components of grid potential except the high-frequency oscillatory voltage.

The proof of this proposition is quite simple. If the oscillating current and grid bias are specified, and the reactance of the grid coil is constant, then the range through which the grid potential oscillates is completely specified. With the plate and filament voltages and the self and mutual reactances of the coils all fixed, it follows that the plate current must then be completely specified. Finally, since the mutual reactance is fixed, the oscillatory voltage fed back into the grid coil, and

hence the ratio of this voltage to the oscillatory current, are also specified. Furthermore, since the range of oscillation of the grid potential is known, the grid current and therefore the hypothetical resistance R_g' (representing grid loss) are uniquely determined. Thus both components of the effective negative resistance, as defined above, are completely specified when the amplitude of oscillating current and the instantaneous grid bias are known.

Experimental Procedure:

In order to investigate the dependence of the effective negative resistance upon the r.m.s. value of oscillating current and the instantaneous value of grid bias, the following experimental method was employed. The receiver was operated as a simple regenerative oscillator, no quenching voltage being used. The data was taken in three groups of runs, each group being for different values of plate voltage and mutual inductance. Within each of these groups, each run was taken with a different value of resistance in the tuned circuit, and was conducted as follows: With the grid voltage sufficiently negative to prevent oscillations from starting, the resistance of the tuned circuit was set at the desired value by adjusting R_{adj} (see Fig. IV - 3b), taking into account the resistances of R_{sig} , the coil, the oscillograph element and the milliammeters. The negative grid bias was then reduced to the point where oscillations started. From that point on, the bias was reduced to zero in small steps, reversed in

polarity, and increased in steps to a positive value sufficiently large to cause oscillations to stop. At each step the r.m.s. value of the current in the tuned circuit was read. In this way a curve of oscillating current versus grid bias voltage was obtained, for a given value of resistance in the tuned circuit. Such curves are sketched in Fig. V-1 for two different values of resistance. As

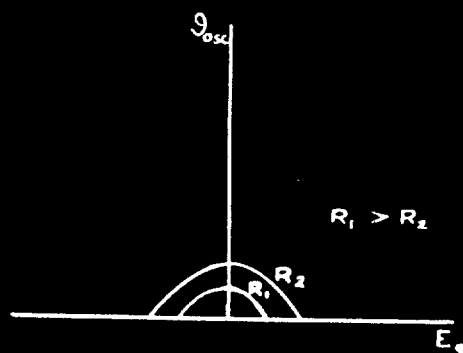


Fig. V-1. "Wobbler graph", or family of curves of oscillating current versus grid bias voltage, for different values of circuit resistance.

might be expected, reducing the resistance of the circuit had the effect of increasing the amplitude of oscillations for a given grid bias, and of increasing the range of grid bias voltage within which the circuit was capable of oscillating.

Now, since these measurements were made with the receiver operating as a simple, unmodulated oscillator, they were taken under steady-state conditions. The amplitude of oscillation was neither building up nor decaying, but was in equilibrium. The net resistance of the circuit was therefore equal to zero during each of the above measurements. This net resistance, however, was simply the sum of two components; the positive resistance of the tuned circuit, and

the negative resistance supplied by the vacuum tube. Consequently, in every case, the negative resistance contributed by the tube was equal to the positive resistance in the circuit. This latter, of course, was easily determinable, being simply the sum of the resistances of R_{adj} , R_{sig} , the coil and the rectifying milliammeter (the oscillograph element and the thermal milliammeter shown in Fig. IV - 3b being omitted during these measurements).

By the foregoing procedure it was possible to determine the negative resistance offered by the tube, as a function of the amplitude (strictly speaking, the r.m.s. value) of the oscillating current and the instantaneous grid bias voltage (already defined). As suggested by Fig. V-1, this function may be expressed by a family of contours of constant negative resistance, plotted against ordinates of oscillating current and abscissae of bias voltage. It has already been demonstrated theoretically that the negative resistance may be expressed as a function of these two variables alone, provided the coil reactances and the filament and plate voltages are kept unchanged. The significance of this theorem is more evident in a corollary which might be stated as follows. For a given combination of values of oscillating current and instantaneous bias, the negative resistance supplied by the tube is always of the magnitude determined for that combination by the above measurements, even though the positive resistance of the circuit may now be different from what it was during those measurements.

But if the negative resistance is independent of the positive resistance, it is necessarily independent of the net resistance, and therefore of the rate of growth or decay of oscillations. Hence follows this important conclusion: The data relating negative resistance to oscillating current and bias voltage, while taken under steady-state conditions, may be used in studying the behavior of a circuit in which the amplitude of oscillations is continually varying -- in other words, a superregenerative receiver. Specific applications of this data will be considered later in the chapter.

It should be realized, of course, that when the negative-resistance contour chart is used in connection with a circuit in which both the grid bias and the oscillating current are continually changing, the coordinates of the chart will refer to "instantaneous" values of these two quantities. The instantaneous grid bias has already been defined as the d.c. grid bias plus the instantaneous value of the quenching voltage. The "instantaneous" value of oscillating current cannot be defined so rigorously, but may be said to mean the root-mean-square value of the current, taken over a period so short that the amplitude of high-frequency oscillations does not change appreciably within the period.

In the course of the negative-resistance measurements described above, there arose a complication which particularly affected the measurements taken with low values of resistance in the tuned circuit. It was found that under these conditions the amplitude of the oscillating current with a given amount of

resistance in the circuit was no longer purely a single-valued function of the grid bias voltage, but followed a curve of the form shown in Fig. V-2 (the three curves in this diagram represent different values of resistance). That is, at one or both ends of the range of grid

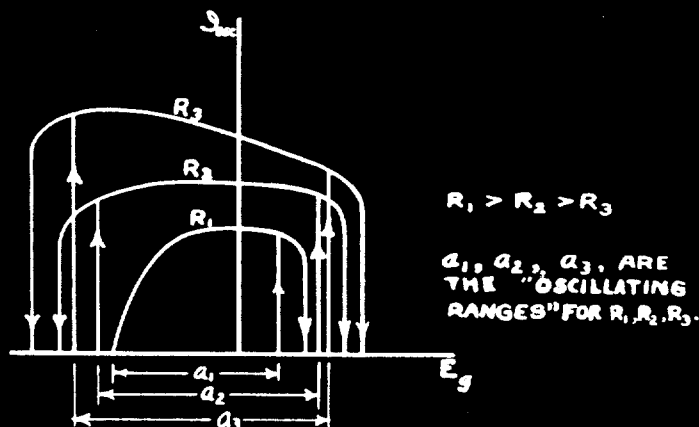


Fig. V-2. "Reissdiagramm", or family of curves of oscillating current versus grid bias voltage, showing hysteresis loops obtained with low values of circuit resistance.

bias voltage in which high-frequency oscillations occurred, there was a hysteresis region in which oscillations would not start when the bias voltage was being brought toward the oscillating range, but would continue when the bias voltage was being brought out of the oscillating range. This phenomenon is by no means a new discovery. It is described by Barkhausen in his *Elektronrohren*, Vol. II, in which he shows a sample "Reissdiagramm" or family of curves similar to those of Fig. V-1 and Fig. V-2.

These hysteresis loops in the curves of oscillating current versus bias voltage for constant values of positive re-

sistance in the tuned circuit do not indicate, however, that similar hysteresis loops exist in the contours of constant negative resistance. In the first place, in the "reissdiagramm", the hysteresis loops for different values of positive resistance overlap each other and even coincide with each other for an appreciable distance along the axis of grid bias voltage. Obviously negative-resistance contours could not contain loops such as these, for this would require the contours to cross each other, whereas it has already been demonstrated on theoretical grounds that the negative resistance supplied by the tube is uniquely determined by the values of oscillating current and instantaneous grid bias.

Furthermore, the hysteresis loops in the "Reissdiagramm" can be readily explained on the basis of negative-resistance contours containing no hysteresis loops, but having the form indicated in

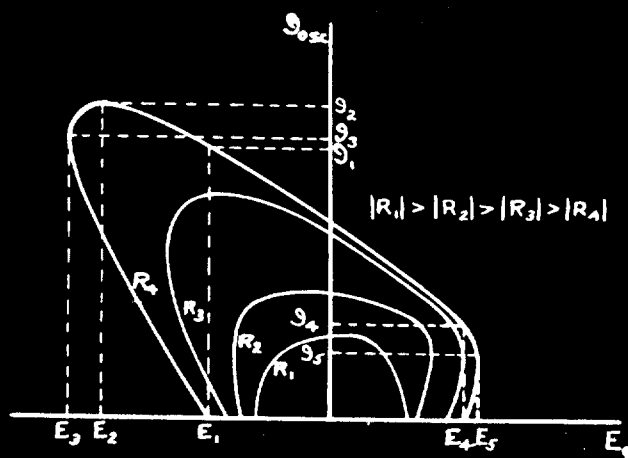


Fig. V-3. Contours of constant negative resistance.

Fig. V-3. Thus, suppose that the positive resistance in the tuned circuit is R_4 ohms, and suppose further that the grid bias, initially highly negative, is being brought toward zero. Until the bias has been reduced as far as E_1 , the negative resistance is numerically smaller than the positive, so that the net resistance of the circuit is positive and tends to damp out any disturbances arising from random noise voltages.

As soon as the bias voltage has been reduced even slightly below E_1 , however, the net resistance is negative, so that the first disturbance which occurs is not damped out but instead builds up. Furthermore, as the oscillation builds up to an appreciable amplitude, the negative resistance becomes greater, on account of the shape of the negative-resistance contours (see Fig. V-3); so that the growth of oscillations is greatly accelerated. The amplitude of oscillation continues to increase, although presently at a decreasing rather than an increasing rate, until the value \mathcal{D}_1 is reached (strictly speaking, approached asymptotically). At this level the oscillating current is in stable equilibrium, since any momentary change in the amplitude of oscillation causes a change in the negative resistance, and therefore in the net resistance, which tends to restore the oscillating current to \mathcal{D}_1 . From the foregoing it may seem that the process whereby the current rises from zero to \mathcal{D}_1 is rather complicated, but it should be realized that it takes place very rapidly.

If now the negative bias is gradually increased, above E_1 , the oscillating current does not fall to zero but instead, follows the R_4 negative-resistance contour. Thus as the negative bias becomes larger the amplitude of oscillations may actually rise for a time. When the bias voltage has reached E_2 , the current has its maximum value of I_2 . Further increase of grid bias causes the oscillating current gradually to fall off again, until the voltage E_3 is reached. Beyond this point it is impossible for the current to adjust itself to any value which will make the negative resistance as great as the positive, and the resulting slightly positive net resistance causes the amplitude of oscillation to decrease. On account of the shape of the negative-resistance contours, this reduction in current decreases the negative resistance further, increases the positive preponderance, and causes the current to fall faster. Thus the amplitude of oscillation quickly falls to zero, and the hysteresis loop is complete.

A similar process accounts for the hysteresis loop between E_4 and E_5 in the positive grid bias region. In general it may be said that wherever the negative-resistance contours exhibit an "undercut" appearance (sloping downward and inward toward the oscillating range of grid bias voltages), as in Fig. 3, the corresponding curves of the "Reissdiagramm" contain hysteresis loops.

There remains, however, the practical problem of determining the course of the "undercut" portions of the negative-resistance contours. All that can be learned about them from the experimental

procedure described on the preceding pages is that, in the case of the R_4 contour of Fig. 3, for instance, the terminal points of one of the undercut sections are $(E_1, 0)$ and (E_3, \mathcal{D}_3) ; of the other, $(E_4, 0)$ and (E_5, \mathcal{D}_5) . Between either of these pairs of points, operation of the receiver is unstable. Any increase or decrease in the amplitude of oscillation causes the operating point to move vertically off the contour and changes the value of negative resistance in such a direction as to increase the original deviation.

A solution of this predicament, for the case of the negative grid bias region, was found in the artifice of inserting a variable grid leak and d.c. voltmeter in the receiver circuit, as shown in Fig. V-4. With a sufficiently high resistance in this leak

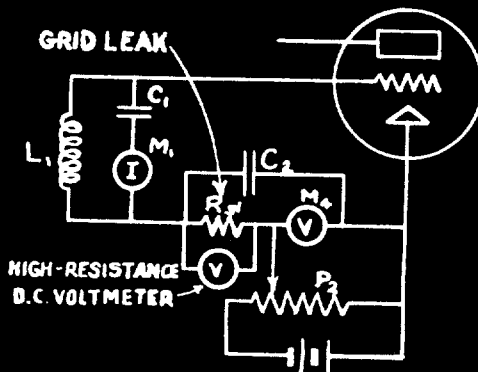


Fig. V-4. Position of grid-leak in circuit.

it was possible to secure stable operation on that portion of the negative-resistance contour which, in Fig. V-3, is bounded by points $(E_1, 0)$ and (E_3, \mathcal{D}_3) .

The reason for this change in behavior is quite simple.

Any momentary variation in the amplitude of oscillation now had a double effect. It not only displaced the operating point vertically, but, by affecting the grid current, changed the d.c. voltage across the grid leak, thus displacing the operating point horizontally as well. The resultant of these two motions was a displacement along a slanting line whose slope could be made smaller than that of the negative-resistance contour by using a sufficiently high grid leak resistance. Under this latter condition, any momentary variation in the amplitude of oscillation altered the negative resistance in such a direction as to restore the oscillating current to its original amplitude, instead of accelerating its departure from the

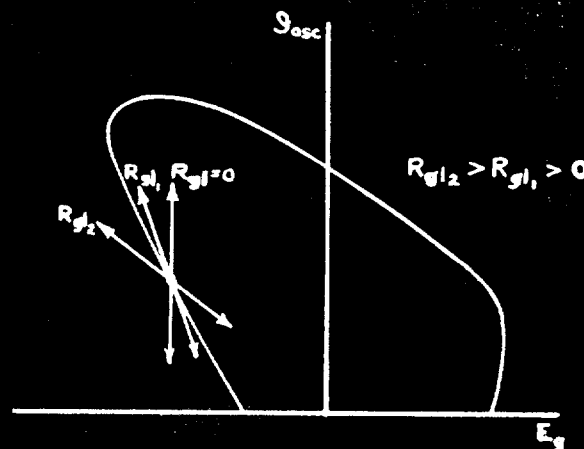


Fig. V-5. Loci of operating point when displaced from equilibrium, with different values of grid-leak resistance.

equilibrium amplitude. This point is illustrated in Fig. V-5, which shows loci of the operating point for different values of grid leak resistance.

The procedure used in locating points on the unstable

part of the negative-resistance contour with the aid of the modified circuit described above was as follows. The positive resistance of the tuned circuit was first set at a value numerically equal to the negative resistance of the desired contour. Next the grid leak and the grid bias potentiometer were adjusted until a desired value of oscillating current was obtained. To the reading of the grid bias voltmeter was then added the reading of the voltmeter shunted across the grid leak, in order to obtain the total bias applied to the grid. This total bias voltage and the oscillating current read on the milliammeter in the tuned circuit were then the coordinates of a point on the negative-resistance contour. The procedure was repeated for other values of oscillating current in order to get a number of points, through which the contour could be drawn.

In practice, it was sometimes unnecessary to shunt the grid-leak voltmeter with a grid leak at all, the resistance of the former serving the purpose quite adequately. Indeed, the only upper limit on the permissible resistance of voltmeter and grid leak combined was imposed by the fact that, with a resistance of more than approximately one megohm, relaxation oscillations occurred. Their frequency was determined by the grid leak resistance and the capacitance shunted across the grid leak and bias supply.

One objection may arise concerning the validity of the foregoing method of obtaining the undercut portions of the negative-resistance contours. It may seem that by the insertion of a grid leak the circuit was so altered that any data gathered with it was

inapplicable to a circuit containing no grid leak. Fortunately this is not true. Because of the large bypass condenser shunting the grid leak and bias supply, the receiver circuit was not changed appreciably by the inclusion of the leak, as far as currents and voltages of the oscillatory frequency were concerned. The only important change was the addition of another source of d.c. grid bias to the potentiometer supply already present, and this additional bias was taken into account in the procedure described above. Consequently, the data on negative-resistance contours obtained with the circuit containing the grid leak is entirely applicable to the circuit containing none.

The principal shortcoming of the grid-leak method of obtaining the undercut portions of negative-resistance contours is that it is applicable only to the negative grid bias region. In the positive grid bias region, the course of the undercut curves can only be estimated from the known end-points (points $(E_4, 0)$ and (E_5, \mathfrak{J}_5) in Fig. V-3).

One point remains to be mentioned, in connection with the foregoing experimental investigation of the negative resistance supplied by the vacuum tube. A set of static characteristic curves of the tube used in the receiver was taken, with the receiver itself serving as the test set, since it contained all of the necessary instruments and controls. Both $I_p - E_g$ and $I_g - E_g$ curves were taken, for a series of different values of E_p .

Experimental Results:

Three families of negative-resistance contours, representing three different combinations of plate voltage and mutual inductance between the grid and plate coils, were taken. They are shown in Fig. V-6 and Fig. V-7. These contours, as has already been explained, give the negative resistance supplied by the vacuum tube of the receiver as a function of the oscillating current and instantaneous grid bias voltage.

The static characteristic curves of the vacuum tube are given in Fig. V-8.

Discussion:

In order to account for the shape of the curves in Fig. V-6 and Fig. V-7, showing the negative resistance contributed by the tube as a function of oscillating current and instantaneous grid bias voltage, it is necessary first to examine the static characteristics in Fig. V-8.

These curves differ from those usually shown for the '01-A tube only in that they are carried well into the positive-grid region. Both the lower and the upper bends in the I_p - E_g curves are to be seen, the lower occurring at cut-off and the upper at saturation of the tube. The I_g - E_g curves for $E_p = 60, 90$ and 180 volts reveal an interesting point. In the range between $E_g = 0$ and $E_g = +20$ (approximately), I_g and E_g are nearly proportional to each other. Their ratio, expressed in terms of resistance, is approximately

FIG. V-6. CONTOURS OF CONSTANT NEGATIVE RESISTANCE

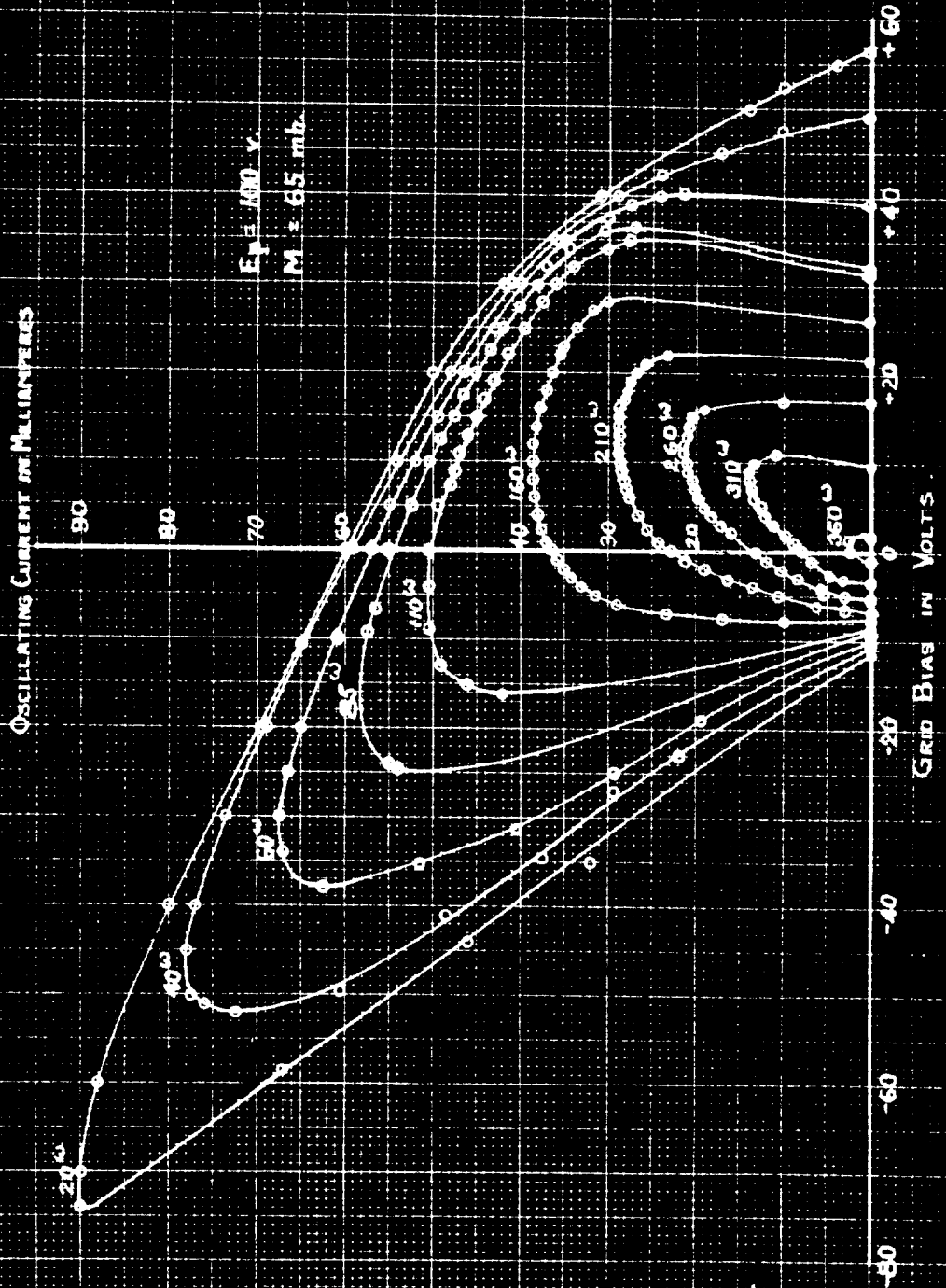


FIG. V-7. CONTOURS OF CONSTANT NEGATIVE RESISTANCE

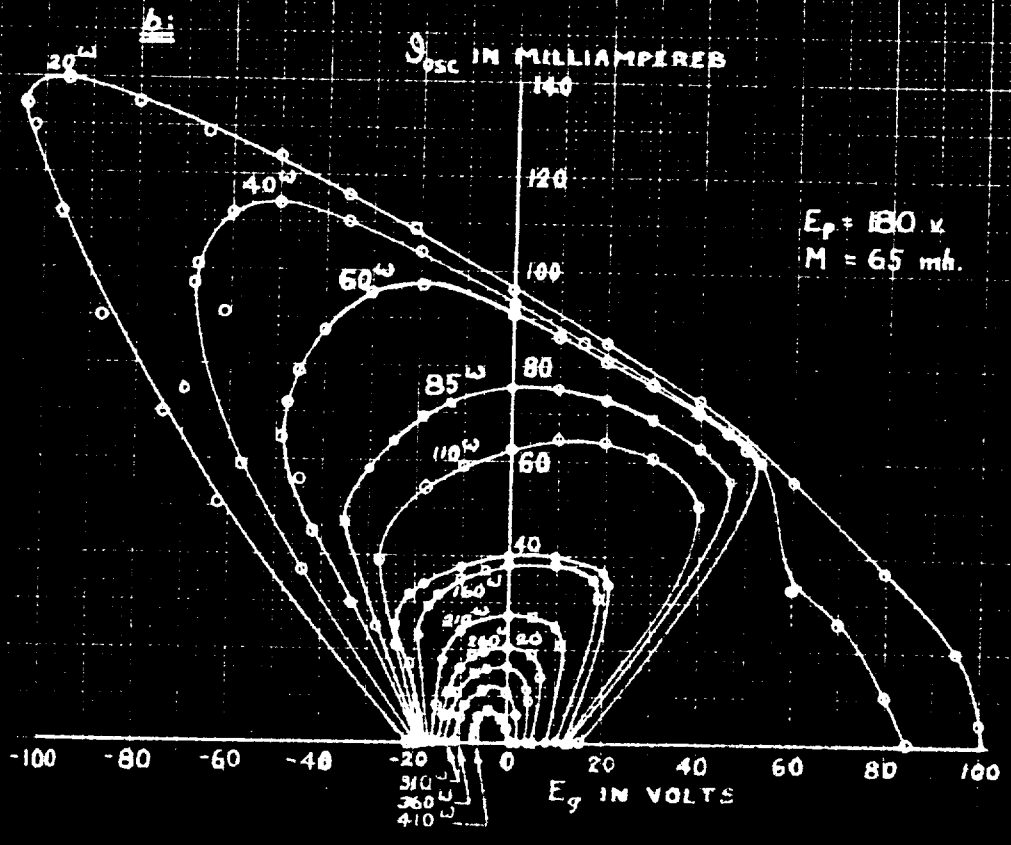
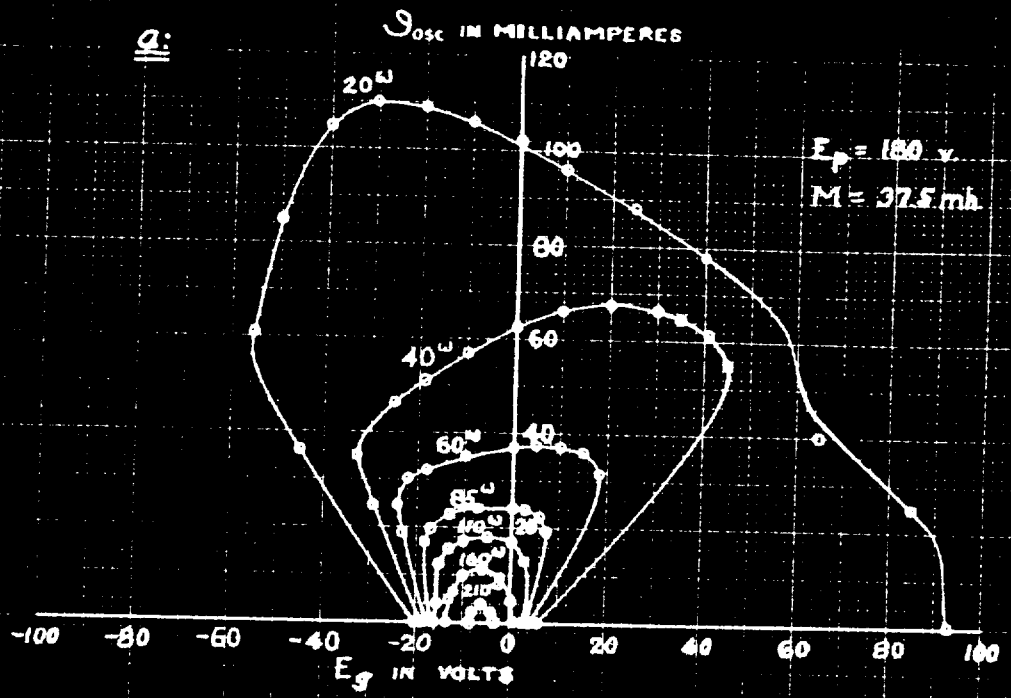
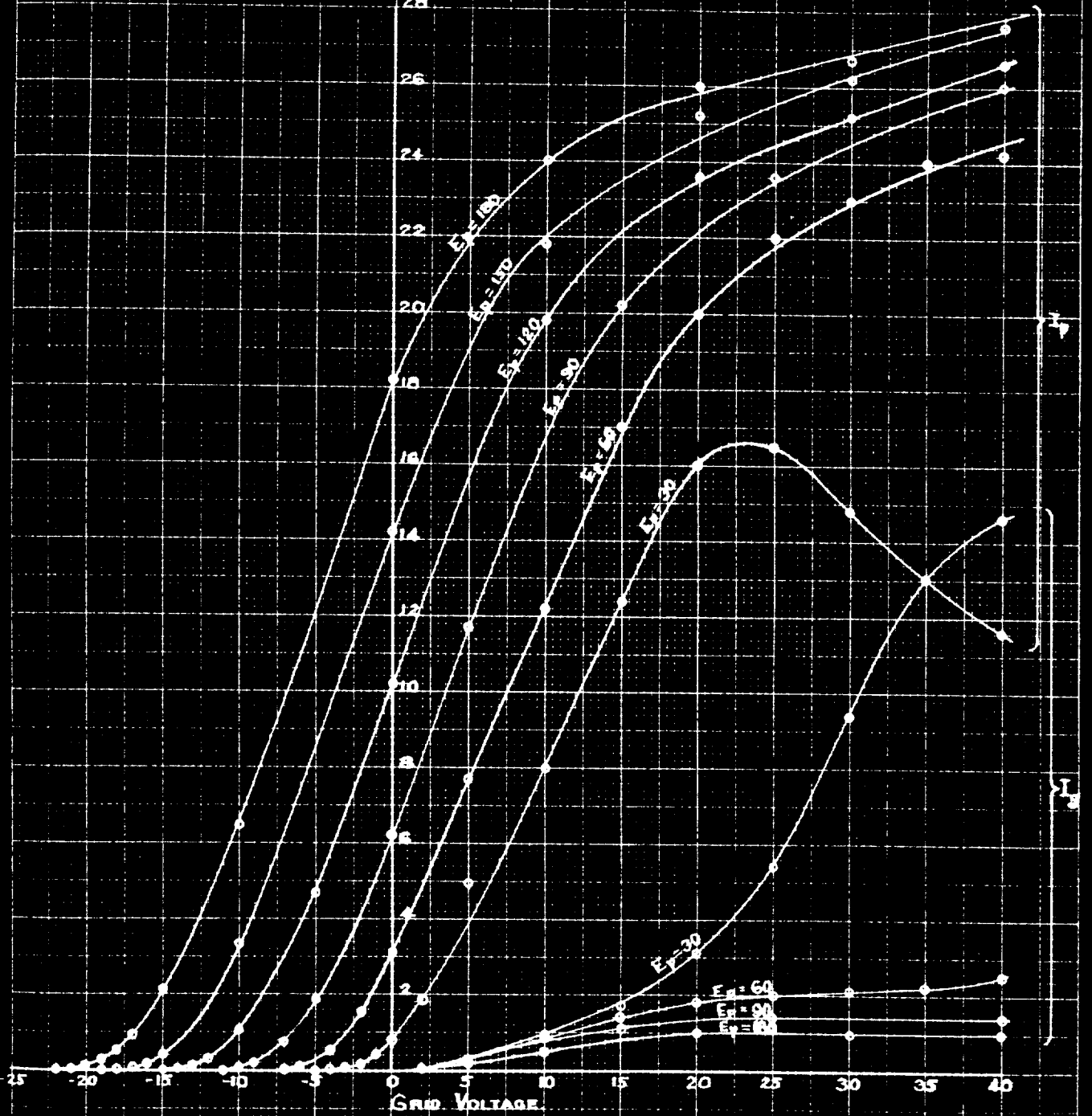


FIG. V-8. VACUUM TUBE CHARACTERISTIC
TYPE 301-A.

PLATE AND GRID CURRENT
(IN MILLIAMPERES).



11,000 ohms for the 60-volt curve; 15,000 ohms for the 90-volt curve; and 20,000 ohms for the 180-volt curve. Outside this 20-volt range of bias voltage, however, in both directions, the slope of the curves decreases practically to zero. That this should be true to the left is to be expected, since no appreciable grid current can flow in the negative-grid region. The levelling off of the curves at grid voltages greater than +20 volts is somewhat surprising, but may be explained on the assumption of secondary emission from the grid.

The shapes of the I_p and E_g curves for $E_p = 30$ are particularly worth noting. At $E_g = +20$, approximately, the I_g curve commences to climb very steeply and continues to do so up to $E_g = +40$, approximately, where it begins to level off. The rapid rise in I_g is accompanied by an actual drop in I_p , indicating that when the grid voltage becomes approximately equal to the plate voltage the grid robs the plate of its space current. While it was impossible to carry the tube characteristics beyond $E_g = +40$ without dangerously overheating the grid, it is to be presumed that the curves for $E_p = 60, 90, 120, 150$ and 180 would reveal the same behavior as those for $E_p = 30$, at positive grid voltages approximately equal to their respective plate voltages.

The significant features of the negative-resistance contour charts, Fig. V-6 and Fig. V-7, can now be explained in terms of the static characteristics of the tube. Consider Fig. V-6 first. Along the axis of grid bias voltage, where the amplitude of oscillation is

equal to zero, the negative resistance supplied by the tube varies quite as would be expected. At negative grid potentials greater than cut-off, which is in the vicinity of -12 volts, the tube is inoperative and supplies no negative resistance at all. As the negative bias is decreased, the mutual conductance of the tube and with it the negative resistance begin to rise from zero. They continue to increase until the bias has been reduced approximately to zero. As a positive bias is applied the negative resistance commences to fall off again, at first not because of a reduction in the mutual conductance but because of the appearance of grid loss. Further increase in bias voltage carries the operating point past the upper bend of the I_p - E_g curve, causing the mutual conductance and hence the negative resistance to fall off steadily. At +56 volts the negative resistance has decreased to 20 ohms, and at a bias of the order of +100 volts the tube would undoubtedly offer a considerable positive resistance to the tuned circuit, because of the steep climb in I_g and the drop in I_p which occur when E_g becomes approximately as great as E_p .

When the oscillating current is not equal to zero, it is apparent from the chart that the situation becomes more complicated. Examining the negative-grid region first, one notes a tendency of the contours representing low negative resistance to stretch out toward the upper left corner of the chart. In order to see the explanation for this "deformation", first choose a line such as $E_g = -50$ and follow it up from $\theta_{osc} = 0$ to $\theta_{osc} = 90$. For small

values of \mathcal{I}_{osc} , the negative resistance remains equal to zero, since the tube is biased nearly 40 volts beyond cut-off. When, however, \mathcal{I}_{osc} becomes large enough to carry the grid potential past cut-off on the positive grid swings, the tube can feed energy back to the tuned circuit, even if only for a small part of the cycle. Hence the negative resistance rises, reaching in this instance a maximum of approximately 40 ohms at $\mathcal{I}_{osc} = 72$. Further increase in \mathcal{I}_{osc} carries the grid potential so far positive on the peak of the grid swing that the grid voltage approaches or even exceeds the plate voltage at the peak of the cycle. This tendency is aggravated by the fact that the oscillating current in the tuned circuit not only applies a large positive peak voltage to the grid, but induces a voltage almost half as great into the plate circuit, in such a phase that at the instant of maximum grid voltage the plate voltage is at a minimum. Consequently, for any given grid bias, there is a fairly definite limiting value which cannot be exceeded by \mathcal{I}_{osc} without sharply increasing the grid loss and reducing the voltage fed back into the tuned circuit. This accounts for the close proximity of the contours along the upper boundary of the chart.

If the line $E_g = -70$ is chosen, instead of the line $E_g = -50$ employed above, it is observed on the chart that the maximum negative resistance now occurs at a higher value of oscillating current, namely, 87 milliamperes. This means merely that it takes a greater amplitude of oscillation to carry the grid potential past cut-off on the positive peak of the cycle. This increased amplitude, in turn,

limits the operative period of the tube to an even smaller portion of the cycle, reduces the amount of energy which can be fed back to the tuned circuit, and therefore decreases the negative resistance. With $E_g = -70$, for instance, the maximum negative resistance is slightly over 20 ohms, whereas approximately 40 ohms was available at $E_g = -50$.

In the positive-grid region, the contours of high negative resistance are observed to lean toward the upper right corner of the chart. Reference to the static characteristics shows that with a positive bias of, say, 10 volts, a considerably larger amplitude of oscillation can exist without carrying the operating point off the steep portion of the $I_p - E_g$ curve than with no bias at all. This explains why the contours of constant negative resistance, which in this case are practically the same thing as contours of constant average mutual conductance, tend to pass through higher values of oscillating current as the bias is made more positive.

The objection may arise that since the $I_p - E_g$ curve is approximately symmetrical, having an upper bend as well as a lower one, the negative-resistance contours discussed above should also be approximately symmetrical instead of leaning toward the upper right. While the complete explanation for the dissymmetry in the shape of the contours is too involved to merit inclusion here, it hinges upon the fact that the upper bend of the characteristic is neither as abrupt nor as acute as the lower one; in other words, upon the imperfectness of the symmetry of the $I_p - E_g$ curve.

The next point to be considered is the relation between

negative resistance, on the one hand, and plate voltage and mutual inductance, on the other. A comparison of Fig. V-6 and Fig. V-7 (b) reveals the effect of changing the plate voltage. In the first place, as might be expected, the entire pattern of contours is shifted horizontally by an amount approximately equal to the change in plate voltage divided by the amplification factor of the tube. Thus in Fig. V-6, in the negative grid region, the 20-ohm contour meets the axis of grid bias voltage at -12 volts, while in Fig. V-7 (b), in which the plate voltage is 80 volts greater, this intersection occurs at about -22 volts. The difference in grid bias, 10 volts, is equal to the difference in plate voltage, 80 volts, divided by the amplification factor, which was approximately 8 in the '01-A tube used in this receiver.

The second obvious result of increasing the plate voltage is an expansion of the pattern in all directions (note that the scale to which ordinates and abscissae are plotted in Fig. V-6 differs from that of Fig. V-7 by a factor of 2). As has already been explained, for any given bias voltage there is a limiting value of oscillating current beyond which the negative resistance falls off steeply. This limiting value is determined by the amplitude of oscillation which makes the grid voltage approximately equal to the plate voltage on the peak of the positive grid swing. Obviously, with increased plate supply voltage, this limiting amplitude is also increased.

It will also be noticed that a slightly higher maximum negative resistance (approximately 440 ohms, as compared with approximately 380 ohms) is obtained with 180 volts plate potential than with 100

volts. This difference is apparently caused by the difference in grid loss in the two conditions. With 100 volts on the plate the maximum negative resistance occurs at $E_g = +\frac{1}{2}$, while with 180 volts it occurs at $E_g = -3$. Reference to the $I_g - E_g$ curves in Fig. V-8 shows that at $E_g = +\frac{1}{2}$ the grid-filament conductance (dI_g/dE_g) is appreciable, while at $E_g = -3$ it is entirely negligible. Hence the grid loss is smaller and the negative resistance supplied by the tube is greater in the former instance than in the latter.

Finally, in order to observe the effect of changing the mutual inductance between the grid and plate coils while keeping the plate voltage constant, compare Fig. V-7 (a) with Fig. V-7 (b). The two families of contours are seen to have very nearly the same shape, provided each curve of Fig. V-7 (a) is compared, not with the corresponding curve in Fig. V-7 (b), but with the contour representing approximately twice as great a negative resistance. Thus the 20-ohm and the 85-ohm curves in (a) are similar to the 40-ohm and the 210-ohm curves, in (b), respectively. This is not surprising, since the mutual inductance is approximately twice as great in (b) as in (a). If it be assumed that a given amplitude of oscillating current in the tuned circuit produces approximately the same alternating component of plate current regardless of the mutual inductance, then the ratio of induced voltage to oscillating current (which is the principal component of negative resistance for negative and moderately positive grid bias voltages) must be proportional to the mutual inductance.

Accurate quantitative comparisons cannot be drawn between

Fig. V-6 and Fig. V-7, since the curves in the latter were taken with different meters from those used in the former, and the calibrations of the two sets of instruments were not identical. However, for qualitative considerations such as those discussed in the preceding paragraphs, they are entirely comparable.

B. THE SUPERREGENERATIVE PROCESS

The material presented in the first section of this chapter, treating the vacuum tube as a source of negative resistance, can now be employed in an examination of the superregenerative process itself. By this term is meant the process whereby the amplitude of oscillations in the tuned circuit periodically builds up from a small initial value and then decays again, as a result of the alternation of the net resistance of the circuit between positive and negative values. The final objective of the analysis will be a determination of the manner in which the net resistance of the tuned circuit varies as a function of time.

The procedure to be followed in studying the superregenerative process will consist of the following steps:

1. Collection of experimental data on the variation of the amplitude of oscillating current as a function of time, using oscillographic records.
2. Analysis of oscillographic data with the aid of the negative-resistance contour chart.

- a. Plotting of "operating loops" on the negative-resistance contour charts.
- b. Plotting of net resistance as a function of time.
- c. Plotting of net resistance as a function of time, directly from oscillographic data; to serve as a check on part b.

With the several steps of the procedure thus outlined, the first of them can now be considered in detail.

1. Oscillographic Study of Oscillating Current as a Function of Time:

The oscillograms now to be considered were taken primarily to supply quantitative data on the manner in which the amplitude of oscillation varied during the quenching cycle. To this end it was necessary that each oscillogram should show both the oscillating current in the tuned circuit and the quenching voltage applied to the grid. Information was also required, either on the oscillogram itself or from supplementary measurements, for "calibrating" the figure on the oscillogram; that is, to permit translating the dimensions of the figure into milliamperes of oscillating current and volts of instantaneous grid bias.

As was mentioned in Chapter IV, two different types of oscillograph were used. For visual observation and for photographs of stationary images, a cathode-ray tube was used on account of its convenience. For records of non-recurrent phenomena it was necessary to

employ a vibration oscillograph.

In using the cathode-ray oscillograph, as has already been explained, it was necessary to superpose the quenching voltage upon the high-frequency voltage in order to show both simultaneously. This was accomplished by means of the circuit connection shown in Fig. IV-3 (b). The principal disadvantage of this superposition is that it makes it somewhat difficult to distinguish at a glance the form of the envelope of oscillations and its phase relation to the sinusoidal quenching voltage. Indeed, before the latter can even be seen in its entirety, it is necessary to locate the midpoints of the high-frequency oscillations and fill in the curve passing through them, as shown in Fig. V-9.

It was found that satisfactory photographs of cathode-ray images could be obtained with an exposure of 1 to 2 seconds on Kodak Verichrome or Agfa Plenachrome film, using a diaphragm opening of $f/4.5$ on the camera.

Two different methods were employed in "calibrating" the oscillograms. In the first of these, after the oscillogram had been taken, the quenching voltage was made equal to zero and the receiver was operated as a simple regenerative oscillator. The oscillating current was adjusted to a convenient known value, measured on either of the milliammeters in the tuned circuit, and a second exposure was taken on the same film as the first, but with the camera shifted slightly to one side. In this way a rectangle whose height represented a known r.m.s. value of oscillating current was obtained

alongside the figure illustrating superregenerative operation. With the inductance, frequency, and therefore the reactance of the grid coil known, this calibration in terms of current could be converted into terms of voltage for the purpose of reading instantaneous grid bias voltages on the oscillogram.

In the second method, it was necessary to determine the calibration of the oscillograph by placing a known oscillating voltage across the vertical deflecting plates and measuring the height of the resulting figure on the screen. On our oscillograph the sensitivity was 39 volts (r.m.s.) per inch (from top to bottom of figure), or about 110 volts per inch of deflection. In order to obtain the calibration of the oscillogram, it was only necessary to find the ratio between the dimensions of the figure on the screen and those of its image on the photographic film. This was done by measuring, say, the horizontal length of the cathode-ray pattern and comparing it with the corresponding dimension on the photograph. Their ratio, multiplied by the sensitivity of the oscillograph, gave the calibration to be used in reading voltages on the oscillogram. When this was divided by the reactance of the coil, the current calibration was obtained.

Examples of the cathode-ray oscillograms taken under various conditions are shown in Figs. V-9, V-10, V-11 and V-12, on the following page. The positive direction is upward for grid voltage and toward the right for time. In Fig. V-9, the sine wave representing quenching voltage has been drawn in. These four pictures will be

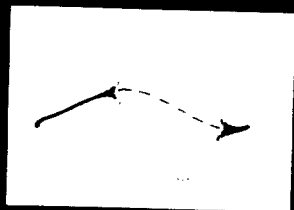


Fig. V-9

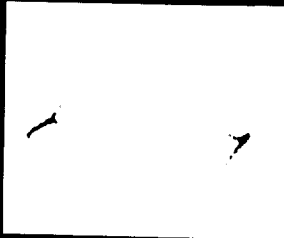


Fig. V-10

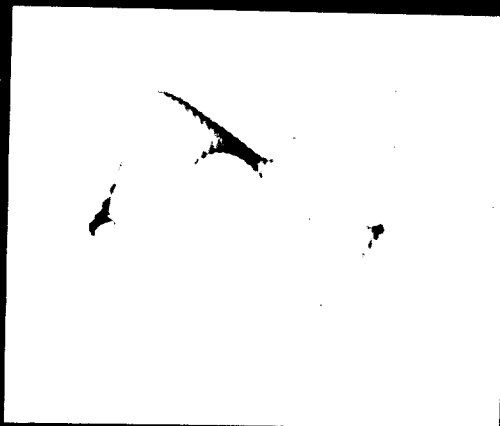


Fig. V-11

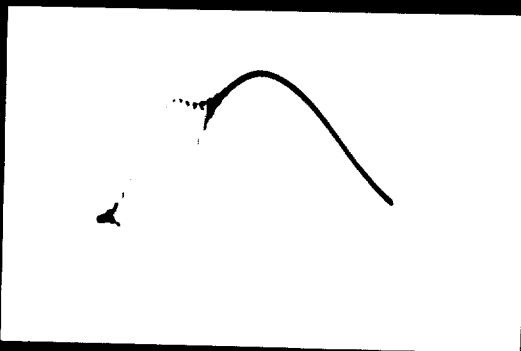


Fig. V-12

TECHNICAL DATA ON OSCILLOGRAMS

<u>Fig.</u>	<u>Circuit Resistance (Ohms)</u>	<u>D.C. Grid Bias (Volts)</u>	<u>Quenching Voltage (Volts)</u>	<u>Quenching Frequency (CPS)</u>	<u>Signal Voltage (Millivolts)</u>
V- 9*	110	-15.0	12.0	25.0	16
V-10	93	-5.3	15.9	25.7	0
V-11	130	16.0	24.8	25.0	0
V-12	130	44.8	33.0	24.8	0
V-13	165	-7.5	10	27	0.16
V-14	165	-7.5	10	27	3.2
V-40*	110	-15.0	12.0	25.0	16
V-41	110	-15.0	10.0	25.0	16
V-42	110	-15.0	7.5	25.0	16
V-43	110	-15.0	7.5	25.0	1.4
V-44	160	-7.5	15	25	0
V-45	160	-7.5	15	25	0.11
V-46	160	-7.5	15	25	0.27
V-47	160	-7.5	15	25	1.1
V-48	160	-7.5	15	25	5.4
V-49				10	
V-54	95	-16.6	10.0	26.7	5
V-55	95	-15.7	9.6	25.7	5
V-56	95	-16.6	10	25.0	5
V-57	110	-17.3	9.8	26.3	4
V-58	105	-15.0	36.0	25.7	0
V-59	75	-15.0	36.0	25.7	0
V-60	57	-14.8	35.7	25.0	0
V-61				25.0	5
V-62	255	-22.5	37	25.3	5
V-63	470	-16.0	38.4	24.7	0
V-64	375	-15	32.6	9.7	0
V-65	410	-14.8	35.7	25.7	0 (sweep cct. on)

A d.c. plate voltage of 100 volts and a mutual inductance of 65 millihenries were used in all of the above oscillograms.

*Note: Figs. V-9 and V-40 are duplicate prints of the same oscillogram.

used shortly in connection with one of the negative-resistance charts described in the first part of this chapter, and consequently are inserted here. Additional cathode-ray oscillograms, taken to illustrate other points, will appear later.

The vibration oscillograph, while less convenient to use, had three advantages over the cathode-ray instrument. In the first place, since separate elements could be used for the oscillating current and quenching voltage, these quantities could be measured more easily on the oscillogram. In the second place, the vibration type of oscillograph was free from errors that were present in the cathode-ray tube on account of distorted electrostatic fields and imperfections in the sweep circuit. Finally, non-recurrent phenomena, such as beats, could be recorded with the vibration oscillograph.

In order to limit the deflections of the beams of light to convenient values, shunts and multipliers were used with the oscillograph elements. The resistance of the element in the tuned circuit and its shunt was taken into account whenever it was greater than one or two ohms.

Calibration of the oscillograph was accomplished by holding a translucent card in the plane normally occupied by the sensitized paper as it passed the light beams, and measuring the length of the illuminated stripe which appeared on the card when a known voltage or current was applied to the element and its multiplier or shunt. This calibration had to be performed only once, whereas with the cathode-ray oscillograph it was necessary to recalibrate frequently

in order to guard against errors resulting from changes in the distance between the camera and the tube.

Reproductions of two oscillograms obtained with the vibration oscillograph are shown in Fig. V-13 and V-14. They were taken under identical circuit conditions, but with different values of input signal voltage. Since the originals were taken on sensitized paper, not film, it was necessary to photograph them in order to

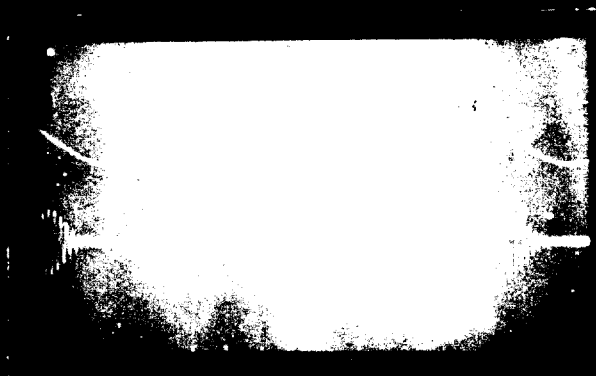


Fig. V-13



Fig. V-14

obtain copies. At the same time, for convenience, they were reduced to approximately one-half size. As in the case of the cathode-ray oscillograms described above, the two oscillograms presented here are ones which will be used in conjunction with negative-resistance data

from the first part of the chapter. Other oscillograms will be shown later, as the points to which they are pertinent come under consideration.

2. Analysis of Oscillographic Data:

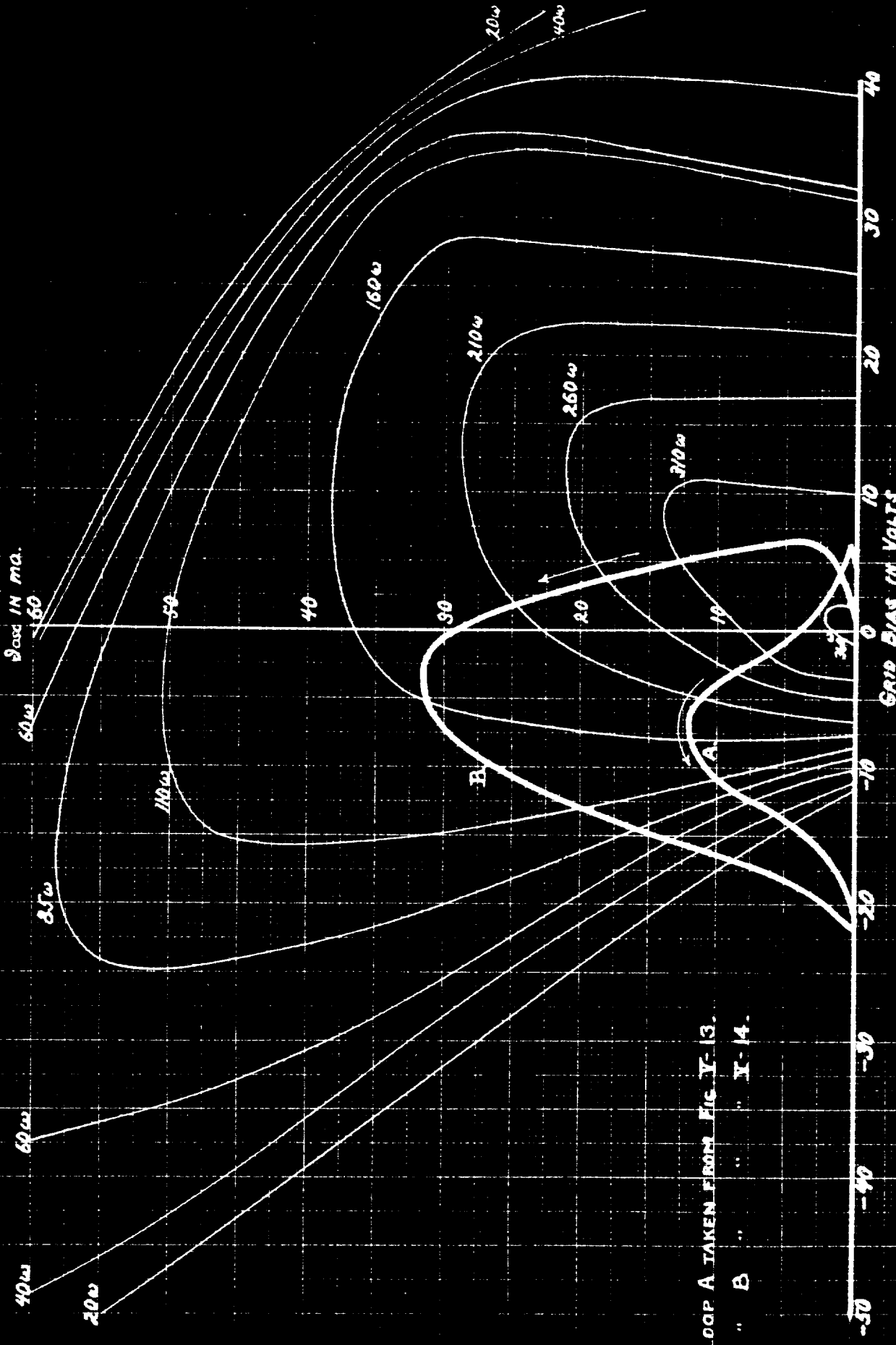
a. Plotting Operating Loops:

Oscillograms of the kind described in the preceding pages, whether taken with a cathode-ray tube or a vibration oscillograph, show oscillating current and instantaneous bias voltage as functions of time. If this information is replotted so that oscillating current and instantaneous bias voltage are the ordinates and abscissae, respectively, a complete cycle of the superregenerative process will appear as some form of a closed curve or "operating loop".

Such a loop reveals little by itself; but if it is plotted on the negative-resistance contour chart for the circuit with which it was taken, a number of significant observations may be made. Accordingly, in Figs. V-15, V-16 and V-17, operating loops are plotted on the contour chart of Fig. V-6, using data obtained from the oscillograms in Figs. V-9 to V-14, inclusive.

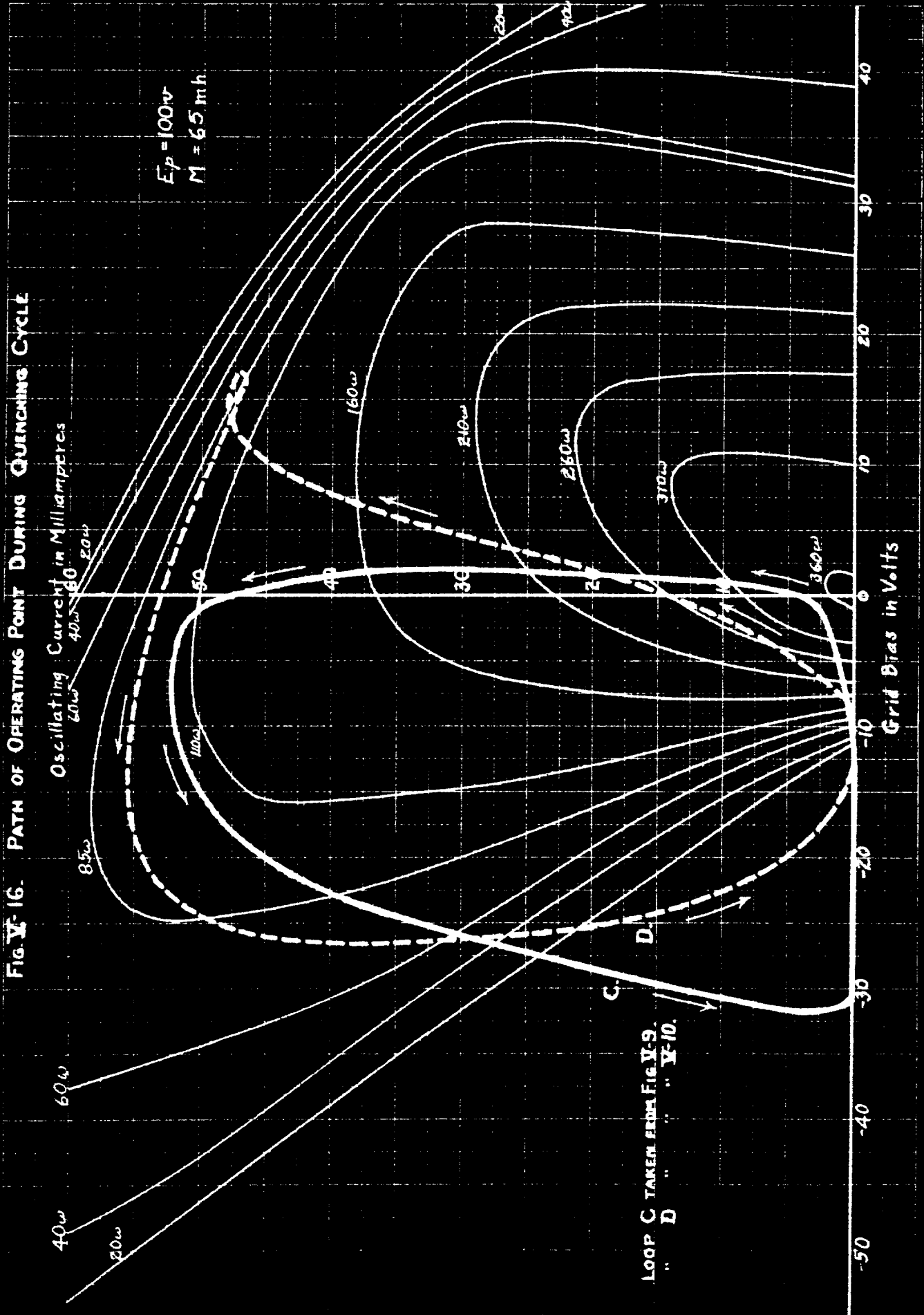
The general form of these loops is very nearly what would be expected on theoretical grounds. The operating point ascends on the chart, indicating increasing \mathcal{D}_{osc} , until it approaches the contour for that value of negative resistance which is numerically equal to the positive resistance in the tuned circuit. As it crosses this

FIG. I-15. PATH OF OPERATING POINT DURING QUENCHING CYCLE



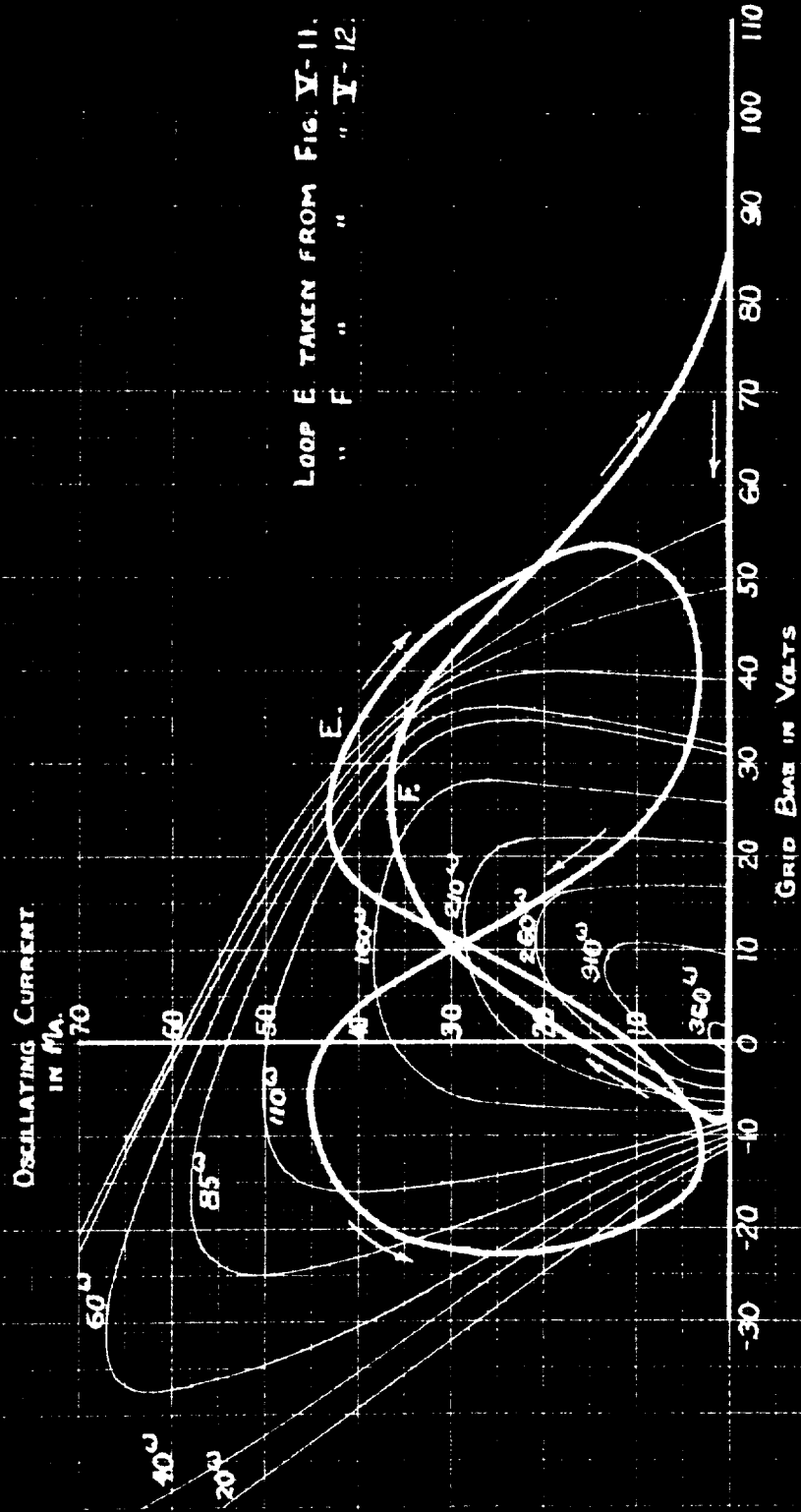
LOOP A TAKEN FROM FIG. I-13.
 " B " " " I-14.

FIG. V-16. PATH OF OPERATING POINT DURING QUENCHING CYCLE



LOOP C TAKEN FROM FIG V-9.
 " D " " " V-10.

FIG. V-17. PATH OF OPERATING POINT DURING QUENCHING CYCLE



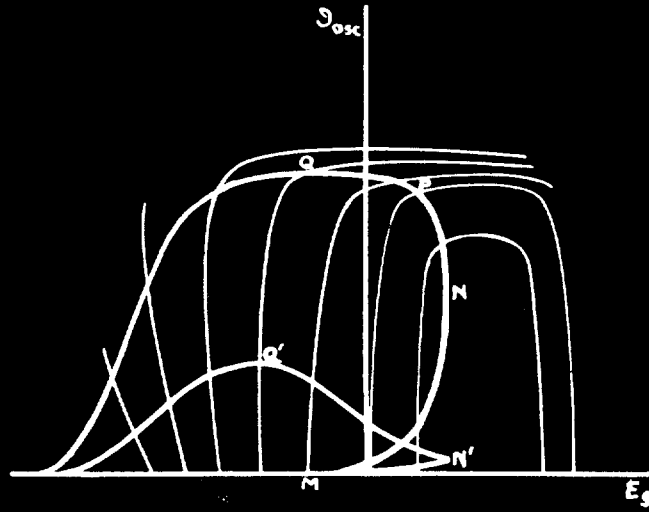
LOOP E TAKEN FROM FIG. V-11.
" F " " " V-12.

contour the path of the operating point should theoretically be horizontal. In Fig. V-15 this condition is fulfilled quite well; the top of the operating loop falls almost exactly upon the 165-ohm negative-resistance contour. In Figs. V-16 and V-17 the agreement with theory is not as good, but the discrepancy is of the order of magnitude of the possible error in the location of the loop on the contour chart. This error may result from inaccuracies in calibrating the oscillograms and in measuring from them, from differences in the calibrations of milliammeters used in taking negative-resistance measurements and calibrating oscillograms, and from differences in the temperature of the tube between the time of taking the negative-resistance measurements and the time of taking the oscillograms.

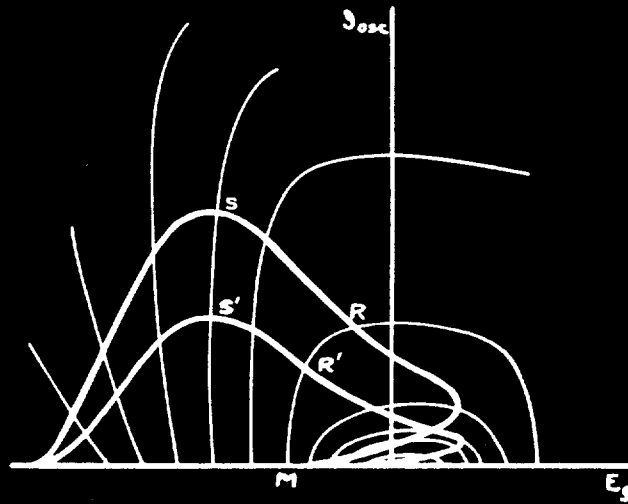
An interesting point is illustrated in Fig. V-15, which shows loops for identical circuit conditions but for two different values of input signal voltage. The ratio of these two signal voltages is 3.2 : 0.16, or 20 : 1, but the ratio of the peak values of oscillating current reached during the quenching cycle is only 31.5 : 12, or 2.6 : 1. This means that the 3.2-millivolt loop represents a saturated condition of the receiver. Yet the oscillogram (shown in Fig. V-14) from which this loop was plotted does not appear to reveal such a condition. The envelope of oscillations certainly does not have the flat-topped appearance which Hassler assumed to exist in all cases of saturation. Indeed, it bears a considerable resemblance to the envelope observed with the 0.16-millivolt signal (see oscillogram, Fig. V-13).

This paradox of saturation without the appearance of saturation may be explained quite simply. The fundamental characteristic of an oscillator circuit which is responsible for saturation is the fact that, for any given grid bias voltage, the negative resistance supplied by the tube decreases when the amplitude of oscillation becomes sufficiently great. The exact manner in which the amplitude of oscillation and the negative resistance are related determines the form of saturation which will occur. To illustrate this point, two hypothetical configurations of negative-resistance contours are shown in Fig. V-18 (a) and (b). In (a) the contours are bunched together at high values of oscillating current; in (b), at low values. In each diagram two operating loops are shown, representing operation with two different signal voltages, one about ten times as large as the other.

Observe what happens as the operating point starts at M and proceeds around the operating loop in a counter-clockwise direction. In (a) the ordinates of the operating points on the two loops remain in the same ratio as the signal voltages until NN'. Between N and P, on the loop representing the stronger input signal, the negative resistance abruptly drops to a value approximately equal to the positive resistance in the tuned circuit. Both the negative resistance and the oscillating current remain virtually constant from P until Q. On the loop representing the weaker input signal, on the other hand, the negative resistance steadily falls and the oscillating current steadily rises from N' to Q'. From QQ' on around to M, the oscillating



(a) "Flat-topped" saturation.



(b) Saturation occurring early in building-up period.

Fig. V-18. OPERATING LOOPS REPRESENTING TWO DIFFERENT FORMS OF SATURATION

current decays in practically the same manner on both loops. Thus the configuration of contours shown in Fig. V-18 (a) causes a strong signal to produce "flat-topped" saturation, the type assumed by Hassler. This form of envelope is strikingly illustrated in the oscillogram in Fig. V-10.

In diagram (b), however, the situation is quite different. Soon after passing through point M, the loop representing the larger input signal begins to encounter lower values of negative resistance than does the loop representing the smaller signal. This condition continues until RR', approximately, and causes the ratio of the ordinates of the two operating points to become much smaller than the 10:1 ratio of the signal voltages. After RR', however, the negative resistance varies in nearly the same way along both operating loops, so that the ratio of the ordinates of the two operating points remains virtually constant at its reduced value. In other words, from RR' on, the envelope of oscillations has nearly the same form regardless of the input signal voltage. This is a characteristic ordinarily associated with the complete absence of saturation. Yet saturation is certainly present in this example, for the ratio of the amplitudes of the two envelopes is far smaller than the ratio of the signal voltages.

Saturation is thus a phenomenon which can manifest itself in a variety of ways. The hypothetical examples discussed above constitute two opposite extremes, while the instance shown in Fig. V-15 is an intermediate case, somewhat more similar to Fig. V-18 (b) than to (a).

One more point deserves mention while operating loops are being considered. The four loops shown in Fig. V-16 and Fig. V-17 form a series in which the d.c. grid bias has the values -15 volts, -5.3 volts, +16 volts and +44.8 volts. The first loop of this series is a simple oval, more or less, upon which the operating point moves in a counter-clockwise direction. In the second of the series, a small reverse loop has appeared at the upper right "corner" of the oval. In the third, this reverse loop has expanded and the original oval contracted, so that the entire loop resembles a figure-of-eight lying on its side. This figure represents a condition in which there are two damping and two "dedamping" periods in each quenching cycle. Such a condition was discussed briefly by Hassler (see Appendix A, Part V. p.288). Finally, in the fourth of the series, the original oval has disappeared completely, leaving only the reverse loop, upon which the operating point travels in a clockwise direction.

This development is interesting in that it points to the possibility of operating a superregenerative receiver in a manner exactly the reverse of conventional practice. That is, the d.c. grid bias could be made positive and the quenching voltage so adjusted that on its negative swing oscillations would build up, while on the positive swing they would be damped out again. Such a mode of operation would ordinarily be quite impractical, however, for the large plate and grid currents would constitute a heavy drain on the "B" and "C" batteries.

VARIATION OF NET RESISTANCE WITH TIME

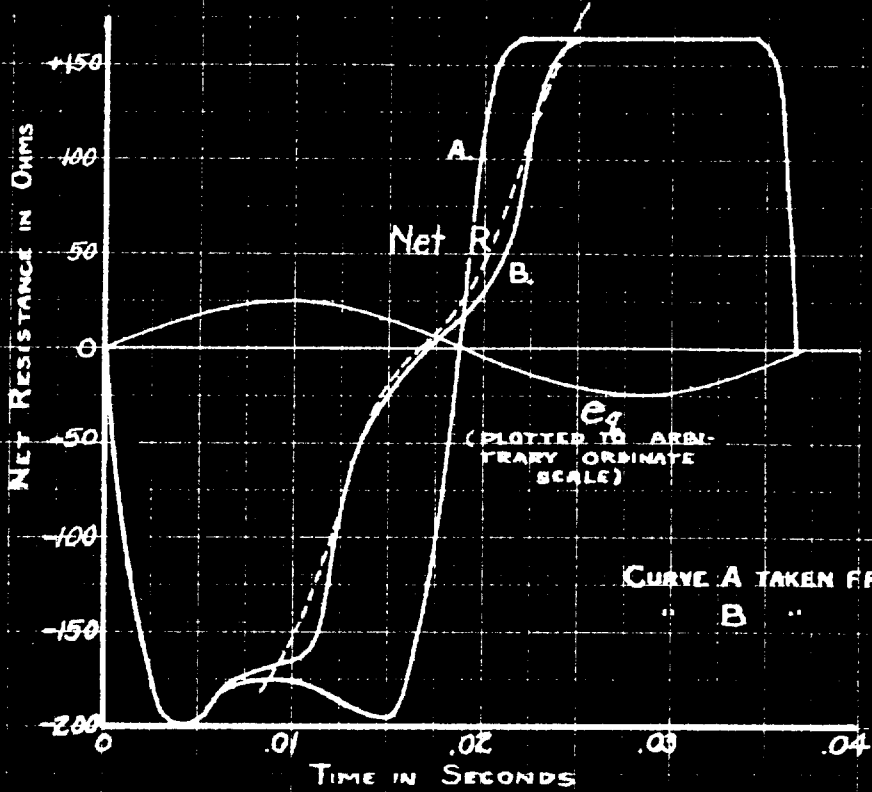


FIG. V-19

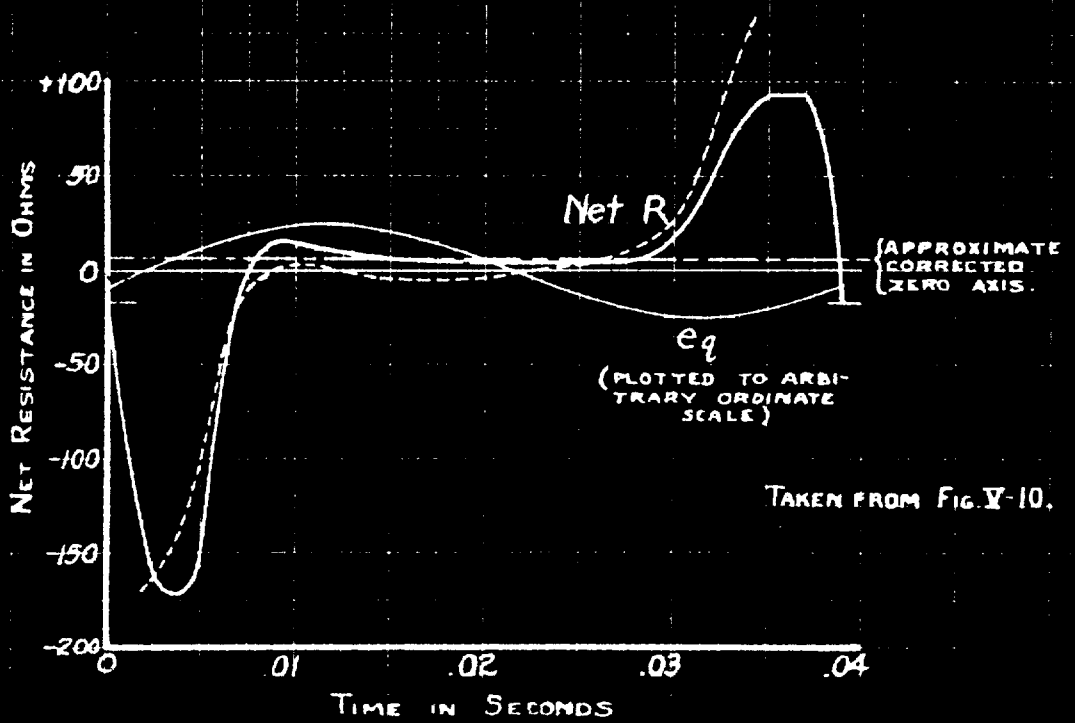


FIG. V-20

VARIATION OF NET RESISTANCE WITH TIME

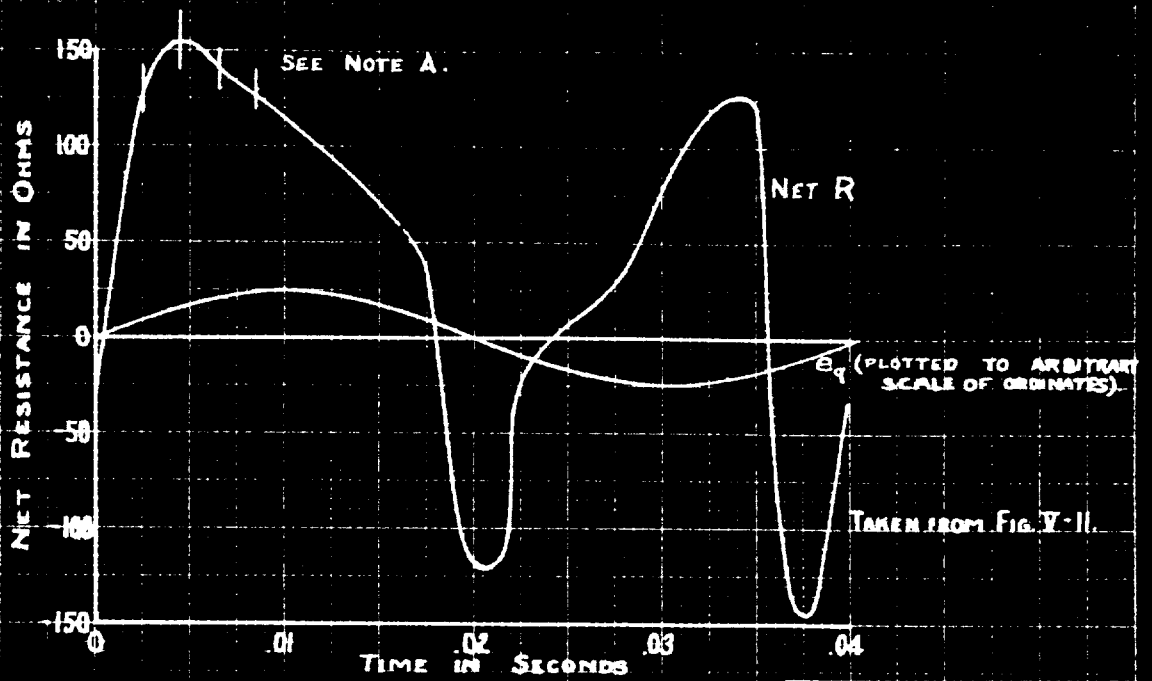


FIG. V-21

NOTE A:
VERTICAL BAR INDICATES UNCERTAINTY IN READING NEG. RESISTANCE ON CONTOUR SHEET

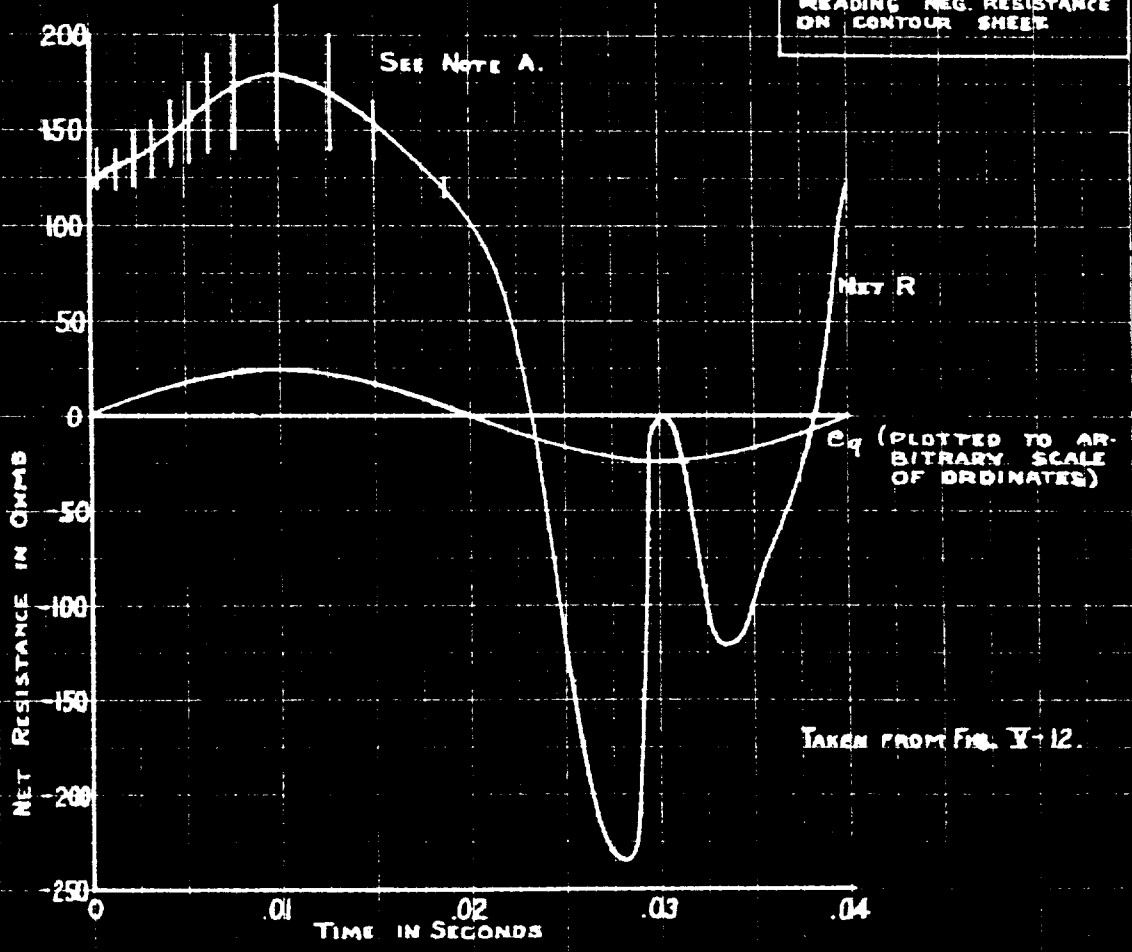


FIG. V-22

b. Plotting Net Resistance Versus Time:

With the operating loops plotted on negative-resistance charts, it is now a simple matter to construct plots showing the net resistance of the tuned circuit as a function of time during the quenching cycle. The procedure is simply to choose points at convenient intervals of time on the original oscillogram, refer to the corresponding points on the operating loop, read the negative resistance by interpolating between contours on the chart, subtract the positive resistance of the tuned circuit, and plot the resulting values of net resistance against the corresponding values of time.

Such plots are shown in Figs. V-19 to V-22, inclusive. They are drawn as solid curves, the dotted curves in Figs. V-19 and V-20 being obtained by another method, which will be considered later. A sinusoid representing quenching voltage is included in each of the four graphs; its amplitude has been chosen arbitrarily, but its period and phase are plotted correctly in order to show phase relations between quenching voltage and net resistance.

Fig. V-19 contains two plots, corresponding to the two operating loops in Fig. V-15 and hence to the two oscillograms in Figs. V-13 and V-14. These, it will be recalled, were taken under identical circuit conditions but with two different values of input signal voltage. The two curves of net resistance versus time are seen to coincide over a large part of their length. Such difference as does exist between them is evidence that saturation occurs when the larger signal voltage is supplied.

In Figs. V-21 and V-22, a series of vertical bars crossing the curves of net resistance may be observed. The portions of the curves in which these bars are found correspond to portions of the operating loops which passed beyond the outermost negative-resistance contours, in Figs. V-17 (a) and (b). It was necessary to extrapolate from the known contours to determine the negative resistance in this region. Such extrapolation could be little more than guesswork, so that considerable uncertainty was introduced in the process. The height of the vertical bars crossing the net-resistance curves is simply an indication of the magnitude of this uncertainty.

Of the four graphs showing net resistance as a function of time, Fig. V-19 is of the most practical interest, since the oscillograms from which it was constructed were taken with the circuit adjusted approximately as it would be in normal reception. It is perhaps surprising to find that the assumption of a square-wave variation of net resistance is not far from the truth after all, particularly in the case of the smaller input signal voltage. Certainly it is more accurate than assuming the variation to be sinusoidal. The conditions which must be satisfied in order that a sinusoidal quenching voltage shall produce a sinusoidal fluctuation of resistance are indeed exacting. Throughout the region traversed by the operating loop on the negative-resistance chart, the contours must be vertical and, in addition, uniformly spaced; that is, the distance between any two contours must be proportional to the difference between their respective values of negative resistance. A glance at the contour chart (see Fig. V-6)

shows that these requirements cannot be even approximately satisfied unless the instantaneous grid bias is restricted to a range of about -3 to -12 volts, and the oscillating current to about 5 milliamperes at the peak of the operating loop. Such a limitation of the dimensions of the operating loop would mean an unnecessary restriction of both the sensitivity and the output of a superregenerative receiver, and hence would not ordinarily be adopted in practice.

Fig. V-20, based on the oscillogram in Fig. V-10, shows the manner in which net resistance varies with time when "flat-topped" saturation occurs. The principal feature of the curve is seen to be an extended period (from $t = 0.009$ to $t = 0.028$ in the diagram) in which the net resistance is constant and very nearly zero. According to the readings of negative resistance on the operating loop in Fig. V-16, this constant value of net resistance is approximately +5 ohms, and is so shown in Fig. V-20. Reference to the oscillogram in Fig. V-10, however, shows that the amplitude of oscillation is slowly increasing, not decreasing, during the period of nearly-constant resistance. Consequently the net resistance must actually be slightly negative, rather than slightly positive. An error of this magnitude is not surprising, in view of the inaccuracy inherent in the entire procedure. In order to make the curve in Fig. V-20 approach more closely to the truth, a "corrected" axis of zero net resistance has been inserted in such a position as to make the horizontal portion of the curve slightly negative.

The next graph of net resistance versus time, Fig. V-21, is

based on the oscillogram in Fig. V-11 and the "figure-of-eight" operating loop in Fig. V-17. The existence of two damping and two "dedamping" periods in each quenching cycle, when the d.c. grid bias and quenching voltage are adjusted as they were in this case, is clearly demonstrated by the form of the net-resistance plot.

In the last graph, Fig. V-22, which is based on the oscillogram in Fig. V-12 and the corresponding operating loop in Fig. V-17, most of the distinguishing features of the preceding graph (Fig. V-21) may still be discerned. The first positive-resistance lobe has been accentuated, however, while the second has been reduced in height and duration until it is only a momentary interruption between the two negative-resistance lobes. In general form the curve in Fig. V-22 is seen to be the direct reverse of that in Fig. V-19, the positive- and negative-resistance half-cycles coming in the opposite order.

The four graphs just described, showing net resistance of the tuned circuit as a function of time during the quenching cycle, all have one feature in common. Because they were constructed with the aid of a negative-resistance contour chart, they are only as valid as the original assumption (see page 70) that these contours, constructed from measurements taken under steady-state conditions, could be employed in a study of superregenerative operation. While this assumption was not adopted until it had been proved on theoretical grounds, it would still be desirable to check it experimentally. Such a check is afforded by the step described in the following section.

c. Direct Plotting of Net Resistance versus Time:

A method of plotting the net resistance of the tuned circuit as a function of time directly from oscillographic data, without recourse to the negative-resistance contour chart, is suggested by the fundamental equation

$$\frac{I}{I_{osc}} \cdot \frac{dI_{osc}}{dt} = - \frac{R_{net}}{2L}$$

Rearranging the equation and substituting the numerical value of L used in the experimental low-frequency receiver,

$$R_{net} = - \frac{2L}{I_{osc}} \cdot \frac{dI_{osc}}{dt} = - \frac{0.280}{I_{osc}} \cdot \frac{dI_{osc}}{dt}$$

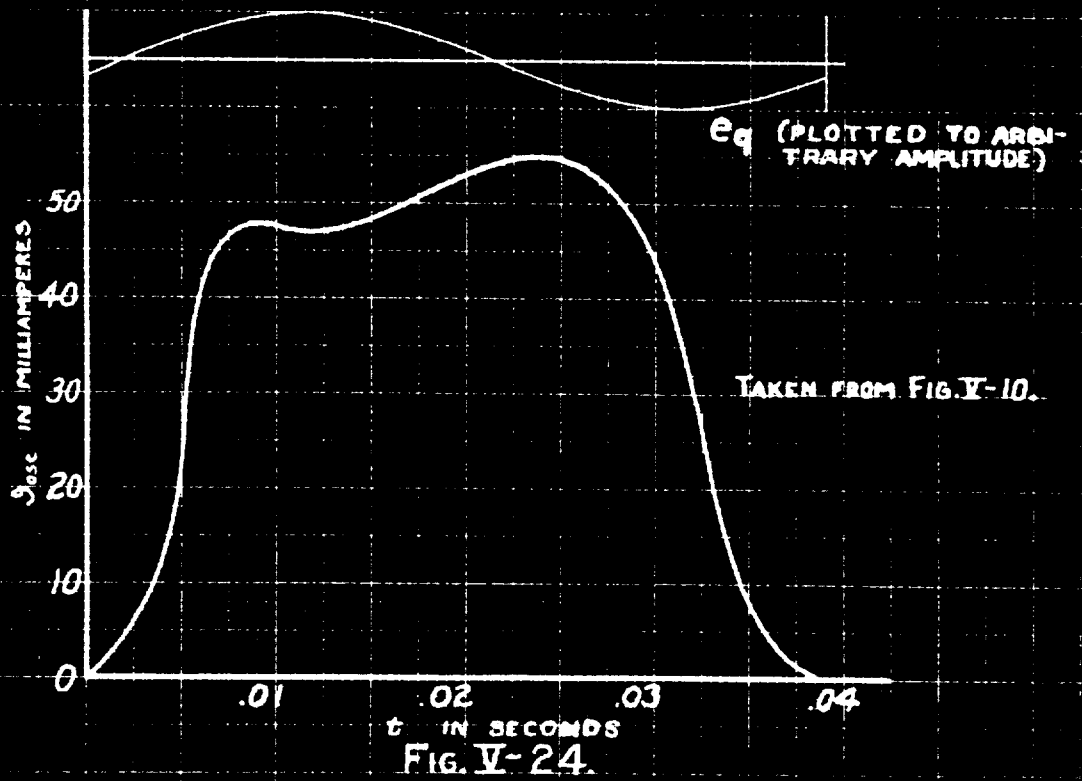
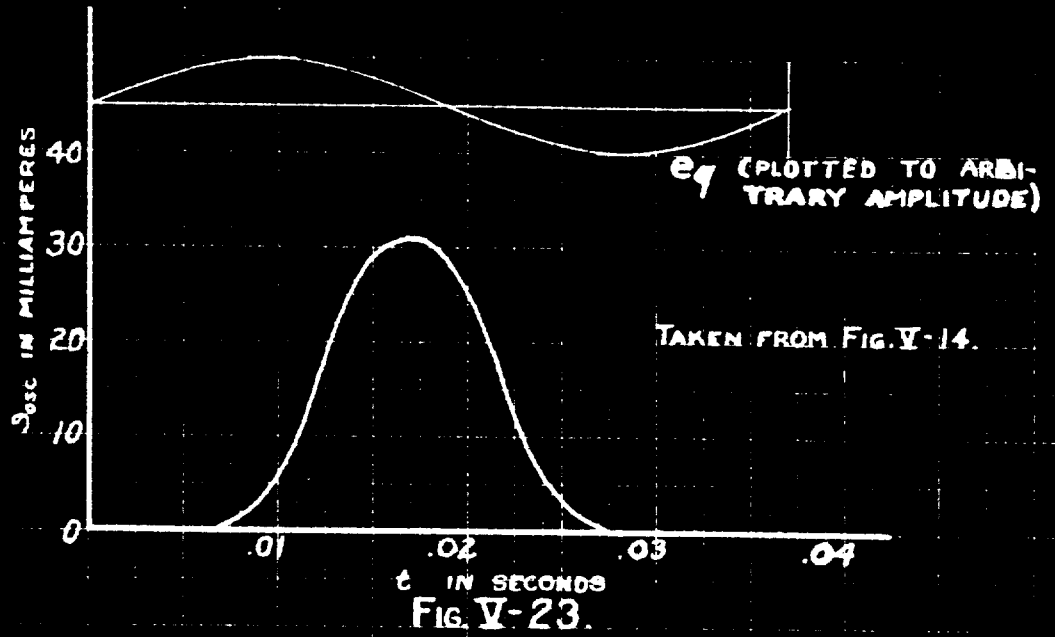
This means that, in order to determine the net resistance at any point in the quenching cycle, it is necessary only to measure the amplitude and slope of the envelope at that point on the oscillogram, convert these into terms of milliamperes and milliamperes per second, and substitute them into the above equation.

As a matter of convenience in making the measurements, it is desirable to transfer the envelope of oscillations from the oscillogram to a piece of graph paper. Only one-half of the envelope need be so transferred.

This procedure has been carried out for the oscillograms of Figs. V-10 and V-14. The envelopes, plotted on graph paper, appear in Figs. V-23 and V-24. From these, curves of net resistance have been plotted with the aid of the above equation. They are shown dotted in Figs. V-19 and V-20.

The principal shortcoming of the method is the fact that I_{osc} and dI_{osc}/dt cannot be measured with adequate accuracy at points on the

ENVELOPES OF OSCILLATIONS



oscillogram where the envelope is less than about 0.3 inch wide. Consequently the dotted curves in Figs. V-19 and V-20 could be drawn through only a portion of the quenching cycle. As far as they go, however, they are in fairly good agreement with the curves plotted by means of the negative-resistance contour chart. The greatest discrepancies occur at points in the quenching cycle where the amplitude of oscillation was small and the measurements of \mathcal{J}_{osc} and $\frac{d\mathcal{J}_{osc}}{dt}$ were relatively inaccurate.

It therefore appears safe to place confidence in the negative-resistance-contour method of plotting net resistance versus time. A theoretical foundation for the method has been presented earlier, and results obtained by means of it have now been checked experimentally.

The superregenerative process has now been discussed in considerable detail. The next step will be to examine the operating characteristics of the superregenerative receiver and to explain them in terms of the mechanics of superregeneration.

C. OPERATING CURVES

In order to obtain quantitative information on the operating characteristics of the low-frequency experimental receiver, an extensive series of measurements was undertaken. These measurements were of the following two types:

1. "Modulation characteristics", or curves of oscillating current versus input signal voltage.

2. Curves of oscillating current versus quenching frequency.

The procedures employed in obtaining these curves, as well as the significant points revealed by them, will be described in the following pages.

1. Modulation Characteristics:

a. Definition:

The term "modulation characteristic", applied to a superregenerative receiver, was first used by Hassler (see page 253). He gave this name to a curve having coordinates as follows. The abscissa was the logarithm of the input signal voltage. The ordinate was the d.c. current obtained by demodulation of the oscillations in the tuned circuit, and, since Hassler used a square-law detector, was proportional to the square of the r.m.s. oscillating current.

The modulation characteristic is one of the most significant pieces of information that can be given for a receiver, whether superregenerative or of any other type. From it can be read the d.c. output produced by a continuous-wave signal of any magnitude. If the input signal is modulated, the modulation characteristic can be used to determine the amplitude of, as well as the distortion in, the audio-frequency output of the detector. The effect of varying either the magnitude or the percent modulation of the input signal, or both, can readily be observed with the aid of the curve. Consequently an

important place in the present investigation was assigned to the taking of modulation characteristics of the low-frequency experimental receiver, with various combinations of circuit parameters and applied voltages.

Certain departures from Hassler's definition of a modulation characteristic were found advantageous. In the first place, most of the curves taken were plotted against the signal voltage itself, rather than against the logarithm of the signal voltage. One purpose of this change was to make the linearity or non-linearity of the relation between the input signal and the resulting amplitude of oscillations as conspicuous as possible. This feature was desired in order to facilitate explaining the shapes of the modulation characteristics in terms of the mechanism of the superregenerative process, discussed in the preceding section of this chapter.

Further deviations from Hassler's definition of "modulation characteristic" were made in the choice of ordinates. In the greater part of the curves plotted, the vertical coordinate represented oscillating current, as indicated by a milliammeter in the tuned circuit, instead of d.c. current resulting from demodulation. This change was made in order to limit the scope of the modulation characteristic to the superregenerative process alone, eliminating the action of the detector from consideration.

The procedure employed in taking the modulation characteristics was quite simple. The plate voltage, grid bias voltage, quenching frequency, quenching voltage and resistance in the tuned circuit were first adjusted to the desired values. The input signal voltage

was then varied in convenient steps from zero to maximum (about 18 millivolts) by adjusting R_s and R_{sig} (see Fig. IV-3 (b), and the oscillating current was read at each step. Whenever R_{sig} was changed, an equal and opposite change was made in R_{adj} in order to keep the total positive resistance constant.

Most of the readings of oscillating current were taken with a thermal milliammeter. The choice of this type of instrument was largely one of convenience. It was desired merely that the milliammeter be sufficiently sluggish to prevent the needle from following the rise and fall of oscillations during the individual quenching cycles. A thermal instrument fulfilled this requirement quite satisfactorily.

During a few runs, however, readings were taken on a rectifier-type milliammeter as well as on the thermal instrument. In addition, a few of the modulation characteristics taken with the thermal milliammeter were replotted in the form used by Hassler; that is, the scale of abscissae was made logarithmic, and the scale of ordinates was changed to read I_{osc}^2 instead of I_{osc} .

b. Experimental Results:

Modulation characteristics of the types described above were taken with the low-frequency experimental receiver, for a variety of combinations of the following variables: quenching voltage, quenching frequency, grid bias voltage, and positive resistance in the tuned

circuit. A plate supply potential of 100 volts was used throughout the measurements.

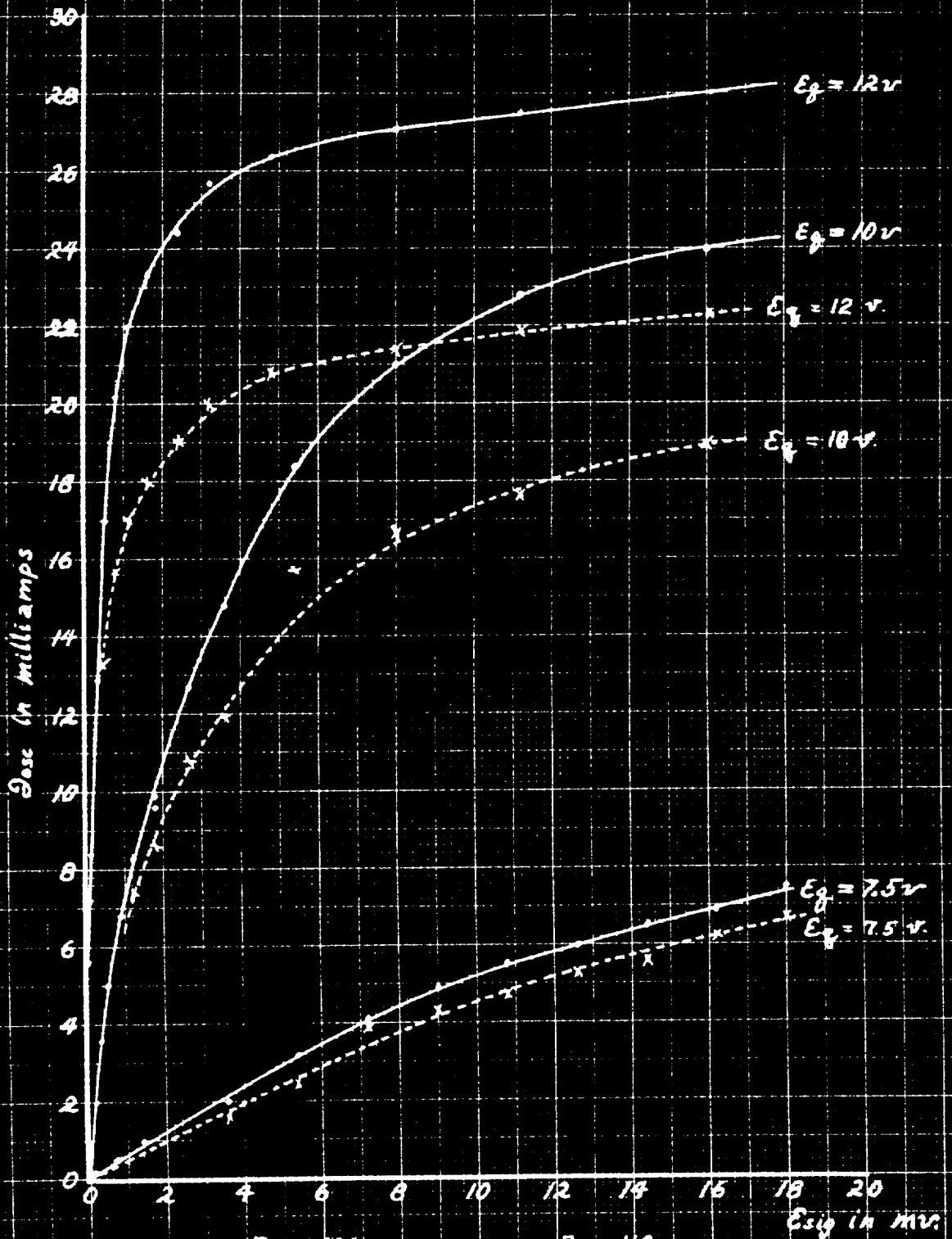
These curves are shown in the series of graphs, Figs. V-25 to V-39, inclusive. The solid curves in Figs. V-25 to V-36, inclusive, show r.m.s. oscillating current as a function of signal voltage. The dotted curves in Figs. V-25, V-26, V-31 and V-32 represent a similar function, except that the current readings were taken with the rectifier-type milliammeter. Figs. V-37, V-38 and V-39 contain the same information as Figs. V-25, V-31 and V-32, but employ Hassler's coordinates; \mathcal{E}_{sig} being plotted logarithmically, and \mathcal{I}_{osc}^2 replacing \mathcal{I}_{osc} as ordinate.

Data on the circuit conditions represented by these curves is tabulated on the graphs. The several curves in each figure were taken with different values of quenching voltage, but otherwise under identical conditions.

It should be understood that the values of \mathcal{I}_{osc} used in plotting all of these curves are mean values; that is, they correspond to the average position of the milliammeter needle during a period of several seconds' duration. In general it was observed that at low values of signal voltage the indication of the milliammeter shifted about in a random manner, but that it became steady at higher values of signal voltage. In a few of the measurements the needle fluctuated so irregularly and over such a wide range that it was difficult to estimate its mean position. In such cases (see Figs. V-34, V-35 and V-36) the value of \mathcal{I}_{osc} for a given \mathcal{E}_{sig} has been indicated on the graph by a vertical bar instead of by a single point. The length of

Fig. V-25

DEPENDENCE OF OSCILLATING CURRENT ON INPUT VOLTAGE



$E_p = 100v$
 $E_g = -15v$

$R = 110 \Omega$
 $f_g = 750 \text{ rpm}$

— Thermal Meter
 - - - Rectifying Meter

FIG. V-26

DEPENDENCE OF OSCILLATING CURRENT ON INPUT VOLTAGE

$E_p = 100 \text{ v}$

$R = 110 \text{ } \Omega$

$E_g = -10 \text{ v}$

$f_g = 750 \text{ rpm}$

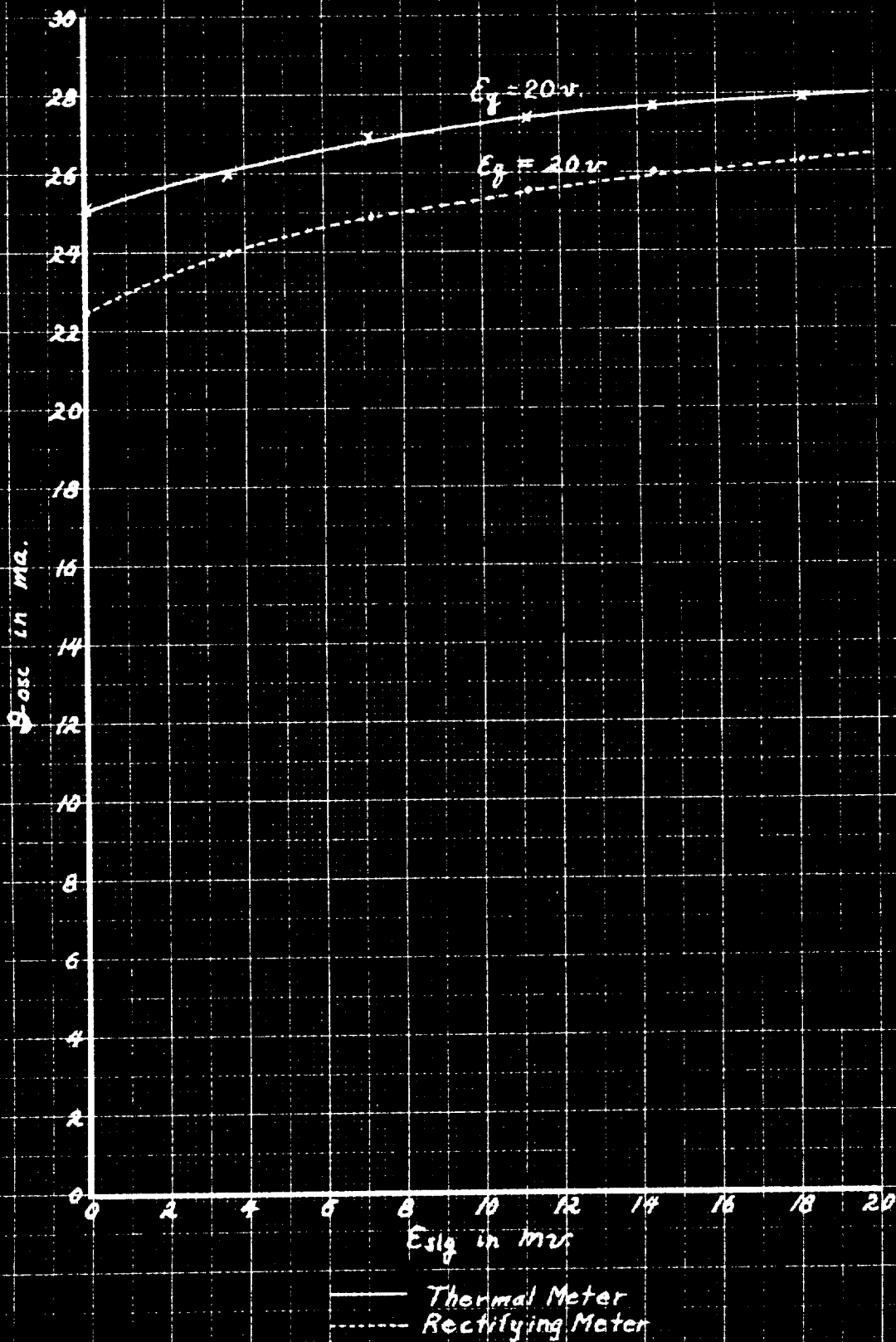


FIG. V-27

DEPENDENCE OF OSCILLATING CURRENT ON INPUT VOLTAGE

$E_p = 100v$

$R = 110 \omega$

$E_g = -25v$

$f_g = 750 \text{ rpm}$

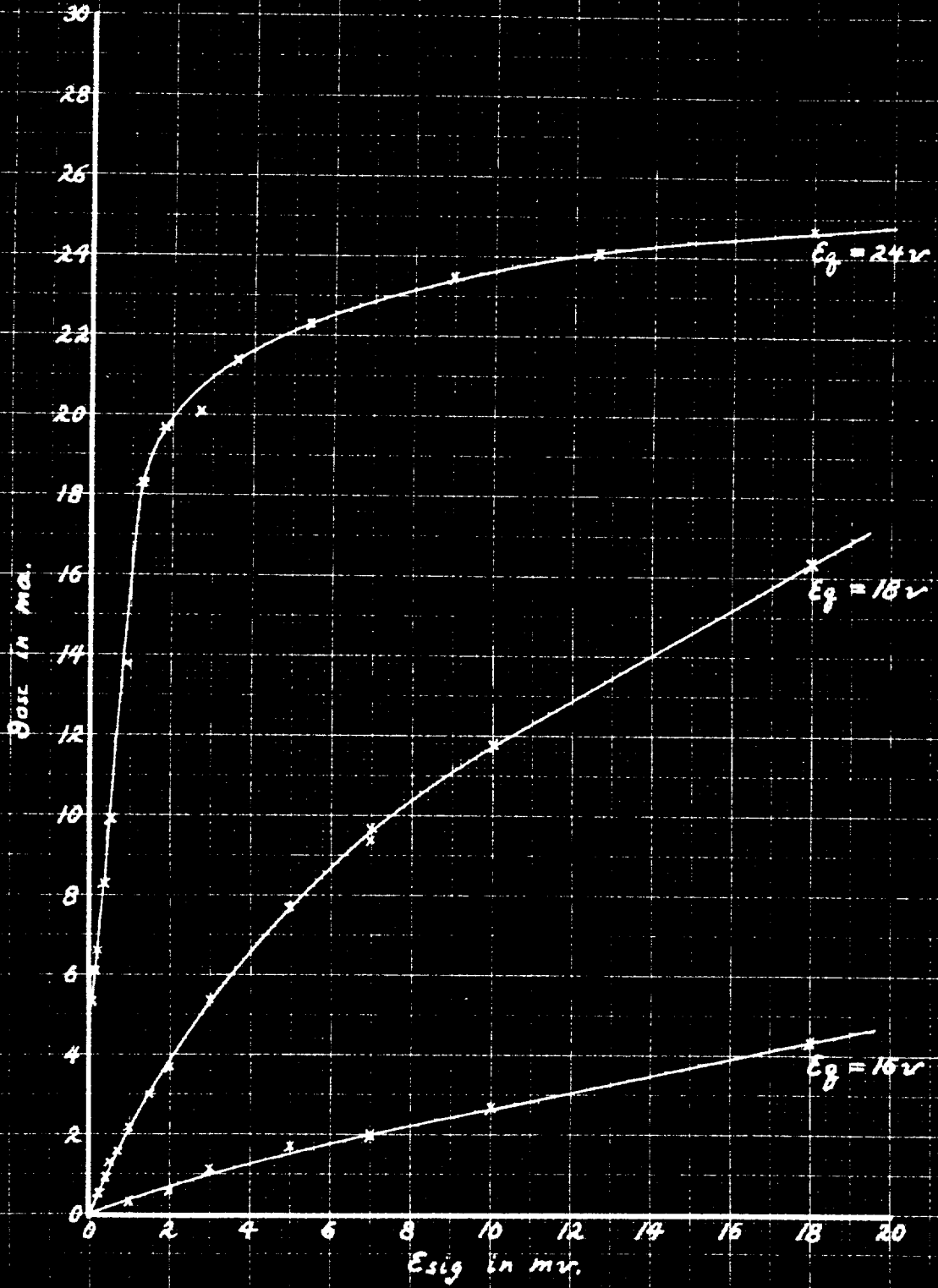


FIG. V-28
 DEPENDENCE OF OSCILLATING CURRENT ON INPUT VOLTAGE

$E_p = 100 \text{ v}$ $R = 110 \Omega$
 $E_g = -45 \text{ v}$ $f_g = 750 \text{ rpm}$

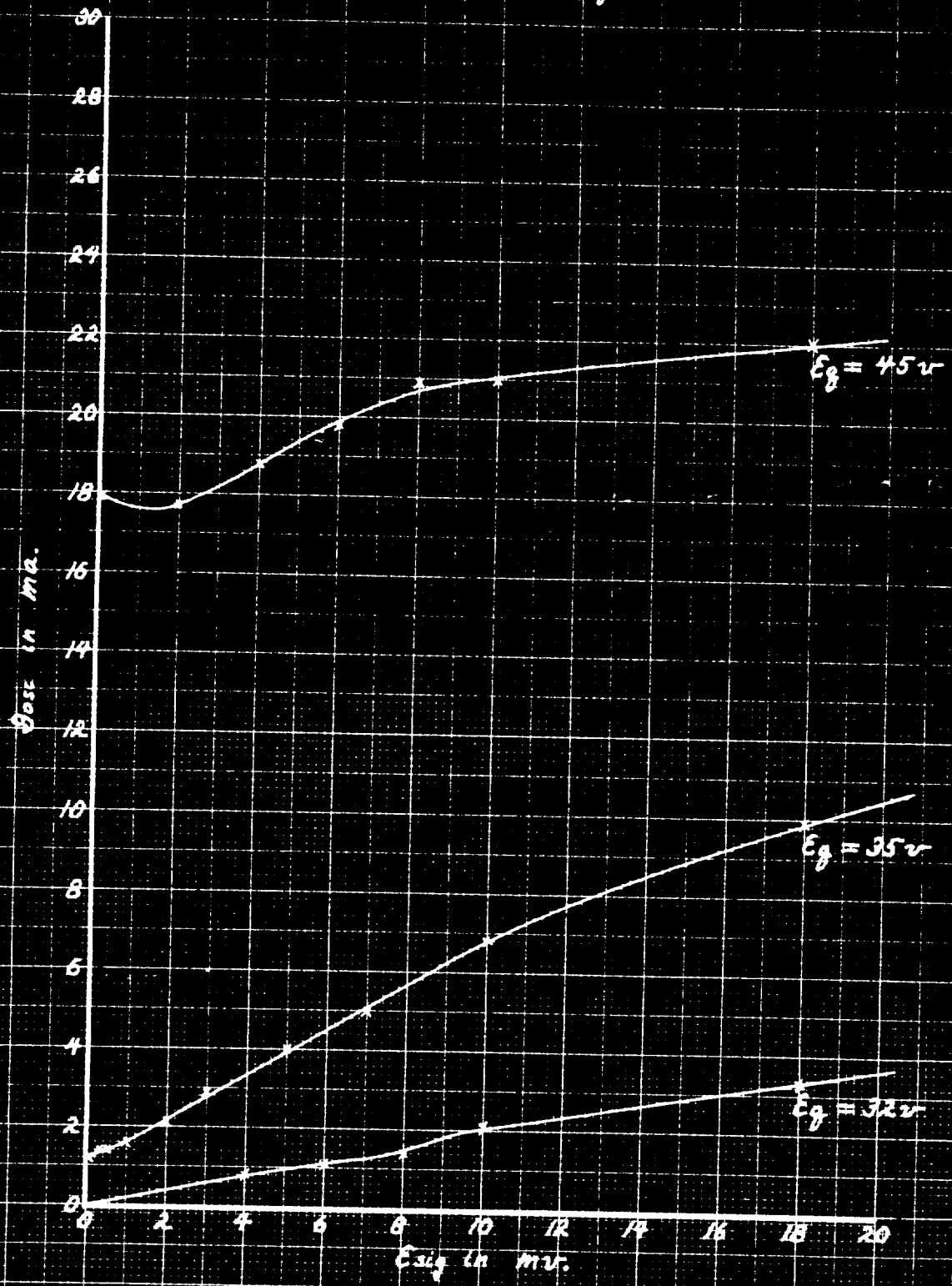


FIG. V-29

DEPENDENCE OF OSCILLATING CURRENT ON INPUT VOLTAGE

$E_p = 100 \text{ v}$

$R = 80 \ \Omega$

$E_g = -25 \text{ v}$

$f_g = 250 \text{ rpm}$

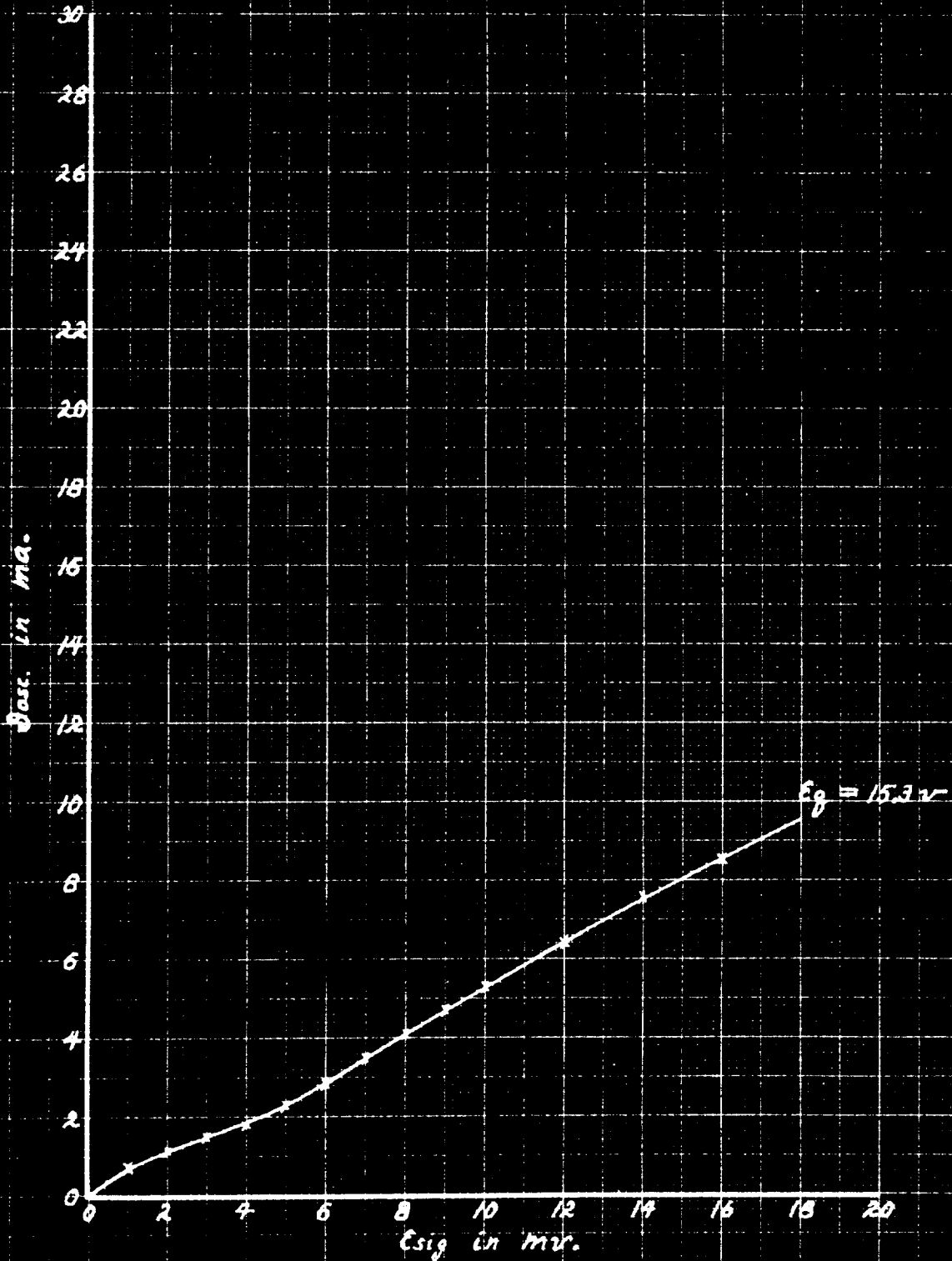


FIG. V-30

DEPENDENCE OF OSCILLATING CURRENT ON INPUT VOLTAGE

$E_p = 100\text{ v}$

$R = 80\ \Omega$

$E_g = -40\text{ v}$

$f_g = 750\text{ rpm}$

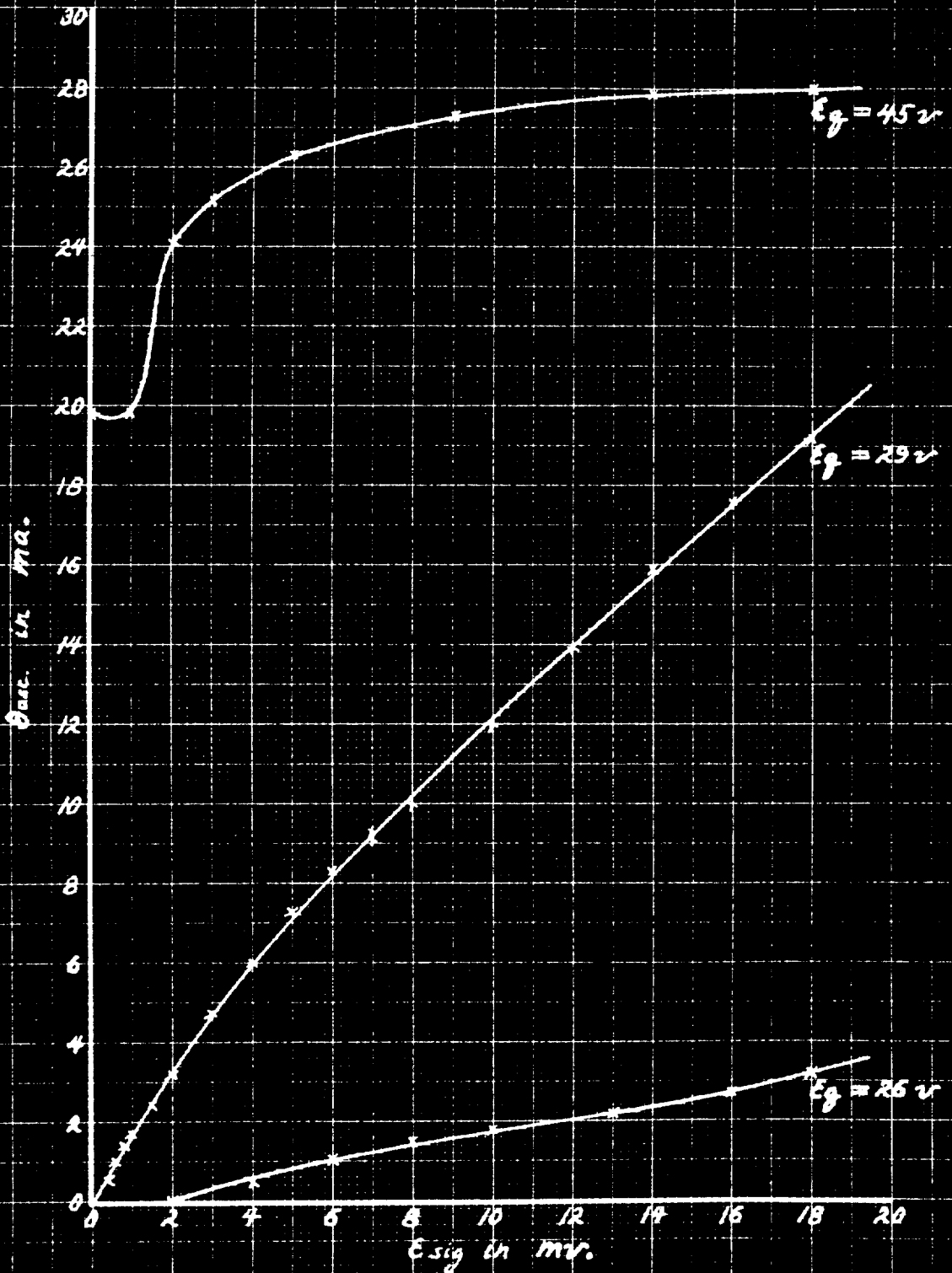


FIG. Y-31

DEPENDENCE OF OSCILLATING CURRENT ON INPUT VOLTAGE

$E_p = 100\text{ v}$

$R = 160\ \Omega$

$E_g = +10\text{ v}$

$f_g = 750\text{ rpm}$

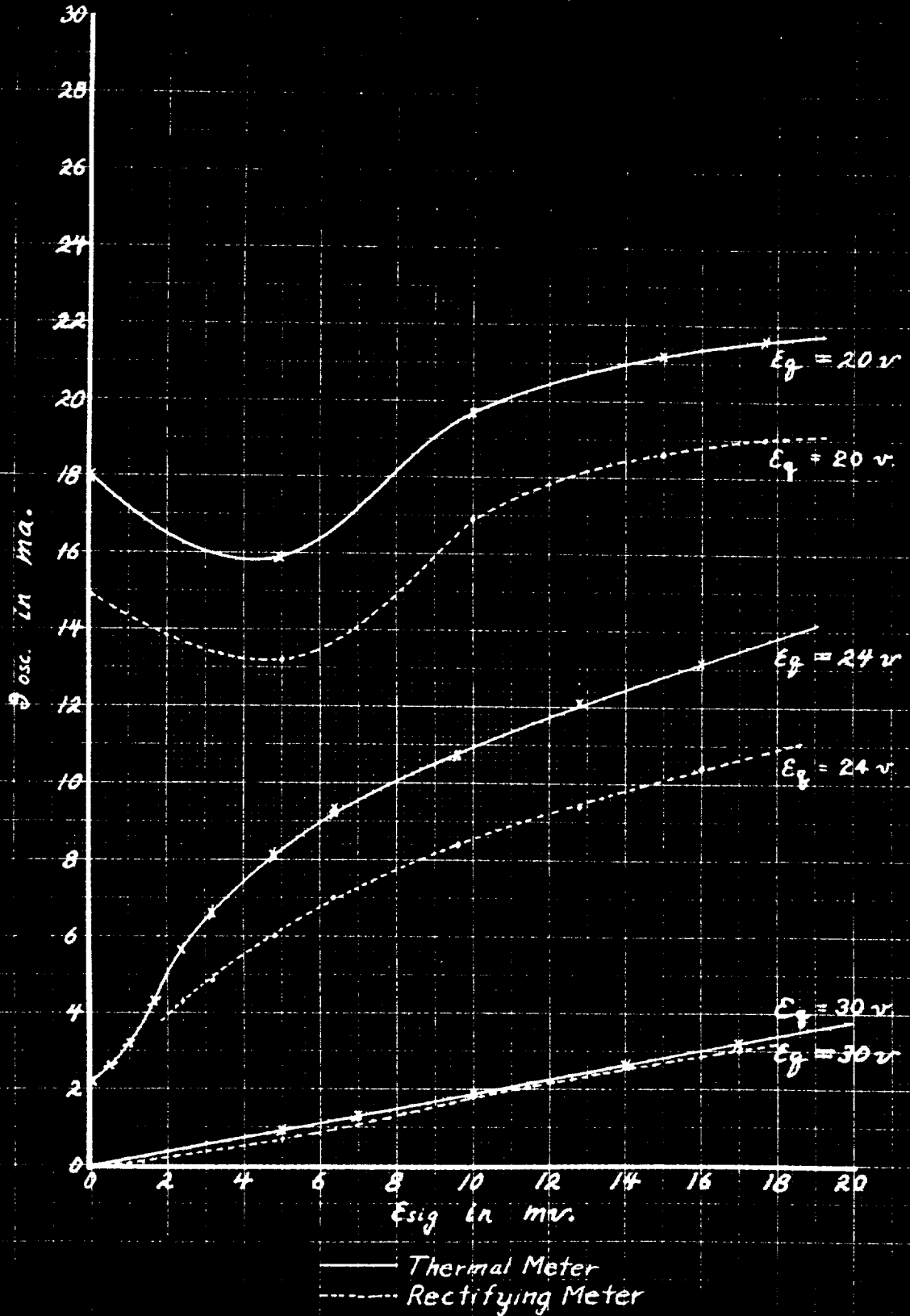


FIG. V-32

DEPENDENCE OF OSCILLATING CURRENT ON INPUT VOLTAGE

$E_p = 100 \text{ v}$

$R = 160 \ \omega$

$E_g = -7.5 \text{ v}$

$f_g = 750 \text{ rpm}$

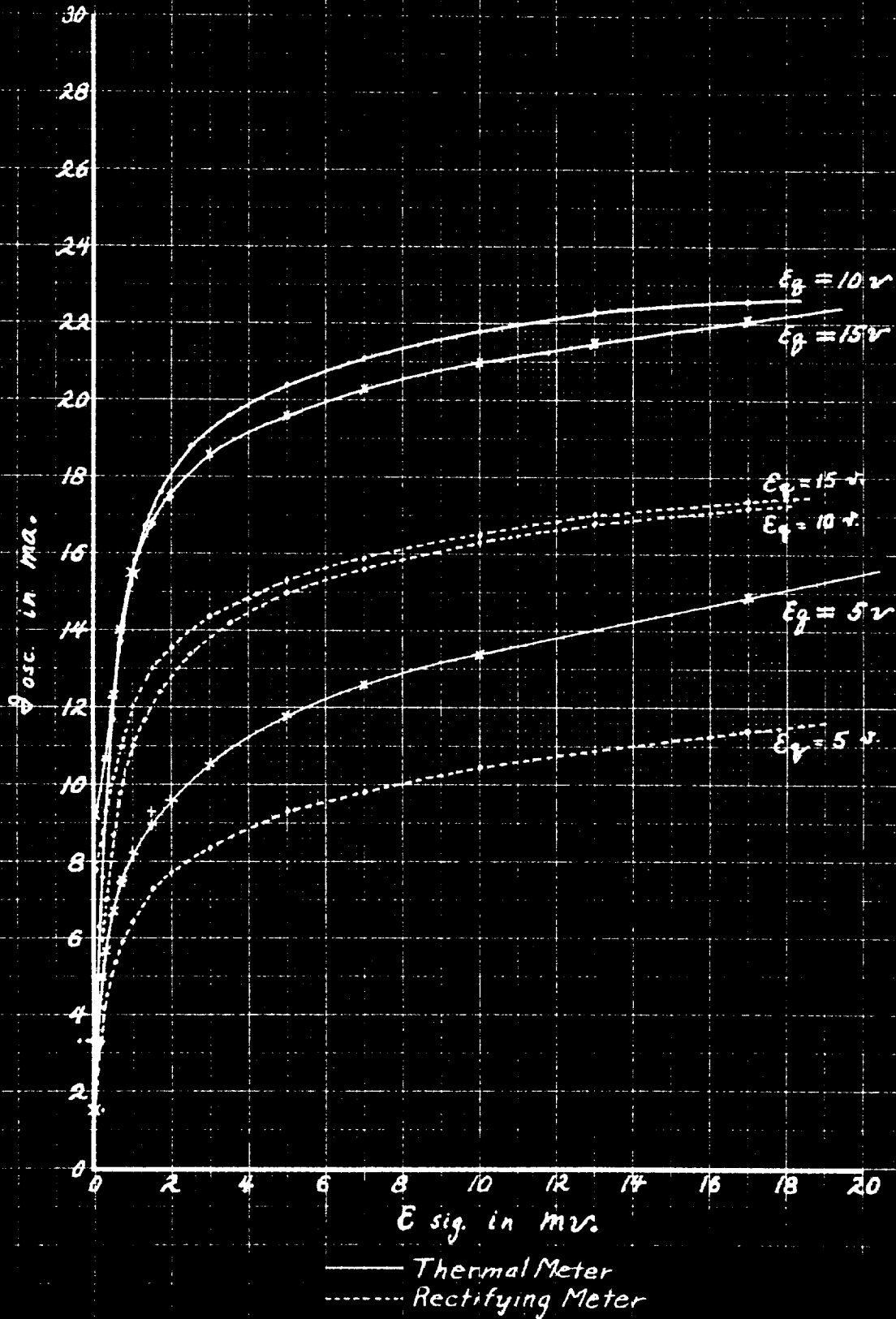


FIG. IX-33

DEPENDENCE OF OSCILLATING CURRENT ON INPUT VOLTAGE

$E_p = 100 \text{ v}$

$R = 160 \text{ } \Omega$

$E_g = -20 \text{ v}$

$f_g = 750 \text{ rpm}$

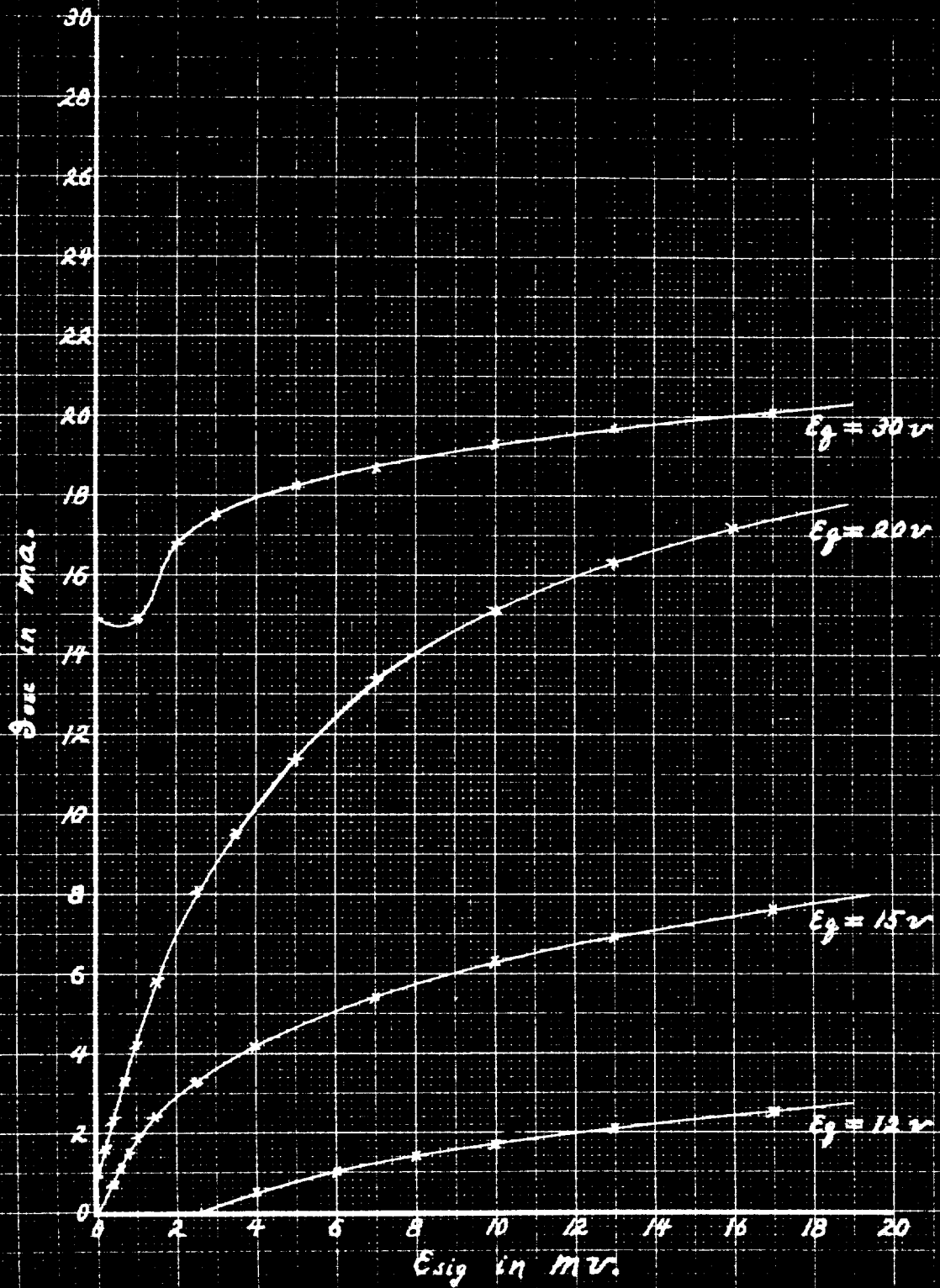


FIG. V-34

DEPENDENCE OF OSCILLATING CURRENT ON INPUT VOLTAGE

$E_p \approx 100 \text{ v}$

$R = 110 \ \Omega$

$E_g = -15 \text{ v}$

$f_g = 300 \text{ rpm}$

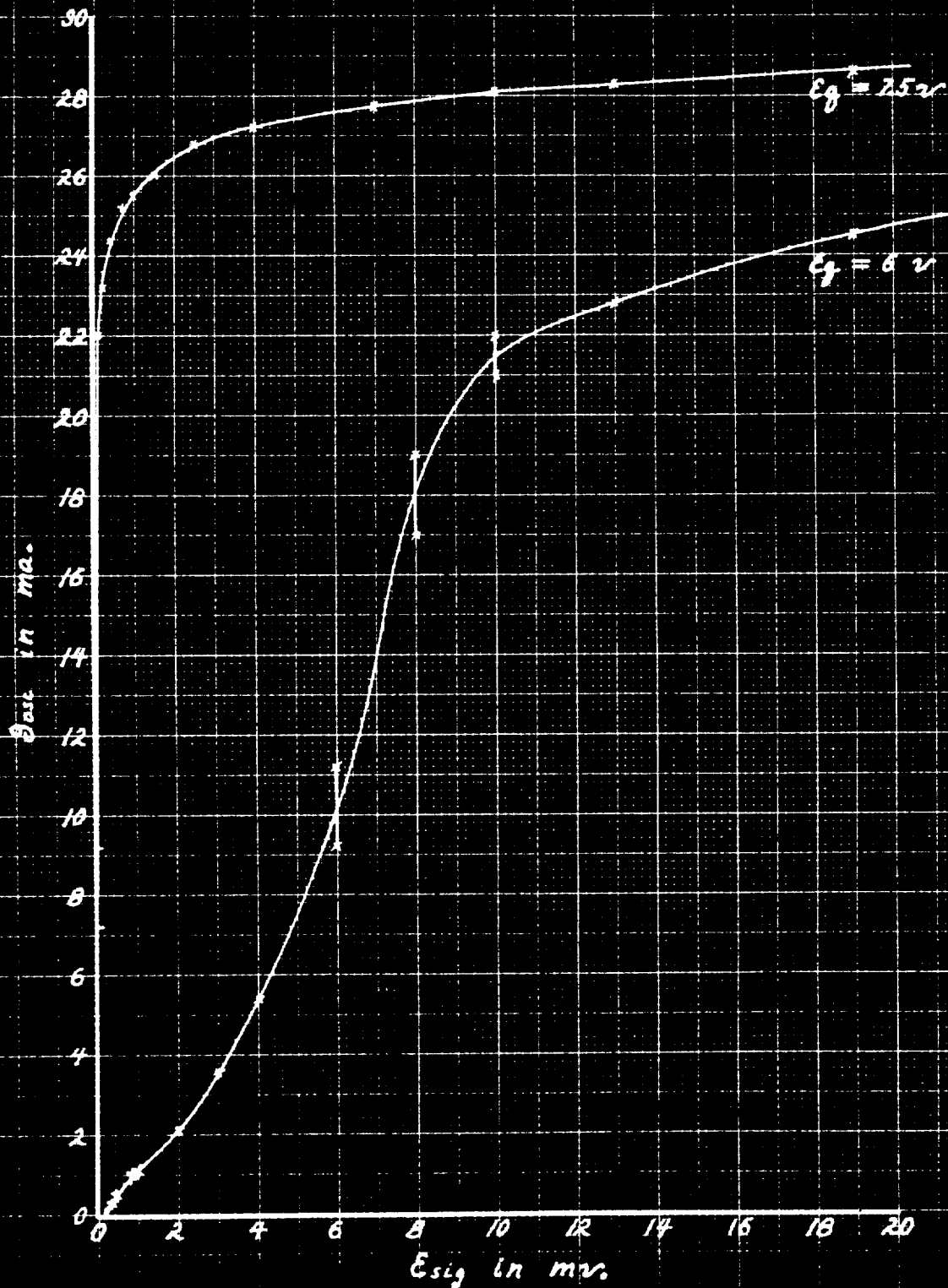


FIG. V-35

DEPENDENCE OF OSCILLATING CURRENT ON INPUT VOLTAGE

$E_p = 100 \text{ v}$ $R = 110 \text{ } \Omega$
 $E_g = -10 \text{ v}$ $f_g = 300 \text{ rpm}$

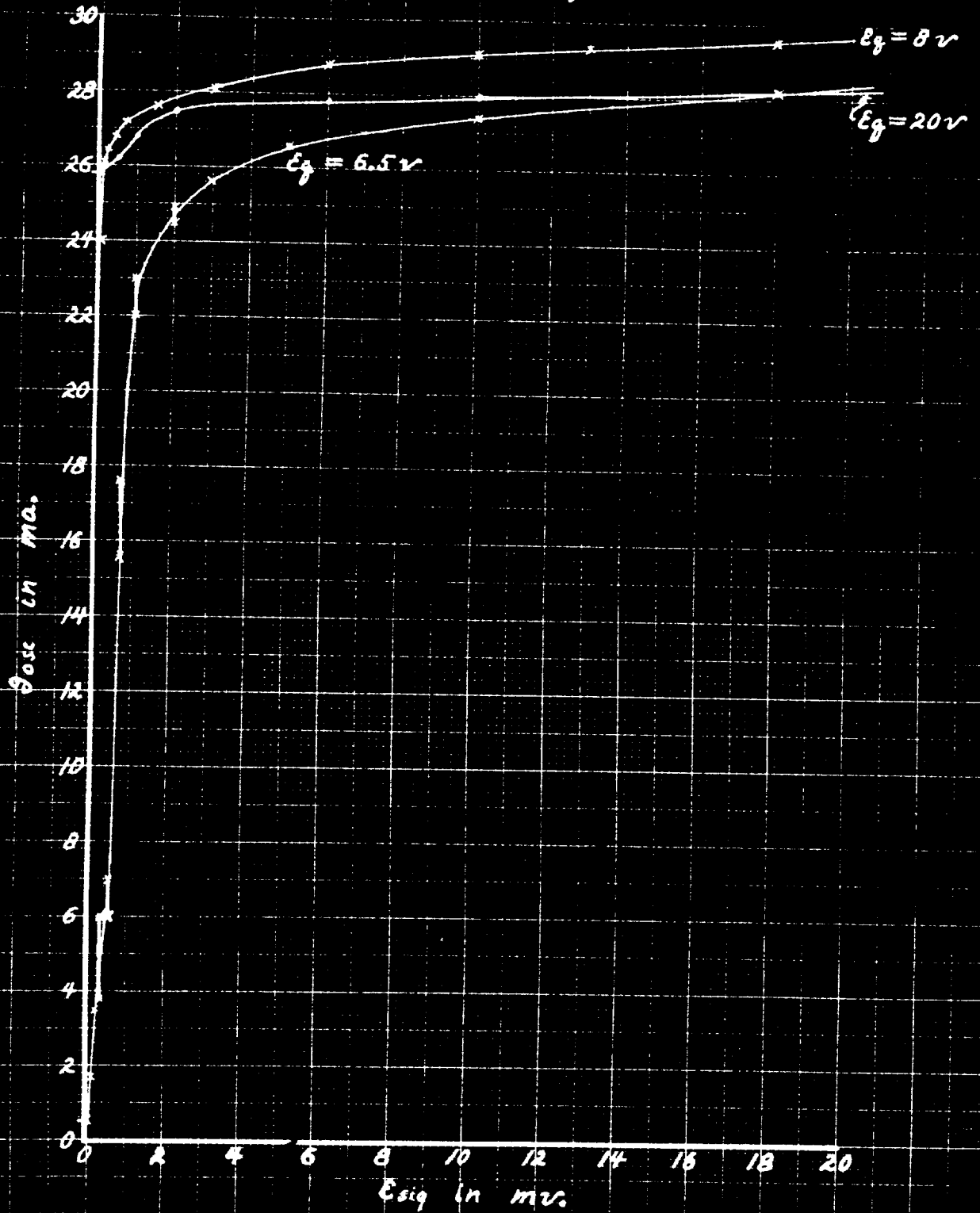


FIG. V-36

DEPENDENCE OF OSCILLATING CURRENT ON INPUT VOLTAGE

$E_p = 100 \text{ v}$

$R = 110 \ \Omega$

$E_g = -2.5 \text{ v}$

$f_g = 300 \text{ rpm}$

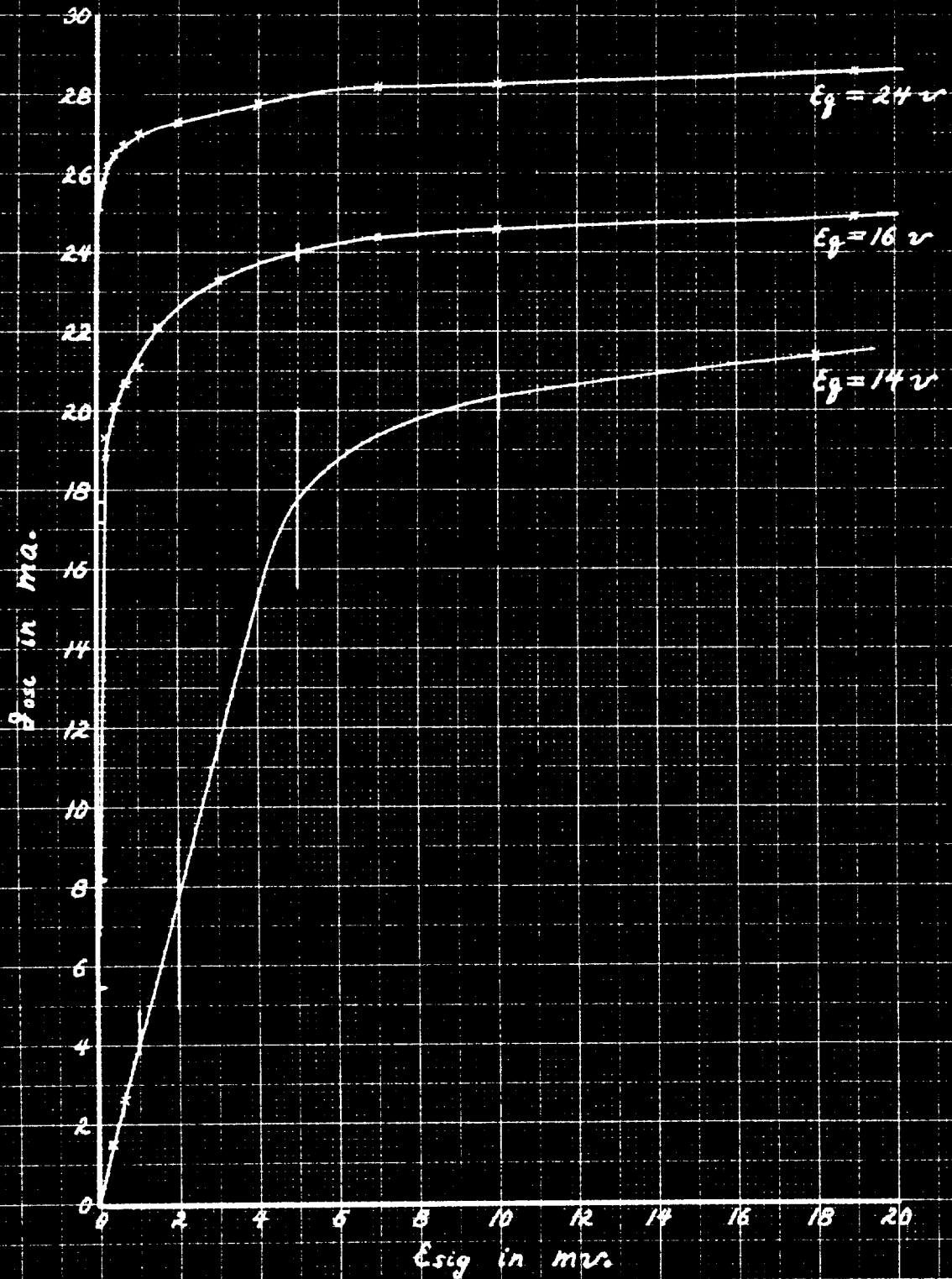


FIG. I-37

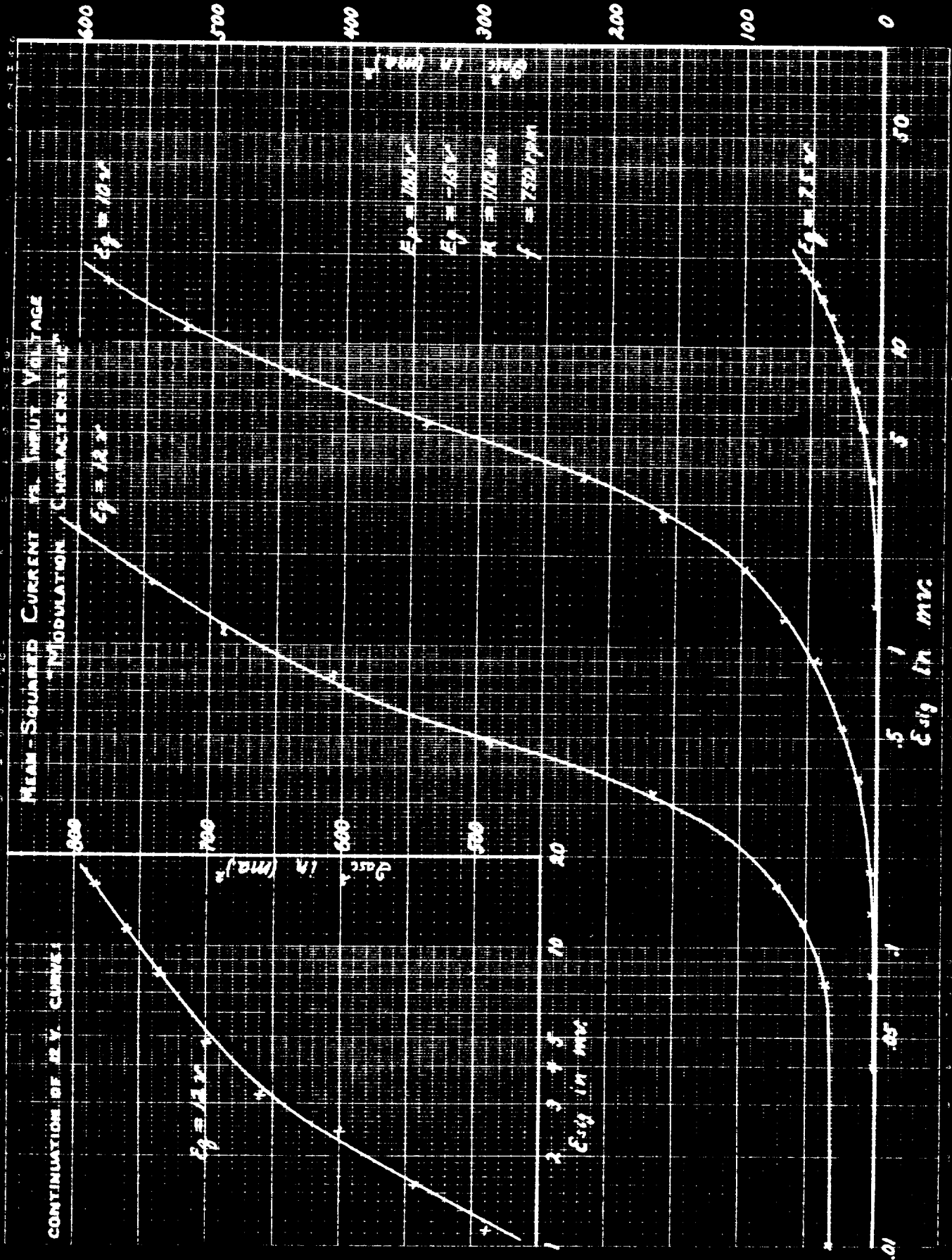


FIG. Y-38
 MEAN-SQUARED OSCILLATING CURRENT
 vs. INPUT VOLTAGE

"MODULATION CHARACTERISTIC"

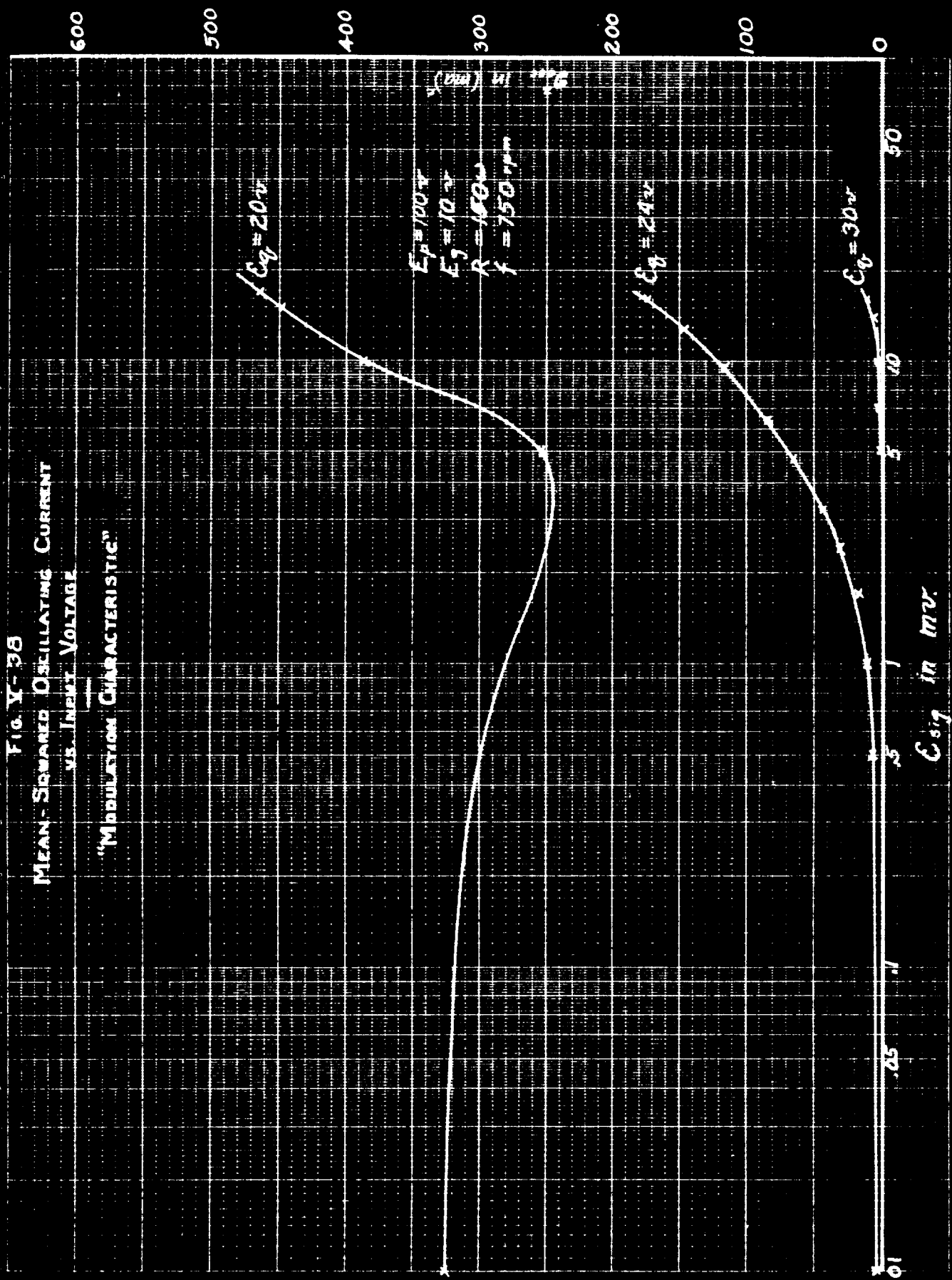
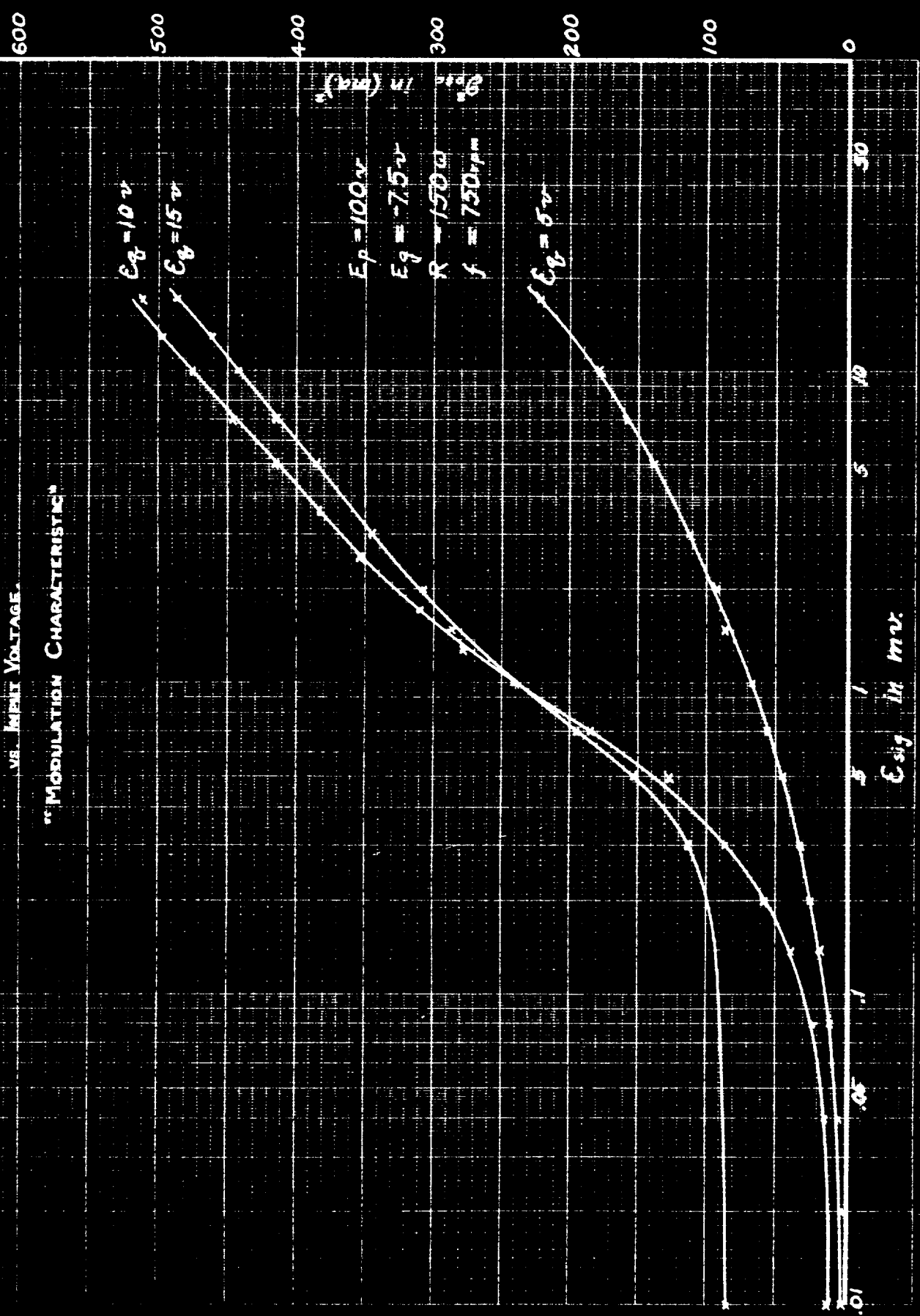


Fig. Y-39
 MEAN-SQUARED OSCILLATING CURRENT
 VS. INPUT VOLTAGE.

"MODULATION CHARACTERISTIC"



the bar is a measure of the range of uncertainty within which the mean value of oscillating current was thought to lie.

Another type of fluctuation was observed during certain of the measurements. In Figs. V-28, V-30, V-31 and V-33, some of the curves commence with negative slopes and shortly thereafter reach minimum values which are appreciably smaller than the values at zero signal voltage. In the vicinity of the "sag" in each of these curves, it was observed on the cathode-ray oscillograph that the amplitude of oscillations was fluctuating up and down with marked regularity, in such a manner as to suggest a heterodyne action between two voltages of slightly different frequencies. The value of \mathcal{J}_{osc} indicated by the milliammeter and shown on the curve under these conditions was again a mean value, taken over a period of several fluctuations.

c. Discussion:

In considering the foregoing group of modulation characteristics it will be convenient to divide the discussion into two parts. The first of these will be devoted to an explanation of the salient features of the curves in terms of the mechanics of superregeneration. In the second part, the relation between the shape of the curves and the operating characteristics of the receiver will be discussed.

Explanation of Form of Curves:

From a survey of the curves in Figs. V-25 to V-36, inclusive, it is possible to identify a certain shape of curve as the basic form

of the modulation characteristic of a superregenerative receiver. As the signal voltage is increased from zero, the curve first passes through a region in which it is very nearly linear, the slope depending upon the adjustment of the receiver. Then comes a portion of the curve which is more or less sharply curved, and finally comes a region in which the curve continues with relatively little curvature. Taken as a whole, the modulation characteristic bears a marked resemblance to the magnetization curve of iron.

In the first of these three sections, the linearity of the curve indicates that the amplitude of oscillation attained during the building-up period is proportional to the signal voltage. This means that the receiver is operating in such a way that the negative resistance supplied by the tube is independent of the amplitude of oscillation; in other words, it is a function of quenching voltage (or, more correctly, instantaneous grid bias) only. In terms of the negative-resistance contour chart, linear operation means that in the region in which the operating loop is located, all the contours are vertical, straight lines. Reference to the contour chart in Fig. V-6 shows that this condition is approximately realized with almost any value of instantaneous grid bias, provided the oscillating current is not greater than about 5 milliamperes; but that in order for it to be realized with values of oscillating current ranging up to, say, 20 milliamperes, the instantaneous bias voltage must be restricted to specified ranges.

For example, if the receiver is to be operated in the conven-

tional manner, with the grid biased negatively, then that portion of the operating loop which extends above approximately 5 milliamperes of oscillating current must be confined to the region between $E_g = -10$ and $E_g = -5$, in order to secure a moderately good approximation of the condition set forth in the previous paragraph. Fortunately, the departure from linearity caused by even a rather large deviation from this condition is not very great. This is obvious from the fact that the linear portions of many of the curves run up to as high as 18 or 20 milliamperes of oscillating current, as indicated by the milliammeter; this of course is equivalent to a much higher amplitude at the peak of the envelope.

If, on the other hand, the grid is to be biased positively by about 25 volts, it appears that a considerably wider range of values of instantaneous bias would be permissible. The contours are seen to be approximately vertical throughout a triangular-shaped area with its base on the axis of grid bias voltage, extending from $E_g = 0$ to $E_g = +40$, and its peak at approximately 30 milliamperes and +25 volts. While no modulation characteristics were taken with a positive grid bias as large as this, it is reasonable to suppose that such a characteristic would reveal linear operation up to a considerable amplitude of oscillating current.

The slope of the linear portion of a modulation characteristic is determined by the average net resistance during the building-up period, and by the length of this period. The first of these two variables is, in turn, determined by the voltages supplied to the tube and by the positive resistance of the tuned circuit. The second

is controlled by the voltages supplied to the tube, by the quenching frequency and to some extent, by the resistance of the tuned circuit. In short, practically every adjustment which can be made on a super-regenerative receiver affects the slope of the linear part of the modulation characteristic.

The second portion of the modulation characteristic to be considered is the "elbow", the part in which the curvature is most acute. The curvature indicates that the receiver has reached a condition where further increases in signal voltage, and therefore in oscillating current, cause the negative resistance supplied by the tube to decrease. The greater the signal voltage, within this region, the greater is the reduction in negative resistance, and the smaller the slope of the curve becomes.

The curves in Figs. V-25 through V-36 reveal a tendency for the sharpness of curvature of the "elbow" to increase when the positive resistance of the tuned circuit is decreased. This trend may be explained qualitatively by a reference to the negative-resistance contour chart of Fig. V-6. The key to the situation lies in the fact that the upper-left-hand corners of the contours representing low values of negative resistance are quite sharp, while on the high-resistance contours these corners appear to be rounded or even "beveled off". Without going into details, this difference in shape of the contours may be interpreted as follows. With a high value of resistance in the tuned circuit, the negative resistance begins to fall off at a relatively low value of oscillating current, and continues to

do so, quite gradually, as the oscillating current is increased to two or three times this value. With a low value of circuit resistance, on the other hand, it is possible for the oscillating current to be increased up to a relatively high value without much reduction in negative resistance; but beyond this point further increases in signal voltage quickly bring the receiver into a state of "flat-topped" saturation.

It is also to be noted that the bend in the modulation characteristic tends to occur at the highest values of oscillating current with the lowest values of resistance in the tuned circuit. This condition is exactly what one would expect from the fact that curvature away from the vertical direction takes place in the contours of high negative resistance at much lower values of oscillating current than in the low-resistance contours.

In the third and final parts of the curve, the degree of curvature becomes much smaller than it was at the elbow, so that a fair approximation to linearity is attained. This portion of the curve represents a saturated condition of the receiver, in the sense that an increase in the signal voltage causes little or no increase in the peak amplitude of the envelope of oscillations. Such increase as does occur in the reading of the milliammeter is caused almost entirely by a "filling out" of the envelope whereby the oscillations attain their peak amplitude earlier in the quenching cycle and hold it for a longer period before starting to decay.

In order to obtain specific illustrations of the relation

between the shape of the modulation characteristic and the form of the envelope of oscillations, a number of cathode-ray oscillograms were taken; they are shown in Figs. V-40 through V-48, on the following page. Figs. V-40, V-41 and V-42 represent conditions on the three curves of Fig. V-25, at a signal voltage of 16 millivolts. The oscillograms confirm what the curves suggest, namely: (a) that with the largest of the three values of quenching voltage, 12 volts, the net resistance goes sufficiently negative during the course of the quenching cycle for oscillations to build up very quickly and reach a condition of "flat-topped" saturation; (b) that with a lower quenching voltage, 10 volts, the oscillations take longer to reach this level, so that the "flat-topped" condition is not so evident; and (c) that with a still lower quenching voltage, 7.5 volts, the oscillations never become large enough to cause saturation. This last point is further confirmed by a comparison of Fig. V-42 with Fig. V-43, which was taken at the same quenching voltage (7.5 volts) but with a signal voltage approximately one-tenth as great. The amplitudes of oscillation in the two oscillograms are seen to bear approximately the same ratio as the signal voltages, so that little or no saturation can be present.

The second series of oscillograms, in Figs. V-44 to V-48, inclusive, was taken with the combination of voltages and circuit parameters represented by the 15-volt curve in Fig. V-32. The signal voltages with which they were taken ranged only from zero to 5 millivolts, but even in this limited range the trend toward a saturated

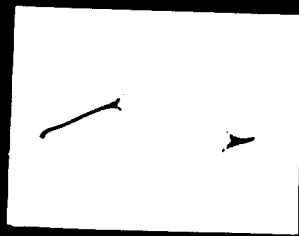


Fig. V-40

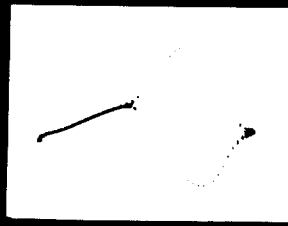


Fig. V-41

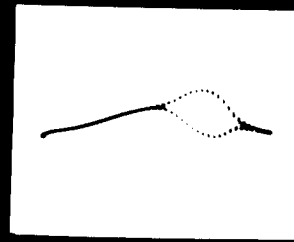


Fig. V-42

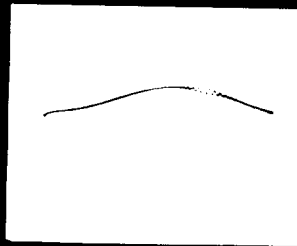


Fig. V-43

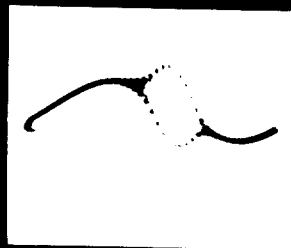


Fig. V-44

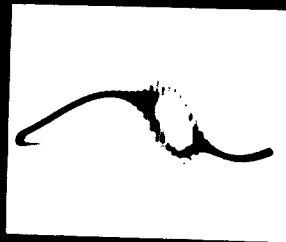


Fig. V-45

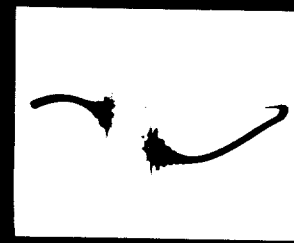


Fig. V-46



Fig. V-47



Fig. V-48

condition at the larger signal voltages is quite evident.

In order to permit comparison with the modulation characteristics given by Hassler, the curves of Figs. V-25, V-31 and V-32 have been replotted in Figs. V-37, V-38 and V-39, respectively, using his choice of coordinates. These three graphs show the same general shape of curve as Fig. 8 of Hassler's article (see Appendix A, Part V).

The lower portion of each curve is approximately parabolic in form, while for values of I_{osc}^2 greater than about 200 ma^2 the curves are more or less straight, having a slope considerably smaller than the maximum slope attained in the "parabolic" portion. The approximation to linearity is much poorer, however, than in Hassler's curves. At high values of signal voltage the slope decreases, so that the modulation characteristic taken as a whole bears some resemblance to an integral sign. This departure from the form given by Hassler is not surprising, in view of the simplified picture of the process of saturation which he employed (see Fig. 4 of his article, in Appendix A, Part V). The remarkable thing is rather the fact that he was able to get experimental data, shown plotted in his Fig. 8, which agreed with this idealized concept.

A number of the modulation characteristics in Figs. V-25 to V-39, inclusive, differ in one major respect from the "basic form" described above. At zero signal voltage they indicate a finite oscillating current of considerable magnitude in some cases. In Fig. V-26, for instance, the oscillating current is 25 milliamperes with no input signal and only 28 milliamperes with the largest signal voltage applied

(18 millivolts). Likewise, the oscillogram in Fig. V-44 shows a considerable amplitude of oscillation, even though it was taken with zero signal voltage.

Such observations do not indicate any flaw in the fundamental theory of the superregenerative process, however. It still remains true that oscillations occur in the receiver only when a voltage is present to start them. What these curves do indicate is the fact that other voltages besides the signal voltage are present in the tuned circuit. When the signal voltage is reduced to zero, provided the receiver is adjusted for high enough amplification, these other voltages alone are sufficient to produce an appreciable oscillating current or even to saturate the receiver.

Such extraneous voltages are normally of two kinds. In the first place, random "noise" voltages arising from a variety of sources are always present in the receiver. In the second place, residual oscillations from the preceding quenching cycle may still be large enough at the end of the positive-resistance period to serve as the initial oscillation in the negative-resistance period immediately following. A third type of extraneous voltage, indirectly caused by the quenching voltage, was encountered in our low-frequency experimental receiver; it will be discussed in Part D of this chapter. Each of these voltages affects the operation of the receiver in its own particular way, so that it will be advisable to consider them separately.

The random disturbances termed "noise voltage" include several different phenomena. Shot effect in the vacuum tube, thermal

agitation and various external disturbances all contribute to noise voltage. These disturbances are spread more or less uniformly throughout the entire frequency spectrum, so that they cannot be completely filtered out. It should be realized, of course, that noise voltage is not peculiar to the superregenerative circuit; it is common to all vacuum tube apparatus, and its effect can be heard in the output of any receiver having sufficient amplification.

The effect of noise voltage in a sensitively adjusted superregenerative receiver is to give rise to trains of oscillations of irregularly varying amplitude. Such a condition is illustrated by the oscillogram in Fig. V-49. The height of the individual envelopes of



Fig. V-49. Oscillogram showing effect of noise voltage.

oscillations is seen to vary up and down with no semblance of order. If the peaks of these individual envelopes were connected up by a pair of curves forming an "envelope of envelopes", the fluctuations in these curves would contain frequency components ranging all the way from the quenching frequency (or possibly harmonics of the quenching frequency) down to zero.

When readings were taken for modulation characteristics with the signal voltage set at zero, the thermal milliammeter gave the

root-mean-square value of an oscillating current which varied in the irregular manner indicated above. Because of the sluggishness of the instrument, the averaging process implied in the term "root-mean-square" took place over a period of the order of magnitude of one second. This means that rapid fluctuations in the "envelope of envelopes", composed mainly of frequency components higher than one cycle per second, did not affect the needle of the meter. Components of noise voltage considerably below one cycle per second, however, caused the needle to shift about from moment to moment. In order to take a reading of oscillating current for the modulation characteristic, it was necessary to estimate the mean position of the needle over a period of several seconds. A meter having an extremely sluggish movement would have arrived of itself at this mean reading and held it steadily.

The observed tendency of "noise" fluctuations in the reading of the milliammeter to become smaller as the signal voltage was increased may be explained on the ground that the receiver was becoming saturated. This caused the sensitivity to fall off, and consequently decreased the response of the receiver to noise voltages.

The second source of extraneous voltage in the tuned circuit is a residual oscillation from the preceding quenching cycle. If insufficient damping is provided during the positive-resistance period, this residual oscillation may be large enough to give rise to a considerable amplitude of oscillating current in the following negative-resistance period. Two cases may be distinguished: (a) if the average net resistance of the circuit, taken over the entire quenching

cycle, is positive, then the residual oscillation at the end of the quenching cycle is smaller than the initial oscillation at the beginning, so that successive trains of oscillations will become smaller and smaller in amplitude; but (b) if the average net resistance of the circuit is negative, then successive trains of oscillations will become larger and larger, until saturation of the receiver makes the average net resistance equal to zero. When the latter condition prevails, the receiver is really generating a continuous oscillation, heavily modulated at the quenching frequency. The root-mean-square value of the modulated oscillation is read by the milliammeter in the tuned circuit.

In the absence of an input signal, then, it is possible for the milliammeter to indicate a definite value of oscillating current as a result of residual oscillations. This is undoubtedly the explanation for the shape of such modulation characteristics as the one in Fig. V-26.

Residual oscillations also account for another peculiarity noted in some of the modulation characteristics, namely, a "sag" in the curve at low values of \mathcal{E}_{sig} . Suppose that the frequency of the signal voltage differs slightly from the natural frequency of the receiver. If \mathcal{E}_{sig} is small, this condition may give rise to a heterodyne or beat effect, whereby \mathcal{E}_{sig} will alternately detract from and add to the residual voltage remaining from the preceding train of oscillations. This beat phenomenon was discussed theoretically in Chapter III, and will be treated more fully from the experimental standpoint in Part D of the present chapter.

Now, if the receiver is at all saturated, the amplitude of oscillation will not be increased as much by the addition of \mathcal{E}_{sig} as it will be decreased by its subtraction. Consequently the net effect of supplying a small signal voltage, instead of no signal at all, is actually to reduce the average amplitude of oscillation. A strong signal, however, completely overrides the residual oscillation and gives rise to larger oscillations than are produced with either a small value of \mathcal{E}_{sig} or zero signal. This phenomenon accounts for the dips observed in some of the modulation characteristics in Figs. V-28, V-30, V-31, V-33 and V-38. It also explains the beat effect observed on the oscillograms in Figs. V-45 and V-46. In these two figures a double envelope may be discerned, indicating that the amplitude of the envelope of oscillations fluctuated between two limiting values during the exposure of the film. In other figures of the same series, taken under the same conditions but with larger signal voltages, or with no signal at all, no beats can be detected.

One point which has not yet been touched upon is the significance of these modulation characteristics which were taken with the rectifier type of milliammeter. These are shown dotted in Figs. V-25, V-26, V-31 and V-32. Their shape is in general the same as that of the corresponding curves taken with the thermal instrument, but they read lower values of oscillating current. Both the thermal and the rectifying meters were calibrated against a standard thermocouple, using unmodulated 1000-cycle current, so that this difference cannot be charged to an error in one of the instruments. Its explan-

ation lies in the fact that a thermal milliammeter in a superregenerative circuit reads true root-mean-square current, while a rectifying meter does not. The latter type does read root-mean-square values if the amplitude of oscillation is constant. As soon as such a "carrier" wave is modulated, however, the reading of a rectifying meter falls below the true root-mean-square value.

The significance of using these two types of meters in a study of superregeneration becomes apparent when the matter of demodulation is considered. The rectifying instrument is essentially a linear detector, while the square of the reading of the thermal instrument is a measure of the output obtainable from a square-law detector. The fact noted above, that the modulation characteristics taken with the thermal meter lie above those taken with the rectifying meter, means that square-law demodulation possesses a slight advantage over linear demodulation in a superregenerative circuit which it does not have in a conventional receiver.

Operating Characteristics

The modulation characteristics discussed in the foregoing pages may now be examined for their relation to certain of the operating characteristics of the superregenerative receiver. Of the latter, perhaps the most important property is sensitivity.

At the outset, it is necessary to distinguish between two types of sensitivity, which may for convenience be termed "telegraphic"

and "telephonic" sensitivity. In the reception of radiotelegraphic signals, the significant point is the difference between the oscillating current produced by the given signal voltage and the oscillating current at zero signal voltage. If the receiver is adjusted so that the modulation characteristic has the basic form described on page 109, in which no appreciable oscillating current exists at zero signal voltage, the sensitivity at a given value of signal voltage may be expressed simply in terms of the oscillating current produced by that voltage. In other words, the telegraphic sensitivity at a given point on the modulation characteristic is simply the ratio of the ordinate of that point to the abscissa.

In radiotelephony, however, the value of the signal voltage does not alternate between a definite value and zero, but varies up and down continuously in the neighborhood of a definite value. Consequently the sensitivity of the receiver at a given point on the modulation characteristic is no longer determined by the ratio of the coordinates, but more nearly by the slope of the characteristic at that point. The smaller the per cent modulation, the more accurately is the slope a measure of sensitivity in telephonic reception.

With these definitions in mind, the relation between sensitivity and the shape of the modulation characteristic may be examined. On the linear portion of the curve, below saturation, the telegraphic and telephonic sensitivities are equal and at their maximum value. In the region of sharp curvature the telephonic sensitivity drops steeply to a much lower level. It then remains nearly constant, fall-

ing off only slightly, in the third or saturated region. The telegraphic sensitivity, on the other hand, starts to decrease gradually in the region of sharp curvature of the modulation characteristic, and continues to do so in the saturated region.

Distortion is of course an important consideration in telephonic reception. From the shape of the modulation characteristic it can be predicted that fidelity will be good in the first or linear part of the curve, and (provided the per cent modulation is not too great) will be fair in the third or saturated portion, where the amplification depends only moderately upon the amplitude of the signal voltage; but that it will be very poor in the intermediate region of high curvature. The fact that fair fidelity of reproduction may be achieved with the receiver highly saturated explains why a musical or vocal program picked up by a superregenerative receiver may effectively suppress the rushing sound which is normally heard as a consequence of noise voltages, and at the same time may be reasonably free from distortion.

So far it has been assumed that the receiver was so adjusted that the modulation characteristic was of the basic form described on page 109. Reference to certain of the modulation characteristics, such as those in Figs. V-25, V-27 and V-33, however, shows that improved sensitivity may sometimes be obtained by a departure from this form to one in which a moderate value of oscillating current exists at zero signal voltage.

With the receiver adjusted in this way, however, the modulation characteristic does not give a complete picture of the situ-

ation. It tells what the r.m.s. value of the oscillating current is at any given value of signal voltage, but it does not tell how widely the amplitude of oscillation fluctuates about this value as a result of either noise voltage or beats between the signal and residual voltages. In terms of the audible output of the receiver, the modulation characteristic makes it possible to determine how loudly a given modulated input signal will be heard, but it reveals nothing about how loud the background noise (or a background whistle, in the case of beats between signal and residual voltages) will be. Obviously, if the intensity of the noise is comparable to or greater than that of the signal, the sensitivity manifested by the receiver in bringing the signal up to the audible level is of little or no use.

The useful sensitivity of the receiver, then, is limited solely by the noise level in the tuned circuit. Any available method of reducing this level makes it possible to adjust the voltages and parameters of the circuit for greater sensitivity without bringing the noise output up to an objectionable level. This statement of course is not peculiar to the superregenerative receiver but applies to any type of receiver whatever.

The low-frequency receiver which was used in this work was at a disadvantage in the matter of noise voltage, for its "radio-frequency" circuits could be neither compact nor properly shielded. However, by shielding the coil and condenser, cabling high-frequency leads, and shunting the bias and plate-voltage supplies with large bypass condensers, it was possible with optimum adjustment of the receiver to detect the effect upon S_{osc} of a signal as small as 10 microvolts.

An important characteristic of any receiver, particularly one which may be used as a field strength measuring set, is its stability; that is, the degree to which its sensitivity is independent of small changes in operating conditions. In a practical superregenerative receiver the quantity most likely to change is probably the quenching voltage, since it is subject not only to fluctuations in battery voltage (that is, in the voltages supplied to the quenching oscillator) but also to such irregularities as variations in tube temperature. It is therefore desirable to know how the receiver should be adjusted in order that the shape and position of the modulation characteristic shall be the least affected by variations in quenching voltage.

Let us see what this objective means in terms of the mechanics of the superregenerative process. At the outset, of course, it means that with any given signal voltage a moderate change in quenching voltage must produce the smallest possible change in oscillating current, as indicated by the milliammeter. This is roughly, although not exactly, equivalent to stating that the average negative resistance supplied by the tube, taken over the period in which the net resistance is negative, must not be materially altered by a small change in quenching voltage.

Assume, now, that the receiver is to be operated in the conventional manner, with a negative d.c. grid bias. It is evident from the negative-resistance contour chart (Fig. V-6) that the condition set forth above could not be realized in our low-frequency receiver with any combination of d.c. grid bias and quenching voltage that

would make the positive peak value of instantaneous grid bias fall between 0 and -12 volts. Suppose that, with the receiver adjusted in this way, a small increase in quenching voltage were to occur. The increase would carry the operating point further to the right during the positive half of the quenching cycle, and in so doing would carry it into a region of higher negative resistance. Thus the objective set forth in the preceding paragraph would not be realized.

A much more satisfactory adjustment, from the point of view of stability, is one in which the instantaneous grid bias reaches a positive peak of roughly +5 volts. Assuming such an adjustment, suppose that a small increase in quenching voltage takes place. The value of negative resistance attained at the positive peak of the instantaneous bias will actually be reduced as a result of the increment, instead of being increased, as it was in the preceding case. In other parts of the positive half-cycle, however, the negative resistance will be increased, so that the net effect of increasing the quenching voltage will be small. This point is illustrated in Fig.V-50. The solid curve represents the negative resistance supplied by the tube as a function of time, with the original value of quenching voltage; while the dotted curve represents the same thing, after a moderate increase in quenching voltage. As may be seen, there is little difference in the areas under the two curves. This means that with the receiver properly adjusted a considerable variation in quenching voltage can occur without much change in the average negative resistance during the building-up period, and hence without

much change in the amount of oscillating current produced by a given input signal voltage.

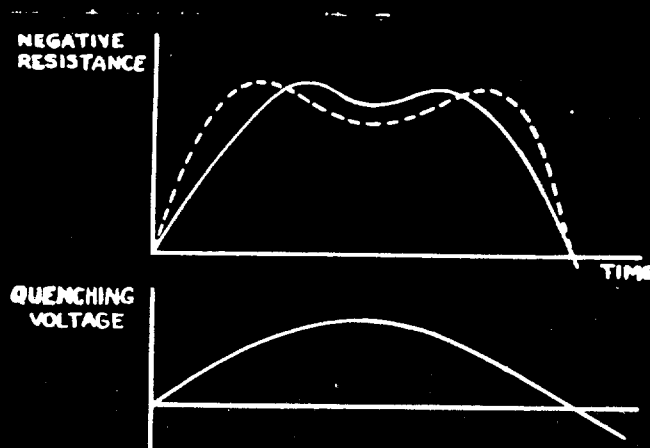


Fig. V-50

This fact is demonstrated in Fig. V-39, which contains the modulation characteristics of Fig. V-32 replotted according to Hassler's definition (\mathcal{D}_{osc}^2 vs. $\ln \mathcal{E}_{sig}$). The ordinates of the 10-volt and the 5-volt curves are seen to maintain approximately a 2-to-1 ratio throughout their length. Since the ordinates represent \mathcal{D}_{osc}^2 , rather than \mathcal{D}_{osc} , it follows that throughout the range of signal voltages shown on the graph the two values of \mathcal{D}_{osc} maintain a ratio of approximately $\sqrt{2}$ to 1, or roughly $1\frac{1}{2}$ to 1. But if a 100% change in quenching voltage produces only a 50% change in oscillating current, it follows that uncontrollable fluctuations in the quenching voltage, which would seldom be greater than a few per cent, would have very little effect on the amplitude of oscillation.

It is not always practicable, however, to adjust the receiver so that the instantaneous grid bias swings as high as +5 or +10 volts. If the resistance of the tuned circuit is low, such an adjust-

ment may make the receiver too sensitive, so that random noise voltages present in the circuit give rise to oscillations sufficiently intense to saturate the receiver, even with no input signal supplied. Or again, if the net resistance of the circuit does not become sufficiently positive during the damping period, so that a residual oscillation of greater amplitude than the noise level is present when the resistance again becomes negative, then this residual oscillation may give rise to oscillations large enough to saturate the receiver. Such a situation is represented by the modulation characteristic in Fig. V-26.

Both of the conditions just described are undesirable from the point of view of reception. There is, to be sure, a way in which they can be avoided in low-resistance circuits and at the same time the instantaneous grid bias can be permitted to swing up to the desired +5 or +10 volts. This is by making the d.c. grid bias highly negative and adjusting the quenching voltage so as to bring the positive peak of the instantaneous bias to the desired point. This procedure overcomes the difficulties of excessive sensitivity described above by reducing the building-up period to a small part of the quenching cycle. It offers no advantage in regard to stability, however, because of the necessity of using a large value of quenching voltage. Fluctuations in quenching voltage of course become correspondingly high, when measured in volts rather than in per cent, so that the advantage of placing the "high-water mark" of the instantaneous bias voltage in the vicinity of +5 volts is largely lost. In

Fig. V-28, for example a glance at the 32-volt and 35-volt curves shows that a 10% increase in quenching voltage is sufficient to treble the oscillating current. Such a condition is of course undesirable from the point of view of stability.

To summarize the foregoing remarks, the optimum combination of sensitivity and stability with respect to quenching voltage was realized in our low-frequency receiver with a d.c. bias of about -10 to -20 volts, a quenching voltage of sufficient magnitude to bring the positive peak of the instantaneous grid bias to approximately +5 or +10 volts, and a value of resistance in the tuned circuit sufficiently large to prevent noise voltage or residual oscillations from producing a large amplitude of oscillating current. This condition also provided maximum stability with respect to d.c. grid bias voltage, since fluctuations in this potential had much the same effect as fluctuations in the quenching voltage. Fluctuations in d.c. plate voltage could be neglected, since they could have only μ times as great an effect as fluctuations in d.c. grid bias. The amplification factor μ had a value of approximately 8 in the tube used in our experimental receiver.

It should be realized, of course, that the quantitative values set forth in the preceding paragraph apply only to the low-frequency receiver with which the experimental investigation was conducted. In any other receiver the numerical values would be different, but the method of determining them would be the same as that which has been described in the foregoing pages.

2. Oscillating Current vs. Quenching Frequency:

The discussion of stability in the foregoing pages, in connection with modulation characteristics, paves the way for consideration of another general class of operating curves. A modulation characteristic, it will be recalled, shows the effect of varying the input signal voltage while the adjustment of the receiver remains fixed. The second type of curve, on the other hand, is designed to show the effect of varying the adjustment of the receiver in a particular "dimension" (quenching frequency, quenching voltage, grid voltage, filament voltage, mutual inductance, etc.) while the signal voltage remains constant. From such curves and a knowledge of the probable amplitude of fluctuation in each of the several dimensions of adjustment, the degree of stability of the receiver can be predicted for any given adjustment.

Such a prediction, to be sure, can be made without the aid of any other curves than a set of modulation characteristics. In Fig. V-25, for instance, a rough notion of the relation between quenching voltage and oscillating current may be obtained by observing the values of current at which a line of constant signal voltage intersects the curves representing the three different values of quenching voltage. Or again, a picture of the relation between d.c. grid bias and oscillating current may be obtained, in an even cruder form, equivalent to a curve plotted through only two points, by a comparison of the ordinates of the 15-volt modulation characteristics in Figs. V-32 and V-33, at a given value of signal voltage.

Such a procedure is obviously awkward. In addition, it gives only very sketchy information, for it is seldom that many modulation characteristics are available which have been taken under identical conditions in all but one dimension of adjustment. Finally, the procedure outlined above is liable to be inaccurate. When a large quantity of test data is taken, the measurements must necessarily last over a considerable period, perhaps several days or weeks. If during this period there occur fluctuations in room temperature, instrument calibrations, etc., then data taken at different times are not strictly comparable. In other words, modulation characteristics taken on different days may be improperly located with respect to each other, although the shape of each of them is probably determined quite accurately. But this means that a curve of oscillating current versus quenching voltage, for instance, which has been compiled from a whole family of modulation characteristics, is likely to be entirely erroneous in shape.

The reasons are then clear for taking curves showing oscillating current as a function of each of the several dimensions of circuit adjustment. The actual work of taking a complete set of such curves would be a large undertaking, requiring more time than could have been devoted to it in the present study. To illustrate the principle, however, curves of this type were taken for a single dimension of adjustment, namely, the quenching frequency.

The experimental procedure employed in obtaining these curves was quite simple. The quenching frequency was first set at a low value (5 c.p.s.) and the receiver was adjusted to a desired combination

of input signal voltage, bias voltage, plate voltage, mutual inductance and resistance in the tuned circuit. The speed of the quenching alternator was then increased in steps, so as to produce increments of 5 c.p.s. in the quenching frequency. At each step the slide-wire controlling quenching voltage was readjusted, in order to compensate for the increase in output voltage of the alternator as its speed was raised, and the oscillating current was read on the thermal milliammeter in the tuned circuit. The run was then repeated with the receiver still adjusted in the same way, but with other values of signal voltage. Three families of curves of this type were taken, using three different values of resistance in the tuned circuit. They appear in Figs. V-51, V-52 and V-53.

In comparing these three graphs, it should be noted that they were not taken under identical conditions of bias voltage and quenching voltage. For example, when 80 ohms was used in the tuned circuit the bias was -40 volts and the quenching voltage was 27 volts, while with the resistance at 160 ohms the voltages were -7.5 volts and 5 volts, respectively. The positive peak of the instantaneous bias was approximately at zero in either case, but the negative peak was at about -80 volts in the first instance and only -15 volts in the second.

Viewed qualitatively, this difference meant that in the 80-ohm case the receiver was adjusted in such a way that the average negative resistance supplied by the tube during the entire quenching-frequency cycle was considerably lower than in the 160-ohm case. This procedure was followed in order to prevent the receiver from

FIG. V-51

DEPENDENCE OF OSCILLATING CURRENT ON QUENCHING FREQUENCY

OSCILLATING CURRENT
IN MILLIAMPERES

28

26

24

22

20

18

16

14

12

10

8

6

4

2

0

$R = 80 \Omega$

$E_d = -40 \text{ v.}$

$E_q = 27 \text{ v.}$

$E_{s1} = 0.66 \text{ v.}$
 $I_{m1} = 3.3 \text{ mA.}$

$C = 0.003$

0 5 10 15 20 25 30 35 40 45 50

QUENCHING FREQUENCY IN CYCLES PER SECOND

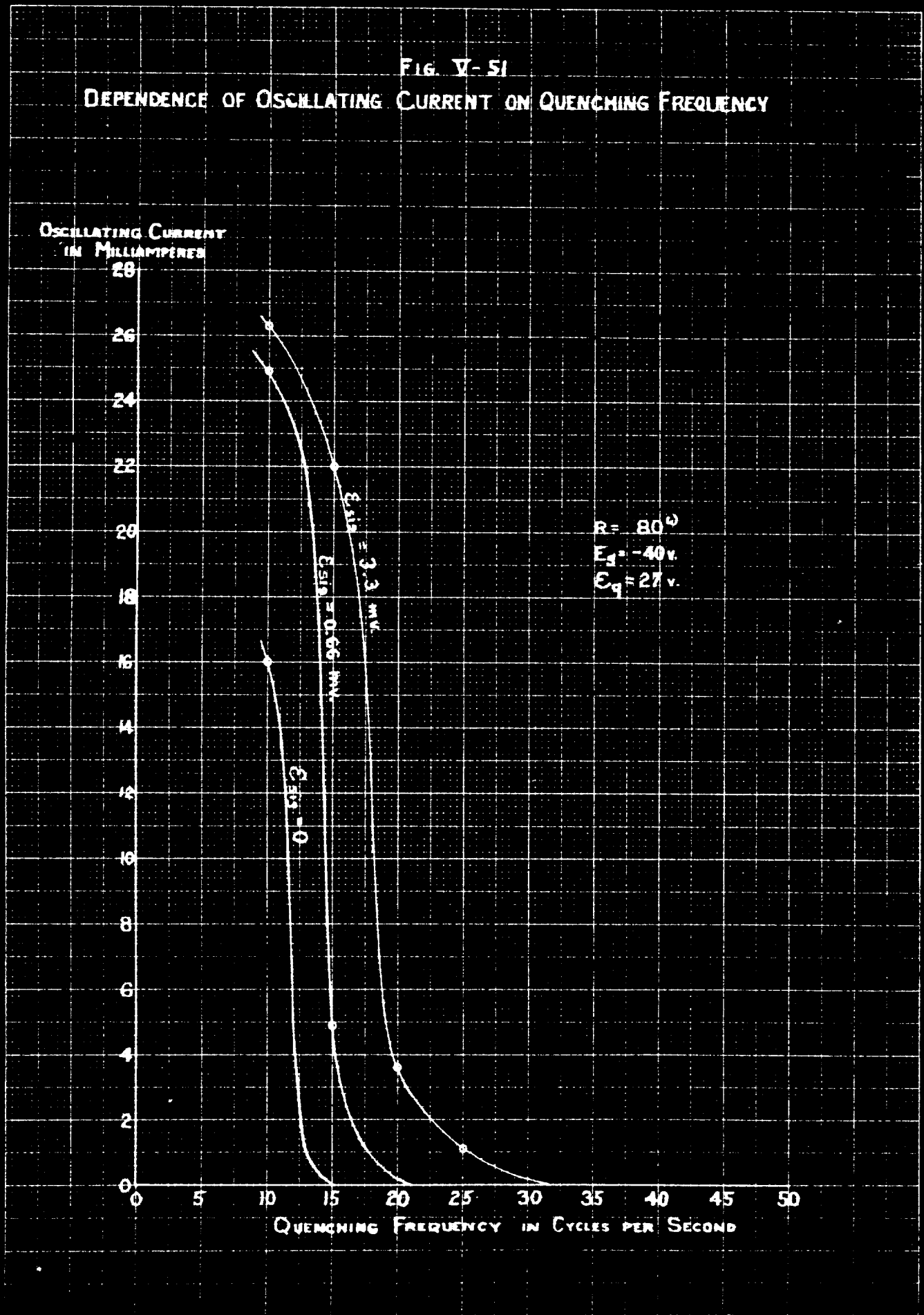


FIG. V-52
 DEPENDENCE OF OSCILLATING CURRENT ON QUENCHING FREQUENCY

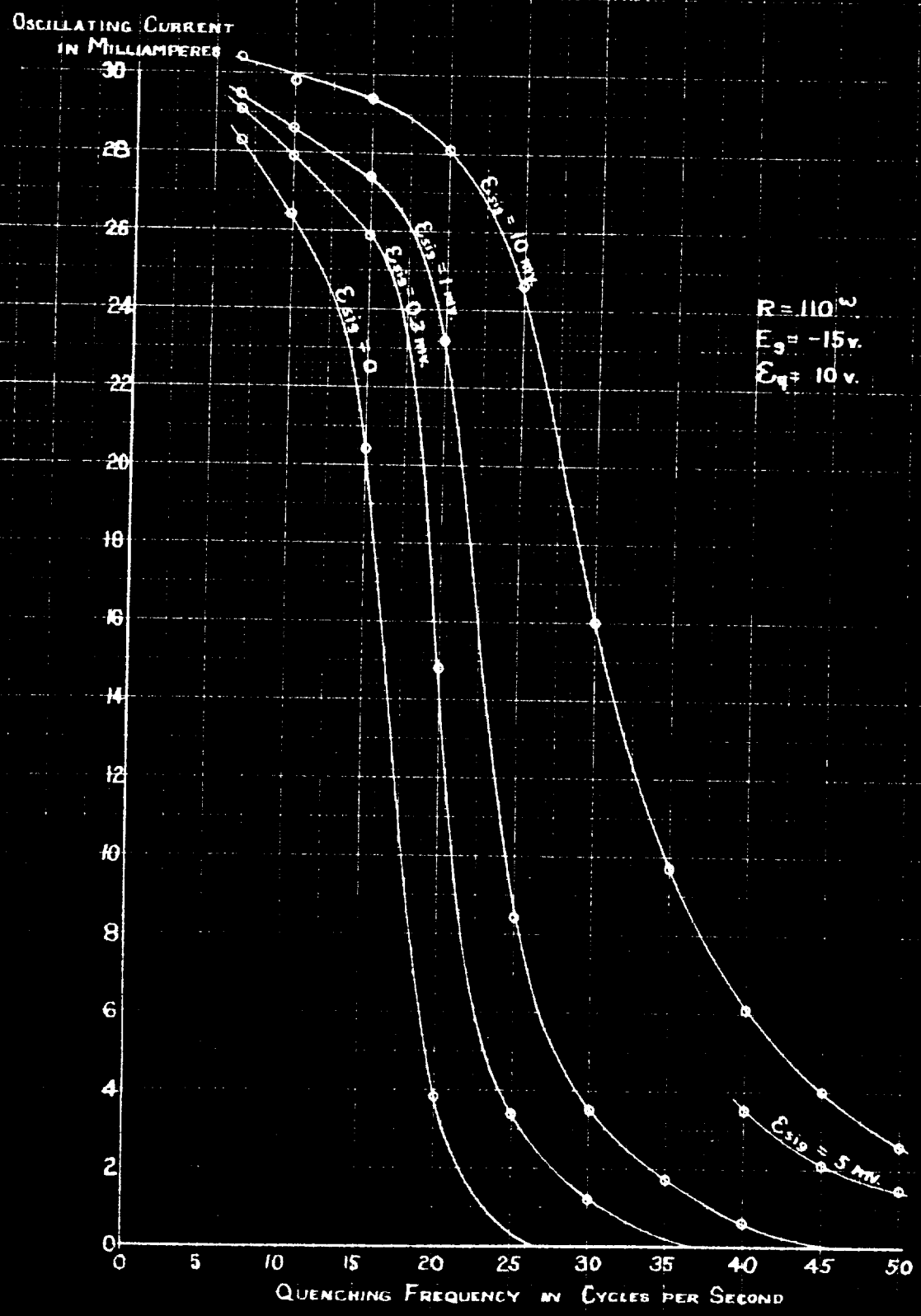
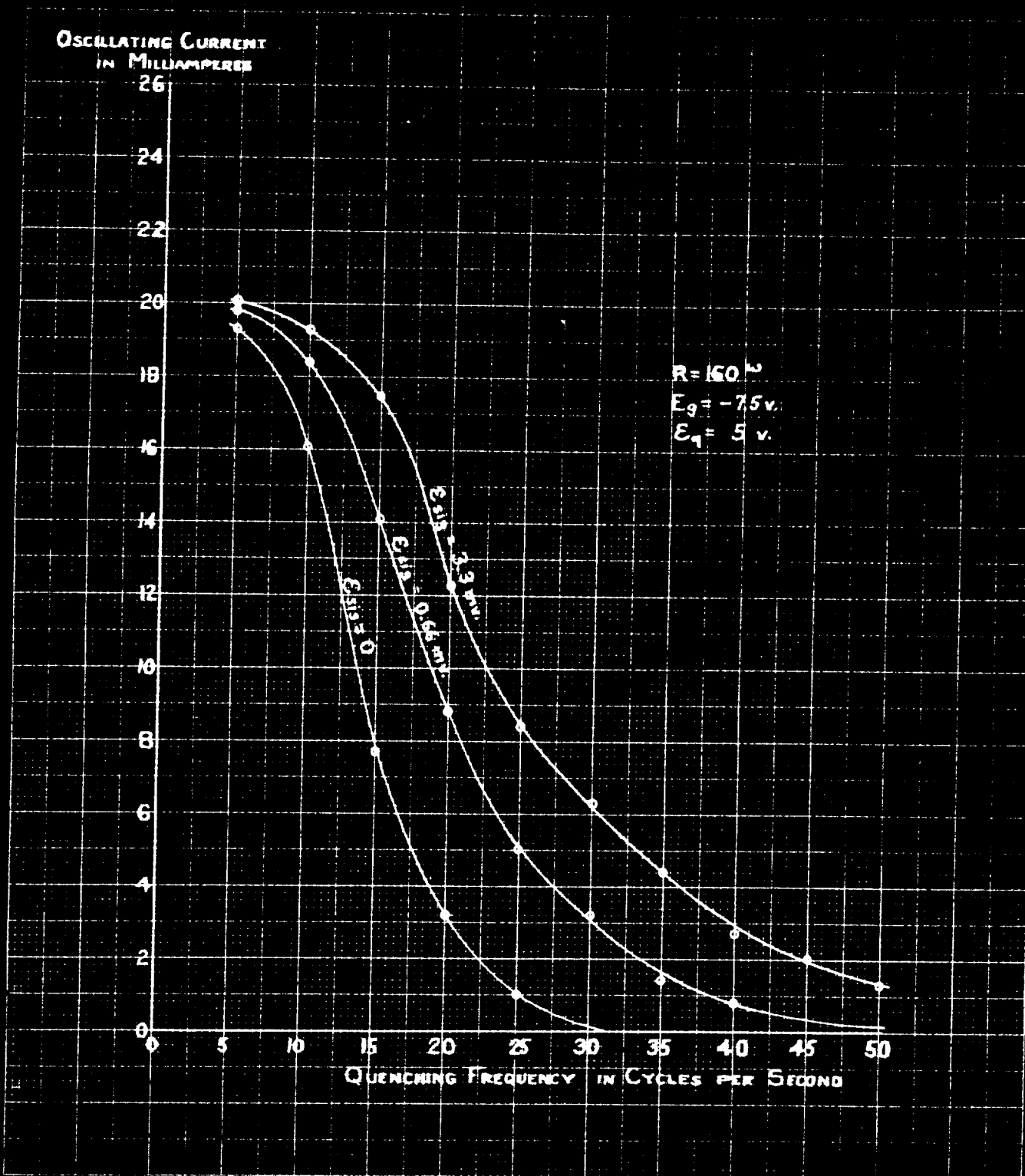


FIG. V-53.

DEPENDENCE OF OSCILLATING CURRENT ON QUENCHING FREQUENCY



saturating at low values of circuit resistance under conditions of quenching frequency and other variables which would not cause it to saturate at higher values of circuit resistance.

An examination of the curves in Figs. V-51, V-52 and V-53 shows that they all slope downward toward the right, exhibiting a form somewhat like that of a reversed integral sign. This confirms a prediction which might be made on theoretical grounds, namely, that if other things are equal the largest amplitude of oscillation will be obtained when the longest building-up period is provided.

The lower ends of the curves are seen to be approximately exponential in shape. They would not be exactly exponential, however, even for an ideal receiver, for the abscissae are plotted in units of frequency, which is the reciprocal of time, rather than in units of time itself.

The bending-over which occurs at the upper ends of the curves is an evidence of saturation. Beyond a certain point, increasing the building-up period causes little increase in the amplitude of oscillation attained. Furthermore, when the building-up period is made sufficiently large, even the random noise voltages in the circuit give rise to oscillations large enough to saturate the receiver, so that the addition of a signal voltage causes little increase in oscillating current. This condition, already illustrated by the 24-volt modulation characteristic in Fig. V-36, causes curves of oscillating current versus quenching frequency to bunch together at the upper left corner of the graph.

One obvious characteristic of the curves is the fact that their steepness appears to vary inversely with the resistance in the tuned circuit. Upon further consideration, however, this relation is seen to be only an indirect one. The primary cause for the variation in steepness is the fact that different values of circuit resistance require the use of different values of grid bias and quenching voltage, as has been explained above. In the 80-ohm case, for instance, the negative bias is so large that the operating loop lies well toward the left of the negative-resistance contour chart (see Fig. V-6). Consequently, during a considerable portion of the building-up period, the operating point may be passing through a region in which the contours have an "undercut" form. If, under such circumstances, the quenching frequency is somewhat reduced, so that the building-up period and consequently the amplitude of oscillation are increased, the net effect will be an actual increase in the average negative resistance supplied by the tube during the building-up period. In other words, an action just the opposite of saturation will take place, causing a large increase in oscillating current. This, then, accounts for the steepness of the curves in Fig. V-51, which were taken with a circuit resistance of only 30 ohms.

The curves in Fig. V-53, on the other hand, were taken with 160 ohms resistance and with much smaller values of grid bias and quenching voltage. Under these conditions, according to the negative-resistance contour chart, the operating point is in a region where the contours are either vertical or inclined to the right, throughout the building-up period. The effect of a decrease in quenching frequency

and a resulting increase in oscillating current is now to reduce the negative resistance supplied by the tube during the building-up period, rather than to increase it. Consequently the magnitude of the rise in oscillating current resulting from the decrease in quenching frequency is relatively small. This reasoning explains the relatively gradual slope of the curves in Fig. V-53, as compared with those in Fig. V-51. Intermediate values of resistance, grid bias and quenching voltage were employed in Fig. V-52, and, as might be expected, this graph is intermediate between Figs. V-51 and V-53 in the matter of the steepness of its curves.

From the foregoing discussion it can be concluded that maximum stability with respect to quenching frequency is realized in a superregenerative receiver when low values of negative grid bias and quenching voltage and, incidentally, high values of circuit resistance are employed. It is interesting to note that this is the very combination of adjustments which was found to give optimum stability with respect to quenching voltage and grid bias.

D. MULTIPLE RESONANCE PHENOMENA

A distinguishing feature of the superregenerative receiver is the fact that under some conditions it has not merely a single resonance point but a number of such points, uniformly spaced in the frequency spectrum, at intervals equal to the quenching frequency. This multiple resonance effect may manifest itself in either of two ways. The output of the detector may simply fluctuate, reaching peak

values at the resonance points and dropping almost to zero in the "valleys" between them. Or, on the other hand, a multiple heterodyne effect may be observed, in which a series of beat notes is heard in the output of the receiver as the latter is tuned through the resonance points.

These two phenomena have been observed by a number of investigators (see, for example, papers by David and Hassler in Appendix A). Theoretical aspects of multiple resonance effects were considered in Chapter III. It was shown there that the receiver must be generating oscillations continuously in order for multiple beats, as distinguished from multiple peaks, to be observed. The present section will deal with experimental observations of multiple resonance phenomena, and will seek to relate them to the theoretical deductions of Chapter III.

Multiple resonance was observed in a very striking manner in the ultra-high-frequency receiver which was built at the start of this investigation. When a small amount of quenching voltage was used and an unmodulated signal was supplied to the receiver by the signal generator, a series of falling and rising beat notes could be heard in the phones when the tuning of either the receiver or the signal generator was varied smoothly through the resonance region. Each of these beats sounded quite similar to the heterodyne note which is heard in the output of an ordinary oscillating detector when it is tuned past a c.w. signal. When a sinusoidally modulated r.f. signal was supplied to the receiver, three beat notes could be distinguished at one time, apparently caused by the carrier and the two sidebands of the input signal.

When a larger value of quenching voltage was used, the beats were no longer audible. No sound could now be detected in the phones when an unmodulated signal was supplied to the receiver, but when the carrier was modulated at 1000 c.p.s. the latter frequency was audible in the output of the receiver. Its loudness passed through a series of sharp resonance peaks when the tuning of either the receiver or the signal generator was varied.

The spacing of these resonance points, both in the case of multiple beats and in that of multiple peaks, was crudely measured by counting the number of resonances between two tuning adjustments whose interval was large enough to be determined, within 10 or 20 per cent, by means of an absorption frequency meter. In every case the spacing between adjacent resonance points was found to be equal to the quenching frequency.

Measurements of d.c. grid current were taken while the quenching voltage was varied. It was found that this current increased abruptly at the point of transition from multiple peaks to multiple beats.

The foregoing observations may all be explained on a basis of theory. The fundamental point, of course, is the fact that when the natural frequency of the receiver is equal to the frequency of the signal, or differs from it by an integral multiple of the quenching frequency, the residual oscillation is always in phase with the input signal at the instant of dedamping. When the receiver is adjusted so that the residual oscillation is almost as large as the initial oscil-

lation which gives rise to it, the reenforcing effect of the residual oscillation upon the signal voltage may be much greater than the signal itself.

What happens when the receiver is not tuned exactly to one of these resonance points depends upon the adjustment of the circuit. If the average net resistance of the tuned circuit taken over a whole quenching cycle is positive, so that the residual oscillation is always smaller than the initial oscillation, then a stable equilibrium position will be reached. The three vectors representing the residual oscillation, the forced oscillation produced by the signal, and the total initial oscillation (equal to the vector sum of the first two) settle into a fixed relation which is repeated at successive instants of "dedamping" (transitions from positive to negative resistance). Consequently the same amplitude of oscillation is attained in successive quenching cycles, and no beats are heard. The vector diagram for this equilibrium (see Chapter III, page 38) shows, however, that the magnitude of the total initial oscillation depends to a very marked degree upon the tuning of the receiver relative to the transmitter. This accounts for the multiple peaks which were heard on the receiver when the quenching voltage was made large enough to give a positive average resistance to the tuned circuit.

If, on the other hand, the receiver is adjusted to have a negative average resistance, then, even in the absence of a signal voltage, oscillations build up rapidly until saturation makes the average resistance, taken over a complete quenching cycle, equal to

zero. This rise in the amplitude of oscillation accounts for the increase in d.c. grid current which was observed experimentally when the quenching voltage was reduced below a critical point. The receiver is now generating oscillations continuously, although under a very high degree of modulation caused by the quenching voltage. In these circumstances, providing certain conditions prescribed in Chapter III are fulfilled, a beat note is observed. Its frequency is equal to the difference between the frequency to which the receiver is tuned and the nearest of the multiple resonance frequencies. Varying the tuning of the receiver necessarily causes this difference frequency to rise and fall between a minimum of zero and a maximum of half the quenching frequency. This statement exactly describes the heterodyne effect which was observed with the ultra-high-frequency receiver.

Multiple resonance phenomena similar to those described above were also observed with the low-frequency experimental receiver. Examples of heterodyne action between the input signal and residual oscillation are shown in the oscillograms in Figs. V-54, V-55 and V-56, on the following page. All three of these oscillograms were taken with a fairly low value of circuit resistance (95 ohms) and with moderate values of grid bias and quenching voltage (-16 volts and 10 volts, respectively). Such an adjustment was responsible for a fairly low rate of decay of oscillations, during the positive-resistance period, and made that period moderately short in duration. Both effects tended to give a substantial residual oscillation, thereby making a heterodyne action possible.



Fig. V-54

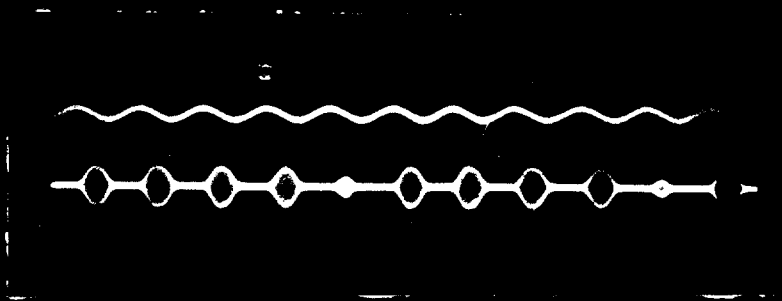


Fig. V-55

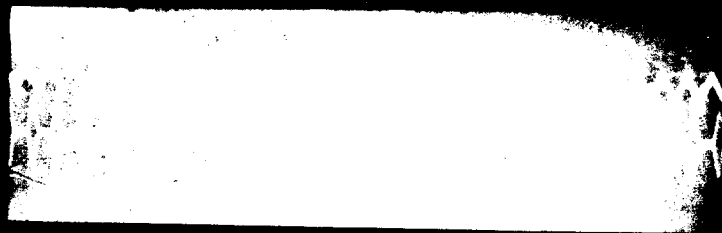


Fig. V-56

OSCILLOGRAMS ILLUSTRATING HETERODYNE ACTION
BETWEEN SIGNAL VOLTAGE AND RESIDUAL OSCILLATION.

In Fig. V-54 the amplitudes of the trains of oscillations are seen to alternate between two definite levels, making the beat frequency in the "envelope of envelopes" equal to half the quenching frequency. The steadiness with which this formation is maintained suggests that, when there are only a few quenching cycles per beat cycle, a locking action occurs which is fundamentally similar to the vector equilibrium condition described above.

In Fig. V-55 the beat frequency is only one-fifth of the quenching frequency. The oscillogram does not cover a sufficient number of quenching cycles to show conclusively whether the beat frequency is locked at a subharmonic of the quenching frequency.

In Fig. V-56 the beat frequency is approximately, but not exactly, one-eighth of the quenching frequency. The two frequencies definitely are not locked together here, for the pattern of the quenching-frequency envelopes within the beat-frequency envelope changes from one beat cycle to the next.

In connection with the multiple beat phenomenon, mention should be made of an interesting effect which was observed when the receiver was adjusted to give beats between the signal voltage and the residual oscillation. The amplitude of oscillations tended to vary with time in a sort of "sawtooth" manner. That is, during the course of the beat cycle, the amplitude attained by the individual trains of oscillations would gradually decrease from its maximum to its minimum, and then would spring up again relatively quickly to its maximum level. This form of behavior is exactly what would be expected on

theoretical grounds, and has already been discussed from that point of view in Chapter III, on page 46.

Further evidence of multiple resonance points occurring with the low-frequency receiver is contained in Fig. V-57. This oscillogram



Fig. V-57

was taken with the drum of the oscillograph rotating at a very low speed, so that the exposure took about 10 seconds to complete. During this time the tuning dial of the signal oscillator was rotated manually at as nearly a constant speed as possible, so that the frequency range from approximately 300 to approximately 1200 c.p.s. was covered during the 10 seconds. In a crude way, then, the oscillogram serves as a frequency-response characteristic.

Prior to the exposure, the receiver was adjusted to such a condition that multiple peaks were obtained when the tuning of the signal oscillator was varied. These peaks are clearly discernible in the oscillogram, although they would be more conspicuous if the drum and the tuning dial had been rotated at a considerably lower speed, so as to cause the envelopes of the individual quenching cycles to run together.

The multiple resonance phenomena discussed so far, let it be

repeated, are of a type caused by the interaction of residual oscillations and the signal voltage. They are by no means new, having been observed by David, Hassler and many others. In the course of the present investigation, however, certain additional multiple resonance effects were noted which could not be explained on the basis of the above interaction, but, instead, pointed to the presence of a third high-frequency voltage which was capable of interacting with either of the voltages already mentioned.

For example, it was found that beats sometimes occurred in the complete absence of an input signal voltage. They were most pronounced at high values of quenching voltage and quenching frequency. Their frequency could be varied by adjusting either the quenching frequency or the tuning of the oscillatory circuit; hence it follows that the extraneous high-frequency voltage, whatever it is, must be closely related to the quenching voltage.

The three oscillograms in Figs. V-58, V-59 and V-60 on the following page were taken under identical conditions, except for circuit resistance. The values of resistance employed were 105 ohms, 75 ohms and 57 ohms, respectively. A fairly high quenching voltage, 35 volts, was used in all three cases, and no signal voltage was supplied. In Fig. V-58, on account of the relatively high damping, the residual oscillation is negligible. Nevertheless, the peak amplitude of oscillation is perfectly uniform from one quenching cycle to the next. Such a condition indicates the presence of a high-frequency voltage in the circuit which remains of constant amplitude at successive instants of "dedamping".



Fig. V-58

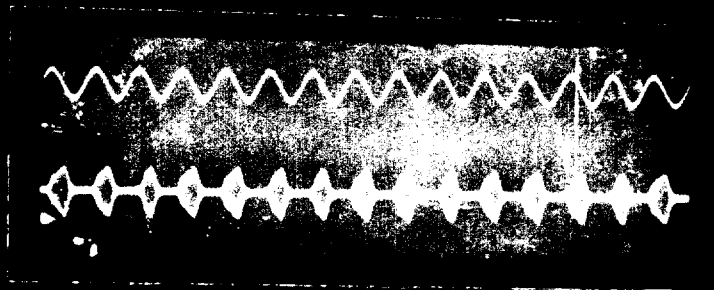


Fig. V-59

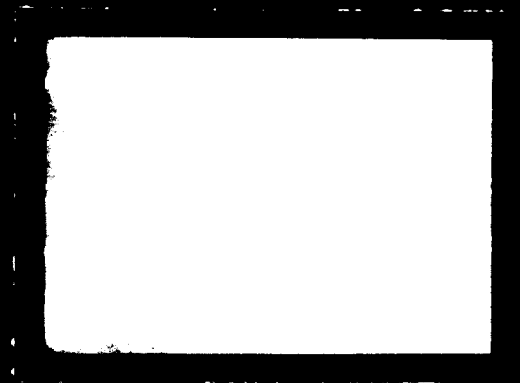


Fig. V-60

OSCILLOGRAMS ILLUSTRATING INTERACTION BETWEEN
RESIDUAL OSCILLATION AND "UNKNOWN" VOLTAGE,
FOR DIFFERENT AMPLITUDES OF RESIDUAL OSCILLATION.

In Fig. V-59, the residual oscillation is large enough to be comparable with this unknown voltage, and perceptible beats occur between the two. The beats take the form of variations in the length, or duration, of the trains of oscillations, rather than in their height, for the receiver is operating in a saturated condition. Finally, in Fig. V-60, the residual oscillation is so large, and the receiver is hence in such a highly saturated state, that the effect of the "unknown" voltage is negligible. Beats undoubtedly occur, but they are too small to be visible in the oscillogram.

Additional evidence of the existence of the "unknown" voltage is presented by the oscillograms in Figs. V-61 and V-62, which were



Fig. V-61

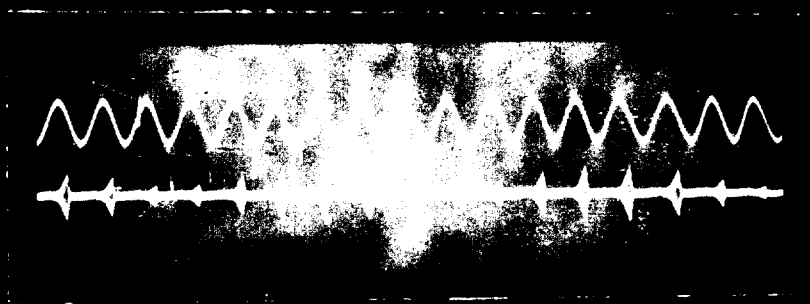


Fig. V-62

OSCILLOGRAMS ILLUSTRATING INTERACTION BETWEEN
SIGNAL VOLTAGE AND "UNKNOWN" VOLTAGE.

taken with such high values of circuit resistance that no appreciable amplitude of residual oscillation can have remained at the instants of "dedamping". In Fig. V-62, for instance, the resistance of the tuned circuit was 225 ohms; and in both figures the abruptness with which the oscillations decay make it appear very unlikely that residual oscillations exerted any appreciable influence.

Nevertheless, beats are clearly visible in both oscillograms. The obvious conclusion is that the input signal was heterodyning with the "unknown" voltage. This conclusion is supported by the observed fact that the beat frequency could be varied by adjusting the quenching frequency or the signal frequency, but did not respond to changes in the tuning of the receiver.

To summarize the foregoing paragraphs, the behavior of the low-frequency receiver indicated that at the instant of "dedamping" there were present not only forced oscillations produced by the signal and residual oscillations from the preceding quenching cycle, but also a third component of radio frequency voltage. This third voltage was definitely related to the quenching voltage, both in magnitude and in phase. The only question was as to the exact mechanism of the action which produced it.

An answer to this question, based on theoretical grounds alone, followed recognition of the fact that, when operating under those conditions which gave the greatest evidence of the "unknown" voltage, the superregenerative receiver was essentially a Class C amplifier, as far as the quenching voltage was concerned. With

large values of negative bias and quenching voltage, the plate current was necessarily equal to zero over a large part of the quenching cycle, rising abruptly to finite values as the instantaneous grid bias swung upward past cut-off. This abrupt bend in the plot of plate current against time, repeated periodically at the quenching frequency, was responsible for the presence of a series of strong harmonics of the quenching frequency in the tuned circuit. These voltages, even as high as the fortieth harmonic, were presumably of appreciable magnitude; so that when a quenching frequency of 25 c.p.s. and an oscillatory frequency of 1000 c.p.s. were used, a transient of considerable magnitude was induced into the tuned circuit by the abrupt rise in plate current as the instantaneous bias passed cut-off. This transient was dependent upon the quenching voltage, both in magnitude and in timing; and it seemed reasonable to expect that it might be sufficiently strong to play an important part in the superregenerative process.

A prima facie confirmation of this hypothesis may be observed in the oscillograms in Figs. V-61 and V-62. In both of these figures, but in the latter particularly, a small but appreciable transient impulse occurs shortly before the beginning of every train of oscillations. These impulses are uniformly spaced, and bear a constant phase relation to the quenching voltage, which is indicated by the sine wave on the same oscillogram.

Further evidence pointing toward the same conclusion appears in the oscillogram in Fig. V-63. The upper curve represents plate current, while the lower represents current in the oscillatory circuit. A sufficiently high resistance (470 ohms) was used in the tuned circuit



Fig. V-63



Fig. V-64

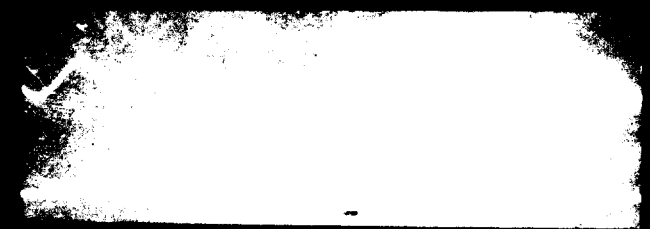


Fig. V-65

to prevent free oscillations from building up during any part of the quenching cycle. Since there could thus be no residual oscillations, and since no signal voltage was impressed, the only remaining voltage to which the tuned circuit was sensitive was the so-called "unknown" voltage. This voltage is clearly visible in the oscillogram, taking the form of transient impulses which repeat themselves periodically at the quenching frequency.

These impulses may be divided into two sets, one of which occurs at that instant in the quenching cycle when the instantaneous grid bias passes cut-off in an upward direction, the other when it passes cut-off headed downward. The former of the two, the "unknown" voltage referred to above, is by far the larger; although just why this dissymmetry between the two types of transients exists is not clear.

The lower curve of Fig. V-64 has the same significance as that of Fig. V-63; that is, it represents current in the tuned circuit. Fig. V-64, however, was taken with a considerably lower value of quenching frequency (10 c.p.s. instead of 25 c.p.s.). All other adjustments remained approximately the same. The effect of reducing the quenching frequency is clearly visible: the transient impulses induced in the tuned circuit through the mutual inductance are now too small to be discernible on the oscillogram. The upper curve of Fig. V-64, incidentally, represents quenching voltage, not plate current.

An interesting phenomenon appears in the oscillogram in Fig. V-65. Here the adjustment of the receiver was practically the

same as in the case of Fig. V-63, but the sweep circuit of the cathode-ray oscillograph was in operation as well. As a consequence of the saw-tooth wave-form of the sweep circuit, there was periodically induced into the oscillatory circuit, through various stray paths, a transient of sufficient magnitude to be visible in the oscillogram. At the time when Fig. V-65 was taken, the fundamental frequency of the sweep voltage was not accurately adjusted to the quenching frequency of the receiver. Consequently, in successive quenching cycles on the oscillogram, there is a steady drift of the transient produced by the sweep circuit, with respect to that produced by the quenching voltage.

From the observations described in the preceding paragraphs it seems clear that, in the low-frequency receiver at least, there were present under the proper conditions not only signal voltage and residual oscillations, but also a third component of radio-frequency voltage induced into the oscillatory circuit by the abrupt rise in plate current which occurred when the instantaneous grid bias swung upward past cut-off. Whereas with two radio-frequency voltages there can be only one interacting pair, with three voltages there are three possible interacting pairs. This statement has been borne out by oscillographic illustrations of the three possible kinds of beat phenomena: (a) forced oscillation produced by signal, versus residual oscillation; (b) transient oscillation due to the intermittent nature of the plate current, versus residual oscillation; and (c) forced oscillation versus transient oscillation.

In practice, it is not expected that this third source of

radio-frequency voltage will ever need to be given much consideration. In the low-frequency receiver in which it was detected, an unusually low ratio of "radio" frequency to quenching frequency -- ranging from 20:1 to 100:1 -- was employed. In a practical superregenerative receiver for reception at, say, 30 megacycles, this ratio would be at least 1000:1. Consequently only very high harmonics of the quenching frequency could be induced into the oscillatory circuit, and these would be so weak as to be negligible.

CHAPTER VI

CONCLUSION

CHAPTER VI

CONCLUSION

To summarize the results of the investigation described in the foregoing chapters, the work may be divided into two general classifications. The first of these has had to do with the factors determining the course of oscillations during the quenching cycle, or the "superregenerative process". The second has dealt with the subject of multiple resonance phenomena. These two parts of the investigation will now be reviewed briefly.

The Superregenerative Process:

The superregenerative circuit is fundamentally an oscillatory circuit with periodically varying resistance. This resistance, alternating between positive and negative values, is a function of both time and the amplitude of oscillating current.

A formal solution of the differential equation for such a circuit would be difficult, if not impossible, to obtain, even if the resistance were assumed to be a very simple function of time and oscillating current. By making the further assumption that the resistance is a simple function of time alone, independent of oscillating current, it would be possible to arrive at an approximate solution, but such a solution would cast little light upon the operation of an actual superregenerative receiver.

Accordingly, an experimental investigation of the superregenerative process was undertaken. The immediate objective was just the reverse of that of a mathematical analysis; instead of trying to find the oscillating current as a function of time, given the resistance as a function of time, we sought to find the course of resistance versus time from experimental data on the course of oscillations versus time. The ultimate objective remained the same, however; the sole reason for attempting to find the resistance as a function of time was to make it possible to predict or to explain the course of oscillating current during the quenching cycle.

For the purpose of the investigation, the net or effective resistance of the tuned circuit was considered to be the algebraic sum of the positive resistance inherent in the circuit and the negative resistance supplied to the circuit by the vacuum tube. This negative resistance component, in turn, was defined as the ratio of the oscillating voltage fed back into the grid coil to the oscillating current in the grid coil, minus a correction to account for grid loss in the vacuum tube. In other words, the negative resistance of the tube was considered to be that resistance which, if placed in series with the oscillatory circuit, would exactly duplicate the effect of the tube upon the circuit.

Experimental data on the value of this negative resistance as a function of oscillating current and grid bias voltage was collected in an extended series of measurements, and was plotted in the form of contour sheets, where the ordinates represented oscillating current,

the abscissae grid bias voltage, and the contours constant values of negative resistance.

Data on the variation of oscillating current and grid bias voltage during the quenching cycle was then obtained from measurements on a series of oscillograms. This data was plotted in the form of operating loops on the negative-resistance contour sheets mentioned above. By interpolating between the contours, it was then possible to read off the negative resistance at any point on the operating loop, and therefore at any point of time during the quenching cycle. These values of negative resistance were added algebraically to the natural positive resistance of the oscillatory circuit, and the resulting series of values of net resistance were plotted against time. In this way it was possible to secure curves showing the variation of the net resistance of the tuned circuit during the quenching cycle.

As a check, curves of net resistance as a function of time were plotted directly from measurements taken on the oscillograms. The agreement with the curves constructed from the negative-resistance charts was fairly good.

The general shape of the curves of net resistance versus time was remarkably close to a square-wave form, for cases representing adjustments of the receiver which would normally be used in reception. For abnormal combinations of quenching and bias voltages the curves departed radically from this form.

The next step in the investigation was the taking of a series of operating curves, showing the dependence of the oscillating current (as indicated by a milliammeter) upon different variables. Most of

these were taken in the form of "modulation characteristics", or plots of oscillating current versus signal voltage. A few curves of oscillating current versus quenching frequency were taken, however. The significant features of these operating curves were explained in terms of the superregenerative process, with the aid of the negative-resistance contour chart.

Multiple Resonance Phenomena:

Multiple resonance effects arise from the fact that when the natural frequency of the receiver is equal to the frequency of the signal or differs from it by an integral multiple of the quenching frequency, the residual oscillation remaining in the circuit at the end of the positive-resistance period is in phase with the forced oscillation produced by the signal, and consequently reinforces it. At other frequencies than these resonance points, the residual and signal oscillations are not in phase at the beginning of the negative-resistance period, and the reinforcing action does not occur.

These resonance effects are of two types, multiple peaks and multiple beats. The former phenomenon manifests itself audibly only when a modulated signal is being received. The modulation frequency can then be heard at a series of points on the tuning dial of the receiver. Multiple beats, on the other hand, may be heard when an unmodulated signal is received, and consist of a series of heterodyne whistles which are heard as the tuning is varied.

Theoretical considerations show that when the receiver is

operating in an entirely unsaturated condition, only the former of these two types of multiple resonance effects may be observed. Sustained beats are impossible in linear operation, for the residual oscillation and signal voltage settle into a fixed phase relation which is repeated at the beginning of every negative-resistance period.

When the receiver is operating partly or completely saturated, on the other hand, so that the residual oscillation is no longer proportional to the initial oscillation which gives rise to it, beats may or may not occur, depending upon how far the receiver is detuned from a resonance point, the magnitude of the signal voltage, and the shape of the saturation curve of residual oscillation versus initial oscillation. A graphical construction has been developed which shows whether or not multiple beats may occur. In their absence, multiple peaks may be observed.

In the experimental investigation, both beats and peaks were observed under different conditions of adjustment, with both the ultra-high-frequency and low-frequency receivers. These phenomena were of the type described above, caused by the interaction between the residual oscillation and the signal oscillation at the beginning of the negative-resistance period.

In addition, a third component of voltage capable of exciting the tuned circuit was found to exist in the low-frequency receiver, under certain conditions. This voltage was found to be a transient impulse caused by a periodic irregularity in the plate current, occurring at the frequency of the quenching voltage. Multiple reso-

nance phenomena were observed which were caused by the interaction of this third voltage with each of the other two radio-frequency voltages mentioned above.

Suggestions for Further Investigation:

The foregoing paragraphs summarize the work of the present thesis investigation. In the course of this work, a number of points were encountered which called for further study, but which we were unable to follow up for lack of time. The more important of these leads are the following:

1. A mathematical approach to the solution of the general equation of the superregenerative circuit, using an experimentally-determined function of oscillating current and time (such as might be obtained from a negative-resistance contour chart, combined with a knowledge of the instantaneous grid bias voltage as a function of time) for the effective resistance of the circuit.

This study might well be carried out on the differential analyzer, or some other mechanical device for the solution of differential equations.

2. An experimental study of a superregenerative circuit in which the negative resistance is supplied by a dynatron. The value of the negative resistance would be under better control in such a circuit than in a regenerative triode circuit such as we used.

3. An experimental study of the negative-resistance contour charts for circuits containing grid-leaks of different values. Our circuit contained none.

4. A theoretical and experimental study of the factors governing selectivity. This would be of considerable practical interest, for the superregenerative circuit is popularly supposed to have very poor selectivity.

5. Further experimental study of the factors controlling stability in a superregenerative receiver. This would probably entail taking curves of oscillating current versus quenching voltage, quenching frequency, grid bias voltage, filament voltage, plate voltage and mutual inductance, one at a time. As this one factor is varied, all of the remaining variables affecting the operation of the receiver, including the signal voltage, would be held constant. In other words, the procedure would be similar to that which was used in taking the curves of oscillating current versus quenching frequency, Figs. V-51, V-52 and V-53.

6. Application of conclusions drawn from the operation of a low-frequency receiver to the design and adjustment of an ultra-high-frequency receiver.

APPENDIX A

TRANSLATIONS AND ABSTRACTS

APPENDIX A

PART I

Brief of

SOME RECENT DEVELOPMENTS OF REGENERATIVE CIRCUITS

Edwin H. Armstrong

Institute of Radio Engineers Proceedings

August 1922

The author first points out that the effect of regeneration, i.e., the reenforcement of oscillations already existing in a circuit, is equivalent to introducing a negative resistance reaction in the circuit, which neutralizes positive resistance and therefore reduces the effective resistance of the circuit.

He then considers the case of a regenerative circuit containing inductance and capacity, when the negative resistance is less than the positive. He points out that if an alternating emf. is suddenly impressed on such a circuit, there will be a steady state value of current which is finite and determined by the circuit parameters, and that there will also be a transient current, the damping of which will be determined by the effective resistance. The maximum amplitude of current in this case is always finite; it reaches this maximum amplitude in a finite time, and when the impressed emf. is removed the current dies

away to zero. This is the action of the common regenerative circuit.

In the case where the negative resistance is equal to the positive resistance, the resultant effective resistance is zero. When an emf. is suddenly impressed on this circuit the current starts to increase at a rate which is directly proportional to the impressed voltage, and in an infinite time it would become infinite. In a finite length of time it attains a finite value. If the impressed voltage is suddenly removed, the current which exists in the circuit at the instant of removal will continue unchanged. It is important to note that although the circuit may have zero resistance, no oscillations will start unless an emf. is impressed.

In the third case considered, the negative resistance is greater than the positive, and the effective resistance is negative. When an emf. is impressed on the circuit, a free and a forced oscillation are set up. The amplitude of the forced oscillation is determined by the impressed emf. and the effective resistance, and is finite. The free oscillation starts with an amplitude which is equal to the forced oscillation and builds up to infinity regardless of whether the external emf. is removed. Here also, it is important to note that there will be no oscillations unless an emf. is impressed, but once started they continue to grow.

In the case where the effective resistance is positive, the forced oscillations contain the greatest amount of energy. In the case where the effective resistance is negative, the free oscillations contain nearly all the energy, and the forced oscillations are

negligible in comparison.

Turner was the first one to use the free oscillations as a means of amplifying signals. He prevented his regenerative circuit from oscillating when there was no signal by biasing the grid negative just enough so that self oscillation could not take place. The introduction of a signal sufficiently large to carry the grid potential over the threshold value would give rise to oscillations which would build up until the tube became saturated. The circuit was then returned to its normal or quiescent state by means of a relay.

Bolitho contributed an important improvement to the above by replacing the mechanical relay by an electrical circuit.

At this point the author states that he wishes to describe a method of operation based on the free oscillation which is quantitative and without a lower limit for the signal. This new method is based on the discovery that if a periodic variation be introduced in the relation between the negative and positive resistance of a circuit containing inductance and capacity, in such a manner that the negative resistance is alternately greater and less than the positive resistance, but that the average value of the resistance is positive, then the circuit will not of itself produce oscillations, but during those intervals when the effective resistance is negative, great amplification of an impressed emf. will be produced. The amplitude of free oscillations set up will be directly proportional to the amplitude of the impressed emf.

The variation in the relation between the negative and positive resistance may be accomplished in three ways. First, by varying the negative resistance with respect to the positive. Second, by varying the positive with respect to the negative. And third, by varying them both simultaneously. The frequency of variation is generally relatively low compared to the frequency which it is desired to amplify.

At this point the author describes three circuits which will produce the desired variation in each of the three ways mentioned above, and includes several oscillograms showing the grid

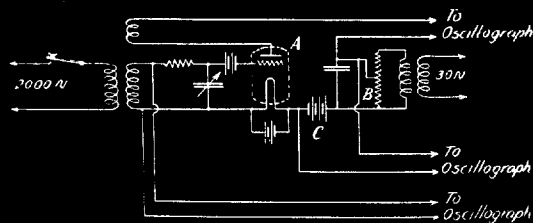


FIGURE 5
A-4 Western Electric Type L₁ Tubes in parallel
B-AC Voltage = 100 Volts
C-DC Voltage = 160 Volts

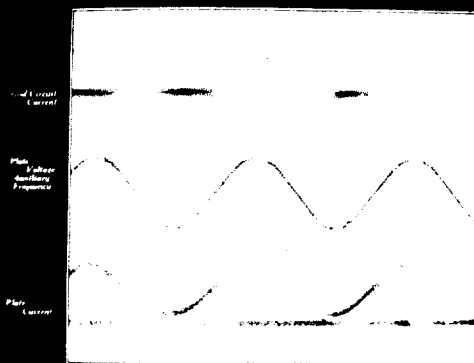


FIGURE 7

and plate currents in two of the circuits suggested. Figures 5 and 7 above show one of these circuits in which the negative resistance is varied and an oscillograph picture of the currents existing in it with and without an input signal. The black arrow in figure 7 indicates the point where the signal voltage was applied. The author points out that in spite of what he has previously said, there is evidence in the oscillograms that there was some self excitation with no signal impressed. This he attributes to random effects in the tube and resistances. Nevertheless the amplitude of oscillations due to noise was much less than the amplitude attained when a signal was impressed because the voltages causing the noise were very small as compared to a normal strength signal. Figure 4 is a sketch of the ideal current and voltage relationships which hold in a circuit of the same general

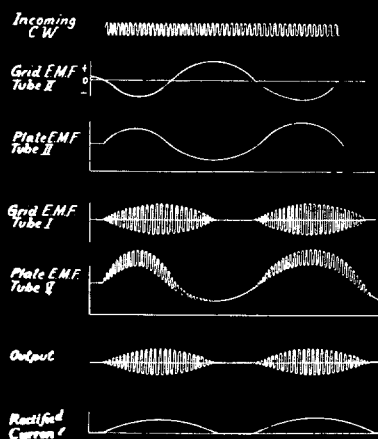


FIGURE 4
 Tube I refers to R in Figure 1
 Tube II refers to O in Figure 1

type as that shown in figure 5. Tube II referred to in the diagram is the oscillator which produces the quenching frequency, and tube I is the superregenerative amplifier.

The choice of quenching frequency is a compromise, particularly in telephony, since obviously the lower the frequency the greater the amplification, and the higher the frequency the better the quality.

Most of the circuits described by the author make use of superregeneration purely as a method of amplification, and the function of detection is carried on in a separate tube. He mentions, however, that when a super-audible quenching frequency is used it is sometimes convenient to perform the function of detection in the same tube as the superregenerative amplification is performed, and he describes a circuit which will do this. He says that it is sometimes necessary to introduce a certain amount of positive resistance into the tuned circuit to insure the dying out of the free oscillation during the period when the resistance of the circuit is positive, and presents a method of doing this.

The use of cascaded superregenerative amplifiers presents severe difficulties because of the reactions of the amplifiers back upon those that precede. This can be overcome by arranging the second stage to operate at double the frequency of the first, etc.

When it is attempted to obtain sharp tuning by placing tuned circuits between the antenna and the amplifier, it is found that the oscillations set up by the amplifier in these tuned circuits,

even when the coupling is very weak, continue during the positive resistance period and re-excite the amplifier when the resistance becomes negative. The simplest solution to this difficulty is to perform the functions of tuning and amplification at two different frequencies, by means of a superheterodyne method which the author describes.

The author states that in general the amplification which can be obtained varies with the frequency of the incoming signal and with the ratio of the wave frequency to the quenching frequency. The higher the signal frequency and the greater the ratio of this frequency to the auxiliary frequency, the greater the amplification. Other things being equal, it appears that the energy amplification varies as the square of the ratio of the signaling frequency to the auxiliary frequency. Hence, it follows that where an audible quenching frequency is employed, much greater amplification can be obtained than in the case of telephony, where a super-audible frequency must be employed.

In a practical way the relative amplification of the new system, as compared with that of the standard regenerative system for reception of telephone signals, may be visualized as follows. With a signal so extremely weak that only the faintest of beat notes can be heard in the ordinary regenerative receiver, the superregenerative receiver will give clearly understandable speech. The new system is singularly selective with respect to spark interference, when a super-audible quenching frequency is

used. This is because although in a normal regenerative receiver, the spark will cause oscillations to be set up which will continue for a thousandth of a second or more, they are damped out inside of a twenty thousandth of a second in the superregenerative receiver because of the periodic quenching.

APPENDIX A

PART II

OSCILLOGRAPHIC STUDY OF SUPERREGENERATION

Messrs. David, Dufour and Mesny

Condensed from L'Onde Electrique,

1925, pp. 175-200.

It was pointed out by Armstrong, in his article in the Institute of Radio Engineers Proceedings, August, 1922, that:

1. The amount of amplification in a superregenerative receiver varies as the square of the ratio between the frequency of the received wave and the frequency of modulation (quenching). This has a practical minimum limit. 2. With the same input signal strength and for the same number of tubes, superregeneration gives a greater output signal than any other system. Nevertheless, it is not possible to receive signals that the superheterodyne, for example, cannot receive.

Upon further investigation, certain difficulties and questions arise in connection with superregeneration. For example, it is not always true that the amplitude of oscillation is proportional to the initial voltage in the tuned circuit. That all depends upon the adjustments of the set. It is possible to obtain the opposite extreme

and have the amplitude of oscillations practically independent of the initial voltage. In such a condition, it is impossible to receive telephony, but the receiver possesses the very interesting property that when receiving a completely modulated signal in telegraphy, the output is practically the same regardless of distance from the transmitter.

The authors have experimented with superregeneration on wave lengths varying from 450 meters to 2 meters. Now, if, as Armstrong has said, the amplification is proportion to the square of the frequency of the carrier (assuming the quenching frequency to be constant), they should have seen it vary in the ratio of one to 50,000 - which they did not. They therefore conclude that the above-mentioned law does not hold indefinitely as the frequency is increased.

Interesting results are obtained when a signal from a local transmitter is superimposed on the signal from a remote transmitter. When the receiver is tuned to the frequency of the latter, and the difference between the two frequencies is in the order of 1,000 cycles, a condition which permits of normal heterodyne detection, it is impossible to receive signals from the remote transmitter by means of superregeneration. The local oscillator makes the receiver oscillate strongly, and the remote one seems to add nothing. If now the frequency difference is progressively increased up to the order of several hundred thousand cycles, it is possible to obtain a great number (100 or more) beats analogous to those of a heterodyne, alternating with silences. Turning the tuning condenser of the local oscillator produces a peculiar warbling sound.

This permits, without particular precautions, extremely sensitive reception of continuous waves, it being easy to adjust for a great number of whistles. To the author's knowledge this phenomenon has not previously been pointed out.

The experimental procedure from which the foregoing observations were taken was as follows. Experiments were carried out on a wavelength of 50 meters. Quenching was obtained by varying the plate voltage at a frequency of about 9000 cycles. The transmitter was placed in the neighboring room. A cathode-ray tube was used to obtain oscillograms.

Pictures were taken of the grid voltage when no signal was impressed. They showed that accidental and random oscillations were much larger and much more frequent for high filament temperatures than for low ones. When a signal was impressed, the resultant oscillations were much greater for higher filament temperatures. The "frying noise" was due apparently to the random oscillations. No noise was observed when a carrier was impressed, and the oscillograph pictures show that the amplitudes of the wave trains are quite uniform.

From the appearance of their oscillograms, the authors deduced that the wave trains always commenced and finished at the same time in the quenching cycle, regardless of their maximum amplitude. To check this theory, they took oscillograms in which the grid voltage was superimposed upon the variations in the plate voltage due to quenching. This permitted them to see the quenching cycles as well as the wave trains in the grid circuit.

From oscillograms taken in this way, they concluded that

when the amplitude of the signal decreased, the amplitudes of the succeeding wave trains decreased also. Furthermore, their duration appeared to grow smaller in such a way that while the wave trains did not begin until later in the cycle, they always ended at the same time.

They next attacked the mathematical analysis of the problem, and started out with considerations of a series circuit containing L , R , and C . They used the equation $L i'' + R i' + \frac{i}{C} = E \omega \cos \omega t$, and solved it by the formal method normally employed in analyzing circuits of constant resistance. Their solution was:

$$i = \frac{E}{\sqrt{R^2 + (\omega L - 1/\omega C)^2}} \left[\sin(\omega t + \psi) + e^{-\frac{R}{2L}t} \left(\frac{CR\omega \sin \psi - 2 \cos \psi}{CS\omega} \sin \frac{St}{2L} - \sin \psi \cos \frac{St}{2L} \right) \right]$$

Where $S = \sqrt{\frac{4L}{C} - R^2}$, $\tan \phi = \frac{L\omega - \frac{1}{C\omega}}{R}$ (phase ϕ between e and i), and $\psi =$ phase of E.M.F. of excitation at $t = 0$.

Assuming that: 1. $R^2 \ll \frac{4L}{C}$, so that $S \cong \sqrt{\frac{4L}{C}}$ 2. $\phi = 0$, i.e., resonance. 3. i and $q = 0$ at $t = 0$. 4. $\psi = 0$.

it follows that:

$$i = \frac{E}{|R|} \left[\sin \omega t - e^{-\frac{Rt}{2L}} \sin \omega t \right]$$

When R is at its maximum positive value, the steady state current is quite small, but it is reached very quickly. The variations in voltage due to this current are too small to be seen in the oscillograms. When R passes through zero, the steady state current becomes infinite, but it requires an infinite length of time to attain that state, and as a result there is a finite value of current at finite values of time. Hence while R is positive, the receiver acts

exactly like a regenerative receiver in that the signal produces a current which is not negligible, and which is proportional to the signal voltage, although too small to be seen on an oscillograph.

When the resistance becomes negative, free oscillations start and rapidly grow. The rate of growth is dependent upon the circuit constants of the set and upon its adjustment. But in a given period it is at each instant proportional to the signal voltage, since the voltage across the tuned circuit at the start of oscillations was proportional to the signal voltage, and since the growth takes place according to an exponential law which means that at any time the amplitude of oscillations is proportional to the initial voltage. The oscillations are limited by the tube characteristics, and by the plate voltage. If the oscillations grow rapidly, the limit is reached at the same time as the plate voltage (quenching voltage) reaches its maximum. If the oscillations grow less rapidly, the maximum is attained some time after the maximum plate voltage is reached. Finally, as the resistance passes through zero and becomes positive, the oscillations grow weaker and die out according to the same law which caused their growth. And thus a return to the original state is made, and the process is repeated.

The preceding explanations show, and the authors' oscillograms confirmed, that for a given signal, it is possible by using different adjustments to obtain different modes of operation, resulting in the growth of oscillations according to different laws. Now in order to receive telephony it is necessary that the maximum amplitude attained by the oscillations be proportional to the received signal at the

beginning of their growth. This will only be true for certain adjustments of the receiver. For, even though during growth the oscillations be proportional to the initial voltage, nevertheless they are limited as to their maximum value. Hence although in the reception of completely modulated telegraph signals it is most convenient to use the maximum possible amplification, it is necessary for telephony that the saturation region be not entered and hence that a lower amplification be used.

In the absence of extraneous voltages, amplification appears to be unlimited. But normally it is impossible to receive signals which generate in the tuned circuit currents which are equal or less than currents due to random effects.

The authors see no reason why the amplification should increase with the square of the frequency of the signal. Of course there exists a lower limit of frequency under which the process of superregeneration becomes impossible, the number of high frequency oscillations in a period of quenching frequency being too small for the above theories and considerations to hold true. In the neighborhood of this limit the amplitude attained by the oscillations is a function of the frequency, and then the amplification does effectively increase with the frequency. But the authors do not believe that when operating at some distance from this lower limit, the frequency can have any effect at all.

In explanation of the previously mentioned phenomenon whereby a musical tone could be produced by two transmitters beating to-

gether at an inaudible frequency, this is due to the fact that the signal is being modulated at a frequency of 1000 c.p.s. Only the forced oscillations which exist in the tuned circuit at the very beginning of the negative resistance period are of importance. Suppose that the two radio frequency signals are beating at a frequency which is an exact multiple of the quenching frequency. Then the forced oscillations which exist at the beginning of the first negative resistance period will be of exactly the same magnitude as those which exist at the beginning of the n^{th} period. Hence all the wave trains will have the same size, and there will be no audible output. However, if the frequency of beats differs by an audible frequency from an even multiple of the quenching frequency, an audible tone of that particular frequency will be heard.

APPENDIX A

PART III

SUPERREGENERATION

Pierre David

Condensed from L'Onde Electrique,

1928, p. 217-260.

DEFINITION

Superregeneration is any method of amplification which depends upon periodic variation of the resistance of the tuned circuit; that is, in which the circuit alternately receives and emits energy.

In many types of receivers use is made of negative resistance, introduced into the circuit by means of regeneration. Only in superregenerative systems, however, is this negative resistance made to vary periodically.

II. STUDY OF THE BEHAVIOR OF A CIRCUIT AS A FUNCTION OF ITS RESISTANCE

General equation:
$$L \frac{d^2 i}{dt^2} + R \frac{di}{dt} + \frac{i}{C} = E \omega \cos \omega t$$

Assumptions:

1. $R \ll L\omega$, so that the natural freq. $\omega_0 = \frac{1}{\sqrt{LC}}$
2. Receiver tuned exactly to r.f. input; $\omega = \omega_0$

When an r.f. E&F is applied, it is meaningless to think of the

initial phase, for practically, on account of inductance in the generator, such an EMF cannot be applied suddenly.

As an example, we shall consider a circuit having the following constants:

$$L = 5 \mu h ; C = 140 \mu \mu f ; \text{ natural resistance } R \cong 10^{\omega} ; \omega_0 = 2\pi(6 \cdot 10^6) ; \lambda = 50 m.$$

A. Resistance constant, not equal to zero:

With the above assumptions, we have:

$$i = \frac{E}{R} (\sin \omega t - e^{-\frac{R}{2L}t} \sin \omega t)$$

$$u = L\omega \cdot \frac{E}{R} (\cos \omega t - e^{-\frac{R}{2L}t} \cos \omega t)$$

When R is positive, the transient term dies out very rapidly.

TABLE I

R	Steady state		Time constant	
	I	U	Sec.	Cycles
10^{ω}	$0.1 E$	$6 \pi E$	$1 \cdot 10^{-6}$	6
5	$0.2 E$	$12 \pi E$	$2 \cdot 10^{-6}$	12
1	E	$60 \pi E$	10 "	60
0.2	$5 E$	$300 \pi E$	50 "	300
0.1	$10 E$	$600 \pi E$	100 "	600
0.01	$100 E$	$6000 \pi E$	1000 "	6000

When $R < 0$, the transient component grows and rapidly becomes predominant. It is limited only by the capacity of the source of power; at which time R ceases to be < 0 . The growth of the exponential term is shown in Table II.

TABLE II

t	$e^{-\frac{R}{2L}t}$		
	R = -1	R = -5	R = -20
$1 \cdot 10^{-6}$	1.1	1.65	7.4
5.	1.65	12.2	$2(10^4)$
10.	2.7	150	$5(10^8)$
20.	7.4	$2(10^4)$	$25(10^{16})$

B. Tuned circuit with $R=0$:

In a tuned circuit having zero resistance, the response to a finite voltage is infinite only if the voltage is maintained for an infinite time. As long as the voltage is maintained, the oscillations grow at a constant rate which is determined by the inductance of the circuit. $i = \frac{E}{2L} t \cdot \sin \omega t.$

If the e.m.f. is applied only for a very short period, it is of almost no advantage to reduce the resistance of the circuit below a certain value, since even with some resistance present the initial rate of growth is practically constant. For substantiation of this point, see Table III.

TABLE III

t	R	I		Total	U
		1st term $\frac{E}{2L} t$	2nd term $\frac{ER}{8L^2} t$		
10^{-6}	0	E/10	0	E/10	$6 \pi E$
10^{-5}	0	E	0	E	$60 \pi E$
10^{-4}	0	10E	0	10E	$600 \pi E$
10^{-3}	0	100E	0	100E	$6000 \pi E$
10^{-6}	0.1	E.10	negl.	E/10	$6 \pi E$
10^{-5}	0.1	E	E/20	19/20E	$57 \pi E$
$2 \cdot 10^{-5}$	0.1	2E	E/5	1.8E	$108 \pi E$
Beyond this point the formula is not applicable.					
10^{-6}	1	E/10	negl.	E/10	$6 \pi E$
$5 \cdot 10^{-6}$	1	E/2	E/8	0.38E	$22 \pi E$
10^{-5}	1	E	E/2	0.5E	$30 \pi E$
Beyond this point the formula is not applicable.					

C. Tuned circuit with R variable:

In the simplest case, the equation for the circuit now becomes:

$$L \frac{d^2 i}{dt^2} + f(t) \frac{di}{dt} + \frac{i}{C} = E \omega \cos \omega t$$

A solution of this equation, however, would fall quite short of showing the true picture of what happens, since it takes no account of the fact that the negative resistance varies with i , as the operating point of the circuit departs from the straight part of the tube characteristic. More correctly, the resistance should be $f(t, i)$; but this equation would be too hard to solve to be worth the trouble, especially since it is not known exactly how the resistance varies with t and i . Therefore the discussion must be limited to a few simple remarks based on physical considerations.

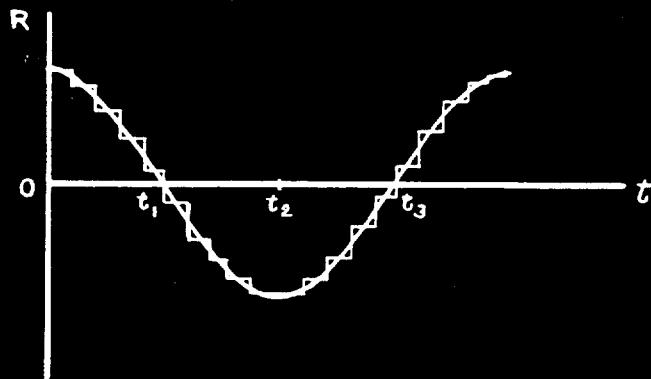
Fundamental Considerations in the case of variable resistance:

Since $R \ll X$ in a practical tuned circuit, the r.f. oscillations are practically sinusoidal, regardless of the wave form of the r.f. input, or of variations in R . The effect of varying R or the r.f. input at a much lower frequency is simply to vary the amplitude of the r.f. oscillations.

III. APPLICATION - SUPERREGENERATION

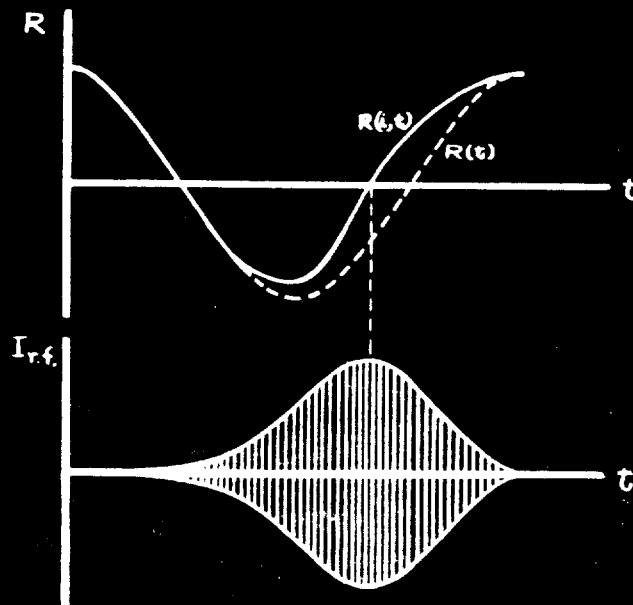
In a superregenerative circuit, one can show approximately how the amplitude of r.f. oscillations varies with time by considering

the resistance to vary in small steps, thus:



In the typical circuit being considered, with an r.f. input voltage of E , the voltage across the condenser may reach $100 E$ by t_1 , (simply an extreme case of the familiar phenomenon of a high resonant voltage across one of the components of a series resonant circuit.)

During the interval t_1 to t_3 , the voltage builds up very rapidly, but remains proportional to the voltage at t_1 , and therefore to E , provided that the voltage does not reach such an amplitude as to change the average slope of that portion of the tube characteristic over which operation occurs. However, because of the tremendous increase of voltage during t_1 to t_3 , even a weak r.f. signal may very well cause the tube to approach saturation, so that R is not simply $R(t)$, but $R(i, t)$. This causes a variation as shown:



Thus, by adjusting the magnitude of the negative resistance introduced into the circuit, one can secure either of these types of operation:

1. Moderate amplification; output signal follows modulation envelope faithfully.
2. High amplification, limited only by capacity of tube; output signal varies but little when input is changed between rather wide limits.

During the positive-resistance period the oscillations decay, reaching a value at τ_1' , of the next resistance cycle, whose ratio to that at τ_1 of the present cycle is determined by the average resistance of the circuit.

(a) If this resistance is positive and large enough (say, a few ohms), the amount of oscillating voltage left over at the beginning of the next negative-resistance period is negligible compared with the forced voltage produced by the signal.

(b) If the average resistance is only very slightly positive, the decaying free oscillations at τ_1 are comparable in magnitude with the forced oscillations produced by the r.f. input. Their effect depends upon their phase relative to the latter.

1. If the number of free oscillations between τ_1 and τ_1' is exactly equal to the number of cycles in the r.f. input, the two voltages are in phase at τ_1 for all quenching-frequency periods. The amplitude of the trains of oscillations, being thus continually reenforced, will build up to saturation of the tube.

2. In general, however, the forced and free oscillations will not be of the same frequency. Let these frequencies be F and F' respectively, and φ the quenching frequency. The relative phase of the two will shift from one t_1 to the next t_1 , causing successive trains to start with different initial voltages; beats are thus produced. If $\frac{F-F'}{\varphi} = n \pm \frac{p}{q}$ (where n is an integer) the beats will have a frequency $f = \frac{p\varphi}{q}$, which may be audible even though $F-F'$ is not.

* * * * *

Because of the above phenomena, there can be several types of superregenerative action. Three will be considered here.

Type A - telephonic:

Conditions necessary:

1. Negative resistance is low enough so that oscillations at no time approach saturation of the tube.
2. Positive resistance is great enough to damp out completely the free oscillations in one quenching-frequency period before the next one begins.
3. Quenching frequency in the range from approximately 12,000 to approximately 20,000 c.p.s.

Result:

Output signal is always proportional to amplitude of input, permitting good reception of modulated signals.

Type B - stroboscopic:

Conditions necessary:

1. Negative resistance is best made large enough to give high amplification, but not to give saturation.
2. Positive resistance is adjusted so that the decaying free oscillations, at the beginning of the following negative resistance period, are still comparable in magnitude with the forced oscillations produced by the r.f. input.

Result:

A series of audible beat notes, separated by intervals equal to the quenching frequency, when the receiver is tuned thru "resonance."

This affords a means of receiving short wave c.w. signals which requires no such precision of tuning as does an autodyne receiver, since a shift of any sort will usually simply transfer the reception to a different one of the series of beats, instead of losing the audible signal entirely.

Reasons why an infinite number of beats are not observed:

1. If $F-F'$ is made too large, the receiver is no longer tuned to the r.f. input, so that an attenuation occurs on this account.
2. The phenomenon of beats demands that $\frac{1}{F-F'}$ be large compared with the interval in which free oscillations are getting under way.

Type C - Anti-noise:

In a regenerative receiver, strong noise voltages are capable of completely preventing reception of a signal, by shifting the operating point of the tube.

In a superregenerative receiver, this noise can be suppressed by fulfilling these conditions:

1. Negative resistance large enough to carry tube to saturation, even with a small initial oscillation.
2. Positive resistance large enough to damp out the oscillations.

Results:

1. C.w. input: all wave trains start off alike and build up to saturation; they all have the same maximum in spite of noise voltages, so no noise is heard.
2. No input signal: tube is no longer saturated. Wave trains start with irregularly varying noise voltages, build up to varying heights, and produce an irregular noise in the output.

This method of reception can best be used when the signal is interrupted r.f., with c.w. between the signals. With this system, no noise can be heard during the intervals, and any noise occurring during the signals cannot interfere with the signal. This method of reception has proven to be of practical value.

* * * * *

Miscellaneous Comments:

Effect of Wave Length:

The shorter the r.f. wavelength, for given positive and

negative resistance, the smaller the time constant, and therefore the higher the rate of growth and decay of oscillations; the limit of this tendency toward increasing amplification being reached when the tube is saturated. The negative resistance contributed by the tube is approximately:

$$R' = \frac{kM}{C\rho} \quad \text{where } k \text{ and } \rho \text{ are constants of the regenerative circuit.}$$

Both from the formula and from practice, it is found that increasing M and decreasing C cause R' to increase. For waves over a few hundred meters long, this limiting value of negative resistance is insufficient to permit the r.f. oscillations to build up rapidly enough to give useful amplification.

Sensitivity and Selectivity:

The amplification of a superregenerative receiver, strictly speaking, can be made almost unlimited, by making the negative resistance sufficiently large. The practical sensitivity, however, is limited by the fact that a signal must be stronger than the background noise in order to be usefully amplified. The height of the noise level, in turn, depends on the selectivity of the receiver. It increases only as the square root of the time constant, while the forced oscillations due to the signal increase directly as the time constant.

In ordinary regenerative reception, the resistance of the tuned circuit is made very small, so that the time constant becomes quite long - 10^{-4} or 10^{-3} sec.

In superregenerative reception, however, the time during

which the receiver is really sensitive and selective, that is, when the resistance is practically zero, is very short - 10^{-6} or 10^{-5} sec. As far as selectivity is concerned, this is the time constant of the circuit. It follows that the superregenerative receiver is less selective than the regenerative receiver.

To increase the selectivity, one must increase the length of time during which the resistance is near zero. This could theoretically be accomplished by adopting a different wave-form of resistance variation, but in practice a resistance variation of the type which leads to "stroboscopic" superregeneration (Type B) keeps the resistance near zero for the greatest part of the time, hence making selectivity highest.

IV. EXPERIMENTAL VERIFICATION (WITH CATHODE-RAY OSCILLOGRAPH)

Methods of connection of oscillograph:

1. A pair of coils deflects the beam at right angles to that of the r.f. oscillations. The photograph is made on a fixed plate. A short pulse of current is sent thru the coils, making the sweep displacement proportional to the time. The result is immediately readable, like a graph plotted on rectangular coordinates. The duration of the exposure, however, is very short. In order to include several modulation periods, it is necessary to sweep slowly, so that only the envelope and not the individual r.f. oscillations can be discerned.

2. To lengthen the permissible duration of the exposure, a double-sweep method was used, in which the following two motions were imparted to the electron beam:

- a. Sinusoidal with respect to time, perpendicular to motion due to r.f. oscillations.
- b. Rectilinear with respect to time, parallel to motion due to r.f. oscillations.

Examples of oscillograms taken in this way are shown in Figs. 13, 14, 20 and 21.

This system was used at two different speeds:

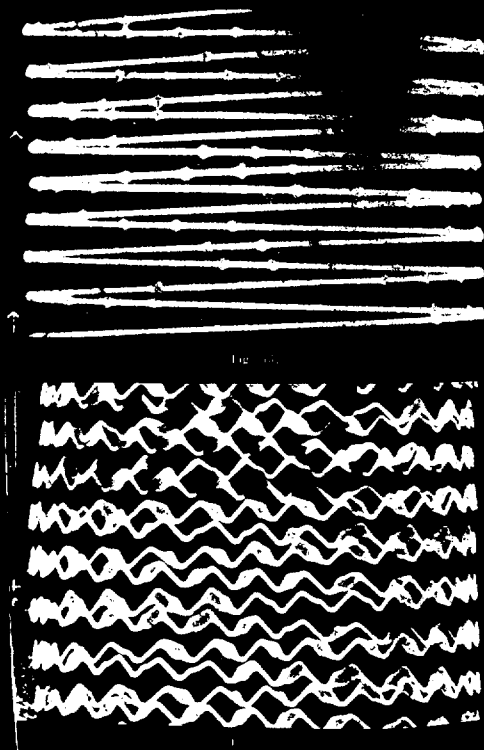
- a. (Sinusoidal sweep: $f = 200$ to 500 c.p.s.
(Rectilinear sweep: $T \cong 0.1$ sec. (produced by rotation of film).
- b. (Sinusoidal sweep: $f = 273,000$ c.p.s.
(Rectilinear sweep: $T = 0.0001$ sec. (produced by electric discharge).

In order to record the phase relation between E_p and the r.f. oscillations, the former was applied to an extra pair of deflecting plates, so that the displacements of the beam by these two voltages were superposed upon each other, as shown in Figs. 14 and 20.

Results:

Type A - telephonic:

Fig. 13 was taken with a sinusoidal sweep frequency of 500 c.p.s. and shows only the r.f. oscillations. The receiver was adjusted to give a clear audible signal. The envelopes are seen to vary in



amplitude, following the modulation. Comparison with Fig. 20 shows that saturation is not reached even in the largest envelopes.

Fig. 14 is similar to Fig. 13, but has the quenching voltage superposed upon the radio-frequency oscillations. The smaller the maximum attained in any envelope, the later it is attained. The weaker the oscillations are, the later they become visible; but they always end at the same instant.

Type B - Stroboscopic:

This is the hardest type to study, for the interesting feature, the beat note of frequency $F-F'$, is normally too weak to be observed on the cathode-ray tube. Consequently it is necessary

to use an abnormally strong input signal.

In Fig. 17, taken with the simple rectilinear sweep first described, the beats of frequency $F-F'$ are easily visible. In the



upper exposure, the beats are slow, because the receiver is nearly tuned to the incoming signal. In the lower, the receiver is further detuned, and the beats are more rapid. In both cases, however, the audible whistle is of the same frequency, about 1000 c.p.s.

An accurate measurement on the plate shows the difference between the maxima attained in two successive periods.

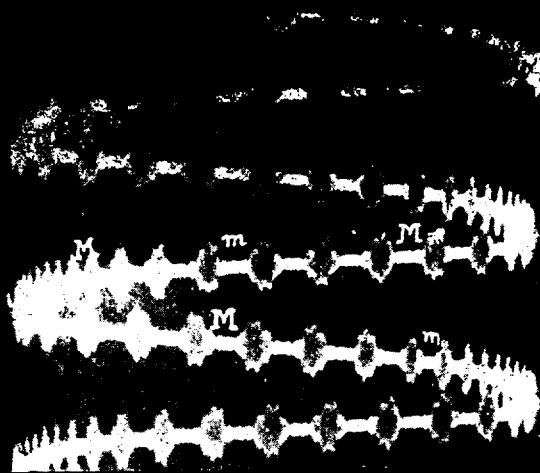


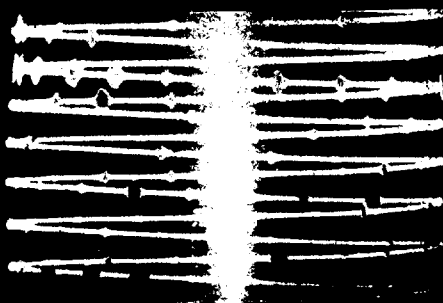
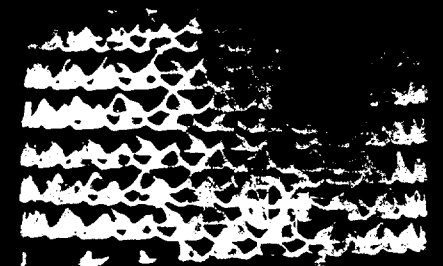
Fig. 19.

Fig. 19 was taken with a sinusoidal sweep frequency of 200 c.p.s. It shows a great number of successive maxima, whose amplitude varies periodically, being maximum at **MM** and minimum at **mm**.

Type C - Anti-noise:

The receiver was subjected simultaneously to the influence of a continuous wave and to that of a source of damped waves having a wavelength of about 200 m.

Fig. 20 shows the behavior of the receiver under these conditions. The r.f. amplitude is now sufficiently great to saturate the tube.



In Fig. 21 no signal is received. It is to be observed that local disturbances suffice to set off oscillations which build up as

high as saturation of the tube. They are irregular, however, sometimes being much smaller or even negligible. The result, after detection, is a confused noise.

APPENDIX A

PART IV

ON SUPERREGENERATION

By Hans Kohn

Institute of Practical Physics, University of Hamburg.

Translated from Zeitschrift für Hochfrequenztechnik,

February, March, 1931

CONTENTS

Introductory considerations.

The regenerative oscillator.

I. Experimental part:

Foreword.

Experimental apparatus.

Damping measurements.

Taking oscillation-characteristics.

Relation between the steepness of the back-coupling
line and the setting of the back-coupling at the
inception of oscillations.

Measurements:

1. Dependence of the minimum quenching voltage upon the quenching frequency.
2. Dependence of amplification upon (quenching) frequency.
3. Accuracy of adjustment and minimum quenching voltage.
4. Dependence of amplification upon damping.

Results of the experimental researches.

II. Theoretical part:

1. Graphical analyses.

Results of the graphical method.

Calculation of Fourier terms.

Relation between back-coupling line and quenching voltage.

2. General theory.

Discussion of results.

Summary.

SYMBOLS

1. Current:

\mathcal{I}_a Amplitude of anode current.

\mathcal{I}_M Amplitude of current of a forced oscillation.

$\mathcal{I}_L = \mathcal{I}_c$ Amplitude of oscillating-circuit current, \mathcal{I}_L in coil,
 \mathcal{I}_c in condenser.

I_a Effective value of anode current.

I_M Effective value of current of a forced oscillation.

I_L Effective value of oscillating-circuit current.

2. Voltage:

U_{st} D.C. control voltage.

U_a D.C. anode voltage.

u_{st} Amplitude of control voltage.

u_a Amplitude of anode voltage.

u_g Amplitude of alternating voltage impressed on grid.

Δu_g Amplitude of the received high-frequency oscillations.

3. Resistance:

R Resultant resistance (impedance) of the high-frequency
oscillating circuit.

R Ohmic resistance.

$$\tan \alpha = \frac{u_{st}}{\mathcal{I}_a} ; S = \frac{\mathcal{I}_a}{u_{st}}$$

4. Wavelengths and frequencies:

λ_M Wavelength of the low-frequency oscillation.

$\lambda = 350m$ wavelength of the high-frequency oscillation employed.

ν Frequency.

- ω Natural frequency of the circuit of the high-frequency oscillations.
- Ω Circuit frequency of the low-frequency oscillation.
- δ Damping = $R/2L$.
- a Rate of growth.
- t Time.

INTRODUCTORY CONSIDERATIONS

(Footnote: Edwin H. Armstrong, L'Onde Electrique 1922, S.625)

Superregeneration was first described by Armstrong. We will consider it in the following manner: an audion is so closely back-coupled that it is brought to self-excitation at a frequency which agrees with the one received. On this high-frequency oscillation is superposed a medium frequency by means of a tube generator which is inductively coupled to the oscillating audion. The high frequency is thus quenched; we shall therefore designate this medium frequency as the quenching frequency.

If the audion receives (a signal from) a distant transmitter, it will be brought into oscillation through the small voltage which is impressed on the grid. Hulbert has made studies of this process of amplification (Footnote: E. O. Hulbert, Proc. Inst. Radio Eng. 11, 391, 1923). He describes a dependence of the amplification upon the high-frequency- and the quenching-voltage.

In the book of K. W. Wagner, "The Scientific Basis of Broadcast Reception", Leuthauser (S. 371) describes in a short article the superregenerative circuit. On the theory, nothing more recent has been put forth. For the adjustment to the most sensitive condition it is remarked only "that the amplitude of the quenching frequency must have a definite value". Further material on this point has been set forth by Barkhausen, Elektronrohren, 3. Bd., Sec. 7 (Footnote: During the carrying out of this work there also appeared Pierre David, L'Onde Electrique 7, 217, 1923; referred to in Ztschr. 33, 153, 1929).

The foregoing work should establish, then, the dependence of the amplification upon the quenching frequency, the quenching amplitude and other factors coming into the question.

Since for very short waves neither high-frequency amplification nor neutrodyning is any longer possible, superregeneration here comes into the question as a possible means of amplification. Its study thus has technical significance as well.

Oscillation problems are conveniently handled by the use of complex representation. For this purpose one uses $Ae^{j\varphi}$ as the complex amplitude, where A is the real amplitude and φ is its phase. Since this system can be used only in linear cases, whereas the characteristics of the tube are not linear, one uses, instead of the tube characteristics, the "oscillation-characteristics" introduced by H. C. Moller: that is, one takes, in place of the instantaneous i_a and u_{st} , the amplitudes \mathcal{I}_a and \mathcal{U}_{st} . To make this clear, the process of oscillation in the case of a tube generator will first be briefly described, and the oscillation-characteristic diagram will be explained on this basis.

The regenerative oscillator:

In the case of the back-coupled oscillator, the control voltage controls the anode current. The relation between the amplitudes \mathcal{I}_a and \mathcal{U}_{st} is shown by the oscillation-characteristic. The anode current, through the oscillating circuit and the back-coupling, induces the control voltage. The relation is linear, and in the oscillation-

characteristic diagram is a straight line. According to H. G. Moller, it is calculated that $\tan \alpha_0 = \frac{1}{2C\delta}$.

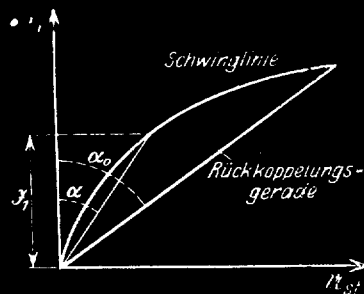


Abb. 1. Röhrengenerator.

Fig. 1. Tube generator.

Key:

Schwinglinie	Oscillation-characteristic
Rückkoppelungsgerade	Back-coupling line

Since the slope of this line is determined by the back-coupling, it is called the back-coupling line. If the current has not yet reached its highest value, but is at the amplitude \mathcal{I}_1 , then there is an excess of control voltage which increases the oscillations. Calculation shows that:

$$\frac{u_{st}}{\mathcal{I}_a} = \frac{1}{2C(\delta + \alpha)} = \tan \alpha$$

for the rate of growth $a = \frac{1}{\mathcal{I}_a} \cdot \frac{d\mathcal{I}_a}{dt}$, one obtains the value:

$$a = \delta \left(\frac{\tan \alpha_0 - \tan \alpha}{\tan \alpha} \right)$$

If one considers a constant for a short time, then one obtains

$\mathcal{I}_a = \mathcal{I}_0 e^{at}$. Ordinarily we always depend upon a small initial current \mathcal{I}_0 which is set up by the switching-on or by shot effect.

EXPERIMENTAL PART

Foreword:

In the case of a superregenerative circuit, as already briefly described in the introduction, the receiver is so strongly back-coupled that inception of oscillations can result; however, an oscillation of considerably lower frequency superposed on the grid circuit immediately suppresses the oscillations. As soon as (the signal from) a distant transmitter is received, the small induced voltage Δu_g suffices to set up oscillations. For simplicity, as a first approximation, we can think of the sinusoidal quenching voltage as supplied by a periodic connection of positive and negative d.c. potential between grid and cathode, which permits the oscillations to increase and decay. The potential, then, remains constant during a half-period. In case, now, the potential is sufficiently negative, so that the slope of the oscillation-characteristic is depressed below that of the back-coupling line (Fig. 2), the oscillations die out. With positive potential, the current can build up again, according to the equation $i_a = i_0 e^{at}$.

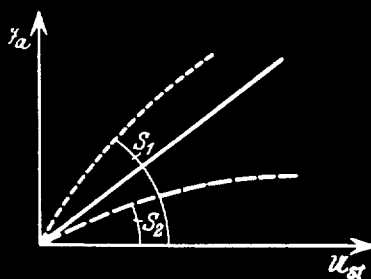


Abb. 2. Schwingliniensteilheiten.

Fig. 2. Steepness of oscillation-characteristic.

For this it is assumed, however, that a current \mathcal{I}_0 is present, in order to bring \mathcal{I}_a back again to a final value during the half-period in which positive voltage predominates (the "positive half-period"). If an external transmitter of the same frequency is received, then the increased ΔU_g is sufficient to produce a current \mathcal{I}_0 and, consequently, a strong oscillation. Upon this depends the amplification process in this circuit. Since $\mathcal{I}_a = \mathcal{I}_0 e^{at}$, \mathcal{I}_a is proportional to the initial value \mathcal{I}_0 , provided again that the expression is given correctly. If one increases the interruption period, which means a decrease of the frequency Ω , then in the now longer "positive half-period" the current can reach greater values, which must increase the amplification as $\frac{1}{\nu}$. If now the back-coupling is also increased, that is, if $\tan \alpha_0$ is increased, and with it a , then a greater quenching potential is also necessary. Furthermore, with closer back-coupling the oscillations become stronger; the amplification, and with it the quenching voltage, thus increase with the back-coupling.

One should now determine first of all the experimental characteristics of superregeneration. The above qualitative theoretical statements should serve as a working hypothesis to the investigator. In the second part an exact theory will then be given for quantitative considerations, and will agree with the experimentally-found values.

Experimental Apparatus:

The experimental apparatus used employs the receiver circuit of Armstrong. It was built as follows (Fig. 3): L_1 and C_1 form the

high-frequency circuit, L_2 is the back-coupling coil and C_2 provides a path for the high frequency from the grid to the cathode. From an external transmitter a small voltage ΔU_g is induced in L_2 . L_4 induces the low-frequency quenching voltage in L_3 .

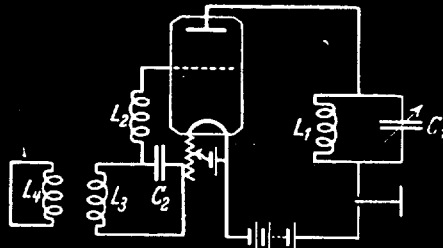


Abb. 3. Gebräuchliche Schaltung.

Fig. 3. Circuit employed.

With this circuit the following questions should be investigated:

1. The dependence of minimum quenching voltage upon quenching frequency.
2. The dependence of amplification upon quenching frequency and damping.
3. The dependence of amplification upon quenching voltage.
4. The dependence of amplification upon the small voltage induced by the transmitter.
5. The dependence of amplification upon the accuracy of adjustment of the minimum quenching voltage.

In the calibration of the apparatus there must be measurements of the resistance of the various parts of the circuit, and also the measurement of damping, the determination of characteristic-fre-

quency, and the taking of the tube characteristic and oscillation-characteristic.

The apparatus finally used for the measurements will now be considered (Fig. 4).

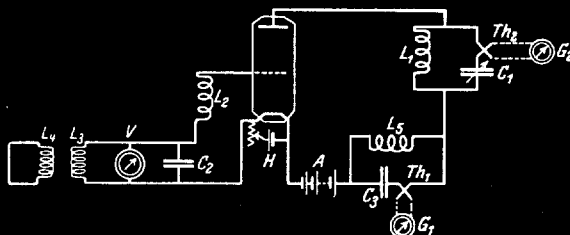


Abb. 4. Meßanordnung.

Fig. 4. Measuring Apparatus.

It is derived from Fig. 3 by the inclusion of measuring instruments. The symbols mean: L_1 - L_5 , coils; C_1 a variable condenser of about 50-700 cm. (55-780 microfarads); C_2 and C_3 , blocking condensers; A, the plate battery; G_1 and G_2 , moving mirror galvanometers; Th_1 and Th_2 , thermo-elements; V, a static voltmeter. In the receiving circuit L_1 and L_2 are coupled together, so that oscillations can be set up. The characteristic wavelength, according to measurement, is 350 m. An outside oscillation of greater wavelength is introduced from another tube generator through L_4 to L_3 . Its voltage is measured by the voltmeter V. Since L_2 possesses only a relatively small inductance (compared with 10^5 cm. (100 microhenries)) and, for the small frequency $\Omega = \frac{2\pi c}{\lambda_m}$

$$(\Omega < 2 \times 10^5 \text{ sec}^{-1}, \text{ that is, } \Omega L < 20 \text{ ohms})$$

has a small resistance (impedance) in comparison with that of the grid-filament path ($\approx 10,000$ ohms), the exact voltage between grid and filament is nearly the same as V . The large condenser C_2 , about 10^4 cm. (0.011 microfarad), bypasses the large impedance ωL_3 , for the high frequency. In order to measure the effective value i_a of the alternating component of the plate current, the high-frequency current going through the condenser C_3 is separated from the direct current which passes through L_5 . The high-frequency current must then pass through thermo-element Th_1 , which is connected with galvanometer G_1 . Since, for the yet-to-be-described damping measurements, the coil current i_L must be known, making allowance for the capacitance current i_C , a second thermo-element Th_2 with galvanometer G_2 , as shown in Fig. 4, will be connected into the oscillatory circuit.

Damping Measurements:

If the voltage across the high-frequency circuit is u_a , the alternating current which flows through L_1 is

$$i_L = \frac{u_a}{j\omega L_1} \quad (1)$$

The current i_a is

$$i_a = \frac{u_a}{R}$$

when R designates the combined resistance (impedance).

Now, for resonance ($R =$ ohmic resistance):

$$R = \frac{L_1}{C_1 R}$$

Furthermore $\delta = \frac{R}{2L_1}$; $R = 2L_1 \delta$.

Consequently $\frac{I_a}{I_L} = \mu_a \cdot 2C_1 \delta$; (2)

and, from (1) and (2), it follows that

$$\frac{I_L}{I_a} = \frac{1}{2C_1 L_1 \delta \omega}$$

and since $1/C_1 L_1 = \omega^2$,

then $\delta = \frac{\omega}{2} \frac{I_a}{I_L}$.

The damping can now be measured for various adjustments of the back-coupling. The back-coupling will be adjusted by shifting the position of the back-coupling coil in proximity to the oscillating coil. The various adjustments of the back-couplings are marked by scale divisions on L_1 . The closeness of back-coupling decreases from 1 to 4 on this scale.

Example

No.	Back-coupling (Scale div.)	I_a^2 (ma ²)	I_L^2 (ma ²)	ω (sec ⁻¹)	$\delta = \frac{\omega}{2} \sqrt{\frac{I_a^2}{I_L^2}}$ *
1	4.1	35	12,000	5.38(10 ⁶)	1.45 (10 ⁵)
2	3.9	73	23,000	5.38(10 ⁶)	1.52 (10 ⁵)

In the second case δ is the larger, since in the case of stronger back-coupling greater loss due to grid current results.

The damping measurements in the various series of measurements were, in part, performed only once, and, in part, repeated for various values as a check.

*The squares of the effective values are proportional to the squares of the amplitudes, $\frac{I_a^2}{I_L^2} = \frac{I_a^2}{I_L^2}$.

Taking Oscillation-Characteristics:

The oscillation-characteristic shows the relation between the amplitude of the anode current I_a and the amplitude of the control voltage U_{st} . I_a is easy to measure. The measurement of U_{st} offers difficulties, however, since electrometers are too insensitive and disturb the circuit by their capacitance, and since other voltage-measuring devices take too much current.

Therefore the slope of the back-coupling line, $\frac{1}{\tan \alpha_0}$, is measured at the position U_{st} , and U_{st} is calculated from $U_{st} = I_a \tan \alpha_0$.

$\tan \alpha_0$ may be very easily measured. At the initiation of oscillations, $\tan \alpha_0 = \frac{1}{S_0}$. It is thus only necessary to so adjust the negative grid voltage, for a given adjustment S_0 of the back-coupling coil, that the oscillations just begin, and to obtain the S_0 -values of the tube characteristic corresponding to the observations U_g , which are first secured.

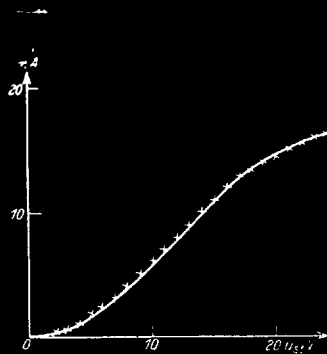


Abb. 5. Röhrenkennlinien.

Fig. 5. Tube Characteristic.

Taking the tube characteristic:

First the characteristic of the tube with d.c. voltage was obtained. In order to prevent oscillations, the back-coupling coil was moved away from the oscillating-circuit coil. The necessary grid bias was adjusted with a potentiometer. Fig. 5 shows the tube characteristic (tube type Valvo H406).

Relation between the steepness of the back-coupling line and the setting of the back-coupling at the initiation of oscillations:

Because of the variation of the control bias U_{st} , which takes place in the way indicated above, the initiation of oscillations occurs at different adjustments of back-coupling. For the inception of oscillations, then, it is always true that $\tan \alpha_0 \cdot S = 1$. The adjustments of the back-coupling and the corresponding control bias voltage were recorded. Knowledge of the mutual inductance is not necessary.

The measurements gave the following values:

L_{12} (Scale div.)	U_{st} (Volts)	$S_0 = \frac{1}{\tan \alpha_0}$ (Milliamps./volt)	
4.20	10	1.175) Obtained, for the specified U_{st} , from the tube characteristic.
4.10	9.5	1.170	
4.02	9.0	1.000	
3.90	8.0	0.910	
3.75	7.0	0.800	
3.50	6.0	0.700	
3.20	5.0	0.626	
2.60	4.0	0.500	
1.30	3.0	0.305	
0.70	2.5	0.250	

Measurement of current for given back-coupling, that is, for given $S_0 = \frac{1}{\tan \alpha_0}$, and therefore for given U_{st} :

Now, with constant d.c. control voltage ($U_a = 100$ v., $D = 10\%$ ($\mu = 10$), $U_g = 0$), I_a^2 is to be measured, with the back-coupling adjusted to the same values as in case 2. For sinusoidal oscillations, I_a is then $\sqrt{2I_a^2}$. Since, now, for each value of back-coupling, $\tan \alpha_0 = \frac{1}{S_0}$ is known, U_{st} can be calculated from $U_{st} = I_a \tan \alpha_0 = \frac{I_a}{S_0}$. The following values were obtained (Fig. 6):

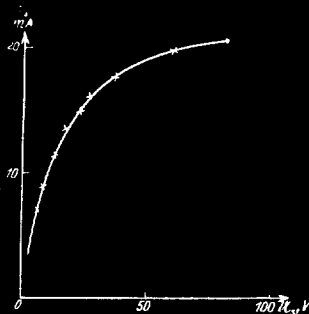


Abb. 6. Schwinglinie.

Fig. 6. Oscillation-characteristic.

L_{12} (Scale div.)	S_0 (Milliamps./volt)	I_a (ma.)	U_{st} (volts)
4.20	1.175	3.47	2.94
4.10	1.170	7.06	6.10
4.02	1.000	8.90	8.90
3.90	0.910	11.50	12.60
3.75	0.800	13.60	17.00
3.5	0.700	15.1	21
3.2	0.62	16.3	26
2.6	0.50	17.3	36
1.3	0.33	20.0	60
0.7	0.25	21.0	84

MEASUREMENTS

1. Dependence of minimum quenching voltage upon the quenching frequency Ω :

As the first question, the dependence of the quenching voltage upon its frequency should be studied. By quenching voltage is to be understood the amplitude of the low-frequency voltage which exactly suffices to suppress the high-frequency oscillations (minimum quenching voltage). The quenching voltage should thus be raised until the high-frequency oscillations just cease. The square of the high-frequency current \mathcal{I}_a^2 or I_a^2 is to be measured by thermo-element Th_2 (Fig. 6) (note: probably this should be Fig. 4). Here, however, the following difficulty presents itself: the longer wave of the quenching oscillator is superimposed upon the characteristic frequency of the receiver, so that a low-frequency forced oscillation will be set up, which will be measured as well as the high-frequency current I_a . Hence it is very difficult to determine I_a at the instant of quenching, since as long as the control voltage is positive the superimposed wave sets up a low-frequency current, even after the stopping of the high-frequency current. In order to separate out this current, a tube voltmeter is loosely coupled to the oscillating circuit as an indicator. This tube voltmeter shows, by means of a milliammeter, the starting and stopping of the high-frequency current, while the low-frequency current can induce no noticeable potential, as can be demonstrated in a separate experiment.

For still greater accuracy of measurement, the tube volt-

meter can be tuned to the high frequency ω by means of a resonant circuit.

The measurements are carried out in the following manner:

1. The receiver is back-coupled sufficiently closely to initiate oscillations.
2. The quenching wave is superimposed and its amplitude increased until the tube voltmeter indicates the quenching of the high-frequency oscillations. This point is located as exactly as possible by repetition of the adjustment. The voltage U_g is read on the static voltmeter and recorded.
3. The measurement is repeated for other quenching wavelengths.

The following results are obtained:

First run: (a) Measurement of square of anode current without quenching voltage: $I_a^2 = 105 \text{ ma}^2$. (b) Measurement of quenching voltage for various wavelengths λ_m . Column 1 gives the square of the anode current I_m^2 which is produced by the quenching voltage. It continues, superfluous, when the monitoring audion shows no more high-frequency oscillation.

(Calculated from U_g)

I_m^2 (ma^2)	λ_m (meters)	U_g (volts)	u_g (volts)
48	7500	6	8.45
47	20000	5.9	8.30
47	25000	5.9	8.30
49	45000	5.9	8.30

Second run: (a) Without quenching wave, $I_a^2 = 91 \text{ ma}^2$. (looser back-coupling). (b) After superimposing λ_m :

(Calculated from U_g)

I_M^2 (ma ²)	λ_M (meters)	U_g (volts)	u_g (volts)
36	5,300	5.1	7.2
34.5	7,500	5.1	7.2
31.0	20,000	5.0	7.05
30.0	29,000	5.0	7.05
31.0	45,000	5.0	7.05

As the measurements show, the quenching voltage is independent of λ_M over a wide range but increases with back-coupling; at the same time it is to be observed that the square of the current of the forced oscillation produced by $u_g \cos \Omega t$ varies only slightly for various quenching wavelengths.

3. Dependence of amplification upon (quenching) frequency:

As a very important subject for study, the dependence of amplification upon frequency now follows.

Experimental Procedure:

1. The receiver, oscillating at its natural frequency, is barely quenched by the superimposed wave. The quenching voltage and the I_M^2 produced by λ_M are measured.

2. A transmitter adjusted to resonance with the receiver is set into oscillation and induces in the grid circuit of the receiver a small voltage ΔU_g , which brings the receiver again to the inception of oscillations. The I_a^2 thus produced adds itself to the I_M^2 and thus can be measured.

3. The same experiment is repeated for different values of λ_M . In connection with this, I_c^2 is measured several times in order to determine the damping. The induced Δu_g is not varied during a run of measurements. Knowledge of Δu_g is not necessary, as only the ratio of the amplifications with different values of λ_M must be measured. The different runs, however, are undertaken, some with the same, and some with different values of Δu_g . The dependence of amplification upon variations in Δu_g will be studied later.

First, four series of measurements taken with the same Δu_g should be discussed. In these the back-coupling, and with it the minimum quenching voltage, were increased in the order 1 to 4. The measured values are represented (Fig. 7) by points, crosses and circles. The ordinates indicate I_a^2 in ma^2 , the abscissas λ_M^2 in km^2 . In the tables values of I_M^2 are also given. u_g is the amplitude of the quenching voltage. L_{12} is the back-coupling setting in scale divisions.

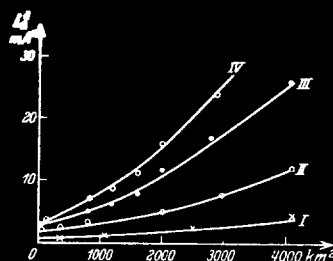


Abb. 7. Meßkurven.

Fig. 7. Measured curves.

The four runs give the following values.

Run No.	I_a^2 without U_g . (ma ²)	I_c^2 without U_g (ma ²)	L_{12} Scale div.	δ sec ⁻¹ (10 ⁵)	U_g (volts)	I_M^2 (ma ²)
1	36	12,000	4.1	1.43	2.96	12.5-13
2	75	23,000	3.9	1.52	4.5	25-31
3	78	23,000	3.7	1.5	8.05	27-34
4	104	—	3.6	1.52	8.5	—

The values of I_a^2 and λ_M^2 in all the measurements are to be taken from Fig. 7.

The I_c value is omitted from the fourth run, since it does not come into the question for our purpose. The damping is repeated in curve 4, in the presence of quenching voltage, and reception is to be measured.

As is evident, the I_a^2 values in runs 1, 2 and 3 are really considerable. The I_M values can be 3 to 4 times as great as I_a . It remains to be observed that the first points of the first curve are uncertain within 30 to 40%, since 1 ma. is at the limit of accuracy of the readings.

For our investigation, the curves show the following results:

1. The amplification increases with decreasing quenching frequency, as is predicted theoretically.
2. The amplification increases with increased quenching voltage, which depends in turn on closer back-coupling, agreeing with theory.
3. By extrapolation to smaller values of λ_M , one obtains a minimum of amplification for $\Omega \rightarrow \infty$ which in the given curves can deviate but slightly from the amplification at $\lambda_M = 5,000$ to 7,000

meters, provided the extrapolation is permissible. To account for this, we assume upon reflection that, with increasing Ω , the time which is available for growth in the positive period decreases toward zero; i.e., the slope of the oscillation characteristic then lies continuously below that of the back-coupling line. Thus, for $\Omega \rightarrow \infty$, one can replace the quenching frequency by a negative grid bias of the receiver which just suffices to suppress oscillations; i.e., $S_0 \leq \frac{1}{\tan \alpha_0}$ continuously. With the reception of ΔU_g , a current I_a now flows again which can be compared with that for large Ω . For the investigation ΔU_g is made larger, in order to obtain sufficiently large values of I_a^2 . The measurements are:

Measurement	Back-coupling	U_g (volts)	Neg.bias (volts)	I_a^2	λ_M (km.)
1	(1a close	8.5	---	9	5.3
	(1b ---	---	3.2	7	neg. bias
2	(2a loose	6.4	---	6	5.3
	(2b ---	---	3.1	7	neg. bias

It is thus shown that our assumption is established as valid, and a lower limiting value of the amplification exists.

3. Accuracy of adjustment and minimum quenching voltage:

For consideration of accuracy of measurement it is now necessary to investigate the quenching voltage most favorable for amplification and the effect of a deviation from it, which might occur

through an error in adjustment. It is already known from practical operation that the quenching voltage should only barely suffice to

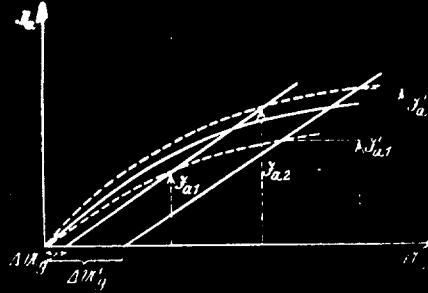


Fig. 8. Accuracy of adjustment.

suppress the oscillations in the absence of a received signal. What effect, now, does supplying too strong a quenching voltage have? When the quenching voltage was adjusted exactly, the oscillation-characteristic was the solid curve in Fig. 8. We will assume that with the adjustment not strictly exact the resulting oscillation-characteristic lies between the two dashed curves. If ΔU_q is very small, then \mathcal{D}_a is uncertain between the wide limits \mathcal{D}_{a_1} , and \mathcal{D}_{a_2} ; if, on the other hand, ΔU_q is larger ($=\Delta U_q'$), then the percentage of uncertainty of \mathcal{D}_a is small (between \mathcal{D}_{a_1}' and \mathcal{D}_{a_2}'). Therefore the amplification will vary only slightly with inaccurate adjustment. The experiment is carried out, again with large ΔU_q , in such a way that first the minimum quenching voltage is established. It is then increased in steps of 1/20 to 1/10 volt.

Fig. 9 shows that the amplification falls rapidly as the

minimum voltage is exceeded; the diminution always proceeds, not

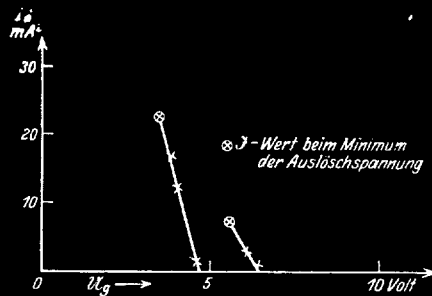


Abb. 9. Verstärkung bei Änderung der Auslöschspannung.

Fig. 9. Amplification with variation of quenching voltage.

Key:

x - Wert beim Maximum der Auslöschspannung

o -value at maximum quenching voltage

abruptly, but continuously. With an excess of 1/10 volt over the minimum voltage, the amplification drops about 10%; since, now, adjustment of the quenching voltage to within 1/10 volt is easily accomplished with the static voltmeter, accordingly the error in every case amounts to less than 10%.

Effect of quenching voltage upon amplification, with constant λ_m :

By "quenching voltage" should always be understood the most favorable value, according to the foregoing investigations; i.e., the minimum quenching voltage. The dependence of the amplification upon it and the back coupling has already been seen in the general curves of Fig. 10 (note: this must mean Fig. 7). To make this more

apparent, this should be shown by yet another measurement, with λ_m held

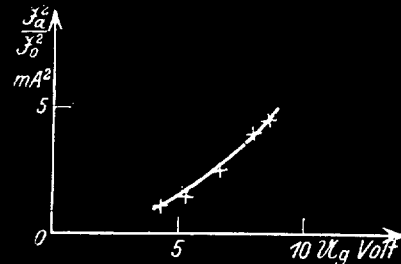


Abb. 10. Verstärkung und Auslöschspannung.

Fig. 10. Amplification and quenching voltage.

constant, and the quenching voltage varied through a variation of the back-coupling.

Instead of the square of the current, the ratio $\frac{I_a^2}{I_0^2}$ is used here, where I_0^2 is the square of that current which flows in the case of minimum amplification. As carried out, this is the case of large values of Ω or of the replacement of quenching voltage by a negative grid voltage. For λ_m a 28,000-m. wave was chosen. As Fig. 10 shows, the amplification in the beginning varies nearly as the square of the quenching voltage.

Effect of variation of ΔU_g upon I_a^2 :

In order to be able to check upon ΔU_g , the voltage applied to the grid of the receiver, in the case of its varying, the following arrangement is used. In the oscillating circuit of the transmitter there is connected a hot-wire instrument before the condenser, in order to measure the high-frequency current in the circuit. ΔU_g is then linearly proportional to the circuit current \mathcal{I}_s or I_s .

. If the high-frequency current I_s decreases by a fractional part, then ΔU_g is also reduced by the same fraction; that is, in general

$$\frac{\Delta U_{g_1}^2}{\Delta U_{g_2}^2} = \frac{I_{s_1}^2}{I_{s_2}^2}$$

where I_{s_1} and I_{s_2} are different high-frequency currents in the circuit, and ΔU_{g_1} and ΔU_{g_2} are the voltages set up by them on the grid of the receiver. For our purpose it is sufficient to know I_s^2 .

The wavelength of the quenching voltage in this investigation was 45,000 meters. As the curve of Fig. 11 shows, the I_a^2 -values are linearly proportional to I_s^2 and therefore to ΔU_g^2 ; thus I_a is proportional to ΔU_g , as long as for the I_a -value the oscillation-characteristic can be closely approximated by a straight line. With

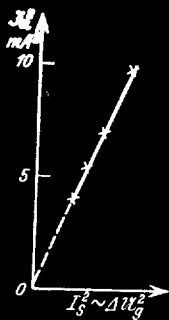


Abb. 11. Kurve.

Fig. 11. Curve.

greater values of current, the linear relation no longer holds, since the amplification tends toward a limiting value independent of ΔU_g and λ_m . We shall observe this again in some measured curves with relatively large ΔU_g .

Since here large values of current are reached very quickly, the rate of rise soon decreases, since because of the bending-over of the oscillation-characteristic the amplification reaches a limit. The measurements were carried out (Fig. 12) in the same manner as previously.

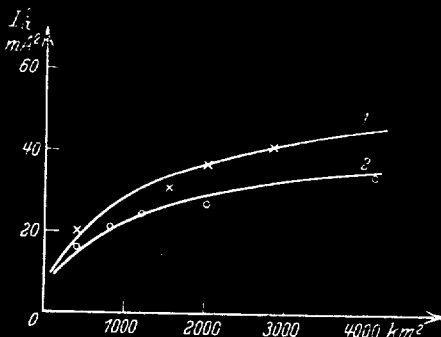


Abb. 12. Meßkurven für großes ΔU_g

Fig. 12. Measured curves for large ΔU_g .

Run	L_{12} Scale div.	I_a^2 (without U_g) ma ² .	δ sec ⁻¹ × 10 ⁵	U_g volts
1	3.7	10.5	1.41	3.8
2	3.8	80	1.41	7.2

$$\omega = 5.3 \times 10^6 \text{ sec}^{-1}.$$

4. Dependence of amplification upon damping:

Heretofore in the measurements the damping was kept nearly constant. Now it should be varied by connecting an ohmic resistance into the oscillating circuit of the receiver. The measurements were carried out in the same manner as before. In place of the I_a^2 -values

the ratio $\frac{I_a^2}{I_0^2}$ should be introduced, in order to reduce to the case $\Delta U_g = 1$ and to be free from any possible variation in ΔU_g between different measured curves. I_0^2 is again the square of the current with minimum amplification. The damping measurement is repeated. Therefore the I_c -values are also given in the table. The measured values are as follows:

Run	L_{12} Scale div.	I_a^2 (without U_g) ma^2 .	δ $sec^{-1} \times 10^5$	U_g volts
1	3	144	2.74	7
2	3.5	104	2.70	6.4

$\omega = 5.3 \times 10^6 \text{ sec}^{-1}$.

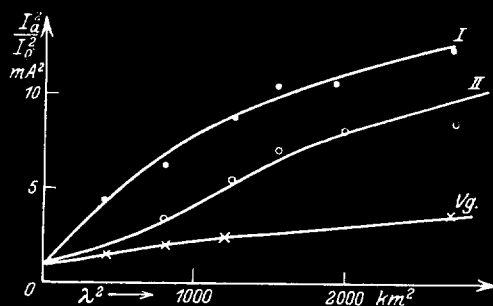


Abb. 13. Reduzierte Meßkurven.

Fig. 13. Reduced measured curves.

These two curves (Fig. 13) are similar to Curve 2, carried out for the same kind of measurement in Fig. 12. The quenching voltage of Curve 1 in Fig. 17 and the corresponding curve in Fig. 18 agree approximately in their U_g . The dampings are in the ratio of

1 to 2. It is seen that with the damping doubled the amplification is already very strongly increased. With $\lambda_M = 3500$ m. for example, in Curve 1, $\frac{I_a^2}{I_0^2} = 9$; while in the corresponding curve, in contrast to the first, this ratio = 2.3 . Also Curve 2, in spite of the smaller quenching voltage, shows a still greater amplification than the corresponding curve. The reason for the greater amplification in the case of higher damping is a greater

$$\frac{dS_a}{S_a dt} = \delta \left(\frac{\tan \alpha_0 - \tan \alpha}{\tan \alpha} \right).$$

In order to see this without calculation, one can employ the following consideration. In the case of greater damping, more energy is used in the oscillating circuit. In the first place, the natural oscillation sets in at greater back-coupling and thereby greater current is induced.

In each oscillation, in a highly-damped, closely-coupled tube, there will issue forth and be consumed in the ohmic resistance perhaps one-third of the oscillating energy $\frac{1}{2}(LI^2 + CI^2)$. In the rebuilding, only a few oscillations (in this case 3) will be necessary. With smaller damping, for example 1/100 of that given above, 300 oscillations are necessary for the establishment of the oscillation condition. Thus, therefore, the oscillations must grow more quickly in the case of greater damping.

RESULTS OF THE EXPERIMENTAL INVESTIGATIONS

We can now set forth the experimental results in the following order: 1. The quenching voltage is independent of the quenching

frequency. 2. The amplification increases with $\frac{1}{\delta}$ (function not yet ascertained). 3. The strength of reception increases, for sufficiently small currents, with the induced grid voltage ΔU_g ; and indeed I_a is linearly proportional to ΔU_g . 4. The amplification increases greatly with damping. 5. The amplification tends toward a minimum at $\Omega \rightarrow \infty$, the same value as attained with negative grid bias. This is the value which one can at most attain with an ordinary back-coupled, undamped receiver. Superregeneration is thus in every case superior to undamped regeneration. It is the task of theory to clarify uniformly and quantitatively these experimentally found facts.

II - THEORETICAL PART

1. Graphical Investigations:

Before we make use of the somewhat complicated theory, a graphical method will be developed which makes it possible to construct I_a -values from damping, oscillation-characteristics and quenching, if one I_a -value is known from measurement. This method will be described and will be used on one of the experimentally-obtained curves in order to investigate its usefulness.

For an oscillatory receiver the following expression, of which we have already made use, holds:

$$a = \frac{d \ln \mathcal{D}_a}{dt} = \delta \left(\frac{\tan \alpha_0 - \tan \alpha}{\tan \alpha} \right).$$

If the small potential ΔU_g is induced by a transmitter, then it is added to the control voltage present at that instant; i.e., (see Fig. 14).

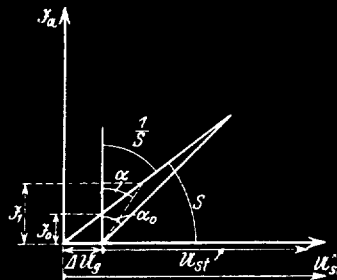


Abb. 14. Anschwingen bei Fremderregung.

Fig. 14. Oscillations with External Excitation.

$U_{st}^x = \Delta U_g + U_{st}$ if U_{st}^x designates the resultant control voltage.

The ratio $\frac{U_{st}^x}{I_a} = \tan \alpha$ is then the instantaneous value in the not-yet-built-up condition, while $\frac{I_a}{U_{st}^x}$ is the slope of the oscillation-characteristic. Then $\tan \alpha = \frac{U_{st}^x}{I_a} = \frac{U_{st}^x - \Delta U_g}{I_a} = \frac{1}{S} - \frac{\Delta U_g}{I_a}$;

Our expression then reads:

$$\alpha = \delta \left(\frac{\tan \alpha_0}{\frac{1}{S} - \frac{\Delta U_g}{I_a}} - 1 \right)$$

δ , $\tan \alpha_0$ and ΔU_g are known to be constant (we also know the oscillation of the quenching voltage to be $U_g = U \cos \Omega t$) and, from the tube characteristic, S is known as a function of U_g . The differential equation therefore gives $\frac{dI_a}{dt}$ as $f(I_a, t)$. But this is a "directional field". In Fig. 15 (a,b,c), such directional fields are shown. Its integration now means to draw in the $I_a - t$ curves. If no initial values are given, and if the integration is described for a stationary state, then the current must have equal values at repetitions of phase.

The curves drawn in the directional field give the resulting oscillations. The direction arrows here show where the currents rise or fall. As can be seen, $\frac{d\vartheta_a}{dt}$ goes from positive to negative values at about 7 volts for all sufficiently large values of current. For $U_{st} > 7$ volts the $\frac{d\vartheta_a}{dt}$ values increase steadily with ϑ_a . (In actuality, for large ϑ_a , in consequence of the bending-over of the oscillation characteristic, which here takes place beyond eight (volts), $\frac{d\vartheta_a}{dt}$ naturally decreases again and finally becomes 0). For $U_{st} < 7$ volts, $\frac{d\vartheta_a}{dt}$ remains greater than zero up to the point of intersection of the back-coupling line with the oscillation-characteristic, then becoming negative. If one compares the form of the curves with

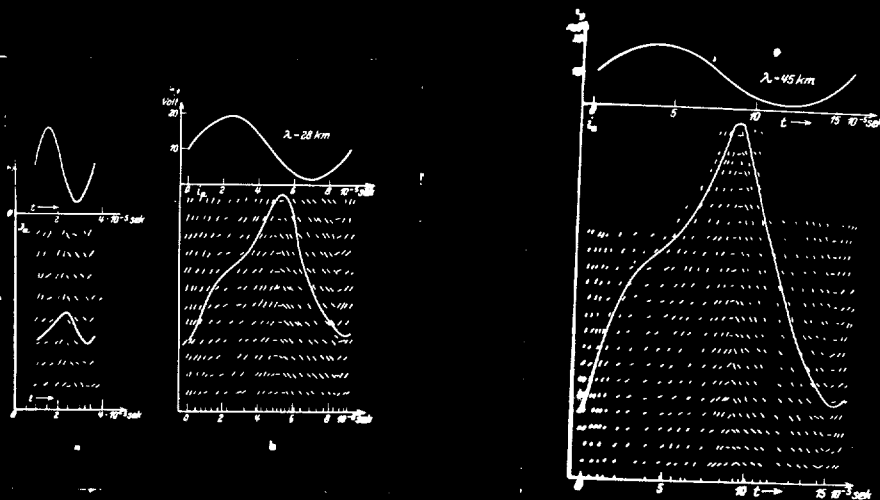


Fig. 15. Graphical Representation.

the quenching waves producing them, one can conceive of the current curve as an approximately sinusoidal oscillation, if one draws a line parallel to the abscissae half-way between the maximum and minimum

of the current values. This oscillation lags after the quenching voltage by somewhat over 90° , if we take as a zero-line of the quenching-wave the control voltage present without it, in our case about 10 volts. The maximum of the current curve then occurs somewhat after the passage of the quenching wave through its zero-line; it is reached when $\frac{d\mathcal{I}_a}{dt}$ again becomes negative, that is, when the control voltage falls below the critical value of 7 volts. The current then falls off sharply, becoming greater again after a new increase of potential beyond 7 volts. As the figure shows, the current first increases rapidly; upon reaching the maximum voltage, however, the rate of growth becomes less, since the slope of the tube characteristic decreases again for high potentials. The curves can be evaluated by dividing the area by the time. We then obtain for the currents, in the case of $\lambda_M = 7, 28$ and 45 km , the following ~~ratios~~ ratios:

$$\mathcal{I}_{\lambda=7 \text{ km}} : \mathcal{I}_{\lambda=28 \text{ km}} : \mathcal{I}_{\lambda=45 \text{ km}} = 1 : 2 : 3.5,$$

and from the measured \mathcal{I}_a^2 , $= 1 : 1.8 : 3.6$.

The results are found to be in good agreement if one observes that the curvature of the oscillation-characteristic present is negligible. The construction also shows that for small λ_M , as is noticeable in Fig. 15a for $\lambda_M = 7 \text{ km}$, the oscillation varies only slightly from the middle value, while for larger wavelengths the oscillations and the middle values become very great. Accordingly it is possible to carry out graphical investigations, especially since it gives not only the dependence of the current upon the quenching frequency, but also the oscillation-forms. The very troublesome and lengthy calcu-

lation is disadvantageous, however, as is the construction of the directional field, which must be constructed especially for every coupling, and then carried out at particular time intervals along the abscissae for each λ_m . Therefore in the next section the theory will be developed, whose derivation will be somewhat detailed, but which after permissible simplifications will lead to an easily usable expression.

Consequences of the Graphical Method:

1. Independence of the quenching voltage from Ω .

First the independence of the quenching voltage from Ω , which was shown in experiment, will also be shown theoretically, since this is possible without further difficulties of calculation. This again follows from the known expression $a = \frac{d \ln \mathcal{D}_a}{dt} = \delta \left(\frac{\tan \alpha_0 - \tan \alpha}{\tan \alpha} \right)$. Let no signal be received, as is the case in the adjustment of the quenching voltage. Then $\tan \alpha = \frac{1}{S}$. For S we write, according to Langmuir's formula,

$$S = \frac{3}{2} c \sqrt{U_{st}} = \frac{3}{2} c \sqrt{U_0 + U_g \cos \Omega t}$$

U_0 (note: this must mean V_0) is the control bias of the receiver without the superimposed frequency and U_g is the amplitude of the superimposed frequency.

Now, and also in further investigations, we take $U_g < U_0$; we can assume this restriction since for $U_0 < U_g$ the current of the low frequency Ω , which as shown in the experimental part, always appears in the presence of $U_g \cos \Omega t$, finally completely suppresses

the high frequency current, so that this case can be eliminated for our investigations. For $U_0 > U_g$ the roots of a converging series, which can be broken off after the second term, can be found. Physically this means that the harmonics may be neglected. Thus we have

$$\frac{g}{2} c \sqrt{U_0 + U_g \cos \Omega t} = A + B \cos \Omega t ;$$

A and B are Fourier terms and should be determined accordingly.

The foregoing equation thus takes the following form:

$$\frac{d \ln \mathcal{I}_a}{dt} = \delta \left[(\tan \alpha_0 A + B \tan \alpha_0 \cos \Omega t) - 1 \right]$$

after integration one has:

$$\mathcal{I}_a = \mathcal{I}_0 e^{\delta \left(A \tan \alpha_0 t + \frac{B \tan \alpha_0 \sin \Omega t}{\Omega} - t \right)}$$

Next let us consider the part $(A \tan \alpha_0 - 1) t$ in the exponent; t grows continuously, and the value must thus become very large, either positively or negatively. The expression is positive, if

$$A \tan \alpha_0 > 1 ; \text{ i.e., } A > \frac{1}{\tan \alpha_0} = S_0,$$

where S_0 is the slope of the oscillation-characteristic at the onset of oscillations. Since the oscillation-characteristic is considered as a straight line after the simplifying assumptions, it is either parallel to or steeper than the back-coupling line; let us now set

$(1 - A \tan \alpha_0) = \varepsilon$, so that we have:

$$\mathcal{I}_a = \mathcal{I}_0 e^{-\varepsilon t + \frac{B \tan \alpha_0 \sin \Omega t}{\Omega}} ;$$

For $A \tan \alpha_0 > 1$, ε is negative, so that \mathcal{I}_0 takes on a very large value, independently of the final factor $\frac{B \tan \alpha_0 \sin \Omega t}{\Omega}$. On the other hand, if $\varepsilon > 0$, that is, if the average slope falls below S_0 , then the oscillations quickly decrease and soon are practically lost, again independently of $\frac{B \tan \alpha_0 \sin \Omega t}{\Omega}$. The periodic term thus has

no marked effect on the quenching of the oscillations, so long as Ω is of finite magnitude. The quenching voltage is thus independent of the frequency.

Calculation of the Fourier Terms:

The Fourier terms will now be calculated:

1. Calculation of A:

$$S = \frac{3}{2} c \sqrt{U_0 + u_g \cos \Omega t} = A + B \cos \Omega t ;$$

the Fourier-series has the form: $f(t) = \frac{A_0}{2} + B \cos \Omega t + \dots$;

the rule for determination of the constants runs as follows:

$$B_n = \frac{1}{\pi} \int_0^{2\pi} f(t) \cos n \Omega t dt \quad ; \text{ and so forth;}$$

we set

$$\Omega t = \alpha ; \quad d \Omega t = d \alpha$$

$$A = \frac{A_0}{2} = \sqrt{\frac{U_0}{2\pi}} \int_0^{2\pi} \frac{3}{2} c \sqrt{1 + \frac{u_g}{U_0} \cos \alpha} d \alpha$$

$$\begin{aligned} A &= \frac{3}{2} c \sqrt{\frac{U_0}{2\pi}} \int_0^{2\pi} \left(1 + \frac{1}{2} \frac{u_g}{U_0} \cos \alpha - \frac{1}{8} \frac{u_g^2}{U_0^2} \cos^2 \alpha + \dots \right) d \alpha \\ &= \frac{3}{2} c \sqrt{\frac{U_0}{2\pi}} \left[\alpha + \frac{1}{2} \frac{u_g}{U_0} \sin \alpha - \frac{\alpha}{16} \frac{u_g^2}{U_0^2} - \frac{1}{16} \sin 2\alpha \frac{u_g^2}{U_0^2} + \dots \right]_0^{2\pi} \end{aligned}$$

$$A = \frac{3}{2} c \sqrt{U_0} \left(1 - \frac{u_g^2}{16 U_0^2} \right) ;$$

the periodic terms drop out when the limits are inserted.

2. Calculation of B:

$$B = \frac{3}{2} c \frac{\sqrt{U_0}}{\pi} \int_0^{2\pi} \sqrt{1 + \frac{u_g}{U_0} \cos \alpha} \cos \alpha d \alpha$$

$$= \frac{3}{2} c \frac{\sqrt{U_0}}{\pi} \int_0^{2\pi} \left(\cos \alpha + \frac{1}{2} \frac{u_g}{U_0} \cos^2 \alpha - \frac{1}{8} \frac{u_g^2}{U_0^2} \cos^3 \alpha + \dots \right) d \alpha$$

the $\cos^3 \alpha$ term falls out after integration and insertion

of limits, since it is purely periodic.

$$B = \frac{3}{2} c \frac{\sqrt{U_0}}{\pi} \left[\sin \alpha + \frac{\alpha}{4} \cdot \frac{u_g}{U_0} + \frac{1}{4} \frac{u_g}{U_0} \sin 2\alpha + \dots \right]_0^{2\pi}$$

$$B = \frac{3}{2} c \sqrt{U_0} \frac{u_g}{2 U_0} .$$

The average slope $S_0 = A$ is thus smaller than the slope of the oscillation-characteristic without quenching voltage, when $S_0 = A$ is again this same slope of the oscillation-characteristic at the exact onset or extinction of oscillations. Upon this depends the quenching process of the low-frequency voltage. If the back-coupling is increased, that is, $\tan \alpha_0$ is made larger, the oscillations will first be quenched at a lower average slope of the oscillation characteristic. In order to depress $S_0 = A$ to this value, U_g must accordingly be increased. This was also discussed further in the experimental part.

Relation between Back-Coupling Line and Quenching Voltage:

To obtain the relation between the back-coupling line $\tan \alpha_0$ and U_g , the expression for A can be used, where A is the average slope and $\tan \alpha_0 = \frac{1}{A}$. If one compares the measured values and the values calculated according to the formula developed above, the calculated ones are approximately correct qualitatively, but quantitatively somewhat too flat: to obtain a better approximation, we will take into account the fact that because of the form of the tube characteristic it is not permissible to use the expression for the whole region. If one takes, instead, for various values of voltage on the characteristics, the corresponding S values from the curve, then the $S \rightarrow U_{st}$ curve can be approximated more closely by a parabola. If one computes at the vertex of the parabola that $S = 11.75 (10^{-4})$ amp/volt and assumes concerning the abscissae that $\frac{U_g}{U_{st}} = U_g$ volts,

then the parabolic equation

$$S = 11.75 \left(1 + \frac{u_g}{U_{st}} \cos \Omega t \right) \cdot 10^{-4} \text{ amp / volt}$$

will be obtained. For the average value A there is then obtained:

$$\frac{1}{\tan \alpha_0} = S_0 = 11.75 \left(1 - \frac{u_g^2}{U_{st}^2} \cdot \frac{1}{2} \right) \cdot 10^{-4} \text{ amp / volt}.$$

The calculated values taken from this (Fig. 16) reproduce better the course of the measured $\tan \alpha_0 \rightarrow u_g$ curve.

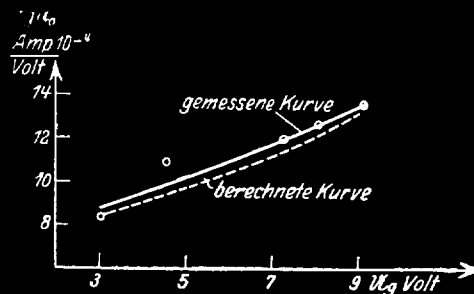


Abb. 16. Zusammenhang von $\tan \alpha_0$ und u_g

Fig. 16. Relation between $\tan \alpha_0$ and u_g .

Key:

Gemessene Kurve	Measured curve
Berechnete Kurve	Calculated curve

2. General Theory:

We proceed from the already derived equation

$$a = \frac{d \ln g_a}{dt} = \delta \left(\frac{\tan \alpha_0}{S} - \frac{\Delta u_g}{g_a} - 1 \right);$$

substituting $S = A + B \cos \Omega t$, we obtain

$$a = \delta \left(\frac{\tan \alpha_0}{A + B \cos \Omega t} - \frac{\Delta u_g}{g_a} - 1 \right).$$

$\frac{\Delta U_g}{I_a}$ is usually small compared to $\frac{1}{S}$, especially if $U_g < U_{st}$; in this case U_g always $< U_{st}$ and S is greater than zero.

$\frac{1}{S} > 10^4$ volts/amp for $I_a > \frac{1}{10}$ milliampere; if, for example, $\Delta U_g \cong 1/10$ volt, then $\frac{\Delta U_g}{I_a}$ is only 10^3 volts/amp.

For still smaller currents, $\frac{1}{S}$ increases approximately in proportion to $\frac{\Delta U_g}{I_a}$. One can therefore revise the expression for a and expand it in a series, whereby the expansion will be divided into two terms.

$$\frac{I_a'}{I_a} = a = \delta \left[\frac{\tan \alpha_0 (A + B \cos \Omega t)}{1 - \frac{\Delta U_g}{I_a} (A + B \cos \Omega t)} - 1 \right]$$

$$a = \delta \left[\tan \alpha_0 (A + B \cos \Omega t) + \tan \alpha_0 (A + B \cos \Omega t)^2 \frac{\Delta U_g}{I_a} - 1 \right]$$

$$I_a' = \delta \left[\tan \alpha_0 (A + B \cos \Omega t) I_a - I_a + \tan \alpha_0 (A^2 + 2AB \cos \Omega t + B^2 \cos^2 \Omega t) \Delta U_g \right]$$

ε will again be substituted for $(1 - A \tan \alpha_0)$; then we obtain

$$I_a' = \delta \left[(B \tan \alpha_0 \cos \Omega t - \varepsilon) I_a + \tan \alpha_0 (A^2 + 2AB \cos \Omega t + B^2 \cos^2 \Omega t) \Delta U_g \right]$$

If $B \ll A$, the last term can be neglected. The permissibility will be investigated later. The equation should now be solved according to Lagrange, by variation of the constants.

Homogeneous Equation:

$$\frac{I_a'}{I_a} = \frac{d \ln I_a}{dt} = \delta \left[-\varepsilon + B \tan \alpha_0 \cos \Omega t \right]$$

$$I_a = C_t \cdot e^{\delta \left[-\varepsilon t + B \tan \alpha_0 \frac{\sin \Omega t}{\Omega} \right]}$$

(Note: in the original article, the 2 terms of the right member are shown added instead of multiplied, but this was evidently an error in printing.)

If C_t were constant, these equations would express the case of quenching without ΔU_g , which has already been considered. It will now be assumed that ϵ is of small magnitude; that is, that the slope of the oscillation characteristic is only slightly less than that of the back-coupling line. The system is therefore almost self-exciting (strongly undamped). As a matter of fact, in the experiment we always have the quenching voltage so adjusted. C_t must still be determined, since the solution is composed of a particular integral of the inhomogeneous equation, added to that of the homogeneous one.

$$C_t' = \Delta U_g \tan \alpha_0 \delta (A^2 + 2AB \cos \Omega t) e^{\delta(\epsilon t - B \tan \alpha_0 \frac{\sin \Omega t}{\Omega})}$$

Carrying Out the Integration:

We develop the e -function in a series, multiply by $A^2 + 2AB \cos \Omega t$, and separate into periodic and aperiodic terms, in which we break off with the quadratic terms. It is to be expected that after the integration the terms will be collectible into an eventually larger number of e -series. The following abbreviations will now be introduced:

$$\delta \epsilon = a; \quad \delta \tan \alpha_0 B = b$$

$$A^2 = c; \quad 2AB = g$$

$$\tan \alpha_0 \Delta U_g \delta = k$$

The equation then reads:

$$C_t' = k(c + g \cos \Omega t) e^{at - b \frac{\sin \Omega t}{\Omega}}$$

Expanded:

$$\frac{C_t'}{k} = (c + g \cos \Omega t) \left[1 + \left(at - \frac{b \sin \Omega t}{\Omega} \right) + \frac{\left(at - \frac{b \sin \Omega t}{\Omega} \right)^2}{2!} + \dots \right]$$

$$\begin{aligned}
&= [c + g \cos \Omega t] \\
&+ \left[c \left(at - \frac{b \sin \Omega t}{\Omega} \right) + g \left(at \cos \Omega t - \frac{b \cos \Omega t \sin \Omega t}{\Omega} \right) \right] \\
&+ \left[c \left(\frac{a^2 t^2}{2} + \frac{b^2 \sin^2 \Omega t}{2 \Omega^2} - \frac{abt \sin \Omega t}{\Omega} \right) \right. \\
&\quad \left. + g \left(\frac{a^2 t^2 \cos \Omega t}{2} + \frac{b^2 \sin^2 \Omega t \cos \Omega t}{2 \Omega^2} - \frac{abt}{\Omega} \sin \Omega t \cos \Omega t \right) \right] \\
&+ \dots \dots \dots
\end{aligned}$$

(Note: a number of typographical errors have been detected and corrected in this and previous equations, during the translation. The impracticability of checking all of the integration and other mathematical work, however, makes it unlikely that the following pages will be free of such errors.)

The terms will be integrated singly after goniometric transformation.

Neglecting the higher terms (harmonics), we obtain the following result:

$$\begin{aligned}
C = k &\left[c \left(t + \frac{at^2}{2} + \frac{b \cos \Omega t}{\Omega^2} + \frac{a^2 t^3}{3!} + \frac{bt}{4\Omega^2} + \frac{abt}{\Omega^2} - \frac{\sin \Omega t}{\Omega^3} \cdot ab + \dots \right) \right. \\
&+ g \left(\sin \Omega t + \frac{at}{\Omega} \sin \Omega t + \frac{a^2}{\Omega^2} \cos \Omega t + \frac{b \cos 2\Omega t}{4\Omega^2} + \frac{a^2 t^2}{\Omega} \sin \Omega t \right. \\
&\quad \left. + \frac{a^2 t}{\Omega^2} \cos \Omega t - \frac{a^2}{\Omega^3} \sin \Omega t + \frac{b^2}{4\Omega^3} \sin \Omega t - \frac{b^2}{8\Omega^3} \sin \Omega t \right. \\
&\quad \left. \left. + \frac{bat}{4\Omega^3} \cos 2\Omega t - \frac{\sin 2\Omega t}{8\Omega^3} \right) \right] + K.
\end{aligned}$$

K is an integration constant.

We can now collect the terms in single e -series. In doing this we further transform the sine- and cosine-free terms, in that we put $\frac{1}{a}$ before the sums, and add to the sums $\frac{1}{a}$ or $\frac{a^2 b^2}{4\Omega^2}$ and subsequently subtract it again. For the single series we obtain:

$$\begin{aligned}
C_t = k &\left[\frac{c}{a} \left(1 + at + a^2 \frac{t^2}{2!} + a^3 \frac{t^3}{3!} + \dots \right) \right. \\
&+ \frac{b^2 c}{4a\Omega^2} \left(1 + \dots \right) + \frac{cb}{\Omega^2} \cos \Omega t \left(1 + at + \dots \right) \\
&+ g \frac{\sin \Omega t}{\Omega} \left(1 + at + \frac{a^2 t^2}{2} + \dots \right) + \frac{ga}{\Omega^2} \cos \Omega t \left(1 + at + \dots \right) \\
&\left. + gb \frac{\cos 2\Omega t}{4\Omega^2} \left(1 + at + \dots \right) - \frac{c}{a} \left(1 + \frac{b^2}{4\Omega^2} \right) \right] + K.
\end{aligned}$$

These series form, as expected, the first terms of an e -series. By the addition of the other terms, there results:

$$C_t = k \left[\left(\frac{c}{a} + \frac{cb^2}{4a\Omega^2} + \frac{cb}{\Omega^2} \cos \Omega t + \frac{g}{\Omega} \sin \Omega t + \frac{ag}{\Omega^2} \cos \Omega t + \frac{gb}{4\Omega^2} \cos 2\Omega t \right) e^{at} - \frac{c}{a} \left(1 + \frac{b^2}{4\Omega^2} \right) \right] + K.$$

But
$$\vartheta = C_t e^{-at} + \frac{b \sin \Omega t}{\Omega}$$

We now introduce the original values again and obtain:

$$\begin{aligned} \vartheta_a = \Delta U_g \tan \alpha_0 \delta \left[\left(\frac{A^2}{\delta \epsilon} + \frac{\tan^2 \alpha_0 A^2 B^2 \delta^2}{4 A^2 \delta \epsilon} + \frac{A^2}{\Omega^2} \tan \alpha_0 B \delta \cos \Omega t + \frac{2AB}{\Omega^2} \delta \epsilon \cos \Omega t + \dots \right) e^{\delta \tan \alpha_0 B \frac{\sin \Omega t}{\Omega}} - \frac{A^2}{\delta \epsilon} e^{-\delta \epsilon t + \frac{\delta \tan \alpha_0 B}{\Omega} \sin \Omega t} \left(1 + \frac{\delta^2 \tan^2 \alpha_0 B^2}{4 \Omega^2} \right) \right] + K e^{-\delta \left(\epsilon t - \frac{\tan \alpha_0 B}{\Omega} \sin \Omega t \right)} \end{aligned}$$

The terms which have ϵ in the denominator are very large compared with the others, as long as Ω is not extraordinarily small, so that one can omit the terms without ϵ in the denominator: 1 can be substituted for $A \tan \alpha_0$, since according to hypothesis A is only slightly smaller than $\tan \alpha_0$. Therefore:

$$\begin{aligned} \vartheta_a = \frac{\Delta U_g A}{\epsilon} \left[\left(1 + \frac{\delta^2}{4 \Omega^2} \tan^2 \alpha_0 B^2 \right) e^{\delta \tan \alpha_0 \frac{B \sin \Omega t}{\Omega}} - e^{-\delta \left(\epsilon t - \tan \alpha_0 \frac{B \sin \Omega t}{\Omega} \right)} \left(1 + \delta^2 \tan^2 \alpha_0 B^2 \right) \right] + \vartheta_0 e^{-\delta \epsilon t + \delta \tan \alpha_0 \frac{B \sin \Omega t}{\Omega}} \end{aligned}$$

where $\vartheta_0 = K$.

Discussion of Results:

1. If $\Delta U_g = 0$: only the last term remains; for $\varepsilon < 0$, i.e., $A > \frac{1}{\tan \alpha_0}$, self-excitation results with an \mathcal{D}_0 present. For $\varepsilon > 0$, i.e., $A < \frac{1}{\tan \alpha_0}$, the oscillation dies out. We thus obtain the already-known special case from the general equation as well.
2. $\Delta U_g > 0, \varepsilon = 0$: this case is not realizable in practice, since it would be possible only for an essentially straight oscillation-characteristic.
3. $\Delta U_g > 0, \varepsilon < 0$: self-excitation results, the current becomes infinite with time (in reality, only up to the intersection of the oscillation-characteristic and the back-coupling line, on account of the bending over of the oscillation-characteristic).
4. $\Delta U_g > 0, \varepsilon > 0$: the terms with $e^{-\varepsilon st}$ are extinguished.

$$\mathcal{D}_a = \frac{\Delta U_g A}{\varepsilon} \left(1 + \frac{\delta^2 \tan^2 \alpha_0 B^2}{4 \Omega^2} \right) e^{\delta \tan \alpha_0 B \frac{\sin \Omega t}{\Omega}}; \quad (4a)$$

this case only is of practical interest, since it corresponds to the conditions of the experimental investigation. It alone will therefore be discussed further. If one considers the term $B^2 \cos^2 \Omega t$ neglected in the beginning of the separation, then, after the corresponding transformation and integration for \mathcal{D}_a , the following additional expression enters in:

$$\mathcal{D}_2 = \frac{\Delta U_g B^2 \tan \alpha_0}{2 \varepsilon} \left(\frac{1 + \delta^2 \tan^2 \alpha_0 B^2}{8 \Omega^2} \right) e^{\delta \tan \alpha_0 B \frac{\sin \Omega t}{\Omega}}; \quad (4b)$$

now, for $U_g < U_{st}$:

$$B < \frac{A}{2}, B \tan \alpha_0 < \frac{1}{2}, \frac{B^2 \tan \alpha}{2} < \frac{A}{8}.$$

therefore:

$$\frac{\Delta U_g B^2}{2\epsilon} \tan \alpha < \frac{\Delta U_g A}{8\epsilon}$$

Since the expression in the parenthesis likewise is smaller than the corresponding one in the first part for \mathcal{D}_a , we can neglect this term. Before the I_a^2 values are calculated, the expression 4(a) will be used to determine, independently of experimental conditions, the course of \mathcal{D}_a in time, and to compare these with the graphically determined ones. For this purpose, we again expand $e^{\delta \tan \alpha_0 \frac{B \sin \Omega t}{\Omega}}$ into a series and stop with the second term, neglecting the harmonics as before.

$$\begin{aligned} \mathcal{D}_a &= \frac{\Delta U_g A}{\epsilon} \left(1 + \frac{\delta^2 \tan^2 \alpha_0 B^2}{4 \Omega^2} \right) \left(1 + \frac{\delta \tan \alpha_0 B \sin \Omega t}{\Omega} \right) \\ &= \frac{\Delta U_g A}{\epsilon} \left(1 + \frac{\delta^2 \tan^2 \alpha_0 B^2}{4 \Omega^2} + \frac{\delta \tan \alpha_0 B \sin \Omega t}{\Omega} \right. \\ &\quad \left. + \frac{\delta^2 \tan^3 \alpha_0 B^3 \sin \Omega t}{4 \Omega^3} \right). \end{aligned}$$

We see that for large Ω , i.e., $\Omega > \delta$, the current tends toward a minimum $\mathcal{D}_0 = \frac{\Delta U_g A}{\epsilon}$, which was also shown experimentally. As Ω becomes smaller, the third term, linear in Ω (translator's note: this must mean $\sin \Omega$, not Ω), first predominates; which only modulates the average value of \mathcal{D}_a , without changing it appreciably, as Fig. 15 shows in the graphical representation for small quenching wave-length, $\lambda_M = 7000$ m. As soon as Ω

is decreased so far that in the second term the numerator is larger than the denominator, then the average value rises very rapidly, almost quadratically, while the sinusoidal form will still be impressed. In this case the high frequency oscillations lag the quenching voltage by 90° , agreeing with the graphical representation. Finally the higher terms predominate, the \mathcal{I}_a curves rise according to a higher power, until the oscillation characteristic bends over and its expression becomes no longer usable.

After we have shown ourselves that the graphical representation and the theory of the formation of oscillations agree with each other, the relationships for amplification should be calculated quantitatively. The expression obtained will be transformed for this purpose so that I_a^2 will be calculated instead of \mathcal{I}_a , since this can be measured with a thermo-element.

$$I_a^2 = \frac{\Delta U_g^2 A^2}{\varepsilon^2} \left(1 + \frac{\delta^2 \tan^2 \alpha_0 B^2}{4 \Omega^2} \right)^2 e^{2 \tan \alpha_0 B \delta \frac{\sin \Omega t}{\Omega}}$$

$$I_a^2 = \frac{\Delta U_g^2 A^2}{\varepsilon^2} \left(1 + \frac{\delta^2 \tan^2 \alpha_0 B^2}{4 \Omega^2} \right)^2 \left(1 + \frac{2 \delta B \tan \alpha_0 \sin \Omega t}{\Omega} + \frac{2 \delta^2 \tan^2 \alpha_0 B^2 \sin^2 \Omega t}{\Omega^2} \right)$$

$$= \frac{\Delta U_g^2 A^2}{\varepsilon^2} \left(1 + \frac{\delta^2 \tan^2 \alpha_0 B^2}{4 \Omega^2} \right) \left(1 + 2 \frac{\delta B \tan \alpha_0 \sin \Omega t}{\Omega} - \frac{\delta^2 \tan^2 \alpha_0 B^2 \cos 2 \Omega t}{\Omega^2} + \frac{\delta^2 \tan^2 \alpha_0 B^2}{\Omega^2} \right)$$

In determining the average value, the purely periodic terms fall away.

$$I_a^2 = \frac{\Delta U_g^2 A^2}{\varepsilon^2} \left(1 + \frac{1}{2 \Omega^2} \delta^2 \tan^2 \alpha_0 B^2 + \frac{\delta^4 \tan^4 \alpha_0 B^4}{16 \Omega^2} \right) \left(1 + \frac{\delta^2 \tan^2 \alpha_0 B^2}{\Omega^2} \right)$$

We can now write for all cases, where Ω is not $\ll \delta$;

$$I_a^2 = \frac{\Delta U_g^2 A^2}{\epsilon^2} \left(1 + \frac{\delta^2 \tan^2 \alpha_0 B^2}{2 \Omega^2} \right) \left(1 + \frac{\delta^2 B^2 \tan^2 \alpha_0}{4 \Omega^2} \right)$$

$\epsilon = (1 - A \tan \alpha_0) > 0$ should be very small. Since $\tan \alpha_0$ is constant for unchanged coupling, ϵ depends only upon A . A , however, is dependent only upon U_g .

Accuracy of Adjustment as Related to ϵ (see Fig. 8):

It is now expedient, as we have already shown, to take ϵ as small as possible, in order to make I_0^2 very large; the induced quenching voltage should only suffice exactly to prevent self-excitation. The adjustment must thus be made very exactly, since a small variation will change the very small quantity ϵ through a considerable portion of its value. Indeed, it was established experimentally (Fig. 9) that I_a^2 falls off rapidly when one increases U_g above the minimum quenching voltage; still a certain region of variation, also in the immediate neighborhood of the minimum quenching voltage, stands in contrast to the theory, so that a small error changes I_a^2 only very slightly. Let us calculate this process for a specific example: Let $\tan \alpha_0 = 10^3$ volts/amp.; in order barely to obtain quenching without ΔU_g , one will adjust the $\tan \alpha$ of the oscillation-characteristic, with the help of $U_g \cos \Omega t$, to a very slightly greater value than $\tan \alpha_0$; e.g., $\tan \alpha_0 = 10^3$ volt/amp, $\tan \alpha = 1,001 \cdot 10^3$ volt/amp, then we have:

$$\epsilon = - \left(\frac{\tan \alpha_0 - \tan \alpha}{\tan \alpha} \right) = \frac{-a}{\delta} = \frac{-1 + 1,001}{1,001} \approx 0.001.$$

If one adjusts to a second value, somewhat different, perhaps $\tan \alpha = 1.01 \cdot 10^3$ volt/amp., which one might obtain by a very small error, then one obtains:

$$\varepsilon = -\frac{a}{\delta} = \frac{0.01}{1.01} \approx 0.01$$

a value ten times greater. We observe the effect of this error, however, in the case of reception of $\Delta \mathcal{U}_g$. The back-coupling line is no longer that for $\mathcal{U}_g = 0$, but for $\mathcal{U}_g = \Delta \mathcal{U}_g$, and intersects the oscillation-characteristic not at $\mathcal{I}_a = 0$ but at a final value, which is determined by the bending-over of the oscillation characteristic. If at the beginning point the oscillation-characteristic has now, as above, the slope $\tan \alpha = 1.001$ or $1.01 \cdot 10^3$ volts/amp, and the back-coupling line, as before, $\tan \alpha_0 = 10^3$ volts/amp., then on account of the bending-over of the oscillation-characteristic, for $\mathcal{I}_a > 0$, α might increase to $\alpha + \alpha^x$; α^x would be perhaps $0.1 \cdot 10^3$ volts/amp, so that for the two $\tan(\alpha + \alpha^x)$ values we have:

$$\varepsilon_1 = \frac{1.101 - 1}{1.101} = 0.092; \quad \varepsilon_2 = \frac{1.111 - 1}{1.1} \approx 0.1$$

Calculation of the Measured Values:

The expression can thus be used in the calculation of the experimentally-found values. Since it depends not upon the absolute values of the currents, but upon their ratios one to another with various values of $\lambda_M, \delta, \mathcal{U}_g$, etc., the amplification will be obtained for $\mathcal{I}_a^2 = \mathcal{I}_0^2$, produced by minimum amplification. From this the remaining \mathcal{I}_a^2 will be calculated.

$$\mathcal{I}_0^2 = \frac{A^2 \Delta \mathcal{U}_g^2}{2}$$

Ω and δ are known by measurement. $B\delta \tan \alpha_0$ can be obtained by the following process:

$$A = \frac{3}{2} c \sqrt{U_{st}} \left(1 - \frac{1}{16} \frac{u_g^2}{U_{st}^2}\right) \approx \frac{3}{2} c \sqrt{U_{st}} \text{ for } u_g < U_{st}.$$

$$B = \frac{2}{3} c \sqrt{U_{st}} \cdot \frac{u_g}{2U_{st}}; \quad A \tan \alpha_0 = 1; \quad \tan \alpha_0 = \frac{1}{A};$$

$$\frac{B \tan \alpha_0}{A \tan \alpha_0} \approx \frac{B \tan \alpha_0}{1} \approx \frac{u_g}{2U_{st}}$$

The calculation can follow in such a manner that we proceed from

$$I_0^2 = \frac{\Delta u_g^2 A^2}{\epsilon^2}, \text{ which was obtained through measurement with large } \Omega.$$

Here it is to be noted, however, that in the measurements in Fig. 17, Curves 1, 2, 3 and 4, the initial values are very small and therefore

cannot be established with very great accuracy. Therefore it is to be connected up with a greater measured value. From it $\frac{\Delta u_g^2 A^2}{\epsilon^2}$

can then be obtained according to the general formula and used to calculate the remaining I_a^2 . These points of connection are given

in Figs. 17 and 18 by the following symbol \otimes . In Fig. 17 the measured values of Fig. 11, and in Fig. 18 the ones from Fig. 13

(large damping) are entered in full lines. The dotted lines represent

the calculated values. In Fig. 17 the calculated and the measured points at first agree very well; for large λ_M , I_a^2 climbs less rapidly than the calculation gives, because of the bending over of the oscillation characteristic, as was theoretically to be expected.

In Fig. 18 such large values of current are already reached with

proportionately small values of λ_M , on account of the larger amplification with higher damping, that the limiting values of amplification

are soon reached. Therefore the measured and the calculated curves agree only in the beginning, as far as the oscillation characteristic can still be considered to be a straight line.

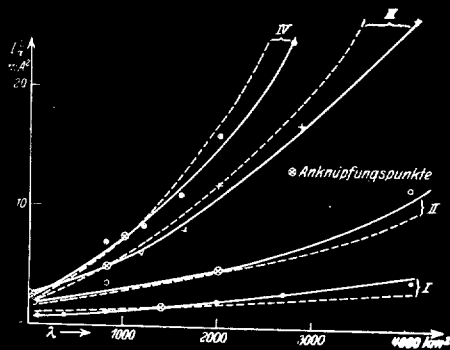


Abb. 17. Gemessene und berechnete Werte.

Fig. 17. Measured and calculated values.

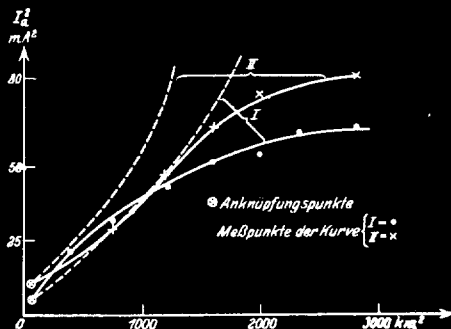


Abb. 18. Gemessene und berechnete Werte bei großer Dämpfung.

Fig. 18. Measured and calculated values with greater damping.

Key:

Anknüpfungspunkte Connecting point

Key:

Anknüpfungspunkte Connecting points

Messpunkte der Kurve Measured points of curve

The foregoing work was carried out at the suggestion of Herrn. Prof. Dr. Moller at the Institute for Applied Physics at the University of Hamburg. For the promotion of this work I must hereby particularly thank Herrn. Prof. Dr. Moller.

CONCLUSION

Fundamentals:

In superregeneration the back-coupling is so close that self-excitation can result, but by means of a low-frequency oscillation the high frequency is periodically interrupted. As a first approximation we consider that the low frequency offers, by a make-and-break connection, a negative grid bias which interrupts the natural oscillation. The oscillations in the receiver, during the positive half-period, run according to $I_a = I_0 e^{at}$, where I_0 is the initial current; I_0 equals the receiver current without back-coupling. During the negative period, I_a decays. From these statements it is to be expected that the final current, and with it the loudness of reception, will be proportional to I_0 ; further, that the amplification $\frac{I_a^2}{I_0^2}$ increases with the time of positive connection t and with the rate of growth a . According to H. G. Moller, a is given by the expression $a = \delta \frac{(\tan \alpha_0 - \tan \alpha)}{\tan \alpha}$ where δ is the damping, α_0 the angle between the back-coupling line and the ordinates, and $\tan \alpha = \frac{U_{st}}{I_a}$ is that for the not-yet-built-up condition. a and with it the amplification must thus increase with δ and $(\tan \alpha_0 - \tan \alpha)$, i.e., with the closeness of back-coupling. These conclusions were verified qualitatively by measurements; for quantitative verification this working hypothesis is still too inexact, since negative and positive grid voltages are not applied suddenly, but are introduced by a sinusoidally alternating current.

Graphical Construction:

First of all, therefore, a graphical investigation is undertaken. One proceeds from the expression $\frac{dI_a}{I_a dt} = \delta \left(\frac{\tan \alpha_0 - \tan \alpha}{\tan \alpha} \right)$ where $\tan \alpha$ depends upon \mathcal{D}_a and the steepness of the oscillation characteristic, and therefore upon $\mathcal{U}_g \cos \Omega t$ and with it the time.

One considers this differential quotient as a function of time and \mathcal{D}_0 and obtains a directional field, in which the course of the oscillations can be sketched out. This process leads to results which are in good agreement with the measurements. Furthermore, the oscillation process can be determined individually with it. The maximum of the high-frequency oscillations lags the amplitude of the quenching voltage by perhaps 90° . With short quenching wave-length, the average value of \mathcal{D}_a remains nearly unchanged and for $\Omega \rightarrow \infty$ tends toward a limiting value which is already practically attained at $\lambda_M = 7000 \text{ m}$, and which agrees with \mathcal{D}_0 , the reception with ordinary back-coupling and no quenching wave. With greater λ_M , the average value of \mathcal{D}_a increases very greatly. The modulation of the high-frequency oscillations is then very strongly impressed. This method is indeed quite direct, but extremely lengthy in its construction.

Theory:

Therefore the more complicated mathematical theory is now derived from the expression

$$a = \frac{d \ln \mathcal{D}_a}{dt} = \delta \left(\frac{\tan \alpha_0}{\frac{1}{A+B \cos \Omega t} - \frac{\Delta \mathcal{U}_g}{\mathcal{D}_a}} - 1 \right).$$

Δu_g is the small alternating grid voltage induced from the transmitter. The expression is expanded into a series and integrated. The terms arising from this are collected into e -series. By neglecting the harmonics and small terms, the simple expression

$$I_a^2 = \frac{\Delta u_g^2 A^2}{\varepsilon^2} \left(1 + \frac{\delta^2 B^2 \tan^2 \alpha_0}{2 \Omega^2} \right) \left(1 + \frac{\delta^2 B^2 \tan^2 \alpha_0}{\Omega^2} \right)$$

is obtained. The discussion gives the small oscillation form obtained with the graphical representation. Let us set $\frac{\Delta u_g^2 A^2}{\varepsilon^2} = I_0^2$, as follows from the equation, for large values of Ω ; then we obtain as the ratio of amplifications:

$$\frac{I_a^2}{I_0^2} = \left(1 + \frac{\delta^2 B^2 \tan^2 \alpha_0}{2 \Omega^2} \right) \left(1 + \frac{\delta^2 B^2 \tan^2 \alpha_0}{\Omega^2} \right).$$

Here there appear only quantities which can easily be measured, δ, B, Ω ; for whose determination only the tube characteristic and the quenching amplitude need be known. Measurements and theoretical calculations then give the following quantitatively agreeing results:

1. The quenching voltage is independent of the quenching frequency.
2. I_a is proportional to Δu_g .
3. All I_a^2/I_0^2 values tend toward the value 1 for $\Omega \rightarrow \infty$.
4. The amplification increases with λ_m .
5. The amplification increases with u_g and the back-coupling.
6. The amplification increases with δ .

All results agree with the final formula given, and are contained in it.

APPENDIX A

PART V

PRINCIPLES OF THE USE OF SUPERREGENERATIVE RECEIVERS

Von G. Hassler

Translated from Hochfrequenztechnik und Elektroakustik,

September 1934

CONTENTS

- I. Creation of the initial amplitude. High frequency amplification.
 - II. Experimental apparatus.
 - III. The receiver with incoherence of the oscillation-trains.
 - (a) Receiver conditions. Modulation characteristics.
 - (b) Resonance curves.
 - (c) Limits of selectivity.
 - IV. The receiver with coherence of the oscillation-trains.
 - (a) Creation of the initial amplitude. Sensitivity.
 - (b) Resonance curves. Multiple resonance curves.
 - V. Deviations from the theory.
- Conclusions.
- Summary.
- Bibliography.

(NOTE: The first few paragraphs of the original article have been somewhat condensed in the following translation).

Of the analyses of superregeneration which have heretofore been published, none has offered an explanation for all of its manifestations and peculiarities. Different writers have obtained different results, through attaching too general interpretations to their observations.

The following work will present a fundamental explanation based on a very simple physical conception, giving a complete and systematic representation of the manner of operation of the superregenerative receiver, in which the correctness of the theory is verified quantitatively by experiment.

I. FORMATION OF THE INITIAL AMPLITUDE.
HIGH FREQUENCY AMPLIFICATION.

By a superregenerative receiver, first described by Armstrong, is meant a receiver of the form of a regenerative circuit in which the operating point of the tube is periodically shifted, so that the regeneration is alternately increased and decreased. The oscillating circuit of the receiver is periodically "dedamped" and then damped again. While doing so, it is acted upon by the high-frequency signal of the transmitter. The high frequency oscillations produced in the receiver are demodulated and then supplied to the audio-frequency part of the receiver. In contrast to all ordinary receivers, the high-frequency amplification of the signal is obtained through a "flaring-up" of oscillations. The resulting oscillation, in the simplest case, takes the course shown in Fig. 1, wherein at time a , the receiver is suddenly dedamped and then during time t_a a constant rate of growth takes place, until at time d , a sudden damping occurs, which remains constant during time t_d .

The oscillations grow exponentially from the instant of dedamping, starting from an initial amplitude u_0 , which arises from the signal \mathcal{E} . In this way an arbitrarily small amplitude u_0 can grow to an arbitrarily large value u^* , provided the time t_a is long enough. There exists however -- and this makes the build-up process a means of amplifying weak signals -- a definite relation between the initial and final amplitudes, regardless of

their values.

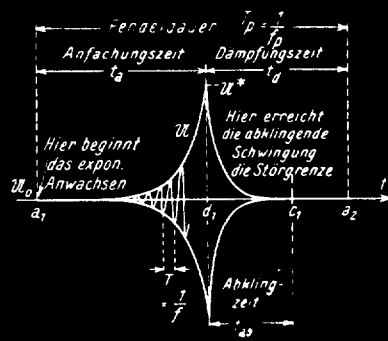


Abb. 1.
Verlauf des Aufbauprozesses bei der Pendelrückkopplung.

Fig. 1

Course of the Building-up Process of Superregeneration.

Key:

Pendeldauer	Period of one quenching cycle
Anfachungszeit	Period of building-up of oscillations
Dampfungszeit	Damping period
Hier beginnt, etc.	Beginning of exponential rise
Hier erreicht, etc.	Decaying oscillation reaches noise level here
Abklingzeit	Period of decay of oscillations

This behavior has already been observed practically by the author (ref. 7). When no signal is present, even with good shielding, shot effect and thermal noise give rise to irregular initial amplitudes.

When the oscillations resulting in the receiver are

applied to the demodulator, the rectified current fluctuates with time, as shown in Fig. 2 for the case of a square-law detector.

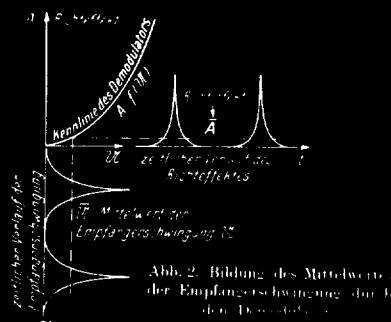


Fig. 2. Derivation of the "average" value of the receiver oscillations, by the demodulator.

Key:

Richteffect	Detector effect
Kennlinie des Demodulators	Characteristic of detector
Zeitlicher Verlauf des Richteffectes	Course of detector effect vs. time
Zeitlicher Verlauf der Empfängerschwingung	Course of receiver oscillations vs. time
Mittelwert der Empfängerschwingung	Weighted average value of receiver oscillations

The average value \bar{A} of the rectified current corresponds to a "weighted average" value \bar{u} of the receiver oscillations. The ratio \bar{u}/u_0 gives the attained high-frequency amplification, since to

produce the rectified current \bar{A} it would be necessary to have a steady oscillation of amplitude \bar{u} , to which the signal would have to be amplified from the value u_0 .

The creation of this "amplified" oscillation \bar{u} from the high-frequency signal E.M.F. \mathcal{E} takes place in two steps:

- (a) The signal \mathcal{E} produces the initial amplitude u_0 .
- (b) The initial amplitude u_0 is then amplified to the value \bar{u} .

(a) CREATION OF THE INITIAL AMPLITUDE

If the circuit is suddenly dedamped, increasing transient oscillations of frequency f result:

$$u = u_0 e^{-(\pi/\rho_a)(t/\tau)} \sin 2\pi ft$$

the initial amplitude being determined by the boundary conditions at the instant of dedamping. The mathematics of this process can be omitted here; the principles underlying it have already been worked out by the author, and, almost at the same time, and more completely, by Roosenstein (ref. 6).

When only the signal voltage is present, u_0 is a function of the forced oscillation before $(u_d \sin 2\pi f_d t)$ and after $(u_a \sin 2\pi f_a t)$ the instant of dedamping. That is:

$$u_0 = u_d - u_a \quad (1)$$

If the receiver and transmitter frequencies are equal, u_d and u_a are 180° out of phase, so that now

$$u_0 = u_d + |u_a| \quad (1a)$$

and the initial amplitude is now the algebraic sum of the forced oscillations under the damped and the dedamped conditions.

For the magnitude of u_d and u_a , in resonance:

$$u_d = \rho_d \cdot \mathcal{E} \quad (2a)$$

$$u_a = \rho_a \cdot \mathcal{E} \quad (2b)$$

where ρ_d and ρ_a are the "resonance heightening effects" (according to the nomenclature of Barkhausen (ref. 10), $\rho = (\pi/d) = (1/R)\sqrt{L/C}$) for their respective conditions. Therefore the overall "resonance heightening effect" of the receiver is:

$$\rho_{eff} = u_0 / \mathcal{E} = \rho_d - \rho_a = \rho_d + \rho_a \quad (3)$$

That is, the creation of the initial amplitude is a simple resonance process. Upon this fact hinge certain considerations of selectivity, which will be taken up subsequently.

Theoretically, the free oscillations arise from u_0 , build up until d , and then require an infinite time to die out to zero. Consequently there is always at the instant of dedamping a residue of oscillations from the preceding period:

$$u_r = u^* \cdot e^{-(\pi/\rho_d)(t_d/T)} \quad (4)$$

so that the individual oscillation-trains exert a mutual effect on each other. This condition is "coherence". Coherence could never be neglected if there were not, in addition to the signal and the residual oscillations, a noise voltage u_{sto} . When the decaying oscillations fall below the noise level (C_1 in Fig. 1), they can no longer exert any effect (see Barkhausen and the author (ref. 8); the oscillation-trains are then "incoherent". The following

chapters will consider the modes of operation of the receiver at coherence and at incoherence, which are fundamentally different.

Actually, the dedamping does not occur abruptly as shown in Fig. 1, but gradually. By setting up an exact equivalent circuit for the superregenerative receiver, one can always calculate ρ as a function of time;* this variation is shown for a particular case in Fig. 3.

We must observe that the finite periods of very high ρ occur only because the damping passes through zero gradually. By tuning the receiver, therefore, there follows merely an enlargement of the effective resonance-heightening ρ_{eff} relative to $(\rho_d + |\rho_a|)$ which is larger the slower the dedamping occurs and the smaller ρ_a and ρ_d are. This is expressed numerically:

$$\rho_{eff} = (\rho_d - \rho_a) + \pi \frac{t_0}{T} \quad (5)$$

($T = \frac{1}{f}$ = period of the high-frequency oscillation, t_0 = duration of extreme resonance-heightening).

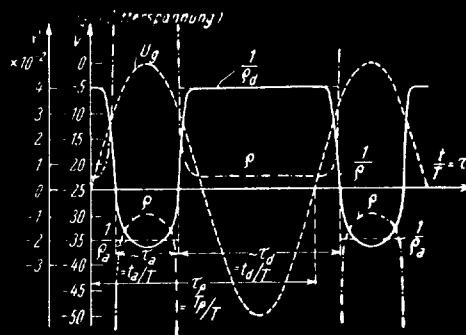


Abb. 3. Zeitlicher Verlauf von ρ bei allmählicher Entdämpfung.

Fig. 3. Variation of ρ as a function of time, with gradual dedamping.

Key:

Gitterspannung

Grid voltage

*See Kautter, ENT 10 (1933) 199.

In practical cases, ρ_{eff} is as much as two times as great as $(\rho_d - \rho_a)$. A sufficiently good approximation of the actual case can be obtained by the assumption of average values of ρ_d and ρ_a for the simple process with sudden dedamping. By detuning the receiver, an important deviation in the form of the resonance curve takes place, and will be referred to later (Part IIIb) in this connection.

(b) High frequency amplification

The growth of the free oscillations cannot continue without limit, for beyond the saturation amplitude u_s set by the non-linearity of the tube characteristic the growth becomes zero.

In the calculation of the amplification there are two cases:

(a) "K"-range. The growing oscillations, during time t_a , do not attain the amplitude u_s (see Fig. 4); that is, the initial amplitude is smaller than the value $u_{0s} = u_s \cdot e^{-(\pi/\rho_a)(t_a/T)}$ which, in time t_a , would grow exactly to u_s . In this case, the amplitude throughout the quenching-frequency cycle is proportional to the incoming signal, and calculation gives a constant amplification V . For linear and for square-law demodulation, if the following relative time terms ⁽²⁾ $\tau_a = t_a/T$; $\tau_d = t_d/T$; $\tau_p = T_p/T = f/f_p = \tau_a + \tau_d$ are introduced, the following expressions for \bar{u} and V are obtained:

Footnote (2): τ_a is the number of growing, τ_d the number of decaying high-frequency oscillations.

Linear demodulation ($A = a \cdot u$):

$$\bar{u} = \frac{\rho_d - \rho_a}{\pi \tau_p} \cdot u_0 \cdot e^{-(\pi/\rho_a) \tau_a} \quad (7a)$$

$$V = \frac{\rho_d - \rho_a}{\pi \tau_p} \cdot e^{-(\pi/\rho_a) \tau_a} \quad (8a)$$

Square-law demodulation ($A = b \cdot u^2$):

$$\bar{u} = \sqrt{\frac{\rho_d - \rho_a}{2\pi \tau_p}} \cdot u_0 \cdot e^{-(\pi/\rho_a) \tau_a} \quad (7b)$$

$$V = \sqrt{\frac{\rho_d - \rho_a}{2\pi \tau_p}} \cdot e^{-(\pi/\rho_a) \tau_a} \quad (8b)$$

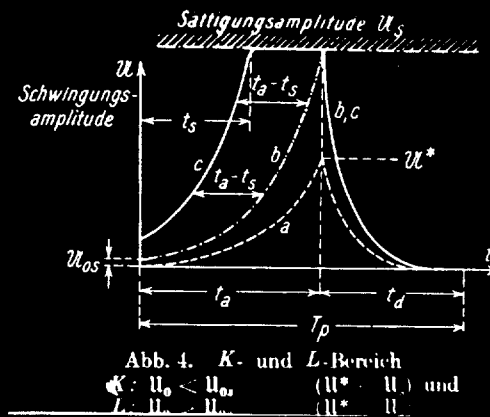


Fig. 4. K- and L-regions.

Key:

Sättigungsamplitude	Saturation amplitude
Schwingungsamplitude	Amplitude of oscillations

The largest amplification in the K-range will be reached when the smallest possible beginning amplitude, i.e., the noise voltage u_{sto} , will give rise to the maximum final amplitude u_s . It is limited only by the noise level, and is:

Linear demodulation:

$$V_{max.} = \frac{\rho_d - \rho_a}{\pi \cdot \tau_p} \cdot \frac{u_s}{u_{sto}} \quad (8e)$$

Square-law demodulation:

$$V_{\max} = \sqrt{\frac{P_d - P_a}{2\pi\tau_p}} \cdot \frac{u_s}{u_{s0}} \quad (8f)$$

(b) "L"-range (u_0 greater than u_{0s}). Here the final amplitude is always the same (u_s), but will be reached earlier the larger u_0 is. The growth curve remains the same but is pushed back toward a as the signal becomes larger. There is a logarithmic law for the amount of this translation (see the author (ref. 7) and Roosenstein (ref. 6)), so the amplification now depends logarithmically on u_0 , becoming:

Linear demodulation:

$$\bar{u} = \frac{1}{\tau_p} \cdot u_s \left[\tau_a + \frac{P_d - P_a}{\pi} + \frac{P_a}{\pi} \ln \frac{u_s}{u_0} \right] \quad (7c)$$

$$V = \frac{1}{\tau_p} \cdot \frac{u_s}{u_0} \left[\tau_a + \frac{P_d - P_a}{\pi} + \frac{P_a}{\pi} \ln \frac{u_s}{u_0} \right] \quad (8c)$$

Square-law demodulation:

$$\bar{u} = u_s \sqrt{\frac{1}{\tau_p} \left[\tau_a + \frac{P_d - P_a}{2\pi} + \frac{P_a}{\pi} \ln \frac{u_s}{u_0} \right]} \quad (7d)$$

$$V = \frac{u_s}{u_0} \sqrt{\frac{1}{\tau_p} \left[\tau_a + \frac{P_d - P_a}{2\pi} + \frac{P_a}{\pi} \ln \frac{u_s}{u_0} \right]} \quad (8d)$$

\bar{u} and V will be calculated for an example and compared with experimental measurements. u is here the high-frequency variation in grid voltage of the receiver. As demodulator there will be used a thermoammeter connected in the anode oscillating circuit of the receiver (see Experimental Apparatus, Part II). With it the squared average value

$$\bar{u} = \text{const} \cdot \sqrt{g_c^2}$$

will be measured. In this case

$$u_s = 14.4 \text{ v.}; f_p = 250 \text{ n}; f = 140,000 \text{ n}; \lambda = 2130 \text{ m.}$$

From the evaluation of the damping values in Fig. 3, we have:

$$\rho_d \cong 25; \rho_a = -50; \tau_a \cong 160$$

The effective resonance-heightening-effect ρ_{eff} , which is somewhat larger than $|\rho_d| + |\rho_a|$, will be valued at 100.

In the calculation, large errors will be made if slight errors occur in the value τ_a/ρ_a . Consequently a check is desired here. This is furnished through a measurement whereby the magnitude of u_{os} may be accurately determined. When $u_o = u_{os}$, the characteristic curve $\bar{u} = f(\epsilon)$ suddenly diverges from its linear beginning, and the transition into the L-region reduces the amplification.

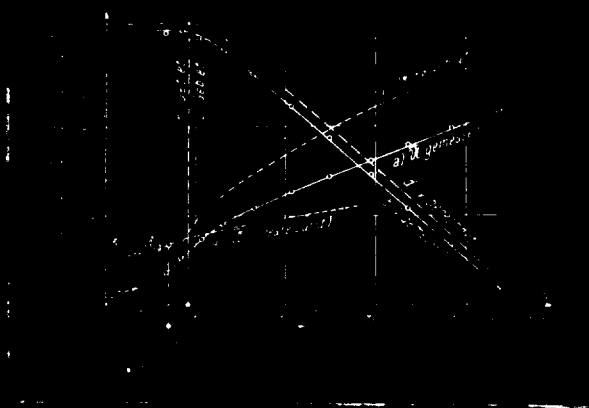


Fig. 5. Slope of amplification (scale for linear representation).

Key:

Gebiet	Region
Berechnet	Calculated
Gemessen	Measured
Lineare Darst	Linear representation

Figure 5, in which curves (a) and (b) show the measured values of \bar{u} and V , shows — especially significantly in the portion of curve (a) which is plotted to linear scales — that this bending-over begins at about $E = 3.5$ microvolts, that is, $u_0 \cong 350$ microvolts. From this we get

$$-\frac{\pi}{\rho_a} \cdot \tau_a = \ln \frac{u_s}{u_{0s}} = 10.6$$

If $\tau_a = 160$, then $\rho_a = -47.5$, almost exactly equal to the graphically-determined value given above. The calculated curves for \bar{u} and V on the assumption of $u_{0s} = 350$ microvolts are shown in Fig. 5 by (c) and (d), and agree well with the measured curves throughout their length.

II. EXPERIMENTAL APPARATUS

The receiver used in the experimental investigations operates at $140,000 \sim$ ($\lambda = 2130$ m). The results, however, can be applied to any desired frequency, if the modulation frequency f_p is correspondingly changed, for all laws of superregenerative receivers are in terms of the ratios τ_p , τ_d , τ_a .

The entire circuit is given in Fig. 6. The receiver oscillating circuit generally is located on the anode side; it can also, however, be placed in the grid circuit.

To the grid circuit of the receiver is supplied the constant bias U_g and the alternating bias U_p , through the low-pass filter HD. The alternating bias is produced by a variable-frequency

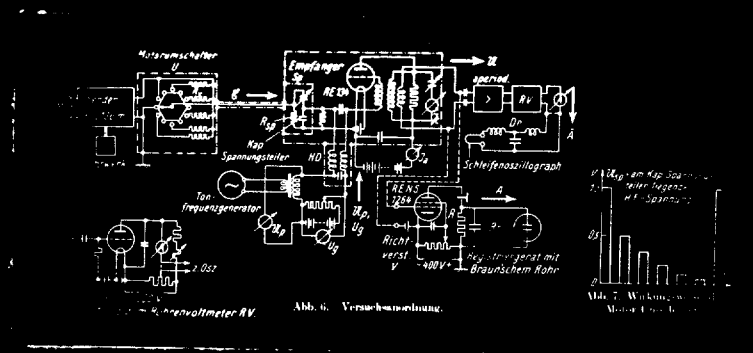


Fig. 6. Experimental apparatus.

Fig. 7. Manner of operation of motor-driven commutator.

Key:

Motorumschalter	Motor-driven commutator
Uhrwerk	Clockwork
Sender	Oscillator
Empfänger	Receiver
Kap Spannungsteiler	Capacitance voltage-divider
Schleifenzillograph	String oscillograph
Tonfrequenzgenerator	Audio-frequency generator
Registriergerät mit Braunschem Rohr.	Recording device with cathode-ray tube.
Schaltung zum Rohrenvoltmeter.	Circuit of vacuum-tube voltmeter.
Am Kap. Spannungsteiler liegende HF-Spannung.	High-frequency voltage applied to capacitance voltage-divider.

audio-frequency-generator. The high-frequency e.m.f. \mathcal{E} of the signal generator S acts upon the grid circuit; its magnitude can be adjusted by the resistance voltage-divider $R_v R_{sp}$, and the following capacitive voltage-divider S_p . R_v , and with it the ratio of the resistance voltage-divider, can be changed in quick succession by the commutator U , so that the voltage entering at S_p follows the variation shown in Fig. 7.

The frequency of the signal generator can be changed continuously by a clockwork with an exactly predetermined speed, in order quickly to register the resonance curve of the receiver.

The demodulator is inductively coupled to the receiver; for this purpose either the rectifier V or the vacuum-tube voltmeter RV is used. The rectified voltage from the former, which no longer contains any high-frequency components, but reproduces, however, the periodic variations occurring at the quenching frequency, controls the deflecting plates of a Zeiss-Ikon "Tremograph", with which the time-variation $A = f(t)$ of the rectified voltage can be photographically recorded. The vacuum-tube voltmeter RV , on the other hand, is so proportioned that the rectified current indicates only the average value \bar{A} . A string oscillograph is connected to RV .

III. THE RECEIVER WITH INCOHERENCE OF THE OSCILLATION PROCESSES.

(a) Receiver conditions. Modulation characteristics.

Under incoherence it is necessary to consider as initial amplitudes only u_{sto} , the noise level, and u_0 , which is produced directly by the signal. In reception, a change of the initial amplitude in a given ratio can produce a large variation $\Delta \bar{A}$ in the average rectified effect. In telephonic receivers this ratio is $(1+m)/(1-m)$, where m is the degree of modulation of the transmitter; in telegraphic receivers it is u_0/u_{sto} , for the initial amplitude in the receiver varies with the transmitter key between these two values.

The best adjustment of the receiver is most easily understood from the logarithmically-represented modulation characteristic $\bar{A} = f(\ln u_0)$; the point of its greatest slope gives the optimum operating point. The slope $S_M = d\bar{A}/d(\ln u_0)$ can be computed as follows:

K-range

Linear demodulation

$$S_{MK} = a \cdot \frac{P_d - P_a}{\pi \tau_p} \cdot u_0 \cdot e^{-(\pi/2)\tau_a} \quad (9a)$$

Square-law demodulation

$$S_{MK} = b \cdot \frac{P_d - P_a}{\pi \tau_p} \cdot u_0^2 \cdot e^{-2(\pi/2)\tau_a} \quad (9b)$$

It becomes a maximum at transition into the L-range:

$$S_{MK_{max}} = a \cdot \frac{P_d - P_a}{\pi \cdot \tau_p} \cdot u_s \quad (9c)$$

$$S_{MK_{max}} = b \cdot \frac{P_d - P_a}{\pi \tau_p} \cdot u_s^2 \quad (9d)$$

L-range

$$S_{ML} = -a \cdot u_s \cdot \frac{P_a}{\pi \tau_p} \quad (9e)$$

$$S_{ML} = -b \cdot u_s^2 \cdot \frac{P_a}{\pi \tau_p} \quad (9f)$$

S_M therefore increases in the K-region almost (as exactly as \bar{A} does) exponentially with u_0 , reaches its maximum at $u_0 = u_{0s}$, and then becomes a constant in the L-region but less than the maximum, according to the relation:

$$S_{MK_{max}} : S_{ML} = \frac{P_d - P_a}{P_a} \quad (10)$$

In the K-region there appear no peculiarities as compared with a normal receiver, for the desired output signal $\Delta \bar{A} = \Delta \ln u_0 \cdot S_M$ is proportional to the input signal strength. In the L-region, on the contrary, because of the constant slope S_M , the audible output signal is completely independent of the size of the signal.

$$\Delta \bar{A} = S_{ML} \cdot \ln \frac{1+m}{1-m}$$

Herein there is afforded an automatic and absolute fading regulator, with which Roosenstein has already dealt further.

A family of such experimentally-measured modulation characteristics is shown in Fig. 8, for these values:

$$U_g = -25 \text{ v.}; P_d = 25; P_a = -40; f_p = 210 \text{ v.}$$

By varying the quenching voltage U_p , the duration of the build-up period was adjusted to different values, and for each of these a modulation characteristic taken. The thermo-ammeter I_c in the oscillating circuit again served as a demodulator.

All of the characteristics may be derived from each other by parallel displacement, as may be expected from equation (9); since the slope S_{ML} in the L-region is independent of τ_a .

In Fig. 8, $S_{MK_{max}} = 2.4 S_{ML}$, while theoretically, according to equation (10), the relation should be $S_{MK_{max}} = 1.75 S_{ML}$.

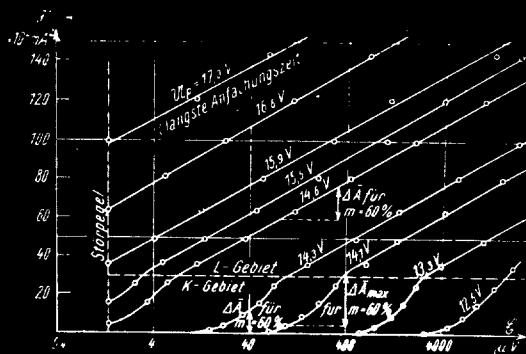


Abb. 8.
Modulationskurven bei verschiedenen Anfachungszeiten

Fig. 8.

Modulation characteristics with different building-up times.

Key:

Langste Anfachungszeit	Longest building-up time
Storpegel	Noise level
Gebiet	Region

For a very weakly modulated telephonic transmission, one would thus be able to reach 2.4 times as great an audible signal in the K-region as in the L-region. For this case the dedamping period must be so adjusted that

$$u_{0\max} = u_0(1+m) = u_{0s}$$

However, even with a degree of modulation of 60%, for which the variation $\Delta \bar{A}$ in the rectified effect is plotted at different points of the modulation characteristics in Fig. 8, the audible signal in the K-region is, with the best adjustment, still 40% to 50% larger

than in the L-region. Consequently the K-region is to be preferred.

All of the characteristics of Fig. 8 may be followed only down to $\mathcal{E} = 1.3 \mu\text{v.}$, that is, $U_0 \cong 120 \mu\text{v.}$, since here the signal vanishes in the noise voltage. $120 \mu\text{v.}$ was therefore the magnitude of the noise level U_{sto} . According to equation (3f), under

optimum adjustment the maximum possible amplification is $V_{\max} = \sqrt{\frac{\rho_d - \rho_n}{2\pi \tau_p}} \cdot \frac{U_s}{U_{sto}}$

= 15,500, which is reached with a quenching voltage of 15.8 volts. In this case the noise disturbance produced the maximum possible audible signal ($U_{sto} = U_{os}$). However, since for useful reception the signal must be at least 4 to 5 times greater than the irregular superimposed noise, an amplification 4 to 5 times smaller than that indicated above is the maximum practically obtainable. In our case $V = 4000$, for which $U_p = 15.6 \text{ v.}$. In this order of magnitude, in general, lies the amplification obtainable from super-regenerative receivers under optimum adjustment.

An increase of the signal beyond the minimum value of $\mathcal{E}_{\min} \cong 5 U_{sto}$, however, produces no increase in the loudness obtainable, as may be seen from Fig. 8; because for each signal strength the receiver may be so adjusted that it works on the steepest part of the modulation characteristic, $U_{o\max} = U_0(1+m) = U_{os}$ (for $\mathcal{E} = 250 \mu\text{v.}$, this is obtained with $U_p = 14.1 \text{ v.}$). For stronger signals, the amplification must simply be correspondingly reduced, through a shortening of the build-up period.

Here there is the possibility of a fading regulator -- to be sure, an indirect one -- in the K-region as well, in that the

build-up period may be controlled automatically by the magnitude of the high-frequency signal; perhaps through the agency of a self-acting variation of grid bias. Since the degree of amplification depends exponentially upon τ_a , only very small changes of voltage, perhaps 1 or 2 volts (note the variation of U_p in Fig. 8) are required, despite the large regulating range. Compared to the direct method in the L-region, this method has the advantage of a greater realizable audible signal, and, above all, of freedom from distortion.

With a sinusoidal modulation of the transmitter, the distortion factor in the L-region is given by

$$k = \frac{m}{4} \left(1 - \frac{m^3}{4} \right) \quad (11)$$

and is thus nearly the same as in a square-law rectifier. In actuality the distortion is even greater than this, which follows from the magnitude of the "modulation factor" μ introduced by Barkhausen (called "m" by him). (See reference #10). μ measures to what degree a high-frequency oscillation superimposed upon a low-frequency oscillation of large amplitude is modulated by the variation in the steepness of the characteristic, and is a better measure of the actual distortion. For characteristics in the L-region, where $\bar{A} = C_1 + C_2 \ln U_0$, this becomes:

$$\mu = 4k \cdot \frac{1}{1-m} = \frac{m}{1-m} \quad (12)$$

as compared with $\mu = 4k = m$ for a square-law rectifier. Even with 40% modulation $\mu = 65\%$, which exceeds the value of 20% to 30% permissible for good reproduction. In the K-region, in which the super-regenerative receiver behaves like every other receiver with a high-

frequency amplifier, the distortion is only of customary magnitudes in linear rectifiers used for very large amplitudes, and is thus essentially much smaller than in the L-region.

There remains to be investigated to what extent the maximum realizable audibility may be increased by suitable choice of other quantities than the building-up period. According to equations (9c) and (9d) this is dependent upon the expression $\frac{\rho_d - \rho_a}{\pi \cdot \tau_p}$, and upon the practically fixed demodulation constant. This expression, however, is essentially constant in value. That is, in order to reach a sufficiently high amplification, $\frac{\tau_a}{\rho_a}$ may not be less than a certain minimum value; thus, for a signal of the order of magnitude of the minimum signal receivable, we have $-\pi \frac{\tau_a}{\rho_a} = 10$, corresponding to a ratio $u_s/u_0 = 20,000$. The expression $\pi \frac{\tau_d}{\rho_d}$ must also have at least approximately the same magnitude, because the oscillations must die away again sufficiently to prevent coherence with its undesirable results (see Part IV). With these practical necessary values:

$$\left(-\pi \frac{\tau_a}{\rho_a}\right)_{\min} = 10; \quad \left(\pi \frac{\tau_d}{\rho_d}\right)_{\min} = 10 \quad (13)$$

then, at the most,

$$\left(\frac{\rho_d - \rho_a}{\pi \tau_p}\right)_{\max} = 0.1$$

and therewith is obtained the maximum audibility, independent of the quenching frequency f_p and the "resonance heightening effect" $\rho_d - \rho_a$, always provided that the minimum values (equation (13)) are not unnecessarily exceeded. For this condition the receiver must be so adjusted that, for a given quenching frequency, the

signal will increase during the build-up time to exactly such a magnitude, and will die away again just sufficiently during the decay period, that coherence will not result. The quenching frequency is then equal to the "limiting quenching frequency" f_{pgr} ($f_p > f_{pgr}$, coherence; $f_p < f_{pgr}$, incoherence; see details in the following paragraphs).

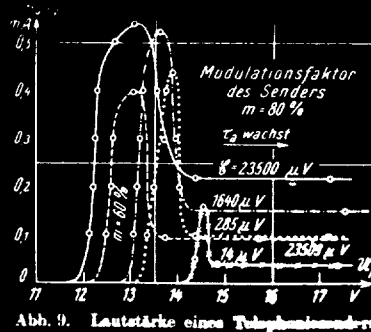


Fig. 9. Audibility of a telephonic transmitter.

Key:

Modulationsfaktor des Senders	Percent modulation of transmitter
wächst	Increases
150 Hz	150 cycles per second

With a stronger signal the minimum values (equation (13)) can be somewhat smaller, so that the audibility may be increased through an increase of the quenching frequency or a decrease of either the damping or the dedamping. However, even if the signal is 150 times stronger than the minimum signal, in which case the amplification only amounts to $V = 27$, the audible signal is only

doubled and acoustically the increase from this is hardly noticeable.

As the one practical means of attaining greater audibility, there remains only (see equation 9c, 9d) the increasing of the saturation amplitude u_s , which can be achieved to any desired degree by the use of more powerful tubes. Usually, however, the addition of one more tube for audio-frequency amplification is to be preferred.

In confirmation of what has been said so far, Fig. 9 shows the results of an experiment in which the audible volume obtained from a transmitter modulated at 150 c.p.s. was measured directly by the magnitude of the alternating current of 150 \sim obtained after detection. The receiver here was an entirely different installation from that of Fig. 8, and the build-up time was accordingly different. The maximum audible volume varies only very slightly, in spite of wide variation of the signal strength; it first encounters a large decrease when the signal approaches the magnitude of the noise voltage. The automatic volume control in the L-region is not absolute here, but is, however, not very far from it.

The smaller amplification corresponding to the reception of a stronger signal has the advantage that it permits a noise-free adjustment of the receiver. In the K-region the rushing sound, produced by the amplified noise voltage after detection, is superimposed upon the signal and acts in reception as a weaker signal; that is, with the application of higher amplifications, it is exactly as disturbing here as in any other receiver. If the receiver is working in the L-region, then there appears the phenomenon

of the suppression of noise by an unmodulated signal, which also occurs in ordinary receivers with automatic volume control (already investigated by David; reference (3)).

On account of the logarithmic amplification, the volume of the noise is here proportional to the ratio $\frac{u_0 + u_{sto}}{u_0 - u_{sto}}$, which with a larger signal approaches unity, with the attainment of which all noise disappears. The oscillogram, Fig. 13c (Part IIIb), shows the difference between the K- and L-regions in this respect. As the signal is increased the disturbances superimpose themselves upon it with unchanged magnitude, in the K-region (under the limiting line (-----)), as the constant spacing of the drawn-in lines shows; but as soon as the L-region (above the (-----) line) is reached they disappear completely.

(b) Resonance curves.

The basis for all possible resonance curves for super-regenerative receivers is the course of variation of the initial amplitude, as the transmitter is detuned with respect to the receiver.

As long as the transmitter frequency f_M and the receiver frequency f are not very far apart, so that the phase condition of the high-frequency oscillations occurring at the instant of dedamping is the controlling influence, there exists here as well, for sudden dedamping, the relation $u_0 = u_d - u_a$

where u_d and u_a must, in general, be combined vectorially. Each of these two forced oscillations has its own normal resonance curve.

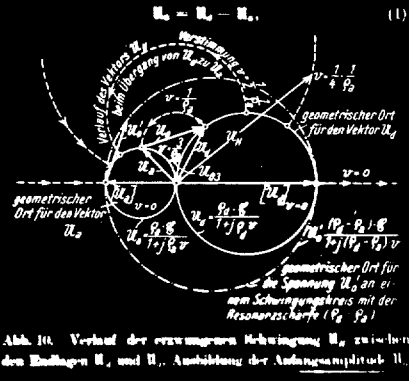


Fig. 10. Course of the forced oscillation u_H between the boundary conditions u_d and u_a . Creation of the initial amplitude.

Key:

- | | |
|--|--|
| Verlauf des Vektors u_H beim Übergang von u_d zu u_a . | Course of the vector u_H in moving from u_d to u_a . |
| Geometrischer Ort für den Vektor | Locus of the vector |
| Geometrischer Ort für die Spannung, etc. | Locus of the voltage u_0' in an oscillatory circuit with the resonance-sharpness $(p_d - p_a)$. |

The graphical construction shown in Fig. 10 then gives u_0 as a function of the "detuning" $v = \frac{f_H}{f} - \frac{f}{f_H}$ (the notation and representation are as given by Barkhausen; reference (11)). It is known that the course of u_0 is not much different from that for the alternating voltage in an ordinary oscillating circuit with resonant sharpness $p_d - p_a$ (--- circle in Fig. 10). Also, even with the largest possible deviation — namely, when

as in Fig. 11 -- there is still a great similarity between these two resonance curves. Only with large degrees of detuning does

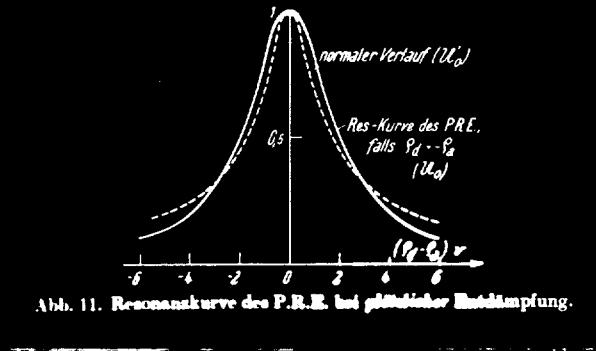


Fig. 11. Resonance curve of superregenerative receiver with sudden dedamping.

Key:

Normaler Verlauf

Normal shape

Res-Kurve des PRE,
falls $\rho_d = -\rho_a$

Resonance curve of
superregenerative
receiver, for the
case of $\rho_d = -\rho_a$

the resonance curve for the superregenerative receiver fall off more steeply than the one for an ordinary oscillating circuit. If, moreover, ρ_d and ρ_a are not of the same magnitude, then the agreement is still better.

The resonance curve for U_0 was determined experimentally in such a way that, regardless of the degree of detuning, the magnitude of the signal was made just sufficient to overcome the noise level. In the experiments, a resonance curve was always obtained which at relatively small detunings fell off much more steeply than was to be expected. In Fig. 12, (b) is an example of a curve

so observed, in comparison to which (a) represents the resonance

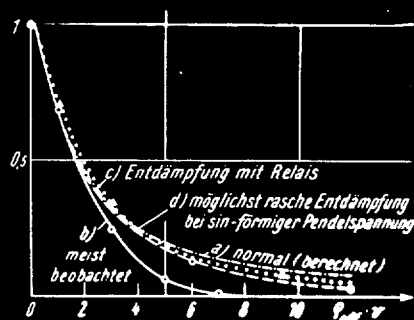


Abb. 12. Resonanzkurven für die Anfangsamplitude.

Fig. 12. Resonance curve for the initial amplitude.

Key:

Entdämpfung mit Relais	Dedamping with relay
Möglichst rasche Entdämpfung bei sin-förmiger Pendelspannung	Most rapid dedamping with sinusoidal quenching voltage
Meist beobachtet	Generally observed
Berechnet	Calculated

curve for an ordinary oscillating circuit. While, for example, in an ordinary receiver a transmitter out of tune by the amount $v = 7/\rho$ must be 7 times as strong as one which is tuned in order to produce the same result, it would have to be about 100 times as strong, according to this, in the case of a superregenerative receiver.

As the cause of this discrepancy, only the gradual dedamping can come into the question; as was to be concluded from the author's earlier experiments.

Therefore it was now attempted to cause the dedamping to occur suddenly, as far as possible. To accomplish this the grid voltage of the receiver was varied, not sinusoidally, but periodically between 2 values by means of a relay operated at 50 \sim . The almost-normal-appearing resonance curve (c) of Fig. 12 was now actually obtained. Moreover, even with sinusoidal quenching voltage, when the dedamping was made to occur as rapidly as possible by setting the grid bias voltage at -130 v. and the amplitude of the quenching voltage at 150 v., the curve (d) was obtained, which approximates much more closely the normal curve.

This experiment verified the assumption that gradual dedamping produces an abnormal steepness of the sides of the resonance curve $u_o = f(\nu)$. Practically the band-pass form of the curve is of advantage.

Theoretically, this behavior of the superregenerative receiver may be explained on the basis of the vector representation of Fig. 10; with gradual dedamping, the vector u_H of the forced oscillation rotates from the initial position u_d to the final position u_a on a circle whose radius is smaller the larger the fixed effective reactance of the oscillating circuit $R_b = 2\pi f_H L - \frac{1}{2\pi f_H C}$. In Fig. 10 there are drawn, for various degrees of detuning, the circles (-----) upon which the endpoint of the vector u_H moves during dedamping. With greater detuning (shown for $\nu = 3/\rho_a$), u_H undergoes only a small phase rotation, without noticeably changing its magnitude; which occurs more slowly

the more gradually the damping passes through zero. In this case a transient process can hardly exist, while with sudden dedamping the considerable initial amplitude u_{03} was obtained. Only for small detuning does the dedamping have the character of a switching process, which was made the basis for all considerations.

Therefore, the resonance curve shows a normal shape only in the immediate vicinity of the resonant frequency, while further away relatively much smaller initial amplitudes are obtained. The more gradually the dedamping takes place, the more strongly this phenomenon occurs.

The effective selectivity curve for reception is connected with the basic resonance curve $u_0 = f(\nu)$ considered above, through the modulation characteristic treated in Part IIIa. It gives as a function of detuning the variation of the rectified effect $\Delta \bar{A}$ -- for telephone receivers, as a consequence of modulation; for telegraph receivers, as a consequence of the variation between the noise and signal levels. In the K-region, because of the constant amplification, the rectified effect varies along the same resonance curve as the initial amplitude (for linear demodulators). In the L-region, on the other hand, the resonance curve must appear flattened out, because with larger initial amplitudes the amplification drops.

Fig. 13 shows some oscillograms of these resonance curves. The ordinate corresponds to the current in the oscillating circuit. The receiver was adjusted with $\rho_d = 30$, $\rho_a = -70$. Fig. 13 (a)

and (b) were taken in the K-region; for (a) the signal was $53 \mu\text{v.}$; for (b) $25 \mu\text{v.}$, for which the dedamping period was so reduced as

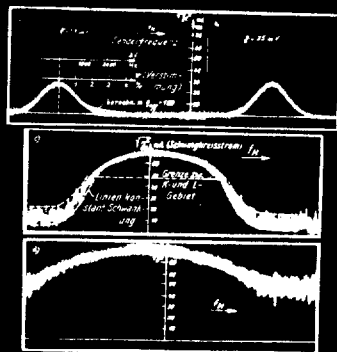


Fig. 13.

Key:

Senderfrequenz	Transmitter frequency
Verstimmung	Detuning
Berechn. m.	Calculated for
Schwingkreisstrom	Oscillating current
Grenze zw. K- und L-Gebiet	Boundary between K- and L-regions
Linien konstant. Schwankung.	Constant lines. Fluctuations.

compared with (a) that the largest initial amplitude at resonance could not build up quite to the saturation amplitude. In both cases the same resonance curves were obtained as previously was secured for u_0 . If one sketches in a normal resonance curve agreeing as closely as possible with that measured above (carried out for (a)), then $P_{\text{eff}} = 180 = 1.8(P_d - P_a)$; the increase of the

effective resonant sharpness, compared with $(\rho_d - \rho_a)$, thus takes place to the extent previously determined theoretically (equation 5). Here also occur the deviations with large detuning explained above.

For (c) the dedamping period was increased, compared with (a), as is to be observed from the noticeable disturbances. When the detuning is decreased, a sharp increase follows at first. Then occurs the change to the L-region, which causes the whole middle part of the curve to be flattened. In Fig. 13 (d) the receiver operates in the L-region from the very beginning; consequently the resonance curve is flattened over its entire length and rises only a little above the disturbance level.

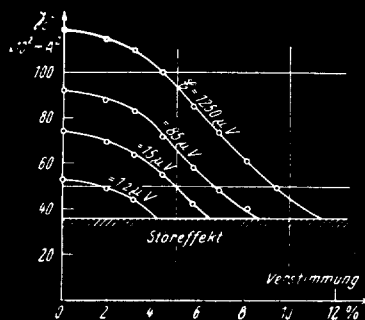


Abb. 14. Parallelverschiebung der Resonanzkurven im L-Gebiet.

Fig. 14. Parallel displacement of resonance curves in L-region.

Key:

Storeffekt	Noise effect
Verstimmung	Detuning

Comparison of Fig. 13 (a) and (b) with (c) and (d) shows that in the L-region a telegraph receiver is extraordinarily unselective.

While in the K-region the resonance curves for signals of different intensities are obtained from each other by multipli-
cation by a constant factor, there corresponds to this in the L-region a parallel displacement of the individual curves. This is very exactly verified by the measurements reproduced in Fig. 14.

With a telephonic receiver, the resonance curve of the audibility in the K-region is naturally also of the form discussed at the beginning. In the L-region, on the other hand, since the audibility is completely independent of the initial amplitude, the receiver may be completely detuned without having the audibility drop in the least, provided that the initial amplitude due to the signal is greater than the noise level.

In Fig. 15, (b) is such a completely horizontally-shaped resonance curve; the lateral drop begins upon reaching the noise level. In taking this, as was described for Fig. 9, the audibility of the 150v -modulated transmitter was measured directly. For comparison, (a) is the resonance curve in the K-region taken under otherwise identical conditions. (c) was obtained as an intermediate form between (a) and (b). In the middle part the receiver operates in the L-region, for larger detuning in the K-region (adjustment about as for Fig. 13c). Since the strongest audibility is reached on the border of the K-region (see Part IIIa), this double-peaked shape is obtained.

The resonance curve of the telephonic receiver undergoes an extraordinary broadening, as well, in the L-region; at least for

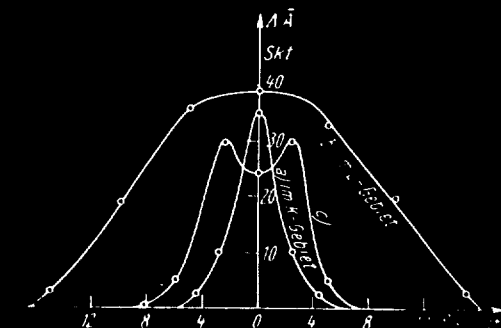


Abb. 15. Resonanzkurven des Telephonie Empfängers.

Fig. 15. Resonance curves of a telephonic receiver.

Key:

Skf	Scale divisions
Im L-Gebiet	In L-region
Im K-Gebiet	In K-region

strong signals. Lack of selectivity is not thereby produced, however, for the same reason as in a receiver with automatic volume control, which has almost the same resonance curve. That is, if two transmitters are operating simultaneously within the resonance curve, then only the one giving the larger initial amplitude will be heard, just as in the case of the receiver noise at the onset of a signal.

In a corresponding experiment, the audibility of transmitter #I, which was somewhat detuned with respect to the receiver, was measured while an equally strong unmodulated transmitter #II acted upon the receiver. Depending upon the detuning of the

latter, the audibility of #I underwent the variations represented in Fig. 16. In the range in which #II produces a greater initial amplitude than #1, the latter transmitter is completely suppressed.

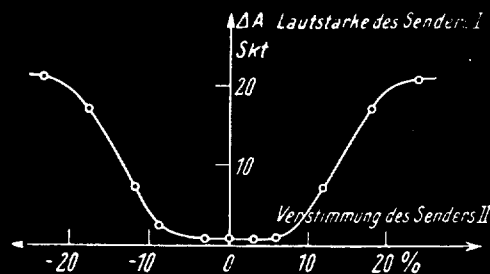


Abb. 16. Auslöschung eines Senders durch einen zweiten

Fig. 16. Suppression of one transmitter by another.

Key:

- Lautstärke des Senders I. Audibility of transmitter I.
- Verstimmung des Senders II. Detuning of transmitter II.
- Skt Scale divisions

To strive for narrower resonance curves through higher ρ_{eff} is of advantage not only for good selectivity, but also for an increase in sensitivity; for the narrower the frequency band of the receiver, the smaller will be the relative noise level. By increasing ρ_{eff} , one may thus reduce the minimum signal \mathcal{E}_{min} . Since ρ_{eff} is proportional to $(\rho_d - \rho_a)$, this may be done equally well by reducing either the damping or the dedamping.

The dependence of the barely-perceptible minimum signal \mathcal{E}_{min} upon the effective resonant-heightening-effect is shown by the series of experiments in Fig. 17. With constant quenching

frequency, the ratio $\frac{\tau_a}{\tau_d}$ was changed by displacement of the operating point. Since the adjustment was always for approximately constant amplification (that is, $\frac{\tau_a}{\rho_a} \approx \text{const.}$), ρ_a is larger the

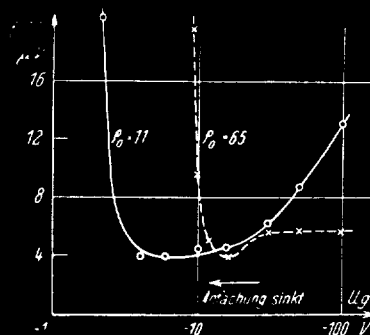


Abb. 17. Mindestsignal abhängig von der Anfachung.

Fig. 17. Minimum signal as a function of amount of dedamping.

Key:

Anfachung sinkt

Amount of dedamping decreases

larger is τ_a , that is, the smaller is the negative grid voltage. In the two tests the oscillating circuit, this time connected in the grid circuit, possessed inherent resonance sharpnesses of $\rho_0 = 65$ and $\rho_0 = 11.5$, respectively.

In the circuit with the higher resonance sharpness, the sensitivity remains unchanged for the higher dedampings; here the effective resonance-heightening-effect is about equal to the positive ρ_d alone, since $\rho_a \ll \rho_d$. In the circuit with $\rho_0 = 11.5$, on the other hand, \mathcal{E}_{min} rises steadily with decreasing ρ_a ; with $U_g = -100$ v. the sensitivity is 2.3 times smaller than in the first circuit. If $\rho_a \gg \rho_d$, then the sensitivity increases more

and more, and is now almost the same for both circuits, since the positive resonance sharpness no longer matters.

There is a certain point, which is different for the two circuits, beyond which the minimum signal suddenly increases very rapidly, even though the rate of build-up drops still lower. Here the damping time has become too short, and coherence occurs (see Part IV).

A corresponding series of experiments (not here presented) with different anode oscillating circuits also gave quantitatively the same sensitivity and dependency on ρ_{eff} , independent of the other constants of the circuit. It may also be shown, in general, that sensitivity depends only on ρ_{eff} ; it is independent of the arrangement of the circuit, as well as of the magnitudes of the inductance and capacitance employed.

The superregenerative receiver possesses the particular advantage that the effective resonance sharpness may be increased arbitrarily without difficulty, through a reduction of the rate of build-up, without the necessity of using low-loss circuits.

(c) Limits of Selectivity

It has already been found in Part IIIa that in the optimum case,

$$\left(\frac{\rho_d - \rho_a}{\pi \cdot \tau_p} \right)_{max} = 0.1 \quad (14)$$

in order, on the one hand, to permit sufficiently high amplification, and, on the other, to prevent coherence. This value depends

only slightly upon the signal strength. When the optimum (equation 14) is reached (at which time the greatest audibility simultaneously occurs), the quenching-frequency period τ_p has its minimum value, for a given resonance sharpness ($\rho_d - \rho_a$); that is, the quenching frequency is then the highest which can be used, and is then equal to the "limiting quenching frequency" (see Part IIIa). With the attainment of the approximate value

$$\rho_{eff} = 2(\rho_d - \rho_a)$$

we obtain:

$$\tau_{pgr} = \frac{f}{f_{pgr}} \cong 1.6 \rho_{eff} \quad (15)$$

Since the sensitivity increases with ρ_{eff} (see Fig. 17), it must be possible by lowering the limiting quenching frequency -- at which the receiver is situated exactly on the boundary between coherence and incoherence -- to reduce the necessary minimum signal. Experiment confirms this: Fig. 18 shows the dependence, both of the limiting quenching frequency and of the magnitude of the minimum signal, upon the grid voltage (see Part V); both curves have the same shape.

Since for the reproduction of the audio-frequency modulation of the transmitter the quenching frequency must be at least four times larger than the modulation frequency f_m , there follows from equation (15):

$$\frac{f}{f_m} \cong 6.5 \rho_{eff} = 13(\rho_d - \rho_a)$$

Therefore, for example, with $\lambda = 300$ m. and a modulation frequency of $f_m = 5000$ m., the highest ρ_{eff} attainable is 30, while with

ordinary receivers one can go considerably higher ($\rho = 200$ to 300). In the broadcast band, therefore, without the introduction of a special pre-selective stage, the superregenerative receiver is not

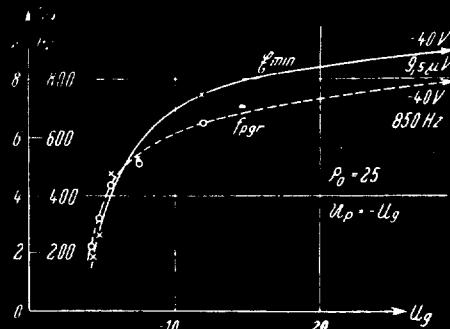


Abb. 18. Grenzpendelfrequenz und Mindestsignal abhängig von U_g .

Fig. 18. Limiting quenching frequency and minimum signal, as functions of U_g .

Key:

Hz

Cycles per second

sufficiently selective, while as a telegraphic receiver it can be used up to long waves; the quenching frequency should then be made an audible frequency, in order to attain sufficient selectivity.

As a short-wave receiver, the telephonic superregenerative receiver also gives sufficient selectivity directly ($\lambda = 30 \text{ m.}; \rho_{\text{eff}} = 300$); for the reception of television signals, however, there are selectivity difficulties even in the short-wave region. For the transmission of 500,000 picture elements there would be required a carrier wavelength of 1 meter in order to attain a $\rho_{\text{eff}} = 100$.

It is to be observed, of course, that with superregenerative receivers the transmitters can be closer together (in frequency) than with an ordinary receiver of equal resonance sharpness, since the resonance curve has a desirable band-pass-filter form, and the value β_{eff} applies to the middle part of the curve but not to the sides (see Fig. 12).

IV. THE RECEIVER WITH COHERENCE OF THE OSCILLATION PROCESSES.

(a) Creation of the Initial Amplitude

Sensitivity

Practically, coherence between the oscillation processes begins when the largest possible residual oscillation, which is still left over from the preceding oscillation process at the instant of dedamping, is several times as large as the noise level. It then has the value

$$u_s \cdot e^{-\frac{\pi}{\beta_d} \cdot \tau_{dgr}} \approx 5 u_{sto} \quad (17)$$

from which the limiting quenching frequency is found to be

$$f_{pgr} = \frac{f}{\tau_{dgr}(1 + \tau_a/\tau_d)} \quad (18)$$

The course of the oscillation processes with coherence is shown schematically in Fig. 19. If at time a_0 the initial amplitude is still u_0 , then at time a_1 it has increased to the residual oscillation

$$u_{r_1} = u_0 e^{-\frac{\pi}{\beta_2} \cdot \tau_a} \cdot e^{-\frac{\pi}{\beta_d} \cdot \tau_d} \approx u_0 e^{\Delta} \quad (19)$$

This step-by-step increasing of the initial amplitude proceeds and after n periods the value

$$u_{on} = u_0(1 + \epsilon^\Delta + \epsilon^{2\Delta} + \epsilon^{3\Delta} + \dots + \epsilon^{n\Delta}) \quad (20)$$

has been established, provided first of all that exact equality of the transmitter and receiver frequencies (i.e., permanent synchronism between the forced and free oscillations) is assumed.

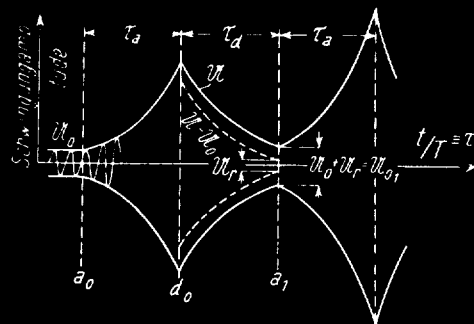


Abb. 19. Kohärente Anschwingvorgänge. (Zur Vereinfachung des Bildes wurde $u_0 = u_d$ gezeichnet, während sie in Wirklichkeit bei der Entdämpfung aus $u_0 = u_d + |u_d|$ besteht.)

Fig. 19. Coherent oscillation-trains. (For simplicity the figure shows $u_0 = u_d$, although strictly, at de-damping, u_0 is formed according to the equation $u_0 = u_d + |u_d|$.)

Key:

Schwingungsamplitude

Amplitude of oscillation

The receiver behaves differently according to whether the residual oscillation is larger ($\Delta > 0$) or smaller ($\Delta < 0$) than the preceding initial amplitude.

In the first case the oscillations "see-saw" up to ever-increasing magnitudes, uninfluenced by the signal; only the reaching of the saturation amplitude sets a limit to the growth. There are then regular steady-state oscillation processes with an initial amplitude of $u_s \cdot e^{-\frac{\pi}{2} \cdot \tau_d} \equiv u_{os} \cdot e^\Delta$.

In order that a signal may now be received, its initial amplitude must be larger than that of the steady state oscillations. The result is an extremely rapid decrease in sensitivity when the limiting quenching frequency is exceeded; when $f_p = 2f_{gr}$ a signal must be at least 150 times as large as the minimum signal at the limiting quenching frequency. Since in this case u_0 is always greater than u_{os} , the receiver operates in the L-region.

If the rate of build-up or the length of the build-up period is so adjusted that $\Delta < 0$ ($\frac{\tau_c}{\rho_a} < \frac{\tau_d}{\rho_d}$), then there results a stationary initial amplitude depending upon the magnitude of the signal:

$$u_0'' = \frac{u_0}{1 - e^{\Delta}} \tag{21}$$

The signal needs only to supply the difference between this stationary amplitude and the somewhat smaller residual oscillation; in case this supply fails because of withdrawal of the signal, then the oscillations die out completely.

The time that is necessary for see-sawing up to 90% of the final value is calculated to be

$$\eta = \left| \frac{2.3}{\Delta} \right| - 1 \quad \text{quenching-frequency periods.} \tag{22}$$

New kinds of phenomena thus enter into the picture, requiring that a signal act for a longer time in order to be correctly received. One consequence of this is that only very low modulation frequencies can be reproduced, as soon as this coherence effect becomes noticeable.

Likewise, the receiver needs a correspondingly longer

time for the effect of a signal to disappear after the signal has stopped. The initial amplitude still has 10% of its original value after

$$n' = \left\lfloor \frac{2.3}{\Delta} \right\rfloor \quad \text{quenching-frequency periods} \quad (23)$$

On account of the nonlinearity of the tube, the maximum initial amplitude attainable is only

$$u_{o_{max}} = u_{os} e^{\Delta} + u_o$$

the highest value up to which the oscillations can seesaw. If the stationary final value $u_o'' > u_{o_{max}}$, then the building-up ends correspondingly sooner, while the amplitude reached remains the same. This shortening of the theoretical "seesawing-up" time is greater, the smaller is the difference between u_o and $u_{os} e^{\Delta}$; for "long seesawing-up times" means at the same time "the residual oscillation is, in the final state, many times as great as the signal". If one prevents this condition through the use of a strong signal which is merely a little smaller than the maximum amplitude (equation 24), in order that the residual oscillation may be appreciably larger than the signal, then the operation of coherence is thereby destroyed; at $u_o = u_{os}$ the receiver immediately reaches a steady condition.

Fig. 20 shows two oscillograms of typical building-up and dying-out processes. Here, through the use of the motor-driven commutator described earlier, signals of different magnitudes were applied and removed in rapid succession, as shown by the curve (----). In Fig. 20 (a) it is seen that the receiver

can no longer follow this rapid modulation; the signals and the pauses run together. For the largest signal, the shortening of

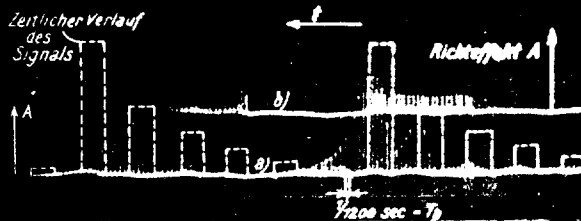


Abb. 20.
 mit länger Ein- und Ausschwingzeiten bei Kohärenz

Fig. 20. Appearance of longer building-up and dying-out times with coherence.

(a) Δ almost equal to zero.

(b) Δ larger (dedamping period shortened).

(Each of the perpendicular stripes is a rectified oscillation-train. The length of the stripes corresponds to the final amplitude reached).

Key:

Zeitlicher Verlauf
 des Signals

Course of signal
 versus time

Richteffekt

Detector effect

the building-up time of the oscillation-trains is also clearly shown. The dying-out lasted, in this experiment, about 16 quenching-frequency periods, corresponding to 15,000 high-frequency oscillations, as may be seen in the oscillogram.

The receiver was indeed rather critically adjusted for this first observation. From the dying-out time, Δ is computed to be -0.15 , while $\frac{\pi \tau_d}{\rho_d} \approx \frac{\pi \tau_e}{\rho_e} = 7.5$. For Δ to be held constant within only 10%, $\frac{\tau_d}{\rho_d}$ and $\frac{\tau_e}{\rho_e}$ must remain unchanged within 0.1%! In Fig. 20 (b), $-\Delta$ was somewhat enlarged through a

wholly insignificant alteration of the quenching voltage. Almost instantaneous building-up and dying-out resulted immediately, but as a consequence the receiver had become about 20 times less sensitive, since the seesawing of the initial amplitude up to higher values could not occur, and since the increase of $-\Delta$, which is attained only through a diminution of $\frac{\tau_e}{\rho_a}$, always reduces the amplification (V is proportional to $e^{\frac{\tau_e}{\rho_a}}$). In the experiment the dying-out time reached values as great as 1 second, in which case the receiver came to rest only after 140,000 oscillations.

The more the limiting quenching frequency is exceeded, the smaller the amplification becomes; for in order that Δ always < 0 , the oscillations will be amplified less, the less they can decay ($\frac{\tau_e}{\rho_a} < \frac{\tau_d}{\rho_d}$). The result would be, were it not for the existence of the seesawing-up process, a decrease in sensitivity in the same degree as occurs in the case of the steady-state oscillations ($\Delta > 0$). It is also to be observed practically that in the coherence condition (with $\Delta < 0$), on account of the low amplification, the receiver's rushing noise is never to be obtained. Also, if one seeks to prevent the unpleasant results of long building-up times through the use of a strong signal $u_0 = u_{0s}$, one does not gain anything over the adjustment $\Delta > 0$; for u_{0s} increases in the same degree as the amplification decreases. As an example, when $f_p = 2 f_{pgr}$ the signal necessary for the suppression of coherence effects is 150 times as large as when $f_p = f_{pgr}$.

Good sensitivity can therefore be obtained in the coherence condition only through continual utilization of the seesawing-up of the amplitude. However, if one takes into the bargain the insufficient reproduction of modulation, practical limits are also very soon reached, since the receiver cannot be sufficiently accurately adjusted. When $f_p = 2f_{pgr}$, in order to lose no sensitivity, one must make $\Delta = -\frac{1}{150}$, and, in order to do this, hold $\frac{\tau_a}{P_a}$ and $\frac{\tau_d}{P_d}$ constant within one part in 15,000, which is impossible. Therefore the sensitivity of superregenerative receivers always falls off very rapidly after the limiting quenching frequency has been exceeded.

This has already been established in Fig. 17, where the receiver came into the coherence range because of extreme shortening of the damping time. Fig. 21 shows further the dependence of the magnitude of the minimum signal upon the quenching frequency, in circuits with various inherent degrees of resonance sharpness ρ_0 . With low quenching frequencies the sensitivity is high and about the same for all circuits; as soon, however, as f_p becomes greater than f_{pgr} for a circuit, \mathcal{E}_{min} rises very rapidly. According to Equation 18, the limiting quenching frequency must be proportional to ρ_d and therefore also somewhat proportional to ρ_0 ; for the more weakly a circuit is damped, the longer time is required for decay of the oscillations. In fact, the result is that:

$$\frac{1}{\rho_{01}} : \frac{1}{\rho_{02}} : \frac{1}{\rho_{03}} : \frac{1}{\rho_{04}} = \frac{1}{65} : \frac{1}{36} : \frac{1}{25} : \frac{1}{15} = 1 : 1.8 : 2.6 : 4.3,$$

and

$$f_{pgr1} : f_{pgr2} : f_{pgr3} : f_{pgr4} = 200 : 400 : 550 : 900 = 1 : 2.0 : 2.7 : 4.5.$$

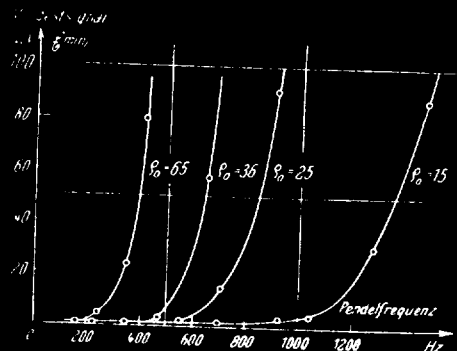


Abb. 21.
Empfindlichkeitsabnahme beim Eintreten von Kohärenz

Fig. 21
Decline of sensitivity with appearance of coherence.

Key:

Mindestsignal	Minimum signal
Pendelfrequenz	Quenching frequency
Hz	Cycles per second

From Fig. 21 it is to be recognized that in the coherence condition the sensitivity becomes extraordinarily large through an increase of the damping of the oscillating circuit. This observation has already been described by Kohn (ref. 4), who undertook all his investigations in the coherence condition, without, indeed, recognizing its peculiarities.

(b) Resonance points. Multiple resonance points.

In the condition of coherence and of adjustment with $\Delta < 0$, the superregenerative receiver shows, because of the long seesawing-up times, the phenomenon of multiple resonant points, which up till

now have been observed only by Gorelik and Hintz (ref. 5), who, however, found no fitting explanation. If an oscillation residue is present, tremors occur between this and the signal as soon as the frequencies do not correspond exactly. The initial amplitude is then not simply $|u_0| + |u_r|$, since the phase of u_0 is continually changing with respect to u_r .

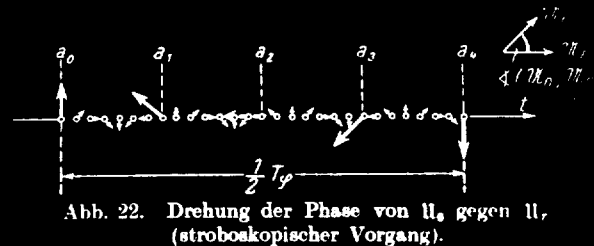


Fig. 22. Phase rotation of u_0 with respect to u_r .
(stroboscopic process).

Fig. 22 shows this process. Here the direction of the single arrows corresponds to the steadily changing phase displacement of u_0 with respect to u_r . With regard to the instant of dedamping a_0, a_1, \dots the phase displacement between u_0 and u_r varies after the manner of a stroboscopic process with period T_ϕ (c.f. also the "super-reaction stroboscopique" of David). It is found that with the receiver adjusted sensitively, considerable time during which the phase of u_0 relative to the free receiver oscillations hardly changes at all is necessary for the building-up of oscillations, since otherwise the seesawing-up process is disturbed.

For this reason the signal can attain a large amplitude

only if the receiver frequency is equal to the transmitter frequency or differs from it by an integral multiple of the quenching frequency; for if the transmitter frequency $f_H = f \pm k \cdot f_p$ ($k = 0, 1, 2, \dots$), u_o always has the same phase relative to u_r at the instant of de-damping. If, however, the stroboscopic period T_p becomes less than the magnitude of the building-up time, then no perceptible initial amplitude can be established. This phenomenon must figure the more significantly the larger the build-up times are; i.e., the smaller $-\Delta$ is.

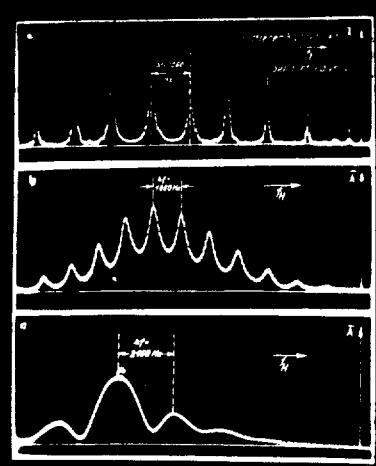


Abb. 23. Resonanzkurven mit multiplen Resonanzpeaks. Auftreten bei Kohärenz und $-\Delta < 0$.

Fig. 23. Resonance curves with multiple resonance peaks. Appearing with coherence (and $\Delta < 0$).

Key:

- | | |
|-----------------------|-------------------------|
| Mittlerer Richteffekt | Average detector effect |
| Senderfrequenz | Transmitter frequency |

Figures 23 (a,b,c) show typical multiple resonance curves in oscillograms. In (a), $-\Delta$ was as small as possible, and building-up times of 10 quenching-frequency periods, with $f_p = 1080 \sim$, were

observed in the Braun tube. A substantial effect is therefore to be expected of the signal only if $\frac{1}{T_{\phi}} < \frac{1080}{10} = 108 \sim$. As a matter of fact, the resonant peaks, lying evenly spaced at intervals of $\Delta f = f_p = 1080 \sim$, are very sharp here; they possess a width of only about $\pm 50 \sim$ with a receiver frequency of $140,000 \sim$. With an increase of $-\Delta$, which was obtained by a slight increase of the quenching voltage over (a), there resulted much more weakly impressed maxima and minima, as Fig. 23 (b) shows. At (c) $-\Delta$ was still larger. The resonance peaks are now very wide, and lie, moreover, because of other reasons (see Part V), at double the spacing.

Through the enlargement of $-\Delta$, there also occurs here a considerable diminution of the sensitivity, on account of the diminished seesawing-up and the lower amplification. The signal was:

(a)	(b)	(c)
130	370	17300 μv .

During reception, multiple resonance peaks are generally disturbing. It is desirable, then, to use them for the establishment of extremely narrow selectivity curves, in conjunction with a pre-stage for the attenuation of side responses.

The multiple resonances may thus be avoided in exactly the same way as the long building-up times, through adjustment of a large value of $-\Delta$ or application of a strong signal $u_0 \cong u_{0s}$; in both cases the sensitivity falls off in the manner already mentioned (see Part IVa). The oscillogram in Fig. 24 is an example

of the latter case; in the center portion u_0 is so great as a consequence of resonance that the multiple resonance peaks almost completely vanish.



Abb. 24. Durch starke Signale werden die multiplen Resonanzstellen zerstört.

Fig. 24.

Multiple resonance peaks destroyed by strong signal.

Key:

Richteff.

Detector effect

Hz

Cycles per second

It is still to be mentioned that only in the coherence condition can a heterodyne whistle appear in superregenerative reception. In the case of maintained oscillations in the receiver ($\Delta > 0$), the interference occurs in the same manner as in every heterodyne circuit. For $\Delta < 0$ also, however, a heterodyne-tone condition occurs in the vicinity of multiple resonance peaks, in case the build-up times are long. Then there occurs a periodic seesawing-up and -down of the stationary initial amplitude, many times greater than u_0 , with a frequency $\frac{1}{T_\phi}$, so that the oscillation-trains are thereby modulated at an audible frequency.

V. DEVIATIONS FROM THE THEORY

Up till now the theory has been quantitatively verified

in all details. Deviations can appear, if the course of damping and dedamping as a function of time is not the same for all oscillation-trains.

This is always the case when the grid bias $U_g \approx 0$, since then in one quenching-frequency period the damping and dedamping alternate twice. That is, if, with a sufficiently high quenching frequency, coherence is to be avoided, then, in order to bring about the necessary damping time, the quenching voltage is so large that the grid also goes strongly positive. Because of the decrease of the "steepness-factor" of the tube in the positive region, it then becomes unavoidable that a damping region shall exist in the ranges of both negative and positive grid voltages, as is explainable from Fig. 25. The dedamping region which lies between is traversed once on the way forward and once on the way back, so that in the course of one quenching period there occur two dedampings with different time-variations.

Whether oscillation-trains are produced by both or only by one of these dedampings depends upon the combined effect of various circumstances. In this way peculiarities of all kinds can arise. For example, it can be explained through these abnormal phenomena how in Fig. 23 the multiple resonance peaks are located partly in single and partly in double spacing of the quenching-frequency.

This peculiarity, while interesting, to be sure, will not be discussed further here, since it has no special significance

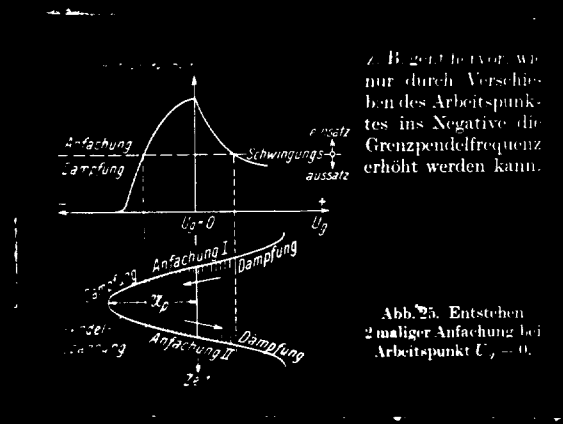


Fig. 25. Dedamping occurring twice with operating point at $U_g = 0$.

Key:

Rohrensteilheit	"Steepness-factor" (a measure of mutual conductance)
Anfachung	Dedamping
Dämpfung	Damping
Schwingungseinsatz	Oscillations start.
Schwingungsaussatz	Oscillations stop.
Pendelspannung	Quenching voltage
Zeit	Time

for superregenerative receivers. To prevent its occurrence, one takes care that only one dedamping occurs in one quenching-frequency period; for this purpose the grid is biased sufficiently negatively that it is raised by the quenching voltage only to the point of maximum slope, or approximately to $U_g = 0$. The necessary ratio $\frac{\tau_a}{\tau_d}$ can then be adjusted by means of the operating point; the larger the negative bias the smaller will be $\frac{\tau_a}{\tau_d}$.

It follows from Fig. 18, for instance, that the limiting quenching frequency can be increased only by the displacement of the operating point toward the negative.

CONCLUSIONS

Since, with a superregenerative receiver, one has the choice between various methods of operation, it can be adapted to almost any special use. Several of these have already been pointed out; in so far as this is not yet done, these are to be kept in reserve for the practical working out of important inferences, as well as certain supplementary technical matters, in a later publication.

Directional experiments with a one-tube short-wave superregenerative receiver have already provided complete confirmation of the fundamentals described here.

In conclusion I might thank Prof. Dr. Barkhausen, especially for the arrangement and many valuable bits of advice; the firm of Zeiss-Ikon, Dresden, for the loan of the Tremograph, by means of which the experiments were made much easier.

SUMMARY

1. The amplification of the signal in superregenerative receivers is accomplished by a periodically-repeated dedamping process of the form:

$$u = u_0 e^{\delta t}$$

The "initial amplitude" u_0 is related to the signal e.m.f. \mathcal{E} by the relation:

$$u_0 = \mathcal{E} \cdot \rho_{\text{eff}}$$

in which the effective resonance-heightening-effect ρ_{eff} consists of positive and negative resonance-heightening-effects: $\rho_{\text{eff}} = \rho_d + |\rho_a|$. If the dedamping of the receiver occurs gradually, then ρ_{eff} is about 2 times as large as $(\rho_d + |\rho_a|)$.

2. With regard to the degree of amplification of the superregenerative receiver, two regions can be distinguished. In the K-region, the degree of amplification has a constant value whose practical maximum depends upon the noise level. In the L-region, on the other hand, the degree of amplification decreases with an increasing signal according to a logarithmic law. In this region there always occurs a distortion factor $k = m/4 (1 - \frac{m^3}{4})$.

3. If the oscillation-trains are "incoherent", that is, in case the excited oscillation always dies out completely before the renewed dedamping, then the best adjustment of the receiver is on the limit of the K-region, directly before the transition into the L-region. Here the greatest audibility is produced by the minimum signal, which is determined by the noise level. By an increase of the signal with respect to the minimum signal there is obtained only an entirely insignificant increase in audibility. The best quenching frequency is then always the "limiting quenching frequency" f_{pgr} which separates the condition of incoherence from

that of coherence, and whose permissible magnitude is determined by the required selectivity. The maximum attainable audibility is, however, independent of f_{pgr} ; its value is influenced only by the size of tube used. In the K-region, the installation of an indirect but distortion-free automatic volume control is readily possible, while the L-region, of course, is inherently free from fading but not distortion-free.

4. The resonance curve for the initial amplitude is, for sudden dedamping only, one of the ordinary smooth curves. With gradual dedamping, on the other hand, it has a band-pass form. In the K-region the resonance curve of the receiver is of the same form; in the L-region there is a flattening, which, however, means no loss in selectivity for telephonic reception.

5. The threshold signal of the receiver, i.e., the necessary minimum signal, is decreased by increasing the effective resonance sharpness ρ_{eff} . This can be accomplished equally well through reduction of either damping or dedamping, the latter method being preferred practically. ρ_{eff} alone determines the threshold signal, which is independent of the other dimensions of the circuit.

6. There is a very definite relationship between the limiting quenching frequency, the effective resonance sharpness, and the highest permissible modulation frequency, which is given, for the practical values used above, by $f/f_{pgr} \cong 1.6 \rho_{eff}$ and

$f/f_m \approx 6.5 \rho_{\text{eff}}$. As a result of this, a lowering of the threshold signal of the receiver can be attained by decreasing the limiting quenching frequency.

7. In the condition of coherence, which occurs when the limiting quenching frequency is exceeded, the oscillations are not yet extinguished at the beginning of the new dedamping-period. Then, depending upon the adjustment, either there are established steady oscillations in the receiver, or it operates in the K-region with a lower amplification the more the limiting quenching frequency is exceeded. In the latter case, to be sure, a large sensitivity could also theoretically be obtained; however, there then result long building-up times in the establishment of the final value of the initial amplitude, and equally long dying-out times after the disappearance of the signal. In practice, at the appearance of coherence, there is always a considerable reduction of sensitivity. Worthy of note is the breaking up of the resonance curve of the receiver into several very sharp resonance peaks which can occur in the coherent condition. The cause of this is a stroboscopic process acting at the instant of dedamping, in conjunction with long building-up times. The effects of coherence, which are generally unfavorable for reception, can also be avoided even with $f_p > f_{pgn}$ through a sacrifice in sensitivity, as, for example, by the use of a very strong signal. With a quenching frequency of double the limiting quenching frequency, the sensitivity is already 150 times smaller.

8. To avoid unexpected and peculiar phenomena, the grid bias is selected so far negative that the grid voltage only attains the point of maximum "tube steepness". In this case there occurs only one dedamping in a quenching-frequency period.

LIST OF REFERENCES

1. Armstrong, E. H., L'Onde Electrique, 1922.
2. Hulbert, E.O., Proc. Inst. Radio Eng'rs., 11 (1923), p. 391.
3. David, P., L'Onde Electrique, 7(1928), p. 217; reference in Hochfrequenztechnik und Elektroakustik, 33 (1929), p. 153.
4. Kohn, H., Hochfrequenztechnik und Elektroakustik, 37 (1931), pp. 51, 98.
5. Gorelik, P., and Hintz, H., Hochfrequenztechnik und Elektroakustik, 38 (1931), p. 222.
6. Roosenstein, H. O., Hochfrequenztechnik und Elektroakustik, 42 (1933), p. 85.
7. Hassler, G., Hochfrequenztechnik und Elektroakustik, 42 (1933), p. 43.
8. Barkhausen, H., and Hassler, G., Hochfrequenztechnik und Elektroakustik, 42 (1933), p. 41.
9. Harnisch, A., Hochfrequenztechnik und Elektroakustik, 38 (1931), p. 181.
10. Barkhausen, H., Elektronenrohren, II, S. 64 (1933).
11. Barkhausen, H., Elektronenrohren, I, S. 136 (1931).

APPENDIX B

STANDARD SIGNAL GENERATOR

APPENDIX B

STANDARD SIGNAL GENERATOR

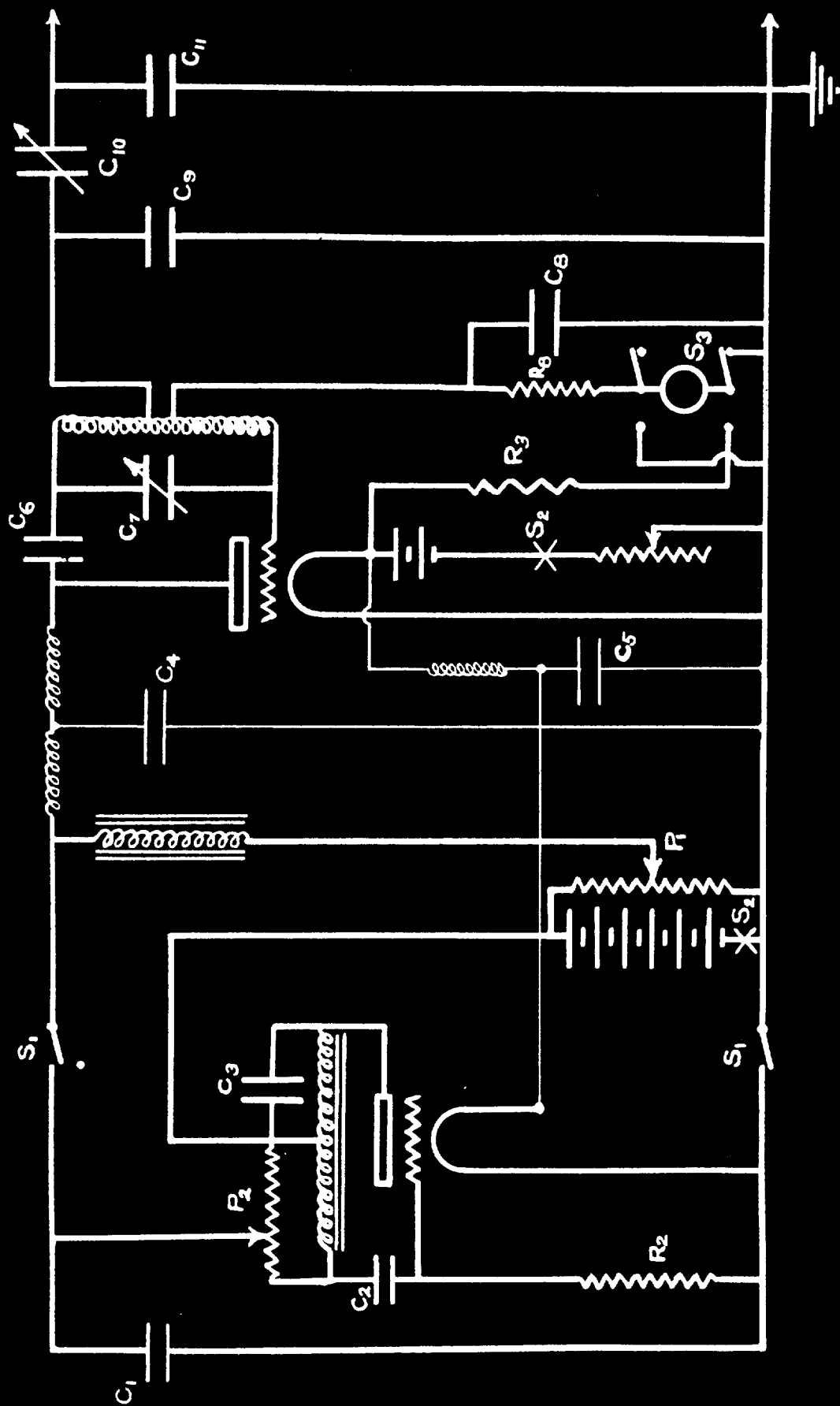
General Characteristics:

The design of the ultra-high-frequency signal generator referred to in Chapter I is quite similar to that of the Model 604B signal generator of the General Radio Company. The radio frequency range is approximately from thirty to fifty megacycles, but can be extended with the aid of additional r.f. tuning coils. The audio frequency used for modulation is 1000 cycles.

As may be seen by referring to the circuit diagram in Fig. 1, the generator consists of an audio frequency oscillator of the tuned plate type (at left of diagram) directly modulating the plate of the r.f. oscillator (at right of diagram), which is of the Hartley type. Type '31 tubes are used in both oscillators. The plate voltage for the audio tube is fixed and equal to the full B battery supply. The voltage on the plate of the r.f. tube is, however, variable by the potentiometer P_1 . Both tubes obtain their respective grid biases by means of grid leak and grid condenser combinations. The amount of modulating voltage used is varied by means of the potentiometer P_2 .

The amplitude of the output signal is made variable by

FIG.1 CIRCUIT DIAGRAM OF SIGNAL GENERATOR



means of the attenuator which is comprised of the π of condensers, C_9 , C_{10} , and C_{11} . C_{10} is a variable condenser of very small magnitude consisting of two circular plates about $\frac{3}{4}$ " in diameter inside of and shielded by a cylindrical metal can. One of the plates is fixed and the other can be made to approach the first from a distance of an inch and a half, up to touching. By means of this system, the ratio of output to input voltage of the attenuator may be varied through a range of approximately 500 to one, meaning that for a given input the ratio of the maximum to the minimum output is 500 to 1.

The meter is so connected up that by means of the double pole double throw switch S_3 , it may be made to read either d.c. grid current of the r.f. tube, or filament voltage. The resistance R_3 is a multiplier which allows the meter to read filament voltage. The grid of the r.f. tube is always connected to ground regardless of which way the switch is thrown.

Those parts of the circuit which have been drawn in lightly are relatively unimportant in the functioning of the set. The branch containing C_1 belongs in this class also. In building the set it was found necessary to include these parts for the prevention of stray induced voltages. They consist of radio frequency chokes and by pass condensers to ground.

Switch S_1 disconnects the audio oscillator and makes it possible to use an external source of modulating voltage connected to the two terminals at the left of the cabinet when it is desired.

Switch S_2 is the main power switch.

Unmodulated output:

To obtain a known output voltage at a certain frequency, the tuning condenser is first adjusted to give the desired frequency. Then the plate voltage potentiometer is adjusted to give a certain specific value of grid current on the grid current meter. This value is determined when the generator is calibrated. When this value of grid current has been obtained, it is understood to mean that a definite known r.f. voltage is being fed to the input of the attenuator. By turning the attenuator dial to the proper setting the desired output voltage is obtained. The statement that the same value of grid current produces the same r.f. input to the attenuator regardless of the frequency, requires some justification.

It is supposed that the d.c. grid current is directly a function of the amplitude of the r.f. oscillations, the wave form, and the grid-current-grid-voltage characteristic. The last is always the same. The wave form of the r.f. oscillations is approximately sinusoidal, and it may be assumed to be practically the same without any dependence upon the frequency. If this is so, the amplitude of oscillations is the only remaining variable, and it follows that if the grid current always reads the same, the amplitude of oscillations will always be the same.

Modulated output:

First, when we speak of the output voltage, we mean the root mean square value of the voltage which the r.f. oscillations would have if unmodulated. If then the percentage modulation is specified, the resultant wave is uniquely determined. The procedure for obtaining a certain percentage modulated output at a certain frequency and of known voltage is as follows.

The adjustments are made by first completely turning off the modulating voltage and turning up the plate voltage on the r.f. tube until the point is reached where oscillations just start. This is determined by watching for an incipient rise in the grid current as shown by the grid current meter. When this has been done, the modulating voltage is turned up until the grid current reaches a certain predetermined value. Then the plate voltage is again turned up still further until the grid current reaches a second predetermined value.

In this case as in the case of the unmodulated output, the grid current is used as the indicator of the voltage fed to the attenuator, and for the same reasons. In both of the above cases, the values of grid current which it is necessary to adjust for are experimentally determined when the generator is calibrated. The attenuator dial is calibrated at the same time. The reason the cut-off point of oscillations (point of incipient rise) is obtained before the modulating voltage is turned on, is that at this point the effect of a given amount of modulating voltages is greatest, in

terms of grid current. The two values of grid current used in adjusting for modulated output determine the percentage modulation, and this figure must also be determined experimentally during the calibration of the signal generator. In general only two values of percentage modulation will be of any practical importance, and these will probably be 100% and 50% or 40%. These are the values used in the General Radio Company's Model 604B.

Physical Characteristics:

The signal generator is contained in a wooden cabinet approximately 18" long, by 9" high, by 12" deep. Covering the entire front of the cabinet is a 1/8" aluminum panel through which pass most of the control knobs. The control for the modulating voltage is at the upper left hand side of the panel as seen from the front. The plate voltage control for the r.f. oscillator is at the lower left, the frequency control is at the lower right, and the knob for filament

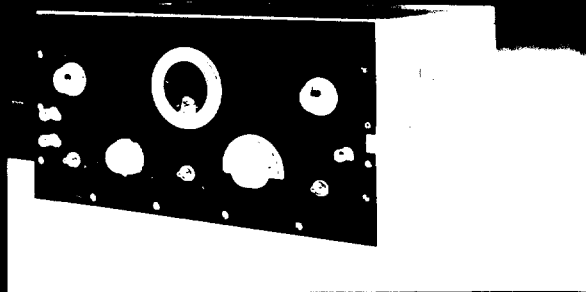


Fig. 2. Front view

voltage is at the upper right. The meter is in the center of the panel, and below it is the switch which enables the operator to read either grid current or filament voltage. At the left of the panel are two binding posts to be used when an external modulating voltage is desired. The switch near these is used to turn off the internal modulation and connect to the binding posts. On the lower right of the panel is the main on-off switch and a ground binding post. Projecting from the right hand end of the cabinet is the

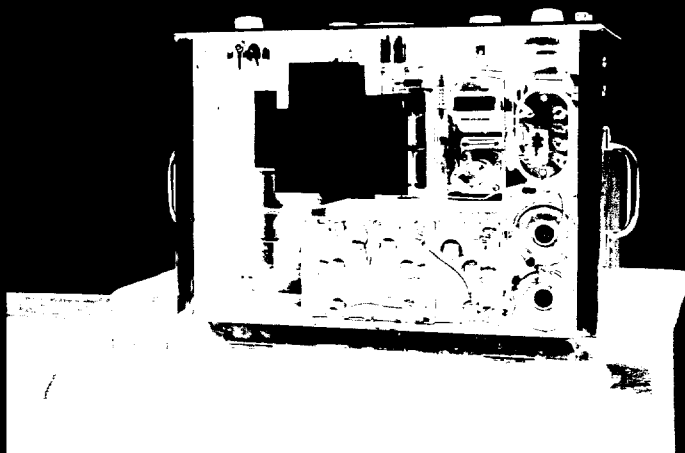


Fig. 3. Top view

drum which bears the attenuator calibration, and varies the attenuator condenser C_{10} . The output from the generator passes through a coaxial cable the terminal for which is at the bottom rear of the right hand side of the cabinet.

The entire inside of the cabinet, with the exception of the panel side, is lined with .005" sheet copper. All the necessary

batteries (three 45 volt "B" batteries and two 1-1/2 volt dry cells) are contained in special compartments at the rear. The audio frequency part of the set is at the left hand end as seen looking in from the top. The r.f. tube, tuning coil and tuning condenser as

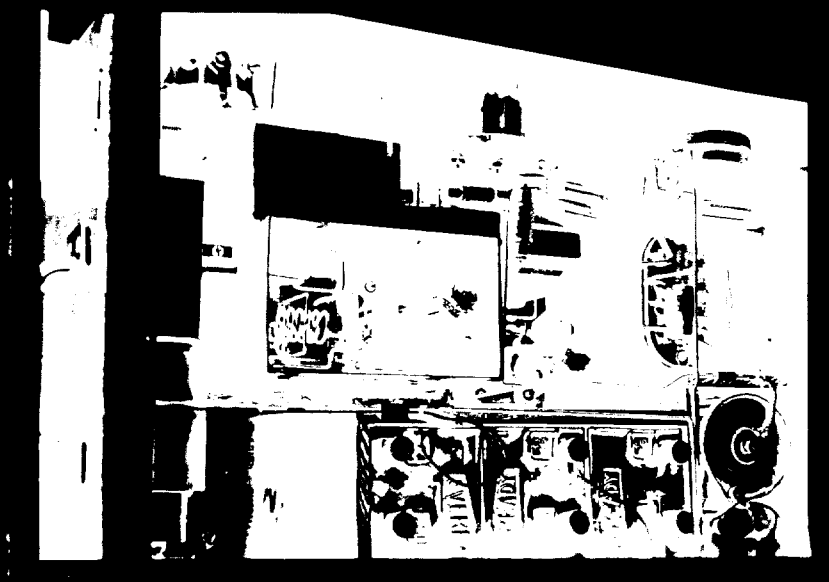


Fig. 4. Close-up view of top, with cover removed from shield can of r.f. oscillator.

well as miscellaneous r.f. chokes and by-pass condensers are contained within a heavy copper can just to the right of center. The entire attenuator is mounted on a separate wooden base at the extreme right, and the connecting leads to the cable terminal and to the r.f. oscillator are completely shielded. The r.f. tuning coil is mounted by means of General Radio plugs and jacks so that it may be removed and another coil may be substituted in order to obtain a different frequency range.

Brief History of Development of Generator:

Many changes were made in the circuit of the generator from the time of the first set-up, and it is unnecessary to tell about them all in detail. The first tentative set-up was made on a large board with little or no shielding present. At least a week was required to get the set to oscillate properly and to obtain the proper audio frequency, etc. Following this, the permanent construction of the generator was undertaken.

When the set was finally installed in the cabinet, it was found that a short-wave receiver near-by would give almost as much output with its antenna lead held outside the cabinet, as it would when the lead was placed in direct contact with the oscillating circuit. In other words we were confronted with a very severe shielding problem, and it was one which consumed a great deal of time. At that time the radio frequency coil and condenser were separately shielded by a heavy copper can. We were troubled by radiation taking place through the shielding of the bottom of the box; and also, separating the plates of the attenuator condenser increased the output instead of decreasing it.

These difficulties were all finally overcome by radically revamping the shielding and arrangement of the radio frequency part of the set. The r.f. tube was placed inside the copper can along with the tuning coil and condenser, and all leads leaving this can had r.f. chokes placed in them with by-pass condensers to ground. The attenuator shielding was augmented and connected directly to

the copper can. Also at the output end, the shielding was connected directly by means of braided tubing to the cable terminal. Radiation still took place through the bottom of the box and it was finally discovered that the screws which held the coil and condenser bases to the bottom of the box were responsible. Since all of these screws did not come through the wooden base, the trouble was corrected by placing a grounded patch of sheet copper over the guilty area and grounding those screws which were exposed. This took care of the largest portion of the stray field. There was still some radiation taking place from some of the control knobs. In one case we grounded the shaft which bore the knob, and in the other case we placed a by-pass condenser from the shaft to ground (see diagram, C_1). At the present time the amount of stray field is very small indeed.

After solving the shielding problem, we noticed another difficulty. The r.f. oscillator could not be made to oscillate for all settings of the tuning condenser, no matter what plate voltage was used. This was a very serious difficulty. We finally found that one of the radio frequency chokes, i.e., the one leading to the plate of the r.f. tube was apparently tuned. In this condition it had not been performing its job of blocking the radio frequency very effectively and for this reason the additional choke just outside the copper box had been added. We detuned the choke just inside the box by unwinding turns until oscillations could finally be produced at all available frequencies.

APPENDIX C

PRELIMINARY OUTLINE OF AUTOMOBILE
ANTENNA INVESTIGATION

APPENDIX C

PRELIMINARY OUTLINE OF AUTOMOBILE ANTENNA INVESTIGATION

(Prepared in July 1934)

Our complete problem is to find the combination or combinations of 9-meter antennas at the fixed and mobile stations which will provide optimum communication between the two stations, especially in city districts.

Because of lack of time we shall probably have to restrict the scope of the investigation to determining what type and position of antenna to use on the mobile unit for best communication when a single type of radiator -- perhaps a vertical half-wave antenna -- is used at the fixed station. At the same time, we recognize that in so restricting the scope of our work we are leaving an important aspect of the job still to be done, since it is conceivable that the best combination of antennas would call for something other than a vertical half-wave radiator at the fixed station.

By the principle of reciprocity, it makes no difference whether we put the transmitter at the fixed station and the receiver at the mobile one, or vice versa. The set-up which gives best communication in one direction will give best communication in the other direction also. However, it will be more convenient

to use a fixed transmitter and mobile receiver, both because the receiver is the more portable and because this arrangement will the more readily permit relationships to be noticed between variations in terrain around the mobile station and variations in received signal strength.

We may therefore restate our problem, at this point, as follows: To find the type and position of antenna to use on an automobile in order to permit optimum reception on 9 meters from a fixed vertical half-wave transmitting antenna, located on top of a city building.

It next becomes necessary to specify what we mean by "optimum reception". Apparently this term implies the following four items:

1. Maximum sensitivity — greatest average received signal, for given transmitter power, under all conditions.
2. Minimum fluctuation as the surrounding terrain varies.
3. Minimum horizontal directivity.
4. Minimum pick-up of noise.

In order to find the antenna or antennas having these four qualities in the highest degree, it would be possible (and this will be done as a last resort) to use cut-and-try methods, testing one type or position of antenna after another by riding through typical city streets and noting the quality of reception

from a fixed transmitter. It might be possible to arrange an automatic continuous recorder for this type of test, so that average results would be more apparent.

Such a method of attack presents two objections, however:

1. Conditions would change from the time of one antenna's test to that of the next. These changes would include traffic conditions, time of day, and weather. We could not afford to spend enough time with any single antenna to learn how to weight these changes.
2. We would not know what made one antenna better than another. In particular, and perhaps most important, we would not know if a particular antenna's superiority resulted from better alignment with the direction of polarization of the field, or from greater field strength at the antenna due to comparative freedom from absorption by the car body.

Consequently, if tests show that it can be used, a somewhat more scientific method, described in the following paragraphs, will be used. Whether or not this method can be expected to give any fruitful results depends upon the outcome of Part I. If Part I yields negative results, we shall be forced to use the cut-and-try method mentioned above.

Part I. To determine if:

1. The direction of polarization of the received

field is essentially constant throughout the immediate vicinity of the car (for any given location of the car).

2. The direction of polarization is not seriously affected in the vicinity of the car by putting a rod, loop or other device suitable for an antenna on the car.

Part II. If Part I yields affirmative results, we shall proceed to make tests, more extensive than time would permit in the cut-and-try method mentioned above (since in that method the tests would have to be repeated for each antenna tried), on the intensity and direction of polarization of the received signal in typical city areas. We shall make these tests with a car carrying a short rod antenna (or, at times, a small loop) mounted on a calibrated swivel joint located in what has been found by test to be a good location (one which is representative in regard to direction of polarization, and favorable in regard to strength of signal for all directions of polarization) on the car.

Initially we shall perhaps use signals received from Station WIXAV, at Squantum, Mass., if the radiated power and degree of modulation of transmissions from that station are found by inquiry or test to be about constant. Soon, however, we shall want to set up a transmitter in Boston, preferably on top of the Berkeley Street police building. Radiated power and per cent modulation will

be kept constant with the aid of meters in the transmitter. The receiver used as a field strength measuring set will be calibrated each day with a signal generator, whose output and per cent modulation will be known. Readings will be of two general types:

Part IIa. Some readings will be taken at intervals of only a foot or two, in order to determine the relation between the interference patterns occurring with different directions of polarization.

Part IIb. Other readings will be taken at random at greater intervals, in order to determine the average direction of polarization. For this latter purpose, it may also be helpful to run over a given route, say, three times, with the antenna oriented in a different direction each time, using an automatic continuous recorder in order to facilitate comparison of the data obtained from the three runs. This would best be done at night, when there would be little traffic to cause changing conditions between runs.

Parts IIa and IIb will be carried out in city streets mainly, but also in suburban districts and, initially, on M.I.T. grounds; in various kinds of weather and times of day; in different traffic conditions; and, if possible, with both rod and loop antennas, in order to gather data on both the electric and the magnetic fields.

Part III. After the average direction of polarization has thus been found, the next step will be to place the car in a

position where the field is so polarized and to explore the vicinity of the car for regions of maximum field strength. This procedure will have to be repeated for enough different positions and orientations of the car to "average out" abnormal effects resulting from reflections from surrounding objects.

This Part III should give the answer to our problem, for it will tell what is the most advantageous location for the antenna, and Part IIb will already have told what is the most advantageous orientation for the antenna. It will remain only to test out the conclusions drawn from Parts II and III.

Part IV. In order to check these conclusions, antennas located and oriented as indicated by the findings of Parts IIb and III will be tried in actual reception, both of the standard signal (perhaps recorded continuously at the receiver) and of voice transmissions. Antennas which parts IIb and III indicate should be poor will also be tried out, for comparison.

Part V. In order to determine the relation between, on the one hand, the horizontal and vertical directivity of an antenna when the car is in the middle of an empty field, and, on the other hand, the directivity observed when that type and position of antenna is used in actual reception in city streets, the antenna arrangements employed in Part IV will be used in tests on Coop Field, in which the transmitter will be in the car and the receiver will be used portably to explore the radiated field. Vertical directivity may be investigated by putting the receiver on one of

the wooden masts located on the field.

In all the tests carried out in this part, it will be necessary to be certain that the same amount of power is being fed to the antenna.

Part VI. If Part IIa indicates that the effect of interference patterns is serious enough to try to overcome, and that their effect can probably be materially reduced by using either of these arrangements:

1. Two (similar) antennas, some distance apart
on the car, or
2. Two dissimilar antennas on the car,

using a switching arrangement to throw the receiver on the antenna receiving the strongest signal, we shall try such systems. At first manual switching will be used, but later on perhaps some automatic mechanical or electronic (two input circuits each with its own detector tube) means will be tried.

It is of course not anticipated that any such antenna system will overcome "dead spots" existing behind hills and large buildings; it would be intended only to reduce fluctuations due to interference patterns.

- - - - -

In summing up this outline of procedure, we see that the four criteria of a good receiving antenna figure in the above six steps in the following manner:

1. Maximum sensitivity: Determined by IIb and III, and checked experimentally by IV.
2. Minimum fluctuation: Determined experimentally by IV, for a single antenna; more complex antenna system to reduce fluctuation designed from IIa and checked experimentally by VI.
3. Minimum horizontal directivity: Determined by III, checked experimentally by IV; general effect of buildings and other surroundings upon directivity revealed by comparison of III and IV, on the one hand, with V, on the other.
4. Minimum noise pick-up: Determined experimentally by IV.